Dissertation zur Erlangung des Doktorgrades

der Fakultät für Chemie und Pharmazie

der Ludwig-Maximilians-Universität München

Proteomic and functional

characterization of

human Argonaute complexes

Julia Regina Stöhr, geb. Höck

aus

Augsburg

2011

SUMMARY

Proteins from the Argonaute (Ago) family act as key factors of small RNA function. In mammalian somatic cells, the predominant class of small inhibitory RNAs is constituted by microRNAs (miRNAs) with a size of 21-24 nucleotides. They are bound by Ago proteins and guide them to their target mRNAs, thereby facilitating regulation of transcription, mRNA stability and translational repression. The complexity of miRNA-guided cellular events implies that a considerable number of additional factors is involved in controlling and fine-tuning these processes. Details on the underlying regulatory mechanisms, however, remain largely unknown.

Therefore, protein complexes containing Ago1 or Ago2 were analyzed for their RNA content as well as for associated protein factors and enzymatic activities. Gradient centrifugation of lysates from human cells revealed three distinct Ago-containing complexes, termed complex I-III, which differed in catalytic activities. While only the smallest complex (complex I) was cleavage competent, both complex I and the largest complex III were able to process a miRNA precursor into mature miRNA. Complex I consists of multiple sub-complexes with distinct enzymatic activities. While all three complexes contain miRNAs, only complex III associates with a translationally repressed mRNA target.

For a comprehensive proteomic analysis, proteins that co-purified with ectopically expressed FLAG/HA-tagged Ago1 and Ago2 were identified by mass spectrometry. Besides factors with reported functions in the miRNA pathway, the majority of Ago-associated proteins were implicated in mRNA binding or RNA metabolism. DEAD/DEAH-box containing proteins and heterogeneous nuclear ribonucleoprotein particles were represented in large numbers as well as ribosomal proteins. Ago interaction was verified for a subset of the identified proteins using immunoprecipitation and *in vitro* pull-down approaches.

Luciferase reporter experiments supported a functional relevance for the RNA binding protein RBM4 in miRNA-mediated repression. Moreover, *in vitro* pull-down approaches confirmed the interaction of RBM4 with all four human Ago proteins. Furthermore, the interaction interface could be narrowed down to the PIWI domain of Ago2, presumably with minor contributions of the N-terminal domain. RBM4 binding appears to be mediated by the second of the two RNA recognition motifs of RBM4 in concert with the Zinc finger domain and the intermediate linker region. Attempting to finally clarify the molecular mechanism of Ago binding to RBM4, first approaches were made towards the identification of common *in vivo* mRNA targets as well as mRNA binding requirements that allow for efficient interaction of RBM4 and Ago proteins. While a relevance in small RNA biogenesis or RISC activity was not observed, RBM4 might cooperate with Ago proteins in target binding and stabilize the Ago-target interaction, thereby increasing the effectiveness of miRNA-mediated gene regulation.

TABLE OF CONTENTS

1. INTRODUCTION

Systematic analysis of the human genome suggested that more than 93 % of the DNA is transcribed into RNA. Less than 2 % is actually translated into protein (Birney et al., 2007). Non-coding RNAs (ncRNAs) play an essential role in a multitude of cellular processes including RNA biogenesis, splicing and translation. In recent years, the relevance of a group of small ncRNAs, also referred to as small inhibitory RNAs, in the down-regulation of gene expression has become more and more apparent.

Effects of small inhibitory RNA functions were first observed in 1990, when Napoli and colleagues reported that overexpression of a pigment synthesis enzyme in petunia flowers resulted in partly or completely white petals (Napoli et al., 1990). Yet, the underlying mechanisms were not understood at the time. A first deliberate and efficient knock-down of target genes was performed in 1998 by Fire and Mellow in *Caenorhabditis elegans (C. elegans)* using long double-stranded RNA (Fire et al., 1998). In subsequent experiments in plants and *Drosophila melanogaster* extracts, it was demonstrated that the introduced long dsRNAs were processed into shorter fragments of about 22 nucleotides (nt) in length (Hamilton and Baulcombe, 1999; Hammond et al., 2000; Zamore et al., 2000). These fragments, termed small interfering RNAs (siRNAs), were shown to induce sequence-specific degradation of complementary target RNAs in a process termed RNA interference. For application in the mammalian system, however, this method proved to be inapt as transfection of long dsRNA into cultured mammalian cells resulted in an interferon response and subsequent cell death (Stark et al., 1998). Elbashir and colleagues were able to show that efficient RNA silencing in mammalian cells could be achieved by transfection of base-paired 21-nucleotide siRNA duplexes with symmetric 2 nt 3' overhangs (Elbashir et al., 2001a).

Meanwhile, small interfering RNAs have become an essential tool for the characterization of protein function and cellular processes. Moreover, several other classes of endogenous small inhibitory RNAs have been identified with functions reaching far beyond cleavage-induced destruction of a complementary target RNA and many aspects of their functions still remain to be elucidated. Their defining characteristics, however, comprise an RNA size of about 20-30 nucleotides and their association with members from the Argonaute protein family, which in turn are essential components of the effector protein complexes guided by small RNAs.

1.1. CLASSES OF SMALL RNAS

Small interfering RNAs can be grouped into classes according to their distinct biogenesis pathways as well as their biological functions, which are also dependent on the constitution of their Argonaute containing effector complexes. In the subsequent paragraphs, the major small RNA classes and their characteristics are outlined.

1.1.1. Small inhibitory RNAs (siRNAs)

Small inhibitory RNAs (siRNAs) guide endonucleolytic cleavage of their complementary target RNAs (Hammond et al., 2000; Zamore et al., 2000). SiRNAs originate from double stranded RNA (dsRNA) from either endogenous or exogenous sources, e.g. viral or transgene RNA.

Exogenous double-stranded siRNA precursors are recognized and cleaved by the dsRNA-specific RNase III enzyme Dicer yielding an RNA duplex of 21 nucleotides, each strand bearing a 5' phosphate and a two nucleotide (2 nt) overhang at the 3' end (Figure 1; Bernstein et al., 2001; Elbashir et al., 2001b; Elbashir et al., 2001c). The duplex is subsequently transferred to a member of the Argonaute (Ago) protein family, the core protein of the RNA-induced silencing complex (RISC; Hammond et al., 2000). One of the strands, termed the guide strand, is bound by the Ago protein, while the other strand, the so-called passenger strand, is ultimately degraded, thereby rendering the RISC complex active (Matranga et al., 2005; Miyoshi et al., 2005; Rand et al., 2005). The incorporated

Figure 1: Biogenesis and function of siRNAs from exogenous sources of double-stranded RNA.
Taken from Jinek and Doudna, 2009.

siRNA eventually acts in guiding the RISC complex to a perfect complementary target, thereby initiating endonucleolytic cleavage and subsequent degradation of its target RNA (Elbashir et al., 2001b; Elbashir et al., 2001c; Schwarz et al., 2002). Notably, only one of the human Ago proteins, Ago2, is endonucleolytically active and capable of target cleavage (chapter 1.2.2.1, Liu et al., 2004; Meister et al., 2004). Further, in plants and flies, siRNAs are

stabilized by methylation at the 3' end prior to loading into Ago proteins (Li et al., 2005; Yu et al., 2005; Horwich et al., 2007; Pelisson et al., 2007; Ramachandran and Chen, 2008).

Initially, the existence of endogenously derived siRNAs seemed to be restricted to *C. elegans* and plants (Hamilton et al., 2002; Ambros et al., 2003). Recently, however, endo-siRNAs have also been detected in *Drosophila* and mammalian systems, suggesting general functions of this small RNA class in higher eukaryotes (Kim et al., 2009).

In plants and nematodes, endo-siRNA production involves RNA dependent RNA polymerases (RdRPs), that allow for the creation of an RNA double strand from a single-stranded RNA template. In *C. elegans*, Argonaute-associated primary siRNAs bind to target mRNAs and recruit the RdRP complex which synthesizes antisense siRNAs to the target mRNA without the requirement of primers (Smardon et al., 2000; Aoki et al., 2007; Pak and Fire, 2007; Sijen et al., 2007). The siRNAs resulting from this process are referred to as secondary siRNAs. In plants, the RdRP complex is recruited upon siRNA-induced target cleavage and produces a long RNA double strand, that is subsequently cleaved by a Dicer-like protein into secondary siRNA duplexes, followed by loading of single stranded siRNAs into Argonaute proteins (Ghildiyal and Zamore, 2009). In both systems, the RdRP synthesis step allows for a self-amplification of the silencing response. In both plants and nematodes, even a spreading of siRNAs from cell to cell has been observed, allowing for a systemic response to exogenous RNA (Voinnet, 2005).

Endo-siRNAs in plants can be distinguished according to their origin and function (reviewed in Kim et al., 2009). Natural antisense transcript-derived siRNAs (natsiRNAs) originate from convergent transcription of a constitutively transcribed RNA strand and a complementary strand that is transcribed in response to cellular stress. *Trans*-acting siRNAs (tasiRNAs) are produced upon cleavage of a pre-tasiRNA. Subsequently, a complementary RNA strand is generated and cleaved into 21 nt tasiRNAs. Both natsiRNAs and tasiRNAs guide cleavage of their respective target RNAs. *Cis*-acting siRNAs (casiRNAs), in contrast, arise from transposons or repetitive elements and initiate heterochromatin formation via DNA methylation and histone modification at their homologous loci. A similar function has also been reported for centromeric repeat-derived dsRNAs in *Schizosaccharomyces pombe* (Volpe et al., 2003; Moazed, 2009). This regulatory mechanism has been termed RNA induced transcriptional silencing.

In *Drosophila* and in mammalian systems, however, RNA dependent RNA polymerases appear to be missing. Here, endo-siRNAs arise from different sources, e.g. from bidirectional transcription, as described for siRNAs against the L1 retrotransposon detected in human cell cultures (reviewed in Ghildiyal and Zamore, 2009). Other endo-siRNAs may arise from RNA transcripts containing intramolecularly paired hairpins, so-called "structured loci", from convergent transcription or read-through transcription of transposons placed in inverted

orientation. Further, a gene transcript may partially pair with that of a cognate pseudogene transcribed in inverted orientation. These endo-siRNAs are believed to maintain genomic stability by repressing mobile genetic elements. Interestingly, some endo-siRNAs in flies also derive from mRNAs, suggesting a possible role in regulating protein expression (Ghildiyal et al., 2008). Except for secondary siRNAs in *C. elegans*, which adhere to specific biogenesis rules, the processing of endo-siRNAs appears to involve Dicer-mediated dsRNA cleavage and subsequent incorporation into Ago proteins as described before.

Current work suggests that abundant expression of endo-siRNAs in mice is restricted to oocytes and embryonic stem cells (Babiarz et al., 2008; Tam et al., 2008; Watanabe et al., 2008). In flies, however, endo-siRNAs have also been detected in somatic cells (Ghildiyal et al., 2008).

1.1.2. MicroRNAs (miRNAs)

In animals, the most prevalent class of small RNAs in somatic cells is constituted by microRNAs (miRNAs). Hundreds of miRNAs have been described in various organisms and viruses and more continue to be discovered, probably regulating more than 60 % of all protein-coding genes on a post-transcriptional level in animals (Friedman et al., 2009).

1.1.2.1. MiRNA biogenesis

MiRNAs are usually transcribed as long, often poly-cistronic, primary miRNAs (pri-miRNAs) by RNA polymerase II in the nucleus (Lee et al., 2002; Lee et al., 2004a). Carrying 5' cap structures as well as introns and poly(A)-tails, these transcripts largely resemble mRNAs (Rodriguez et al., 2004). Additionally, a considerable number of miRNAs is encoded in the intronic regions of protein-coding transcripts.

In a first processing step, the stem-loop-structured miRNA precursors (pre-miRNAs) are liberated from the primary transcript (Figure 2, left and upper right panel). The cleavage reaction is performed by a multiprotein complex termed microprocessor containing the RNase III enzyme Drosha and its double-stranded RNA binding domain (dsRBD)-containing partner DGCR8 (or Pasha in *Drosophila*) (Lee et al., 2003; Denli et al., 2004; Gregory et al., 2004; Han et al., 2004; Landthaler et al., 2004). This cleavage yields hairpin-structured pre-miRNAs of a size of 60-70 nucleotides with a 2 nt 3' overhang as is characteristic for products of RNase III enzymes. They are recognized by the nuclear export factor Exportin 5 and transferred to the cytoplasm in a Ran-GTP dependent manner (Yi et al., 2003; Bohnsack et al., 2004; Lund et al., 2004). Another RNase III enzyme, Dicer, and its dsRBD partner

TRBP (or the homologous Loqs in *Drosophila*), removes the hairpin from the pre-miRNA, yielding a short-lived duplex intermediate that consists of the mature miRNA and the miRNA*, which usually is degraded subsequently. Mature miRNAs – and in some cases also miRNA*s (Packer et al., 2008) - are then incorporated into their effector complexes termed microRNA containing ribonucleoprotein particles (miRNPs) and guide them to their target mRNAs, which are subsequently regulated on the level of translational inhibition and/or mRNA degradation (Fabian et al., 2010).
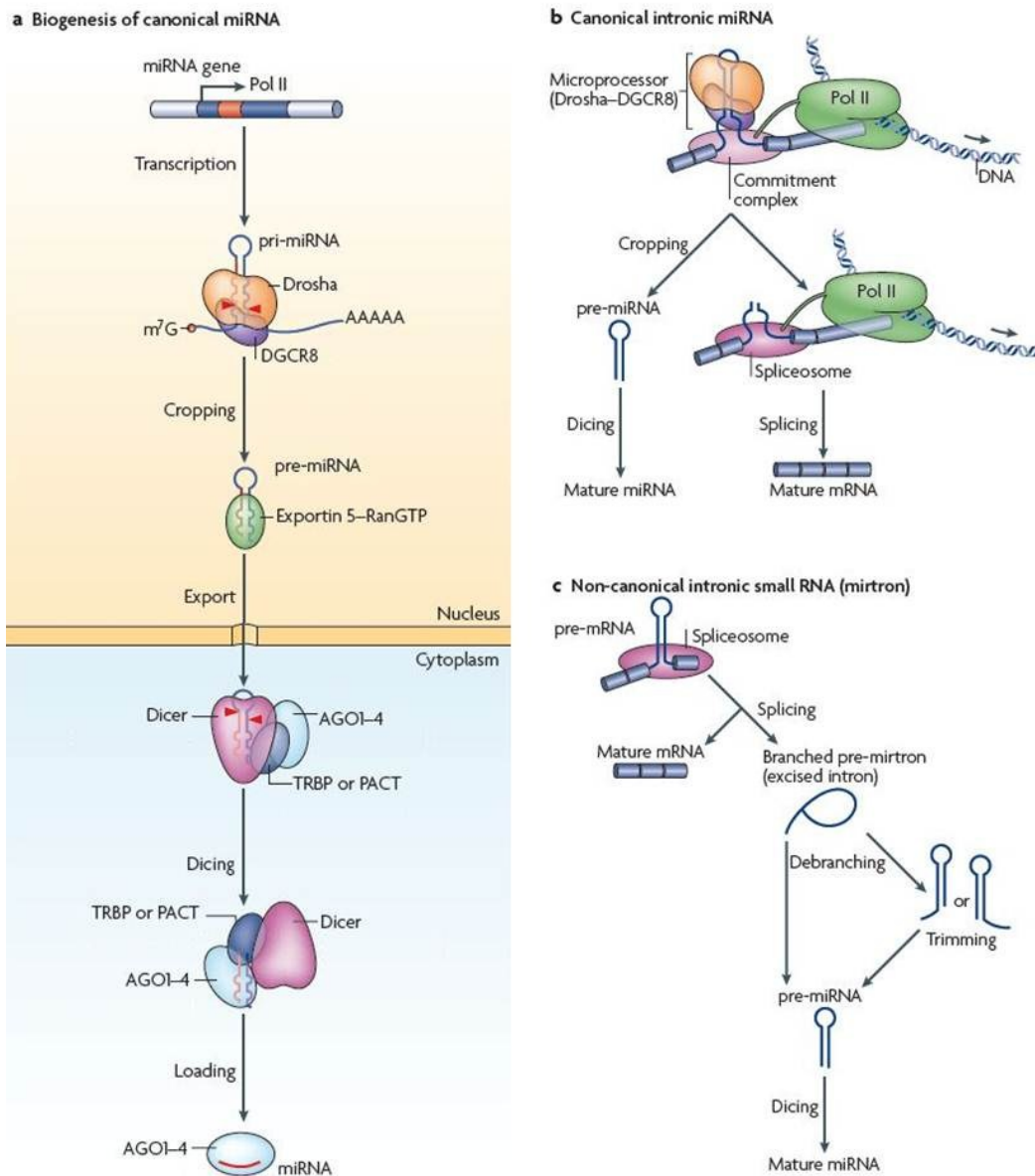
Figure 2: MiRNA biogenesis pathways
(a) MiRNA processing from a non-coding RNA transcript, (b) Biogenesis of an intronic miRNA, (c) Drosha-independent miRNA biogenesis from a "mirtron" (modified from Kim et al., 2009).

Moreover, alternative miRNA processing pathways have been discovered in the meantime. Some miRNAs are produced in a Drosha-independent manner from pre-miRNA-resembling

introns, so-called "mirtrons" (Figure 2, lower right panel). They are liberated from protein-coding transcripts during nuclear pre-mRNA splicing and primarily accumulate as branched pre-mirtrons (Okamura et al., 2007; Ruby et al., 2007; Babiarz et al., 2008). After debranching and sometimes also trimming, the resulting pre-miRNAs are exported into the cytoplasm and further processed by Dicer. Other studies identified small nucleolar RNAs (snoRNAs) as sources of small RNAs with miRNA-like functions (Ender et al., 2008; Saraiya and Wang, 2008; Taft et al., 2009). Recently, a Dicer-independent miRNA biogenesis pathway has been described for miR-451 (Cheloufi et al., 2010; Cifuentes et al., 2010; Yang et al., 2010). Both miR-144 and miR-451 are cleaved from a poly-cistronic primary transcript by the Drosha complex. While the miR-144 precursor enters the canonical miRNA biogenesis pathway, pre-miR-451 is directly loaded into Ago2 in the cytoplasm. Bypassing Dicer processing, the miR-451 precursor is cleaved by Ago2 and probably trimmed by an unknown exonuclease to yield the mature miR-451.

MiRNA function is highly regulated cell-specifically as well as temporally (Landgraf et al., 2007). This is also reflected in the post-transcriptional regulation of miRNA biogenesis. As an example, maturation of miRNA let-7 in murine embryonic stem cells is prevented on the pri- as well as on the pre-miRNA level by Lin28 (Heo et al., 2008; Newman et al., 2008; Viswanathan et al., 2008). Contrarily, the proteins hnRNP A1 as well as the RNA helicase p68 have been reported to enhance pri-miRNA processing (Guil and Caceres, 2007; Davis et al., 2008).

1.1.2.2. MiRNA binding to target mRNAs

In contrast to siRNAs, miRNAs usually exhibit only partial complementarity to the binding sites on their target RNAs. Perfect pairing of 5' nucleotides 2-8 of the miRNA, the so-called "seed" sequence, is, however, of particular importance for miRNA function (Lewis et al., 2005; Rajewsky, 2006). Complementarity of the 3' nucleotides is in many cases of minor importance for miRNA function, though it may stabilize the interaction (Fabian et al., 2010). As a rule, miRNA-mRNA duplexes contain mismatches or bulges in the central region, preventing endonucleolytic cleavage of the mRNA in an siRNA-like manner. As partial complementarity is sufficient for miRNA targeting, a single miRNA may control a large number of mRNAs (Bartel and Chen, 2004). This consideration illustrates the impressive regulatory potential of this small RNA class, but, on the other hand, the difficulties in the prediction of target mRNAs.

Most miRNA binding sites are located in the 3'-untranslated regions (3'-UTRs) of mRNAs. They are frequently found in AU-rich regions in close proximity to the open reading frame (ORF) and/or the 3' end of the 3'-UTR (Rajewsky, 2006; Grimson et al., 2007; Nielsen et al.,

2007). In many cases, multiple sites for a single or different miRNA are clustered and act cooperatively to increase functional efficiency (Doench and Sharp, 2004; Grimson et al., 2007). More rarely, miRNA binding sites in the 5'-UTR or the coding region of mRNAs have been reported as well (Kloosterman et al., 2004; Easow et al., 2007; Orom et al., 2008; Gu et al., 2009; Rigoutsos, 2009).

Despite their distinct biogenesis, siRNA and miRNA pathways are not strictly separated. In rare cases, mammalian miRNAs have been reported to induce cleavage of highly complementary targets (Doench et al., 2003; Yekta et al., 2004; Davis et al., 2005), whereas siRNA binding to imperfectly matching target RNAs can influence their translation and/or turnover rate. While this opens up additional regulatory options, it also poses a considerable problem for the use of siRNAs as a scientific tool, as so-called "off-target effects" caused by imperfect binding of the guide strand to a number of unintended targets may overlap with actual siRNA effects (Jackson and Linsley, 2004).

1.1.2.3.   Mechanisms of miRNA function

1.1.2.3.1.   Translational repression

While the repressive effect on translation is a widely acknowledged function of miRNAs, the mechanisms by which it is achieved continue to be under debate (Figure 3).

Some studies observed a miRNA-mediated decrease in translation initiation. For efficient translation initiation of capped mRNAs, several initiation factors are required: among them, eIF4A destroys secondary structures in the 5'-UTR of the mRNA through its RNA helicase function, allowing for AUG-scanning by the small ribosomal subunit. EIF4G acts as a scaffold that binds eIF4A and the m^7G-cap-binding factor eIF4E as well as the poly(A)-binding protein (PABP) at the 3' poly(A)-tail of the mRNA, thereby circularizing the mRNA and enhancing translation initiation rates (Fabian et al., 2010). Transfection of miRNA target reporter constructs resulted in a shift of the respective mRNAs to lighter fractions in polysome gradients, presumably caused by a block of ribosome subunit joining to the mRNA (Pillai et al., 2005; Bhattacharyya et al., 2006a). This was attributed to miRNA interference with eIF4E binding to the 5' cap (Humphreys et al., 2005). Further, the Ago effector complex might disturb the association of eIF4G with PABP, thereby preventing mRNA circularization (Humphreys et al., 2005). This theory was supported by observations that mRNAs either lacking a functional 5' cap or possessing certain internal ribosome entry sites (IRES) were either not or only weakly affected by miRNA-mediated repression (Humphreys et al., 2005; Pillai et al., 2005; Wang et al., 2006; Mathonnet et al., 2007; Thermann and Hentze, 2007; Wakiyama et al., 2007). Another theory assumes that Ago directly binds to the cap-structure

and thereby displaces eIF4E. The Ago MID domain shows limited sequence homology with eIF4E and mutation of two aromatic residues within this sequence impaired translation repression (Kiriakidou et al., 2007). However, this model was questioned as mutation of said residues interfered with binding of an essential Ago partner, GW182 (Eulalio et al., 2008); moreover, no significant structural similarities could be observed between human Ago2 and eIF4E (Kinch and Grishin, 2009). Some data suggest that 60S ribosomal subunit joining and subsequent formation of the 80S ribosome might be another process disturbed by miRNAs (Mathonnet et al., 2007; Thermann and Hentze, 2007; Wang et al., 2008a). This was also supported by co-immunoprecipitation results that found eIF6, a translational regulator that can associate with the 60S subunit and prevent its premature joining to the 40S subunit, to be associated with the ternary Ago2-Dicer-TRBP complex (Chendrimada et al., 2007).
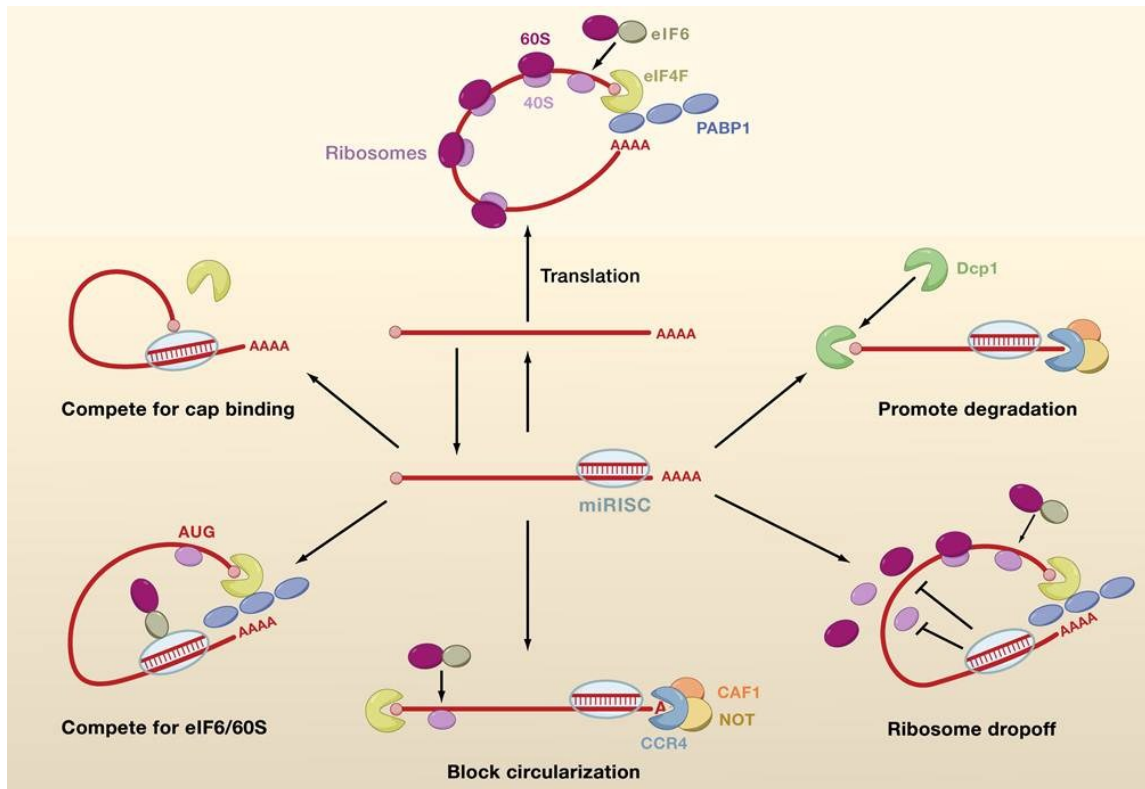
Figure 3: Mechanisms of miRNA-mediated translational repression.
MiRNPs may interfere with efficient translation by competition of Ago with eIF4E for cap binding (upper left), by preventing 60 S ribosomal subunit joining (lower left), by blocking mRNA circularization through competition for PABP (lower middle) or by facilitating premature ribosome drop-off (lower right). Alternatively, mRNA decay may be promoted by a concerted process of deadenylation, decapping and subsequent degradation (taken from Carthew and Sontheimer, 2009).

A number of studies proposed that miRNA-mediated translational repression might function at post-initiation steps. Polysome sedimentation analyses found repressed miRNA target mRNAs in fractions also containing actively translating polysomes, supporting the idea that miRNAs might function in blocking translation elongation (Olsen and Ambros, 1999;

Seggerson et al., 2002; Maroney et al., 2006; Nottrott et al., 2006; Petersen et al., 2006; Gu et al., 2009). In contrast to aforementioned studies on IRES-dependent translation, some groups also observed IRES-driven translation to be repressed by miRNAs (Seggerson et al., 2002; Lytle et al., 2007) and therefore claimed that translation inhibition may take place at a step other than initiation. Another approach concluded that miRNAs may act by causing premature translation termination and subsequent ribosome drop-off (Petersen et al., 2006). Nottrott and colleagues finally proposed that repression is facilitated via co-translational degradation of the nascent polypeptide chain (Nottrott et al., 2006). This theory is controversial as, accordingly, degradation should not occur with polypeptides targeted to the endoplasmatic reticulum (ER); however, miRNA-mediated repression remained unaffected by ER targeting. Further, translation of a high number of membrane and ER proteins was shown to be regulated by miRNAs (Pillai et al., 2005; Selbach et al., 2008).

The present data are in many points controversial or even contradictory. Partly, this may be attributed to differing experimental approaches. However, it seems plausible that miRNAs interfere with translation in multiple ways to facilitate target mRNA repression. It is even conceivable that repression modes vary in dependence of the present mRNA target. For example, Kong et al. have proposed that the promotor of an mRNA might influence whether miRNA repression occurs on translation initiation or elongation levels (Kong et al., 2008). Further, other factors may influence accessibility of miRNA binding sites, e.g. under conditions of cellular stress, thereby adding another layer of complexity to the regulation of translation (Bhattacharyya et al., 2006b). Other proteins might either positively or negatively interfere with the function of certain miRNAs by interacting with miRNA-associated protein factors, as described for murine Ago1 and TRIM32 or the *C. elegans* TRIM-NHL and the nematode Ago proteins ALG-1/2 and AIN-1 (Hammell et al., 2009; Schwamborn et al., 2009).

1.1.2.3.2.   mRNA deadenylation and decay

A second functional miRNA mechanism is marked by a decrease of target mRNA levels due to degradation (Behm-Ansmant et al., 2006; Giraldez et al., 2006; Wu et al., 2006). MiRNA-mediated mRNA decay is a concerted process that requires both Ago and GW182 family proteins and usually starts with the removal of the poly(A)-tail by the CCR4-NOT1 complex of 3'-5' exoribonucleases (Behm-Ansmant et al., 2006). Subsequently the mRNA is either degraded in 3'-5' direction or decapped by the DCP1-DCP2 decapping enzyme complex followed by complete degradation by the 5'-3' exonuclease Xrn1 (Orban and Izaurralde, 2005). MiRNAs were associated with deadenylation and destruction of a variety of mRNA targets in many organisms. During development and cell differentiation, for example, miRNAs control the destruction of maternal mRNAs and transiently required transcripts

(Giraldez et al., 2006; Wu et al., 2006; Wakiyama et al., 2007; Fabian et al., 2009; Iwasaki et al., 2009).

The ribonuclease CAF1, an essential component of the CCR4-NOT1 complex, interacts with Ago proteins (Fabian et al., 2009). Another crucial protein factor for deadenylation is the poly(A)-binding protein PABP, that directly interacts with GW182, placing the mRNA poly(A)-tail in close proximity to the deadenylase complex and at the same time blocking translation initiation and termination (Tarun and Sachs, 1996; Uchida et al., 2002; Kahvejian et al., 2005; Fabian et al., 2009). Translational repression and deadenylation are not strictly separated processes but may occur subsequently or even simultaneously (Wu et al., 2006; Fabian et al., 2009; Hu et al., 2009). In some cases, the two mechanisms complement each other while regulation of other miRNAs seems to be restricted to either of the processes (Selbach et al., 2008; Fabian et al., 2009).

1.1.2.3.3. Translational activation

Occasionally, miRNAs have also been reported to act as activators of translation rather than as repressors. As an example, the miRNA-regulated translation of the TNFα mRNA was increased in growth arrested cells. In proliferating cells, however, translation of the same mRNA was repressed (Vasudevan and Steitz, 2007; Vasudevan et al., 2007).

Moreover, mRNAs with 5'-UTR miRNA binding sites have been associated with translational activation as well (Henke et al., 2008; Orom et al., 2008).

Still, reports on miRNA-mediated translational activation have been rather rare and further investigations will be necessary to clarify the underlying mechanisms and also the relevance of this miRNA function.

1.1.3. Piwi-interacting RNAs (piRNAs)

Another class of small RNAs with a size of 25-30 nucleotides is implicated in germ line development and maintenance of genomic stability (Aravin et al., 2006; Girard et al., 2006; Lau et al., 2006; Siomi and Siomi, 2009). These small RNAs associate with the Piwi subfamily of Argonaute proteins and accordingly have been termed Piwi-interacting RNAs (piRNAs). PiRNA expression seems to be restricted to germ cells and is particularly prominent in testes. While piRNA sequences are highly diverse, they mostly map to a few hundred discrete genomic clusters (Aravin and Hannon, 2008). They are not conserved across species, but still are expressed from syntenic regions. In *Drosophila*, piRNA biogenesis was proposed to function via an amplification loop according to the so-called

"ping-pong" mechanism that requires neither Dicer processing (Vagin et al., 2006) nor small dsRNA intermediates (reviewed in Kim et al., 2009). The *Drosophila* Piwi subfamily is constituted by the proteins Piwi, Aubergine (AUB) and Ago3. Piwi and AUB typically bind piRNAs with a sequence antisense to transposon transcripts and a strong nucleotide bias towards uracil at their 5' end, whereas Ago3-associated piRNAs arise mostly from sense transcripts and carry an adenine at nucleotide position 10 (Brennecke et al., 2007; Gunawardane et al., 2007). Strikingly, the first 10 nucleotides of AUB-associated piRNAs are usually complementary to Ago3-associated piRNAs. Based on these observations and the detection of endonucleolytic Piwi-activity (Saito et al., 2006; Gunawardane et al., 2007), it was proposed that AUB or Piwi loaded with antisense piRNA might cleave sense retrotransposon transcripts, thereby creating the 5' ends of a sense piRNA that can associate with Ago3. In turn, Ago3 cleaves antisense retrotransposon transcripts, producing the 5' end of the antisense piRNA that subsequently binds to AUB or Piwi, ultimately resulting in an amplification of the piRNA population (Brennecke et al., 2007; Gunawardane et al., 2007). *Drosophila* and mammalian piRNAs are 3' methylated, similar to siRNA modifications in *C. elegans* and plants (reviewed in Siomi and Siomi, 2009). The mechanism defining the 3' ends of the newly created piRNAs has yet to be determined. Initiation of the ping-pong cycle during development was attributed to maternal inheritance of piRNAs as well as AUB and probably also Piwi proteins (Brennecke et al., 2007; Nishida et al., 2007; Brennecke et al., 2008).

In mammals, piRNAs can be grouped into two classes that act in distinct stages of sperm development. Mouse piRNAs, that are expressed before meiotic pachytene and – in analogy to *Drosophila* piRNAs - originate from repeat- and transposon-rich clusters, are presumably created via a ping-pong-resembling mechanism (Watanabe et al., 2006; Aravin et al., 2007; Aravin et al., 2008). These pre-pachytene piRNAs interact with the murine Piwi proteins MILI and MIWI2. Intriguingly, MILI and MIWI2 also display DNA methylation activity in fetal male germ cells, indicating their importance for transcriptional silencing rather than degradation of abundant transposon transcripts (Aravin et al., 2008; Kuramochi-Miyagawa et al., 2008). The second piRNA class is very abundant in spermatocytes in the pachytene stage and associates with MIWI and MILI (Girard et al., 2006; Aravin et al., 2007; Aravin et al., 2008). However, pachytene piRNAs do not adhere to the sequence characteristics described for *Drosophila* but rather seem to be derived from large genomic clusters with marked strand asymmetry and a lower repeat frequency (Aravin et al., 2006; Girard et al., 2006). The exact function of pachytene piRNAs in mammals still remains elusive.

While piRNAs are predominantly detected in mammalian testes, female germ cells are strikingly enriched in endo-siRNAs (Tam et al., 2008; Watanabe et al., 2008), indicating a possible cooperation of both pathways in transposon repression (Ender and Meister, 2010).

1.2.   PROTEINS INVOLVED IN SMALL RNA FUNCTION

1.2.1. The RNase III ribonucleases Drosha and Dicer

SiRNA- and miRNA biogenesis generally requires the endonucleolytic cleavage of dsRNA precursors by proteins of the RNase III family: Dicer and Drosha. Both Drosha and Dicer are monomeric proteins with two tandemly arranged RNase III domains that constitute the catalytic site (Figure 4). As all RNase III-processed RNAs, their products are characterized by a monophosphorylated 5' end and a 2 nt overhang at the 3' ends (MacRae and Doudna, 2007).

The nuclear RNase III protein Drosha acts in liberating miRNA precursors from primary transcripts in an initial cleavage reaction (Lee et al., 2003). Its substrate specificity, however, is dependent on association with the dsRBD protein DGCR8 (DiGeorge syndrome critical region 8) or its homologue Pasha in *Drosophila* in a complex termed microprocessor (Giot et al., 2003; Gregory et al., 2004; Han et al., 2004; Landthaler et al., 2004). By binding to the base of the pri-miRNA hairpin, DGCR8 positions Drosha to cleave the primary transcript at a distance of 11 base pairs from the junction between hairpin structure and flanking single-stranded RNA regions, releasing the respective pre-miRNA (Han et al., 2006).

Dicer, the second RNase III enzyme involved in small RNA biogenesis, uses long dsRNAs as well as pre-miRNAs as substrates, creating short dsRNA fragments with a defined length of 21-25 nucleotides, depending on the organism studied (Bernstein et al., 2001). In *Drosophila*, miRNA and siRNA processing is performed by two distinct Dicer proteins – Dcr-1 and Dcr-2, respectively (Lee et al., 2004b). Nematodes and mammals, however, possess only one Dicer protein that acts indiscriminately on both small RNA classes (Hutvagner et al., 2001; Ketting et al., 2001; Knight and Bass, 2001). Human Dicer is characterized by an N-terminal DEXD/H box, a Domain of Unknown Function (DUF) and a PAZ domain, followed by a connector helix, two RNase III domains and the C-terminal dsRBD (Figure 4, Jinek and Doudna, 2009).
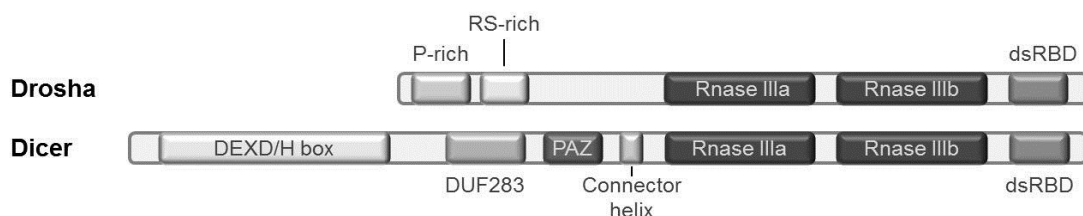
Figure 4: Schematic depiction of the human RNase III enzymes Drosha and Dicer.
DUF: Domain of Unknown Function, PAZ: Piwi-Argonaute-Zwille domain, RNase IIIa and -b: RNase domains, dsRBD: double-stranded RNA binding domain. Modified from Jinek and Doudna 2009.

While Dicer structures from higher eukaryotes have not been solved to date, crystal structures of Dicer from the unicellular eukaryote *Giardia intestinalis* as well as biochemical approaches elucidated some of the mechanistic details of Dicer function (Zhang et al., 2004; Macrae et al., 2006). The *G. intestinalis* Dicer lacks the DEXD/H box as well as DUF and dsRBD domains, providing a minimal Dicer protein. The PAZ domain is connected with the tandem RNase III domains via a connector helix that is not conserved through species. The PAZ domain acts in anchoring the 3' end of the RNA duplex. The RNA establishes electrostatic interactions with a number of positively charged residues, while the intramolecular RNase III domain dimer cuts the double strand in dependence of Mg^{2+} cations, creating characteristic double-stranded RNA intermediates of a defined size carrying the RNase III specific 5' phosphate-2 nt 3' overhang pattern (Macrae et al., 2006; MacRae et al., 2007). The distance from PAZ (3' RNA anchor) to RNase III domains (5' cleavage site) – which is mainly defined by the connector helix - thereby acts as a molecular ruler that determines the product size (MacRae et al., 2007). The dsRBD appears to act as a clamp that locks the RNA substrate; deletion of the dsRBD from human Dicer decreases enzyme efficiency while substrate affinity remains unaffected (Ma et al., 2008). Moreover, the DEXD/H box domain was proposed to have auto-inhibitory functions, implying that a conformational change occurs prior to substrate binding (Ma et al., 2008). A possible function of the DEXD/H box in duplex unwinding during small RNA loading to Argonaute proteins still awaits closer examination.

Apart from RNA duplex cleavage, Dicer also participates in the loading of Ago proteins and selection of the miRNA or guide strand, respectively. Just as Drosha, Dicer functions in tandem with a dsRBD protein. In *Drosophila*, the dsRBD partner of Dcr-1 in the miRNA pathway is an isoform of the protein Loquatious, Loqs-PB (Forstemann et al., 2005; Saito et al., 2005), while Dcr-2 associates with R2D2 in RISC assembly (Liu et al., 2003; Tomari et al., 2004b). Interestingly though, the endo-siRNA pathway in *Drosophila* appears to require the interaction of Dcr-2 with the Loquacious isoform Loqs-PD (Zhou et al., 2008; Hartig et al., 2009; Hartig and Forstemann, 2011). The human Dicer-associated dsRBD proteins TRBP and PACT reside independently in a complex with Ago2 and Dicer and depletion of either TRBP or PACT resulted in defects in miRNA processing and function (Chendrimada et al., 2005; Haase et al., 2005; Lee et al., 2006; Paroo et al., 2009). For TRBP, a function in strand selection from the RNA duplex intermediate has been proposed in analogy to R2D2. Guide strand selection in most cases depends on differences in the thermodynamic stability of the RNA duplex ends (Khvorova et al., 2003; Schwarz et al., 2003). In *Drosophila*, R2D2 binds to the more stable end of the duplex while Dicer associates with the opposing end (Liu et al., 2003; Tomari et al., 2004b). In a concerted process, the duplex is transferred to an Ago protein where the strand whose 5' end is less stably paired is preferentially incorporated into

the effector complex while the passenger strand is cleaved by Ago2 or removed by passive unwinding (Khvorova et al., 2003; Schwarz et al., 2003).

1.2.2. Argonaute proteins

Proteins of the Argonaute family are essential components of small RNA guided effector complexes. They are conserved throughout species; however, the number of encoded Argonaute proteins varies considerably (Hock and Meister, 2008). *Schizosaccharomyces pombe* possesses one Ago protein, as well as some species of the budding yeast (though not *Saccharomyces cerevisiae*). 10 Ago proteins were found in *Arabidopsis thaliana* and five in *Drosophila melanogaster*. *C. elegans* even encodes for 27 Argonaute proteins that mainly act in the secondary siRNA pathway.

In mice and humans, 8 Ago proteins were identified that can be further grouped into two subclasses. The human Ago subclass comprises 4 members, Ago1 through -4, and is expressed ubiquitously. The expression of the Piwi subclass members - HILI, HIWI, HIWI2 and HIWI3 in humans (Sasaki et al., 2003) - however, appears to be restricted to germ cells, where they associate with piRNAs. In *C. elegans*, a third subclass is constituted by the WAGO clade, whose members are loaded with secondary siRNAs resulting from RdRP synthesis through an unknown mechanism (Pak and Fire, 2007; Sijen et al., 2007; Tolia and Joshua-Tor, 2007; Hutvagner and Simard, 2008).

1.2.2.1. Structure of Argonaute proteins

Ago proteins contain four defined domains: An N-terminal domain and the highly conserved PAZ (Piwi-Argonaute-Zwille), MID and PIWI domains (Figure 5a). Crystallization attempts of complete Argonaute proteins from higher eukaryotes have not yet been successful, however, structural analysis of isolated domains and archaeal and bacterial Argonaute proteins have shed some light on the properties of the protein (Ma et al., 2004; Song et al., 2004; Parker et al., 2005; Yuan et al., 2005; Wang et al., 2008b; Wang et al., 2008c).

N-terminal and PAZ domains as well as MID and PIWI domains constitute a bilobal structure (Figure 5b). The PAZ domain was revealed to contain a specific binding pocket that anchors the characteristic 2nt 3' overhangs produced by RNase III cleavage during siRNA and miRNA biogenesis (Lingel et al., 2003; Song et al., 2003; Yan et al., 2003; Lingel et al., 2004; Ma et al., 2004). At the opposite end, the phosphorylated 5' terminal nucleotide of the small RNA is buried in a deep pocket within the MID domain, which also explains the minor importance of the 5' nucleotide for "seed" formation with the miRNA target. The two lobes

form a positively charged tunnel in which miRNA nucleotides 2-6 contact the Ago protein via their sugar-phosphate backbone. They fold into a semi-helical conformation that allows for hydrogen bonding of their bases with those of the target mRNA. Target binding is accompanied by a significant conformational change that moves the lobe containing N-terminal and PAZ domains away from MID and PIWI domain, thereby reaching a more open conformation (Wang et al., 2008b). The PIWI domain, finally, displays an RNase H fold and contains the catalytic center that – in the case of Ago2 - cleaves the target mRNA between nucleotides 10 and 11 of the guide RNA (Elbashir et al., 2001b; Haley and Zamore, 2004; Wang et al., 2008b; Wang et al., 2008c), producing a 5' RNA fragment with a 3' hydroxyl group and a 3' fragment with a 5' phosphate (Martinez and Tuschl, 2004; Schwarz et al., 2004).
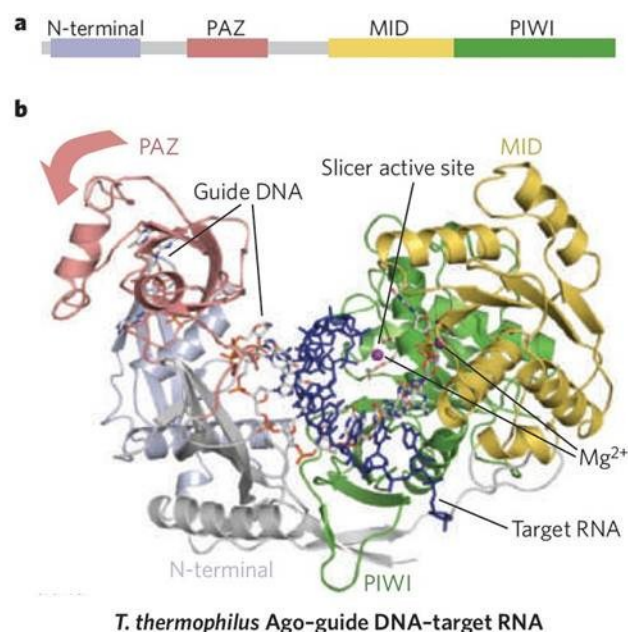
Figure 5: Argonaute protein structure.
(a) Schematic depiction of the Argonaute domain structure. **(b)** Crystal structure of *Thermus thermophilus* Ago in complex with a 5'-phosphorylated 21 nt guide DNA strand (grey backbone) and a 20 nt target RNA (blue). Structural rearrangements of the PAZ domain upon target binding are indicated by an arrow (modified from Jinek and Doudna, 2009).

The cleavage reaction requires Mg^{2+} ions and is ATP independent. Within the active center of human Ago2, the residues Asp_{597}, Asp_{669} and His_{807} have been identified as the catalytic triad (Song et al., 2004; Rivas et al., 2005). However, only one out of four human Ago proteins, Ago2, exhibits cleavage activity when binding to perfect or nearly perfect complementary targets (Liu et al., 2004; Meister et al., 2004). In Ago1 and Ago4, this catalytic inactivity can be attributed to a variation of the catalytic DDH triad towards a DDR or GDR motif, respectively. Strikingly though, Ago3 is cleavage incompetent despite the presence of the

DDH motif (Liu et al., 2004; Meister et al., 2004); while the reason for this behavior has not been clarified yet, it suggests that Ago activity might be controlled by posttranslational modifications or interaction with additional protein factors. However, as siRNA-induced target cleavage is a rather rare event in mammalian somatic cells, Ago cleavage (in)competence might simply reflect the major importance of miRNA-mediated repression.

In *Drosophila*, Ago1 and Ago2 differ in their preference to bind miRNAs or siRNAs, respectively (Forstemann et al., 2007; Tomari et al., 2007). Further, the terminal nucleotides of the guide strand play a role in Ago loading (Czech et al., 2009). Similar distinctions have also been reported in *C. elegans* (Steiner et al., 2007; Jannot et al., 2008). In contrast, mammalian Ago proteins do not show loading preferences and to a considerable degree appear to be functionally redundant (Meister et al., 2004; Yoda et al., 2010). Ago2, however, seems to take an exceptional position among members of the Ago subfamily due to its cleavage compentence. Effects of Ago2 knock-down on miRNA-mediated repression exceed those of depletion of the other Ago proteins (Schmitter et al., 2006). Further, it is essential for murine hematopoiesis (O'Carroll et al., 2007), presumably due to its role in Dicer-independent maturation of mammalian miR-451 (Cheloufi et al., 2010).

Furthermore, Argonaute function may be regulated by protein modifications. For Piwi proteins, dimethylarginine modifications catalyzed by the methyltransferase PRMT5 proved to be important for protein stability, localization and function (Kirino et al., 2009; Reuter et al., 2009; Vagin et al., 2009). Hydroxylation of human Ago2 in Pro_{700} appears to be of importance for protein stability (Qi et al., 2008). Phosphorylation of Ser_{387}, on the other hand, seems to be related to P body localization (Zeng et al., 2008). In contrast, phosphorylation of Tyr_{529} in the 5' binding pocket of the MID domain can interfere with small RNA binding and may play a role in Ago loading (Rudel et al., 2010).

1.2.2.2. Argonaute loading

During RISC or miRNP formation, Ago proteins are loaded with the small RNA duplex intermediate that results from Dicer processing in a concerted process that requires ATP (Nykanen et al., 2001; Pham et al., 2004; Yoda et al., 2010). In several organisms, Argonaute proteins were recently reported to interact with the heat shock protein HSP90 or a chaperone complex involving the heat shock cognate 70 (HSC70) as well as HSP90 during this process (Iki et al., 2010; Iwasaki et al., 2010; Johnston et al., 2010; Miyoshi et al., 2010). This resulted in a model proposing that binding of the chaperone complex might bring the Ago protein into an "open" conformation that allows for loading of a small RNA duplex. Upon ATP hydrolysis and subsequent dissociation of the chaperone complex, the miRNA* or passenger strand is discarded or cleaved, respectively, rendering the RISC/miRNP complex

active. The removal of the miRNA* strand seems to be achieved by a passive, ATP-independent unwinding process, possibly facilitated by the mismatches within the miR/miR* duplex resulting in the degradation of the miRNA* upon its release (Forstemann et al., 2007; Kawamata et al., 2009; Yoda et al., 2010). Another theory proposes the involvement of a yet unknown RNA helicase in the unwinding process.

The minimal complex required for RISC cleavage is composed of Ago2 in concert with a single-stranded RNA (Rivas et al., 2005). For loading with an RNA duplex, a trimeric RISC complex comprising Ago2, Dicer and its dsRBD partner TRBP (or R2D2 in *Drosophila*) is required, constituting a trimeric RISC complex (Gregory et al., 2005; Maniataki and Mourelatos, 2005). Still, efficient incorporation and RISC activity presumably involves a number of additional proteins. For example, the *Drosophila* RNA helicase Armitage and its human homologue MOV10 were implicated in siRNA function though their specific modes of action remain elusive (Tomari et al., 2004a; Meister et al., 2005; Klattenhoff et al., 2007). Moreover, the endoribonuclease C3PO enhanced RISC activity in flies by removing siRNA passenger strand fragments (Liu et al., 2009). A homologous factor in mammals, however, has not yet been described.

1.2.2.3. Argonaute localization to processing bodies

Cytoplasmic localization studies demonstrated Ago proteins to accumulate in distinct cytoplasmic foci called processing bodies (P bodies). These structures seem to be involved in storage and degradation of translationally repressed mRNAs (Eulalio et al., 2007a; Parker and Sheth, 2007). According to their integral protein component GW182, P bodies are sometimes also referred to as GW bodies. GW182 belongs to the TNRC6 (trinucleotide repeat containing 6) protein family which comprises three members in the mammalian system: TNRC6A (GW182), TNRC6B and TNRC6C. For Ago function in translation inhibition and deadenylation, its interaction with the GW182 protein family is crucial (Eulalio et al., 2009c).

GW182 possesses several N-terminal glycine-tryptophan (GW) repeats, a ubiquitin-associated domain (UBA) and a glutamine (Q)-rich domain. These domains are required for localization GW182 to P bodies (Behm-Ansmant et al., 2006). Further, GW182 contains a Domain of Unknown Function (DUF) and a C-terminal RNA recognition motif (RRM). It binds to the Ago PIWI domain via its N-terminal GW repeats and interacts with the poly(A)-binding protein (PABP) via its DUF (Figure 6, Till et al., 2007; Eulalio et al., 2009a).
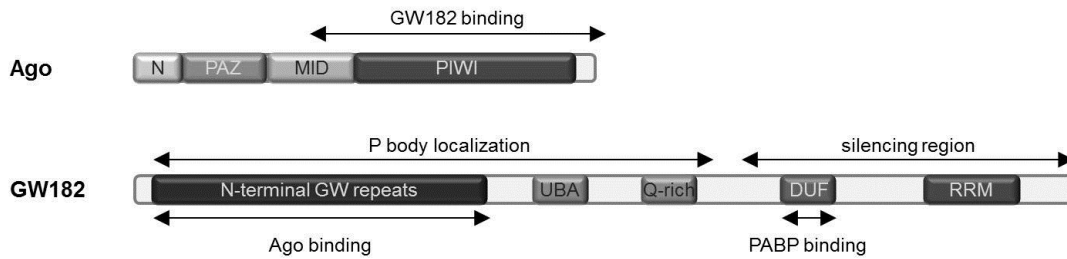
Figure 6: Schematic depiction of Ago and GW182.
Regions relevant for mutual interaction as well as functional regions of GW182 are denoted by arrows. UBA: ubiquitin-associated domain, DUF: domain of unknown function, RRM: RNA recognition motif (modified from (Fabian et al., 2010).

The repressive function of GW182 is mediated by the C-terminus containing the DUF and an RNA recognition motif (RRM) domain that, together with its adjacent regions, acts in protein rather than RNA binding (Eulalio et al., 2009b; Fabian et al., 2010). GW182 is the actual effector of miRNA-mediated posttranscriptional gene silencing (Behm-Ansmant et al., 2006). Ago proteins located on 3'-UTR miRNA-binding sites act in recruiting GW182 which in turn through its interaction with PABP can disrupt translation initiation and/or recruit the deadenylase complex. When GW182 is tethered to the 3'-UTR of an mRNA, repression can even take place independently of Ago binding (Baillat and Shiekhattar, 2009; Zipprich et al., 2009).

P bodies are highly enriched in translationally repressed mRNAs as well as in proteins involved in mRNA deadenylation, decapping and degradation, e.g. the DCP1-DCP2 complex, the exonuclease Xrn1 and the Lsm protein family (Eulalio et al., 2007a; Parker and Sheth, 2007). Ribosomes and the majority of translation initiation factors, however, were not found in P bodies. P bodies are highly dynamic structures and can adjust in number and size according, for example, to the translational status of the cell or to the stage of the cell cycle (Lian et al., 2006; Pauley et al., 2006; Eulalio et al., 2007a; Eulalio et al., 2007b; Parker and Sheth, 2007). Still, they are not essential for miRNA-mediated repression itself but rather seem to occur as a consequence of this process. Depletion of GW182 or other proteins involved in the miRNA pathway disrupts visible P bodies. However, submicroscopic complexes of P body components may persist and facilitate miRNA function (Pauley et al., 2006; Eulalio et al., 2007b). Together with the observation that many P body components are also present in the cytosol (Eulalio et al., 2007a), this suggests that miRNA-mediated repression starts in the cytosol and repressed mRNAs are subsequently transported to P bodies where they may be either stored in a translationally blocked state or be subjected to degradation. However, translation repression and P body localization is not an irreversible process, as repressed mRNAs may be released from P bodies upon cellular signals and resume translation (Bhattacharyya et al., 2006a).

1.3. THE RNA BINDING PROTEIN RBM4

The RNA binding protein RBM4 - in *Drosophila* and mice termed LARK - is an evolutionarily highly conserved protein. In humans, two highly related copies of RBM4, RBM4a and RBM4b, are present on chromosome 11q13.2; however, only RBM4a has been investigated to date and will subsequently be referred to as RBM4 in this work. The human RBM4 protein is about 40 kDa in size and carries two N-terminal RNA recognition motifs (RRMs) and a CCHC-type zinc finger domain (Figure 7). The C-terminal part of the protein contains three alanine-rich stretches and has been shown to be involved in protein-protein interaction as well as correct nuclear localization (Lai et al., 2003; Markus and Morris, 2006).
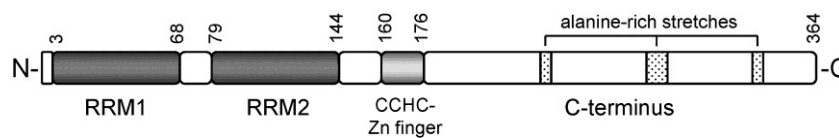
Figure 7: Schematic depiction of the RBM4 protein.
RRM1 and -2: RNA recognition motifs (taken from Markus and Morris, 2009).

LARK was first identified in a genetic screen for mutations that perturb the circadian regulation of *Drosophila* adult eclosion (Newby and Jackson, 1993). It is an essential factor in *Drosophila* embryogenesis and both maternal and zygotic LARK expression are required for normal development (Newby and Jackson, 1993, 1996; McNeil et al., 1999). LARK abundance oscillates in a circadian manner in flies as well as in the mammalian system and protein levels of murine LARK (mLARK) where shown to be related to the length of circadian periods in cycling cells (McNeil et al., 1998; Kojima et al., 2007). mLARK further was demonstrated to bind to the 3'-UTR of the Period1 (Per1) mRNA and to regulate its expression. Per1 is an essential factor for maintenance of circadian rhythms, itself possessing a rhythmic transcription coupled to delayed protein expression. This posttranscriptional regulation strengthens the functional relevance of mLARK in the circadian system. Another function of *Drosophila* LARK was described by Sofola and colleagues (Sofola et al., 2008). LARK was shown to bind and stabilize dFMR and to collectively regulate eye development and circadian behavior in adult flies.

Human RBM4 has been described as a ubiquitously expressed nucleocytoplasmic shuttling protein with a predominantly nuclear localization to speckles and regulatory functions in pre-mRNA splicing and 5' splice site and exon selection (Lai et al., 2003; Kar et al., 2006). Exemplary, RBM4 was presented to activate the selection of skeletal muscle-specific exons in the α-tropomyosin pre-mRNA by antagonizing the splicing regulator PTB (pyrimidine tract binding protein) through binding to intronic pyrimidine-rich elements (Lin and Tarn, 2005). In alternative splicing, RBM4 function was further demonstrated to be affected by a specific

isoform of Wilms tumor protein 1 (WT1), an RNA-binding post-transcriptional regulator that interacts with splicing components (Markus et al., 2006). This points towards a more complex interplay of RNA processing factors in the modulation of alternative splicing.
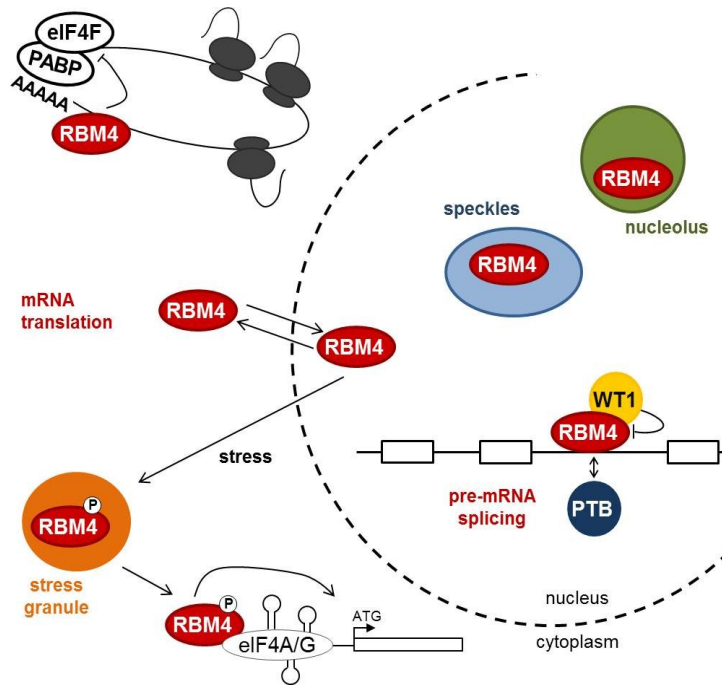
Figure 8: Known cellular functions of RBM4.
RBM4 is a nucleocytoplasmic shuttling protein with nuclear concentration in speckles and nucleoli. Its functions range from splicing regulation to cytoplasmic translation control, suppressing cap-dependent translation and, upon cellular stress, activating IRES-dependent translation (modified from Markus and Morris, 2009).

Apart from interfering with splicing of pre-mRNAs, RBM4 has also been implied in translational control. As mentioned before, RBM4 regulates expression of murine Per1 in a Cap/poly(A)-dependent manner (Kojima et al., 2007). The aforementioned interaction of *Drosophila* LARK with dFMR (Sofola et al., 2008), an established translational regulator, may also imply a participation of RBM4 in translational control. Further, phosphorylated RBM4 was shown to translocate to the cytoplasm and cytoplasmic stress granules and to inhibit translation of cap-dependent mRNAs under cellular stress conditions, while concomitantly facilitating IRES-mediated translation (Lin et al., 2007). Activation of internal ribosome entry sites (IRES) is presumably mediated by stabilizing eIF4A-containing initiation complexes. RBM4 therefore exhibits a complex functional pattern within numerous cellular processes (Figure 8).

1.4. AIM OF THE THESIS

In recent years, small inhibitory RNAs have emerged as key players in a large number of cellular events including transcriptional and post-transcriptional regulation. Argonaute proteins act as binding partners of small RNAs and their significance as effectors of small RNA-mediated silencing is undisputed. However, to allow for the large variety of observed small RNA functions, effector complexes are bound to include various additional factors that allow for specific regulation of individual events.

Therefore, the aim of this work was to characterize Ago1- and Ago2-containing protein complexes by investigating their sedimentation behavior in sucrose gradients, their mRNA- as well as miRNA content and their catalytic activities. Further, Ago-associated proteins were to be identified in a comprehensive approach to acquire an overview on the protein network involved in small RNA function. The thereby established protein interactions were to be verified by various experimental approaches. Finally, this work attempted to demonstrate the functional relevance of Ago-interacting proteins in miRNA-mediated regulation of target mRNAs.

2. RESULTS

2.1. ANALYSIS OF ARGONAUTE CONTAINING mRNA-PROTEIN COMPLEXES

2.1.1. Human Ago1 and Ago2 form distinct protein complexes

Previously, it has been demonstrated that mammalian Ago proteins and miRNAs sediment with polyribosomes (Kim et al., 2004; Nelson et al., 2004; Maroney et al., 2006; Nottrott et al., 2006). In other studies, however, the majority of Ago proteins and miRNAs migrate together with untranslated ribonucleoproteins (mRNPs; Kim et al., 2004; Nelson et al., 2004). For a detailed characterization of Ago protein complexes, Ago sedimentation in polyribosome fractionations was revisited (Figure 9A). Extracts from human embryonic kidney (HEK) 293 cells were separated on a sucrose gradient ranging from 0.5 M to 1.5 M sucrose. Fractions were analyzed by western blotting against the ribosomal protein S6 (rpS6) to identify ribosome-containing fractions. RpS6 was detected in fractions 10-12, representing ribosomal subunits as well as monosomes, and in fractions 14-27, indicating polyribosomes. Probing with antibodies against Ago1 showed that human Ago1 predominantly migrated in fractions with low sucrose density corresponding to mRNPs and to some extent also with monosomes. Only a small portion of Ago1 was found in higher molecular weight fractions also containing polyribosomes (fractions 14-27).

For a closer analysis of Ago-containing mRNPs, lysis buffer as well as gradient conditions were modified to allow for further separation of the mRNP pool (Figure 9B). Due to the presence of EDTA in the buffer, polyribosomes were not preserved in these experiments. HEK 293 lysate was loaded onto a 15-55 % sucrose gradient and fractionated by centrifugation for 18 h. To roughly estimate the size range of Ago protein complexes, marker proteins of known size were separated by gradient centrifugation under the same conditions and visualized by coomassie staining. Western blotting using α-Ago1 and α-Ago2 antibodies showed that both Ago1 and Ago2 sedimented in three distinct complexes which are furthermore referred to as Ago complexes I-III. A large portion of Ago1 or Ago2 was found in complex I, which has a molecular mass of about 250-350 kDa (lanes 2-7). Complex II constitutes a second prominent peak, which sediments similarly to a 19 S particle and is about 600-700 kDa in size (lanes 10-13). Complex III peaks in fractions 15 and 16 indicative of a molecular mass of more than 900 kDa or 25-30 S (lanes 15-16).
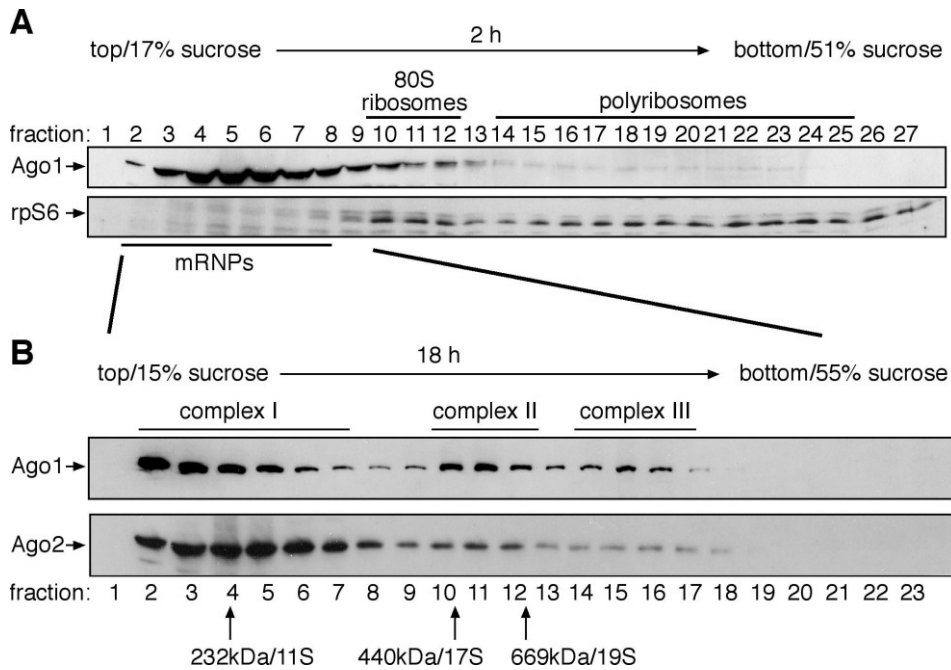
Figure 9: Association of human Ago1 and Ago2 with distinct protein complexes
(A) Individual fractions of polyribosome gradients were analyzed by western blotting against endogenous Ago1 (upper panel) and rpS6 (lower panel). (B) Lysates from wild-type HEK 293 cells were separated by sucrose density centrifugation under conditions that allow for separation of mRNPs. Endogenous Ago1 and Ago2 were analyzed using specific antibodies.

The migration of Ago proteins with mRNPs in polyribosome gradients implied that Ago complexes I-III contain mRNAs and form mRNPs. To assay this, HEK 293 cell lysates were subjected to RNase A treatment prior to separation by gradient centrifugation. Ago1 complexes II and III were clearly visible in untreated lysates (Figure 10, upper panel), but not in RNase-treated extracts (lower panel), indicating that complexes II and III indeed constitute RNA-containing protein complexes.
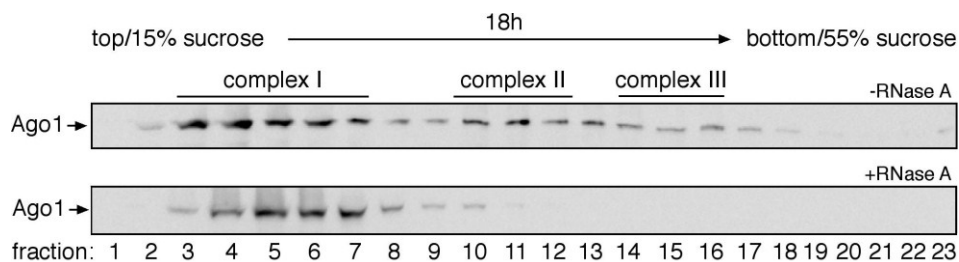
Figure 10: RNase sensitivity of Ago complexes II and III
Lysates from wild-type HEK 293 cells were separated by sucrose gradient centrifugation as in (9B) and analyzed for endogenous Ago1. Lysates shown in the lower panel were treated with 100 µg/ml RNase A prior to centrifugation.

For further evaluation of the aforementioned experiments, it was necessary to use tagged Ago proteins. Therefore, HEK 293 cells were transiently transfected with FLAG/haemagglutinin (HA)-tagged Ago1 through -4 and lysates were subjected to gradient

27

centrifugation as before. Subsequent western blotting against the HA-tag produced a distinct complex pattern similar to that of endogenous Ago1 and -2 (Figure 11). Individual gradient fractions were subjected to western blotting using antibodies against the HA-tag. All four FLAG/HA-tagged Ago proteins yielded three complexes in lanes 3-8 (complex I), lanes 11-13 (complex II) and lanes 15-17 (complex III), indicating that the tagged proteins associated with native protein complexes and were suitable for further analysis.
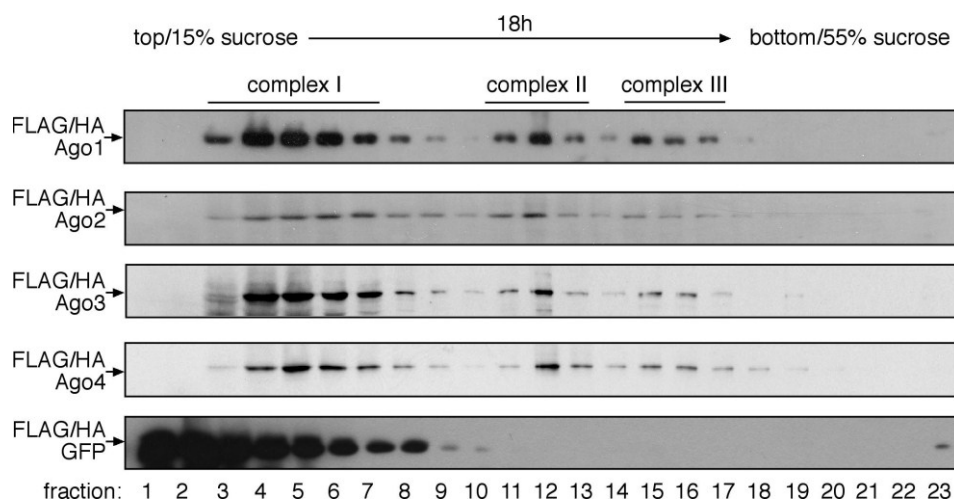
Figure 11: Protein distribution of FLAG/HA-Ago1-4 on sucrose gradients
Lysates from HEK 293 cells transiently transfected with FLAG/HA-Ago1-4 were separated by sucrose gradient centrifugation as in **(9B)**. The presence of FLAG/HA-Ago1-4 was analyzed by western blotting using α-HA antibodies.

As a control, HEK 293 cells were transfected with FLAG/HA-tagged green fluorescent protein (GFP). Separation of FLAG/HA-GFP lysates yielded strong signals in the low density fractions, whereas no protein was shifted to the higher fractions corresponding to complexes II and III.

In summary, endogenous as well as ectopically expressed Ago1 through -4 could be separated into three distinct complexes by gradient centrifugation. The smallest complex, complex I, appeared to be resistant to RNase treatment while complexes II and III were dependent on RNA.

2.1.2. Ago distribution in nuclear and cytoplasmic extracts

It has been shown that Ago proteins can be found in the nucleus as well as the cytoplasm of human cells (Meister et al., 2004; Robb et al., 2005; Janowski et al., 2006; Rudel et al., 2008). To further characterize the observed Ago protein complexes, nuclear and cytoplasmic extracts were prepared from HEK 293 cells.
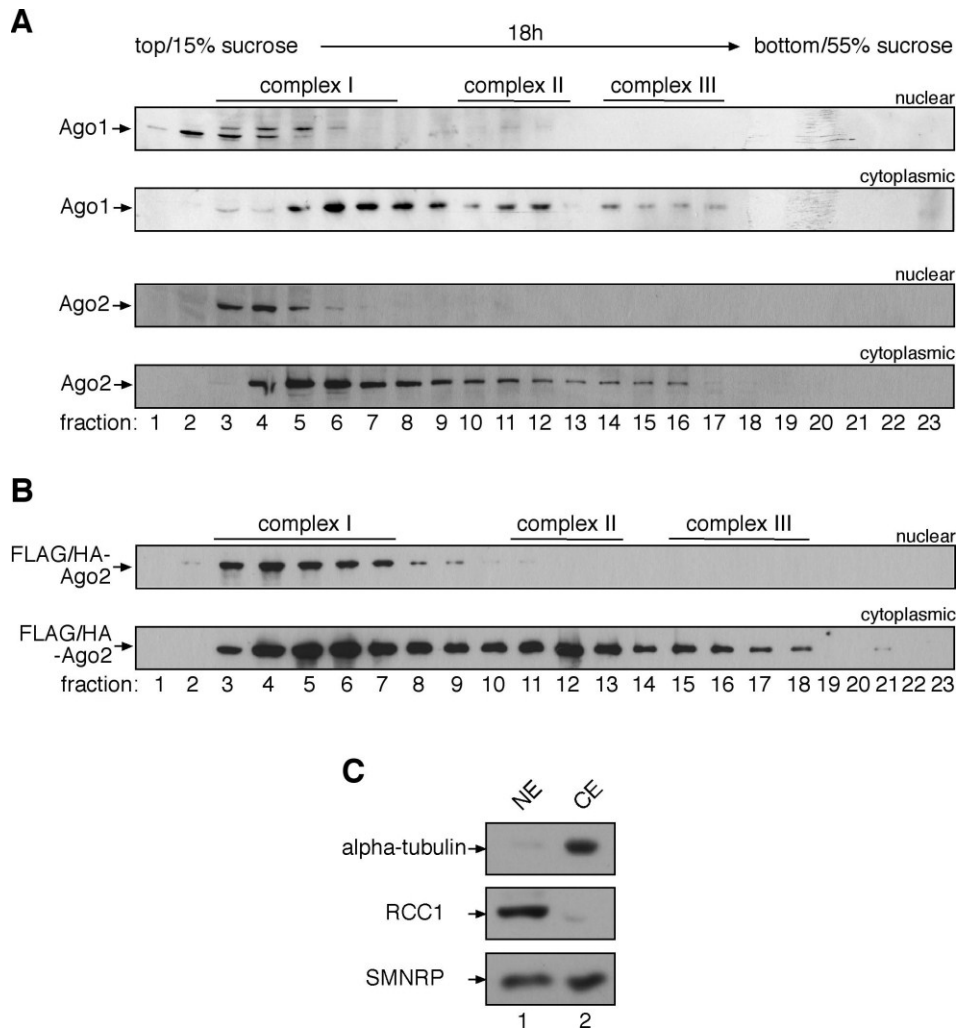
Figure 12: Distribution of endogenous Ago1 and -2 in nuclear and cytoplasmic fractions
(A) Nuclear and cytoplasmic extracts from HEK 293 cells were subjected to gradient centrifugation as described in **(9B)**. Fractions were analyzed by western blotting for endogenous Ago1 (upper panels) and Ago2 (lower panels). **(B)** Nuclear and cytoplasmic gradients from HEK 293 lysates containing FLAG/HA-Ago2 were analyzed by western blotting using α-HA antibodies. **(C)** Nuclear (NE) and cytoplasmic (CE) extracts from **(A)** before gradient centrifugation were analyzed for alpha-tubulin (upper panel), RCC1 (middle panel) and SMNRP (lower panel) by western blotting.

Gradient centrifugation and subsequent western blotting showed that endogenous Ago1 and Ago2 from nuclear extracts is restricted to low density fractions (Figure 12A, lanes 2-5). Cytoplasmic extracts also show signals in higher fractions corresponding to complexes II and III. Notably, in the cytoplasmic complex I, Ago1 and Ago2 signals were shifted slightly towards higher fractions so that nuclear and cytoplasmic signals (lanes 2-5 and lanes 5-9, respectively) only partially overlapped.

Transient overexpression of FLAG/HA-Ago2 yielded similar results: FLAG/HA-Ago2 was present only in the nuclear fractions corresponding to complex I, while it was detectable in all three complexes in cytoplasmic extracts (Figure 12B). A clear shift of the nuclear signals to lower molecular weight was not detectable with these samples; however, this could be due to FLAG/HA-Ago2 overexpression.

As a control for successful extract preparation, nuclear (NE) and cytoplasmic (CE) extracts were subjected to western blotting using antibodies against alpha-tubulin, RCC1, and SMNRP (Figure 12C). As expected, alpha-tubulin could be detected in cytoplasmic, but not in nuclear extracts. RCC1, a chromatin-bound nuclear protein, was restricted to nuclear extracts. The nucleoplasmic protein SMNRP, which is not tightly associated with nuclear structures, could be detected in both nuclear and cytoplasmic extracts. Therefore, even though the separation of nuclear and cytoplasmic extracts was not complete, nuclear extracts are not contaminated by cytoplasmic proteins and the results concerning nuclear Ago gradient migration can be regarded as reliable.

2.1.3. Ago complexes I-III associate with miRNAs

As Ago proteins are the binding partners of mature miRNAs, Ago complexes were also analyzed for their miRNA content. HEK 293 lysates containing FLAG/HA-Ago1 or FLAG/HA-Ago2 were separated by gradient centrifugation. Proteins were immunoprecipitated from individual fractions using FLAG-antibodies and associated RNA was extracted, reverse transcribed and analyzed by semi-quantitative PCR for miR-16 or let-7a, respectively. Both miR-16 and let-7a were found in all Ago-containing fractions, whereas only weak signals were found in other fractions (Figure 13A).

MiRNA distribution was also analyzed by northern blotting. HEK 293 cells were transiently transfected with FLAG/HA-Ago1, -Ago2 or -GFP. Lysates were subjected to gradient centrifugation and complex fractions were pooled. FLAG/HA-tagged proteins were immunoprecipitated from the pooled fractions, RNA was extracted and northern blotting for miR-19b, a miRNA abundant in HEK 293 cells, was performed. MiRNA-19b signals could be detected in all three complexes of FLAG/HA-Ago1 and -Ago2 in amounts that roughly corresponded to the protein abundance in the respective complexes visualized by western blotting against the HA-tag (Figure 13B). As expected, co-immunoprecipitation of miR-19b with FLAG/HA-GFP could not be detected despite the high protein expression level.

Taken together, miRNAs could be shown to specifically associate with all three Ago complexes. MiRNA levels visualized by northern blotting correlated with Ago protein levels.

30
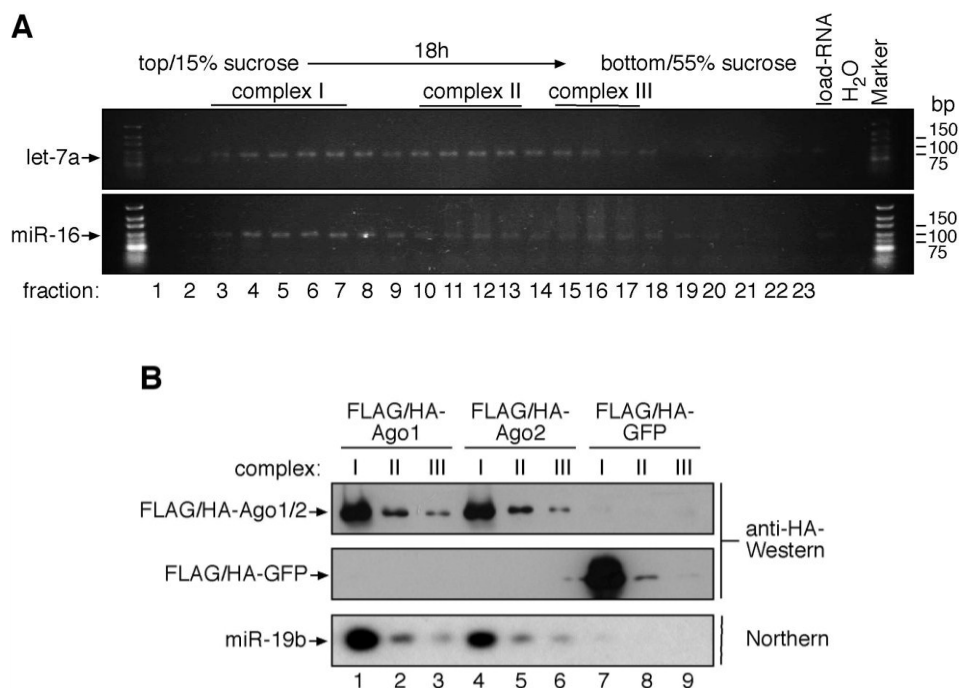
Figure 13: Distribution of miRNAs on FLAG/HA-Ago1 and -2 gradients
(A) Lysates from HEK 293 cells expressing FLAG/HA-Ago1 or -Ago2 were separated as in **(9B)**. Individual fractions were subjected to immunoprecipitation using α-FLAG antibodies. RNA was extracted and the presence of endogenous let-7a (upper panel, FLAG/HA-Ago1-IP) and miR-16 (lower panel, FLAG/HA-Ago2-IP) was determined using semi-quantitative RT-PCR. **(B)** Sucrose gradient centrifugation was performed as described in **(9B)** using lysates from HEK 293 cells containing FLAG/HA-Ago1, -2 and -GFP. Fractions corresponding to complexes I to III were pooled individually and immunoprecipitation was performed using FLAG agarose. Co-precipitated miR-19b was analyzed by northern blotting (lowest panel). 20 % of the beads were used for western blotting against the HA-tag (upper and middle panel).

2.1.4. Ago complex III co-sediments with the KRAS mRNA

Small RNA effector complexes exert their regulatory functions by binding to target mRNAs. As RNase treatment of cell lysates prior to gradient centrifugation had eliminated complexes II and III, it was tempting to speculate that these complexes contain translationally repressed mRNAs. To address this, gradient samples were analyzed for their association with a known miRNA target mRNA. HeLa cells were transiently transfected with a luciferase reporter construct carrying the 3'-untranslated region (3'-UTR) of the Kirsten rat sarcoma viral oncogene homologue (KRAS). KRAS has been shown to be translationally regulated by let-7a in human cells (Johnson et al., 2005). Cell lysates were separated on a 15-55 % sucrose gradient, RNA was extracted from individual fractions, reverse transcribed and analyzed by quantitative PCR (qPCR). While KRAS mRNA was absent from the fractions corresponding to Ago complex I, fractions 10-13 (complex II) contained small amounts of the target mRNA (Figure 14). Strikingly, high amounts of KRAS mRNA co-sedimented with Ago complex III, suggesting that this complex forms large mRNPs with miRNA target mRNAs.
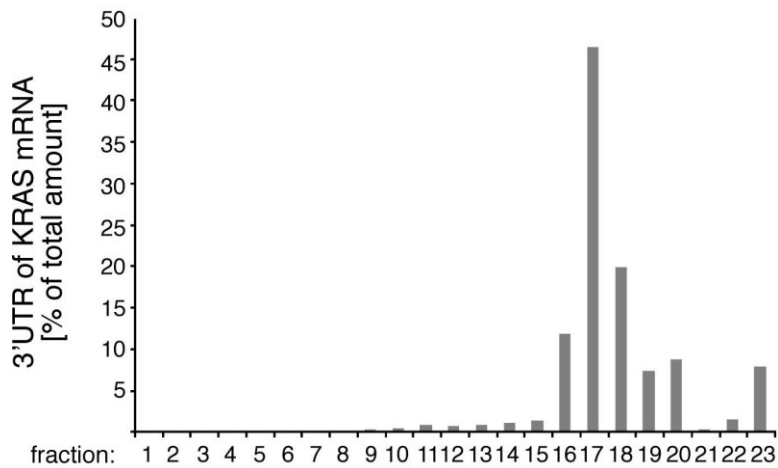
Figure 14: KRAS 3'-UTR distribution in HEK 293 gradients
A reporter construct containing the KRAS 3'-UTR was transfected into HEK 293 cells and lysates were separated as in **(9B)**. Total RNA was extracted from the individual fractions and analyzed by qPCR. The distribution of the KRAS 3'-UTR is shown as a percentage of the total amount of the KRAS reporter construct.

2.1.5. Analysis of Ago-associated RISC and Dicer activity

Ago2 has been shown to be the endonucleolytic component of the human RNA induced silencing complex (RISC; Liu et al., 2004; Meister et al., 2004). Therefore, the observed Ago2 complexes were tested for association with RISC activity.
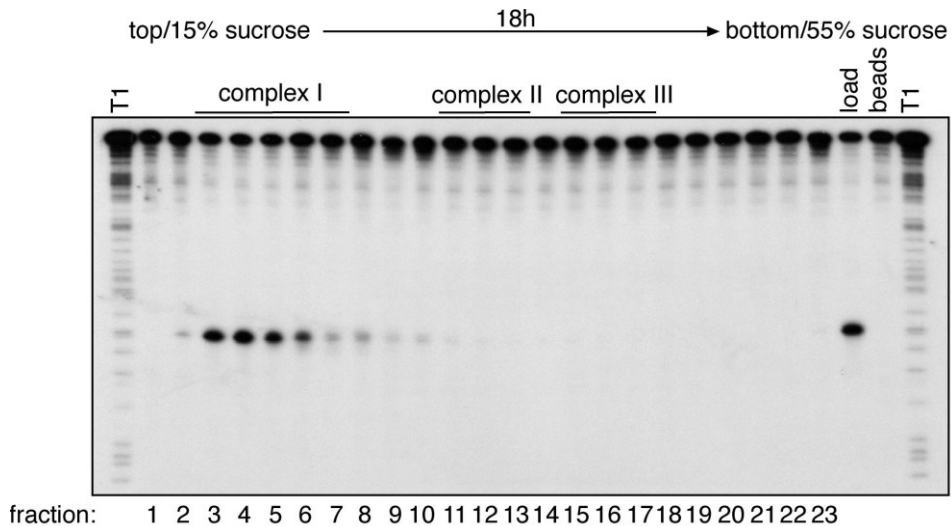
Figure 15: RISC assay analysis of FLAG/HA-Ago2 gradient fractions
Lysates from FLAG/HA-Ago2 transfected HEK 293 cells were separated as in **(9B)** and subjected to immunoprecipitation using FLAG agarose. Immunoprecipitates were incubated with a ^{32}P-cap-labeled RNA, which contained a perfect complementary sequence to the endogenous miR-19b. Lanes indicated with T1 show RNase T1 digestions of the RNA substrate. The RNA sequence complementary to miR-19b is indicated by a black bar to the right.

Lysate from HEK 293 cells transfected with FLAG/HA-Ago2 was fractionated by gradient centrifugation and FLAG/HA-Ago2 complexes were immunoprecipitated from individual fractions using FLAG antibodies. Immunoprecipitates were incubated with a ^{32}P-cap labeled RNA complementary to miR-19b (Figure 15). Fractions 3-6, as well as the total lysate prior to gradient centrifugation (load), showed strong cleavage activity, whereas no cleavage was observed in higher molecular weight fractions, indicating that Ago2 complex I represents active human RISC.

It has been demonstrated that human Ago proteins stably associate with Dicer and that this complex is able to generate small RNAs from double-stranded RNA (dsRNA) precursors (Gregory et al., 2005; Meister et al., 2005). Hence, individual Ago complexes were also tested for Dicer activity. HEK 293 lysates containing FLAG/HA-Ago1 were fractionated and immunoprecipitated as described above. Immunoprecipitates were incubated with an internally ^{32}P-labeled primary miR-27a precursor and accumulation of mature miR-27a was analyzed by denaturing RNA polyacrylamide gel electrophoresis (RNA-PAGE; Figure 16A). Ago1 complex I (fractions 3-7) as well as Ago1 complex III (fractions 15-17) was associated with Dicer activity, whereas only very weak Dicer activity was observed in Ago1 complex II (fractions 10-13). Similar results were obtained when using FLAG/HA-Ago2 lysates (data not shown).
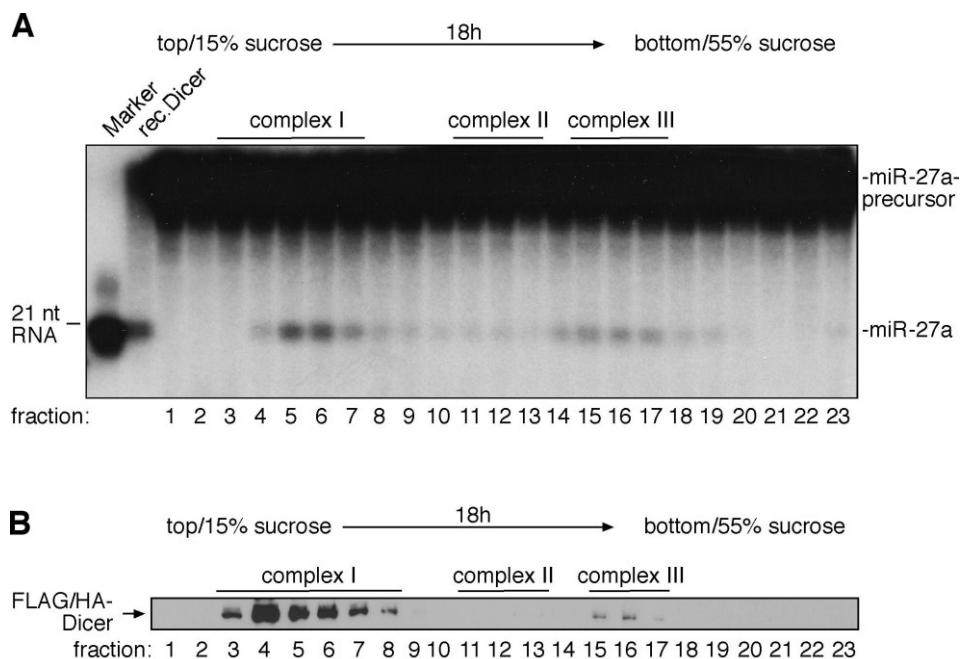
Figure 16: Analysis of Dicer activity and distribution on sucrose gradients
(A) FLAG/HA-Ago1 containing HEK 293 lysate was separated and immunoprecipitated as in **(15)**. The immunoprecipitates or recombinant Dicer were incubated with an internally ^{32}P-labeled pri-miR-27a substrate. A 21-nucleotide marker is shown to the left. **(B)** Lysates from HEK 293 cells expressing FLAG/HA-Dicer were separated as in **(9B)**. Fractions were analyzed for FLAG/HA-Dicer by western blotting using α-HA antibodies.

This was also consistent with results from a gradient fractionation of HEK 293 lysate containing FLAG/HA-Dicer (Figure 16B). Western blot analysis using antibodies against the HA-tag showed a strong Dicer signal in complex I as well as a weaker signal in complex III. In complex II, however, Dicer could not be detected.

To exclude that the observed pattern of RISC and Dicer activity was mainly due to the Ago protein abundance in the respective complexes, both experiments were repeated with adjusted Ago protein levels (Figure 17). Lysate from FLAG/HA-Ago2 containing HEK 293 cells was separated by gradient centrifugation, the fractions of each complex were pooled and Ago2 levels in the pooled fractions were estimated by western blotting. The volumes of the pooled complexes used for immunoprecipitation were adjusted to give approximately equal Ago2 levels in all three samples. As a control, fractions 20-23 were pooled and a volume equal to that of complex III was used. RISC and Dicer assays were performed as described above.
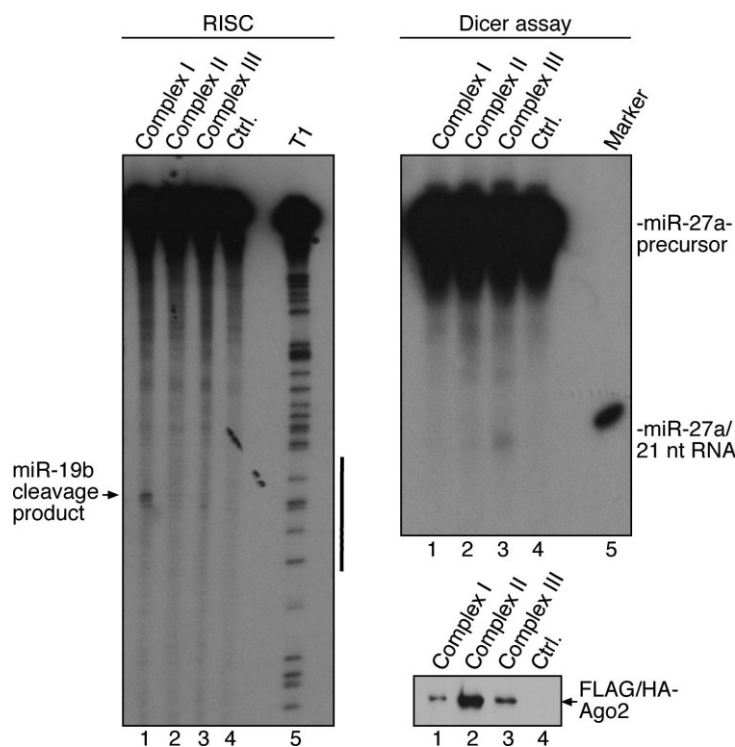
Figure 17: RISC and Dicer assays with adjusted Ago2 levels in pooled complex fractions
FLAG/HA-Ago2 containing HEK 293 lysates were separated as in **(9B)**. Fractions corresponding to complex I (fractions 3-6), complex II (fractions 11-13), complex III (fractions 15-17) and fractions 20-23 (as a control) were pooled. To adjust for equal Ago2 amounts, different volumes from pooled complex fractions were subjected to immunoprecipitation using α-FLAG antibodies. The volume of the control fraction equaled the pooled complex III sample volume. Subsequently, RISC (left panel) and Dicer (upper right panel) assays were performed as described in **(15)** and **(16A)**. FLAG/HA-Ago2 levels were checked by western blotting using α-HA antibodies (lower right panel). The RNA sequence complementary to miR-19b is indicated by a black bar to the right (left panel).

Though FLAG/HA-Ago2 levels in the adjusted samples proved not to be as equal as intended (Figure 17, lower right panel), Ago2 levels in complexes II and III were considerably higher than in complex I and therefore, samples should be suitable for the indented experiment. Indeed, RISC activity could only be detected in complex I while higher molecular weight complexes were not cleavage competent (left panel). Also, even with high FLAG/HA-Ago2 levels in the complex II sample, Dicer activity could not be detected (upper right panel). Therefore, the RISC and Dicer activity pattern observed in Figure 15 and Figure 16 cannot simply be attributed to Ago protein abundance in the samples, but is specific to the distinct Ago complexes.

Taken together, these experiments demonstrate that the identified Ago complexes I-III contain distinct enzymatic activities. Ago2 complex I contains a low molecular weight RISC whereas Ago complexes I and III are associated with Dicer. Interestingly, Ago complex II does not contain RISC and shows only little detectable Dicer activity.

2.2. ARGONAUTE PROTEINS AND THEIR INTERACTION PARTNERS

2.2.1. Proteomic analysis of Ago complexes I-III

In order to identify co-factors that function together with Ago1 and Ago2, the protein composition of Ago complexes I-III was analyzed using a proteomic approach. FLAG/HA-Ago1 or FLAG/HA-Ago2 was transiently expressed in HEK 293 cells, and the lysates were separated by sucrose gradient centrifugation. Fractions 3-8, 10-13 and 15-18, representing Ago complexes I, II and III, respectively, were combined and Ago complexes were immunoprecipitated using FLAG antibodies.

While in a previous study the investigation of Ago-associated proteins had been restricted to only a few visible gel bands (Meister et al., 2005), the aim was now to analyze all proteins that were present in the Ago immunoprecipitates. Therefore, co-immunoprecipitated proteins were separated by SDS-PAGE and analyzed by mass spectrometry (Figure 18A). Antibodies not specific for the FLAG-tag were used for control purifications (Figure 18B).
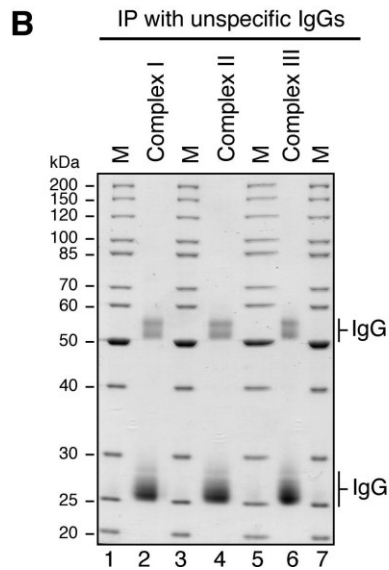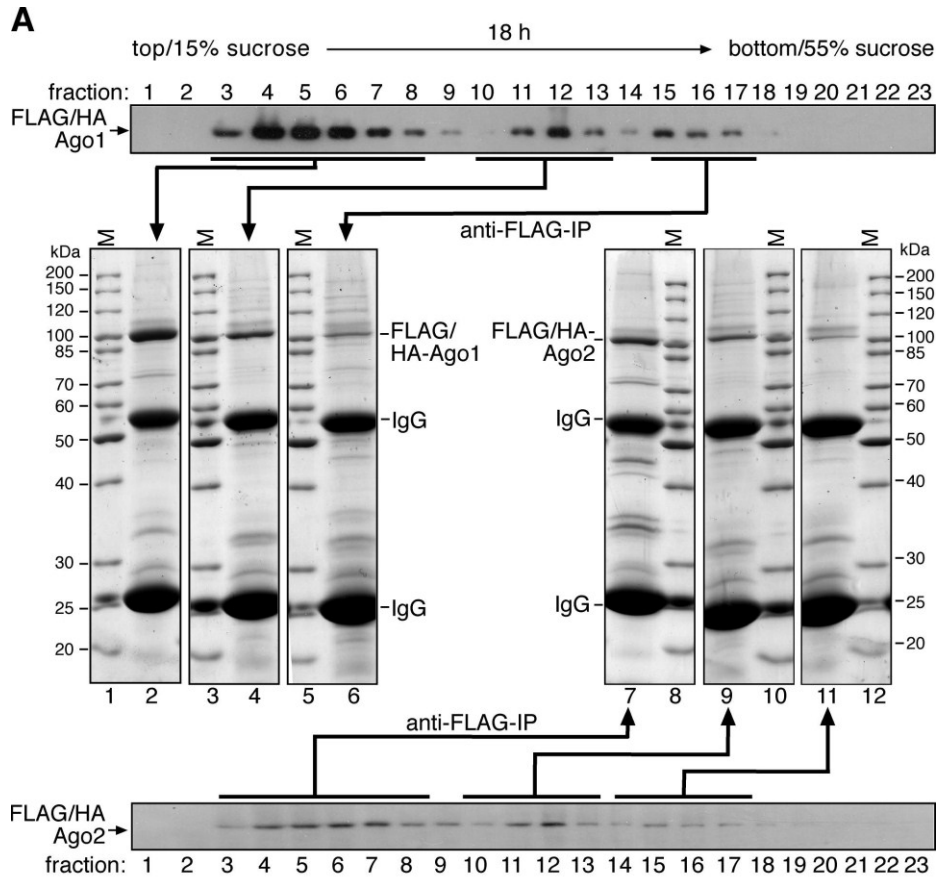
Figure 18: Proteomic analysis of Ago complexes I, II and III.
(A) Lysates from HEK 293 cells containing FLAG/HA-Ago1 or -Ago2 were separated on 15-55 % sucrose gradients. Fractions 3-8 (complex I), 11-13 (complex II) and 15-17 (complex III) were pooled and subjected to immunoprecipitation using α-FLAG antibodies. Immunoprecipitated FLAG/HA-Ago1 complexes (lanes 2, 4 and 6) or FLAG/HA-Ago2 complexes (lanes 7, 9 and 11) were separated by SDS-PAGE and proteins were analyzed by ESI TOF mass spectrometry. Lanes 1, 3, 5, 8, 10 and 12 show molecular weight markers (M). IgG as well as FLAG/HA-Ago1 and -Ago2 bands are indicated. **(B)** FLAG/HA-Ago2 gradient fractions were pooled as in **(A)** and immunoprecipitated using agarose coupled mouse IgG as control antibody. Proteomic analysis was performed as in **(A)**. Lanes 2, 4 and 6 show immunoprecipitates from Ago complexes I, II and III, respectively. IgG bands are denoted to the right. Lanes 1, 3, 5 and 7 show molecular weight markers.

Table 1 shows a list of proteins that were specifically found in Ago samples, but not in control purifications (see also the supplementary tables in the appendix for a more detailed listing).

Table 1: Proteins associated with human Ago1 and Ago2

Name	Domains/motif	Ago1 complex	Ago2 complex	Accession No.
Proteins involved in gene silencing				
Dicer	DEAD box, RNase III, PAZ, dsRBD, DUF	I, III	I, III*	gi|21665773/gi|5019620
TNRC6B	RRM	-	I	gi|14133235
MOV10	DExH box	III	III	gi|14424568
TRBP	dsRBD	I*	I*	gi|107904
Gemin3	DEAD box	-	II*	gi|14209614
Gemin4	Leucin Zipper	II*, III	II, III	gi|7657122
DEAD/DEAH box containing proteins				
RNA helicase A (RHA)/DHX9	DEAH box, helicase domain, dsRBD, DUF1605	II, III	II, III	gi|1806048/gi|1082769
DDX30	DEAH box, helicase domain, dsRBD, DUF1605	II, III	II, III	gi|20336294
RENT1/Upf1	DEAD box, exoV	III	-	gi|1575536
DHX36	DEAH box, helicase domain, DUF1605	II*, III*	II*	gi|7959237/gi|23243423
DDX21/ RNA helicase GuA	DEAD box, helicase domain, GUCT	II, III	II	gi|2135315
DDX50/ RNA helicase GuB	DEAD box, helicase domain, GUCT, RESIII	III	-	gi|55664207
DDX46	DEAH box, helicase domain, DUF1605	II*	II*	gi|2696613
DDX48	DEAD box, helicase domain	II*, III	-	gi|496902
DDX18	DEAD box, helicase domain	III	-	gi|1498229
DDX5/p68	DEAD box, helicase domain	-	II*	gi|57165052
DDX39/BAT1	DEAD box, helicase domain	III*	II*	gi|1905998
DDX47	DEAD box, helicase domain, Apolipoprotein L	III	-	gi|20149629
hnRNPs				
hnRNP-U	SAP, SPRY, SCOP	II, III	II, III	gi|32358
hnRNP-U-like	SAP, SPRY, SCOP	I*	-	gi|3319956
hnRNP-H2/H'	RRM, RNPHF zinc finger	II*	-	gi|6065880
hnRNP-F	RRM, RNPHF zinc finger	II*	I*	gi|16876910
hnRNP-C	RRM	II, III	II, III	gi|13937888/gi|14250048
hnRNP-E2	KH1, KH2	III*	-	gi|460773
NSAP1/SYNCRIP	Phox-like, PX-associated motif, RRM	II, III	-	gi|5031512

Name	Domains/motif	Ago1 complex	Ago2 complex	Accession No.
hnRNP-L	Enoyl-CoA hydratase/isomerase, RRM	III*	-	gi|11527777
mRNA binding proteins				
Poly(A)-binding proteins	RRM	II, III	II, III	gi|46367787/gi|693937
Nuclear cap binding protein 80kDa	MIF4G	III	-	gi|3153873
YB-1	Cold shock domain	II	II, III	gi|181486/gi|55451
FMRp	Agenet, KH1	III*	-	gi|182673
FXR1	Agenet, KH1	-	III	gi|1730139
FXR2	Agenet, KH1	III	-	gi|4758410
IMP1	RRM, KH1	II, III	III	gi|7141072/gi|56237027
IMP3	RRM, KH1	III	-	gi|30795212
HuR	RRM	III*	-	gi|1022961
RBM4	RRM, Zn-finger	-	III*	gi|4506445
Proteins involved in RNA metabolism				
NF-90/ILF3/NFAR-1	dsRBD, DZF	II, III	II	gi|1082856/gi|5006602
NF-45/ILF2	DZF	II, III	II, III	gi|532313
SART3	Lsm interaction motif, RRM	I, II, III	-	gi|7661952
RBM10	D111/G-patch, RRM, Zn finger, Ran binding	-	I*, II*	gi|12644371
Fibrillarin	Fibrillarin motif	-	II*, III*	gi|182592
NOP56	Pre-mRNA processing RNP, NOP5NT, NOSIC	III	-	gi|2230878
Nucleolin	RRM	III	-	gi|128841
eIF2bδ	Initiation factor 2B	I*	-	gi|6563202
eIF4b	RRM	-	I*	gi|288100
PTCD3/FLJ20758	Pentatricopeptide repeat	II	II	gi|38683855
Other proteins				
Myb binding protein 1a	DNA polymerase V	III	III*	gi|7657351
Matrin 3	RRM, Zn finger	III*	III*	gi|6563246
Motor protein	-	II, III	-	gi|516764
ZNF326	AKAP95	II, III	-	gi|31807861/gi|47125447
Ku70	Ku70/80 motif, DNA-binding SAP	-	II*	gi|57165052
DDB1	CPSF A subunit	I	I*	gi|418316
RuvB-like II	AAA ATPase, Tip49b	I	I, II	gi|5730023/gi|12653319
Coatomer protein	WD-40, COPB2	III	II	gi|1002369

*identified by a single peptide

38

As expected from the Dicer activity assay as well as the western blotting results in Figure 16, Dicer was found only in Ago1/2 complexes I and III. TRBP, a protein that has been shown to be part of a minimal RISC complex (Gregory et al., 2005), was identified only in complex I of both Ago1 and Ago2. Moreover, with TNRC6B, MOV10, RNA helicase A (RHA), Gemin3 and Gemin4, a number of additional proteins that had been found in Ago complexes previously (Mourelatos et al., 2002; Meister et al., 2005; Robb and Rana, 2007) were among the identified proteins. Proteins that have not yet been implicated in RNA silencing in mammals were grouped according to their domains and function (Table 1). A prominent group among the identified proteins was constituted by the DEAD/DEAH box helicases. DDX5, an orthologue of *Drosophila* p68, which has been shown to associate with *Drosophila* Ago2 (Meister and Tuschl, 2004), was found as well as DDX18, a putative helicase that has been implicated in Drosha function (Gregory et al., 2004) and DHX36 (RHAU), a protein involved in mRNA degradation (Tran et al., 2004). Another prominent protein group was formed by the heterologous nuclear ribonucleoprotein (hnRNP) family, which is known to associate with mRNAs and to have specific functions in the regulation of gene expression (Han et al., 2010). Consistent with the hypothesis that Ago complexes II and III are mRNPs, various isoforms of poly(A)-binding proteins were identified, indicating that mRNAs were present in the purifications. Strikingly, many mRNA-binding proteins that are involved in translational regulation were identified, including FMRp and its homologues FXR1 and FXR2. It was reported previously that FMRp associates with Ago proteins as well as miRNAs in both human and *Drosophila* cells (Meister and Tuschl, 2004). Further identified proteins with regulatory functions in translation were NSAP1/SYNCRIP, YB-1, HuR, RBM4, IMP1 and IMP3. Furthermore, various ribosomal proteins were found in the Ago complexes (see supplementary tables), suggesting that ribosomal proteins might have other functions as components of mRNPs.

Besides the known Ago interactors Dicer, TNRC6B and TRBP, a number of proteins were identified in Ago1/2 complex I. For example, hnRNP U-like, a protein that had been found in Drosha complexes in the nucleus (Gregory et al., 2004) was restricted to Ago1 complex I, consistent with the migration of nuclear Ago in complex I (Figure 12). DDB1, HSP70, HSP90 and members of the solute carrier family were found in both Ago1 and Ago2 complex I. SART3, an RNA binding protein implicated in pre-mRNA splicing and transcription (Bell et al., 2002) as well as the eukaryotic initiation factor eIF2bδ was specific to Ago1 complex I. The RNA binding protein RBM10, however, was found in Ago2 complex I only. Complete lists of all identified proteins of Ago1 and Ago2 complex I are presented in Supplementary Table 1 and Supplementary Table 4, respectively.

2.2.2. Ago complex I distribution into distinct subcomplexes

The observation that the number of proteins identified would form a much larger complex than Ago complex I led to the question whether Ago complex I is formed from different subcomplexes. To investigate Ago complex I in more detail, FLAG/HA-Ago1 or -Ago2 were transfected into HEK 293 cells. Lysates were loaded onto a sucrose gradient ranging from 5-25 % allowing for a better separation of smaller protein complexes. The individual fractions were first analyzed by western blotting using antibodies against the HA-tag (Figure 19A).
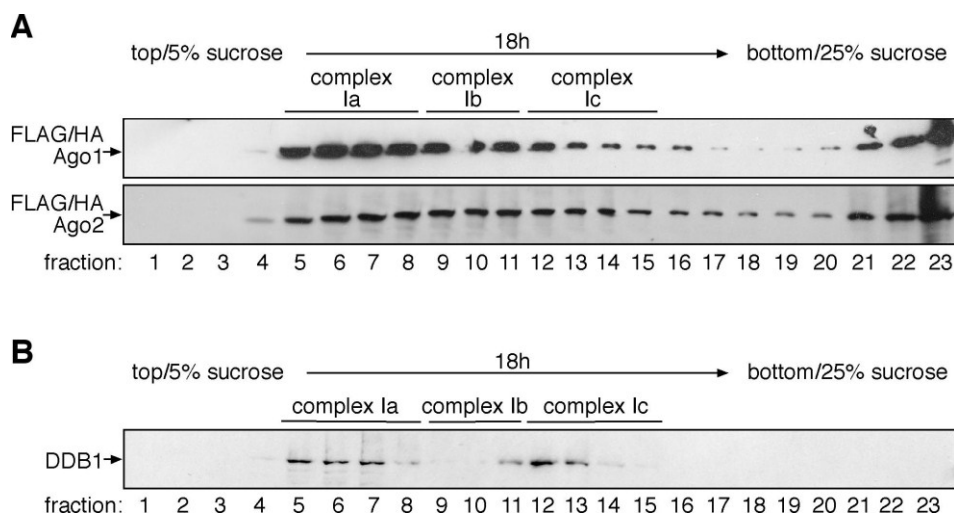
Figure 19: Further division of Ago complex I into subcomplexes
(A) HEK 293 cell lysates containing FLAG/HA-Ago1 (upper panel) or FLAG/HA-Ago2 (lower panel) were separated by sucrose gradient centrifugation ranging from 5 -25 %. Individual fractions were analyzed by western blotting using α-HA antibodies. **(B)** Wild-type HEK 293 lysate was separated as in **(A)** and analyzed by western blotting using specific antibodies against DDB1.

As expected, Ago complexes II and III migrated into the highest fractions (lanes 21-23). Ago complex I was found in fractions 5 to 17. Interestingly, when HEK 293 lysate was separated on a 5-25 % sucrose gradient, western blotting of individual fractions using antibodies against the complex I component DDB1 yielded two signal peaks in fractions 5-7 and fractions 11-13 (Figure 19B), indicating that Ago complex I could further be divided into several subcomplexes.

Next, endonucleolytic activity of Ago2 as well as Dicer activity in a 5-25 % sucrose gradient was analyzed. Again, FLAG/HA-Ago2 was immunoprecipitated from individual fractions of the gradient using α-FLAG antibodies. Immunoprecipitates were incubated with a ^{32}P-cap labeled miR-19b substrate RNA. RISC activity was observed in fractions 4-14 with varying signal intensities (Figure 20A). Again, no cleavage signal was detected in the higher molecular fractions corresponding to complex II and III.
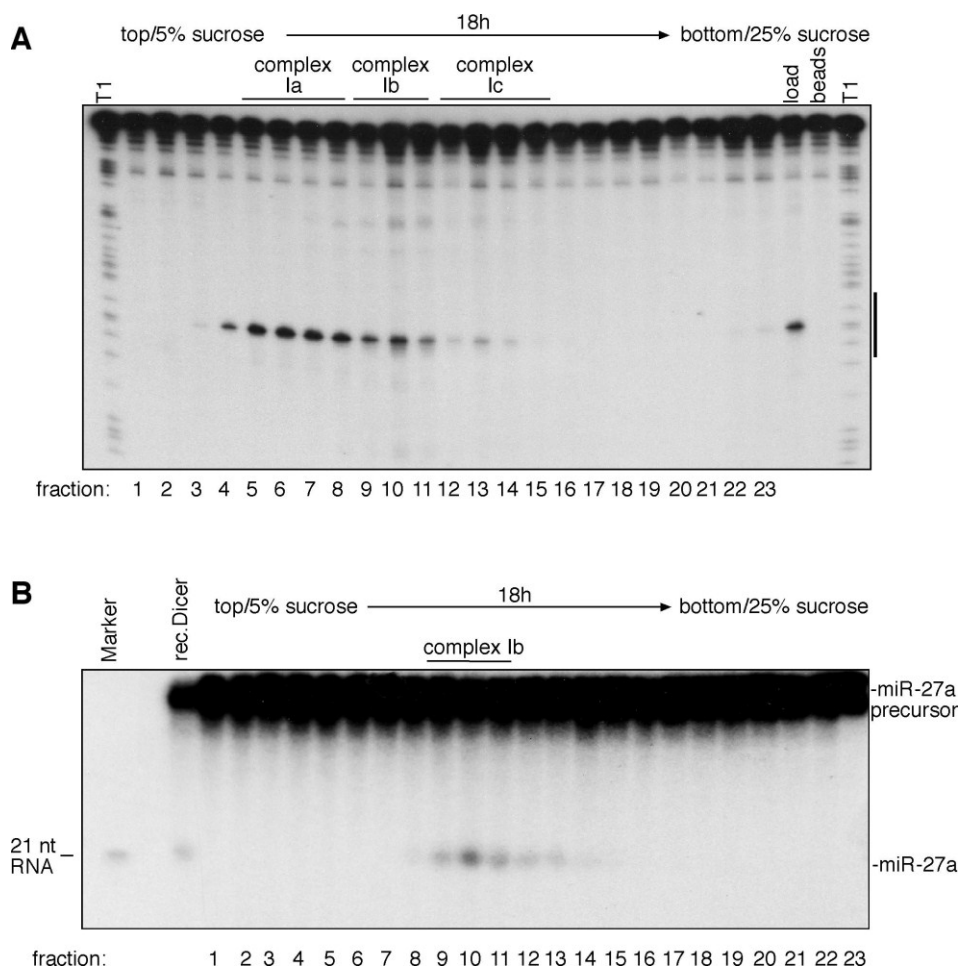
Figure 20: Analysis of Ago complex I subcomplexes for RISC and Dicer activities
(A) FLAG/HA-Ago2 was immunoprecipitated from gradient fractions from **(19A)** using α-FLAG antibodies and incubated with a ^{32}P-cap-labeled target RNA complementary to miR-19b. Cleavage products were analyzed by denaturing RNA-PAGE. T1 indicates RNase T1 digestion of the RNA substrate. The RNA sequence complementary to miR-19b is indicated by a black bar to the right. **(B)** FLAG/HA-Ago2 was immunoprecipitated from HEK 293 cells as in **(A)** and incubated with a ^{32}P-labeled pri-miR-27a substrate. Dicer products were analyzed by 15 % denaturing RNA-PAGE. A 21-nucleotide marker is shown to the left.

The analysis of Dicer activity resulted in a different picture. Dicer activity peaks in fractions 9-11, with weaker activity also detectable in fractions 12-14 (Figure 20B). In fractions 5-8, which produce the strongest RISC signals, Dicer activity was hardly detectable.

Taken together, these results indicate that Ago complex I indeed can be further divided into subcomplexes with different characteristics. Ago complex Ia (lanes 5-8) most likely forms a Dicer-free minimal RISC as described by Martinez et al. (Martinez et al., 2002). Ago2 complex Ib (lanes 9-11) associates with Dicer as well as RISC and is presumably a trimeric complex formed by Ago2, Dicer and TRBP (Gregory et al., 2005). Ago2 complex Ic (lanes 12-15), which shows only low RISC and Dicer activities, presumably is formed by various Ago-protein interactions including the other protein factors identified by mass spectrometry analysis.

2.2.3. Sedimentation of co-purified proteins with Ago complexes

In order to validate the mass spectrometry data, several different assays were performed. In a first approach, the identified factors were examined for specific co-sedimention with Ago-containing fractions in sucrose gradients. HEK 293 lysates were subjected to gradient centrifugation followed by western blotting analysis using specific antibodies (Figure 21, upper panels). For several factors, antibodies were not available; hence FLAG-HA-tagged fusion proteins were expressed and analyzed by western blotting against the HA-tag (Figure 21, lower panels). However, due to the large number of protein interactors, experiments were restricted to a selection of the identified factors.

Consistent with the proteomic data, hnRNP-U, NF-90, IMP1 and IMP3 co-migrated with both Ago complexes II and III, whereas TRBP was found in low molecular weight fractions co-migrating with Ago complex I. However, NF-45 and YB-1, which had been identified in complexes II and III by mass spectrometry, were detected in fractions containing Ago complex III only.
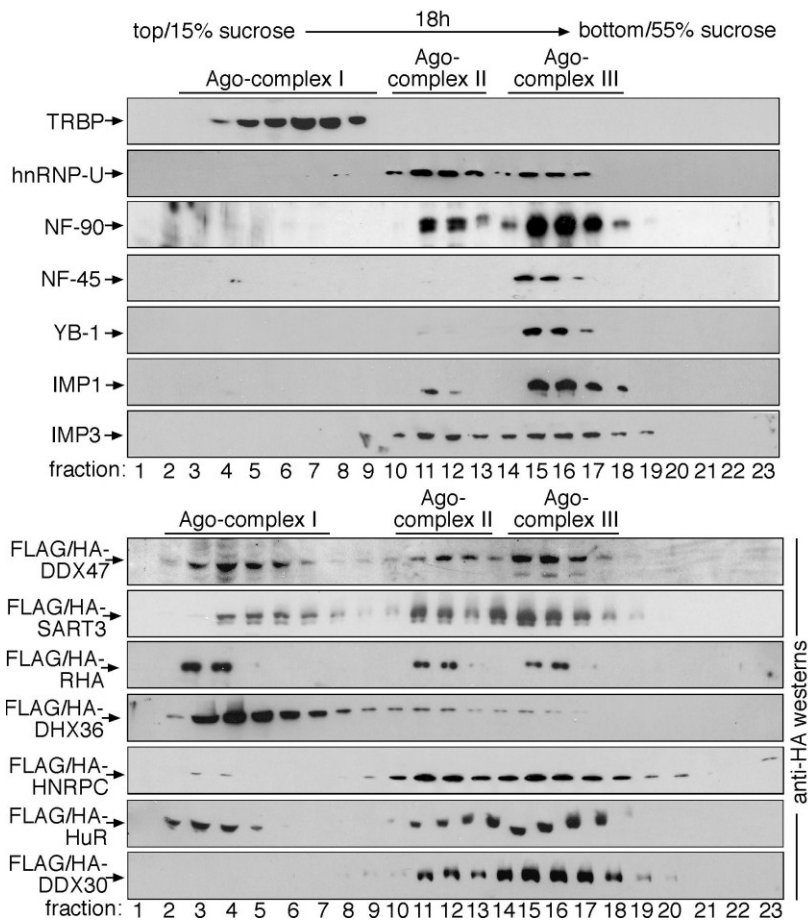
Figure 21: Co-migration of Ago-interacting proteins with Ago complexes
HEK 293 cell extracts were separated by gradient centrifugation and fractions were analyzed by western blotting against the proteins indicated to the left (upper panel). HEK 293 cells were transiently transfected with FLAG/HA-tagged expression constructs as indicated to the left and analyzed by western blotting using α-HA antibodies (lower panel).

For further co-sedimentation studies the proteins DDX47, DHX36, DDX30, RHA (DHX9), hnRNP C, HuR and SART3 were expressed as FLAG/HA-fusion proteins. All tagged proteins migrated in fractions also containing Ago complexes II and III. Notably, while SART3 was the only of the mentioned proteins that had been identified in all three Ago complexes I-III, a large portion of the tagged proteins migrated at the top of the gradient, presumably owing to overexpression.

Therefore, the migration behavior of the tested proteins largely corresponded with the mass spectrometry data.

2.2.4. Verification of Ago-protein-interactions by co-immunoprecipitation

To validate a specific interaction with Ago complexes, co-immunoprecipitation experiments were performed. Samples were further subjected to RNase A treatment to allow for a distinction of RNA-dependent and RNA-independent protein interactions. Again, due to the large number of identified proteins, co-immunoprecipitation experiments were focused on some exemplary proteins.

FLAG/HA-Ago1 and -Ago2 were immunoprecipitated from transiently transfected HEK 293 cell lysates using FLAG antibodies (Figure 22A). RNase A-treated and untreated samples were analyzed by western blotting for co-purified endogenous interaction partners. As negative controls, FLAG/HA-GFP as well as unloaded FLAG beads were used. HnRNP-C1/C2, IMP1, IMP3 and YB-1 disappeared from the FLAG/HA-Ago1/2 immunoprecipitates when RNase A was added, indicating that the tested proteins were not associated with Ago proteins through protein-protein interactions, but bound to the same RNAs (Figure 22A, left panels). NF-90, SART3, DDX5 and DDB1 immunoprecipitated with both FLAG/HA-Ago1 and -Ago2 in the presence of RNase A, thus indicating protein-protein-interactions.

A western blot using α-HA antibodies is shown in the upper right panel of Figure 22A, demonstrating that Ago1- and Ago2 levels in RNase A-treated and untreated samples are equivalent. Furthermore, the efficiency of RNase A treatment was examined by northern blotting. RNase A-treated and untreated FLAG/HA-Ago2 samples were separated by denaturing RNA PAGE and RNA was visualized by UV-illumination (Figure 22C, left panel). RNA fragmentation is clearly visible in the RNase-treated sample (lane 2). Also, endogenous miR-19b levels were massively decreased upon RNase-treatment, as analyzed by northern blotting (Figure 22C, upper right panel), indicative of effective RNA degradation even of Ago-bound miRNAs.
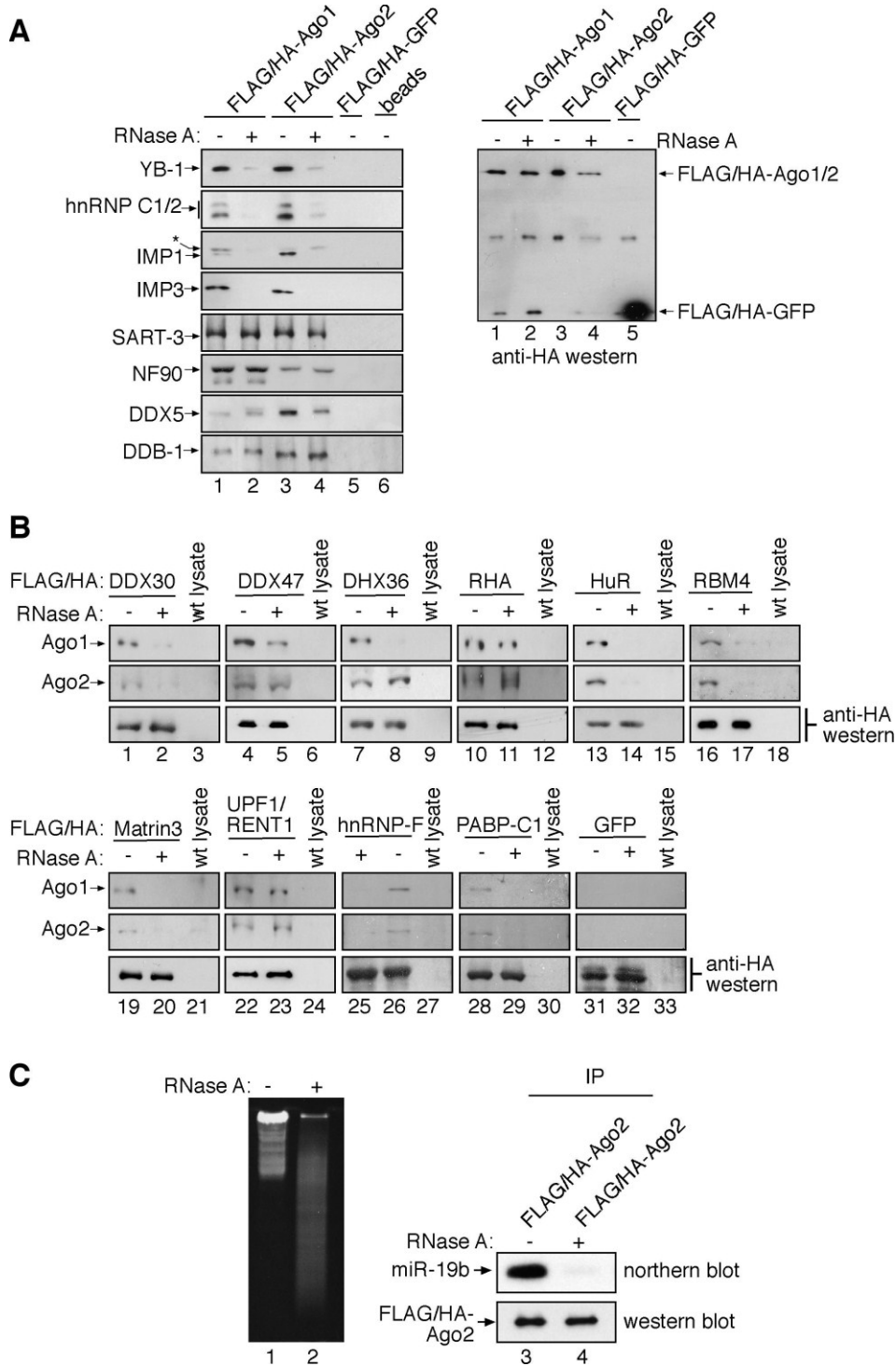
Figure 22: Verification of Ago-protein interaction by co-immunoprecipitation
(A) HEK 293 cells were transfected as indicated. Ago complexes were immunoprecipitated using α-FLAG antibodies and probed using specific antibodies with (+) or without (-) prior RNase A treatment (left panel). The asterisk denotes unspecific interactions of the IMP3 antibody. A western blot using α-HA antibodies is shown to the right. **(B)** HEK 293 cells were transfected with FLAG/HA-tagged expression constructs as indicated. Immunoprecipitations and RNase treatment were carried out as in **(A)**. Wild-type HEK 293 lysate was used as a control. Interactions were analyzed by western blotting against Ago1 (upper panels), Ago2 (middle panels) or HA (control; lower panels). **(C)** Total RNA from HEK 293 cells was incubated with (+) or without (-) RNase A, separated by RNA PAGE and visualized by ethidium bromide staining (left panel). FLAG/HA-Ago2 lysates were immunoprecipitated using α-FLAG agarose (right panels). Beads were incubated with or without RNase A followed by RNA extraction and northern blotting against miR-19b (upper panel). As a loading control, 15 % of the beads were used for western blotting against the HA-tag (lower panel).

44

In a reverse co-immunoprecipitation experiment, Ago-interacting factors were expressed as FLAG/HA-fusion proteins and co-immunoprecipitated endogenous Ago1 and Ago2 was detected by western blotting using specific antibodies (Figure 22B, upper and middle panels). Wild-type HEK 293 lysate was used as a negative control and anti-HA western blots were performed to check for equal levels of the FLAG/HA-tagged proteins (lower panels).

Endogenous Ago1 and Ago2 clearly co-precipitated with all FLAG/HA-tagged proteins except the FLAG/HA-GFP control (lanes 31-33). The binding of DDX30 (lanes 1-3), HuR (lanes 13-15), RBM4 (lanes 16-18), hnRNP F (lanes 25-27), PABP C1 (lane 28-30) and Matrin3 (lanes 19-21) to Ago1 and Ago2 was sensitive to RNase A treatment, whereas the binding of DDX47 (lanes 4-6), RHA (lanes 10-12) and UPF1/RENT1 (lanes 22-24) was not, suggesting protein-protein interactions. Interestingly, the binding behavior of DHX36 (lanes 7-9) reproducibly differed with Ago1 and Ago2. While Ago1 binding seemed to be RNA-dependent, Ago2 binding was not, implying a distinct interaction mode with the different Ago proteins.

In summary, the interaction of Ago1 and Ago2 with all of the tested proteins could be confirmed by co-immunoprecipitation. Still, results from RNase treated immunoprecipitates suggested that a number of the observed interactions is mediated by RNA rather than direct protein-protein interaction.

2.2.5. Analysis of Ago-interactions by in vitro pull-down experiments

As another approach to validate Ago interactions, *in vitro* pull-down experiments were performed with a small subset of proteins.

To cross-examine its binding behavior to the Ago proteins, DHX36 was recombinantly expressed as a GST-fusion protein. His-tagged Ago1 through -4 as well as the negative control His-Sip1 were *in vitro* translated in presence of ^{35}S-Methionine and subsequently incubated with GST-DHX36. In contrast to the co-immunoprecipitation experiments in Figure 22B, GST-DHX36 did not show distinct binding to Ago2, but displayed binding to all four Ago proteins (Figure 23A, lanes 1-4). Control reactions where GST alone was immobilized did not yield any signal (lanes 6-9) and Ago input protein levels where equivalent (left panel). However, expression levels of GST-DHX36 were quite low and degradation products were visible in the coomassie staining, hence it cannot be excluded that the indiscriminate Ago binding observed in the *in vitro* pull-down assay might to some degree be unspecific.

As mentioned before, TRBP has been demonstrated to form a complex with Ago2 and Dicer and to be part of a minimal RISC complex (Gregory et al., 2005). Consistently, *in vitro* pull-down experiments showed a strong interaction of GST-TRBP with all four Ago proteins (Figure 23B).
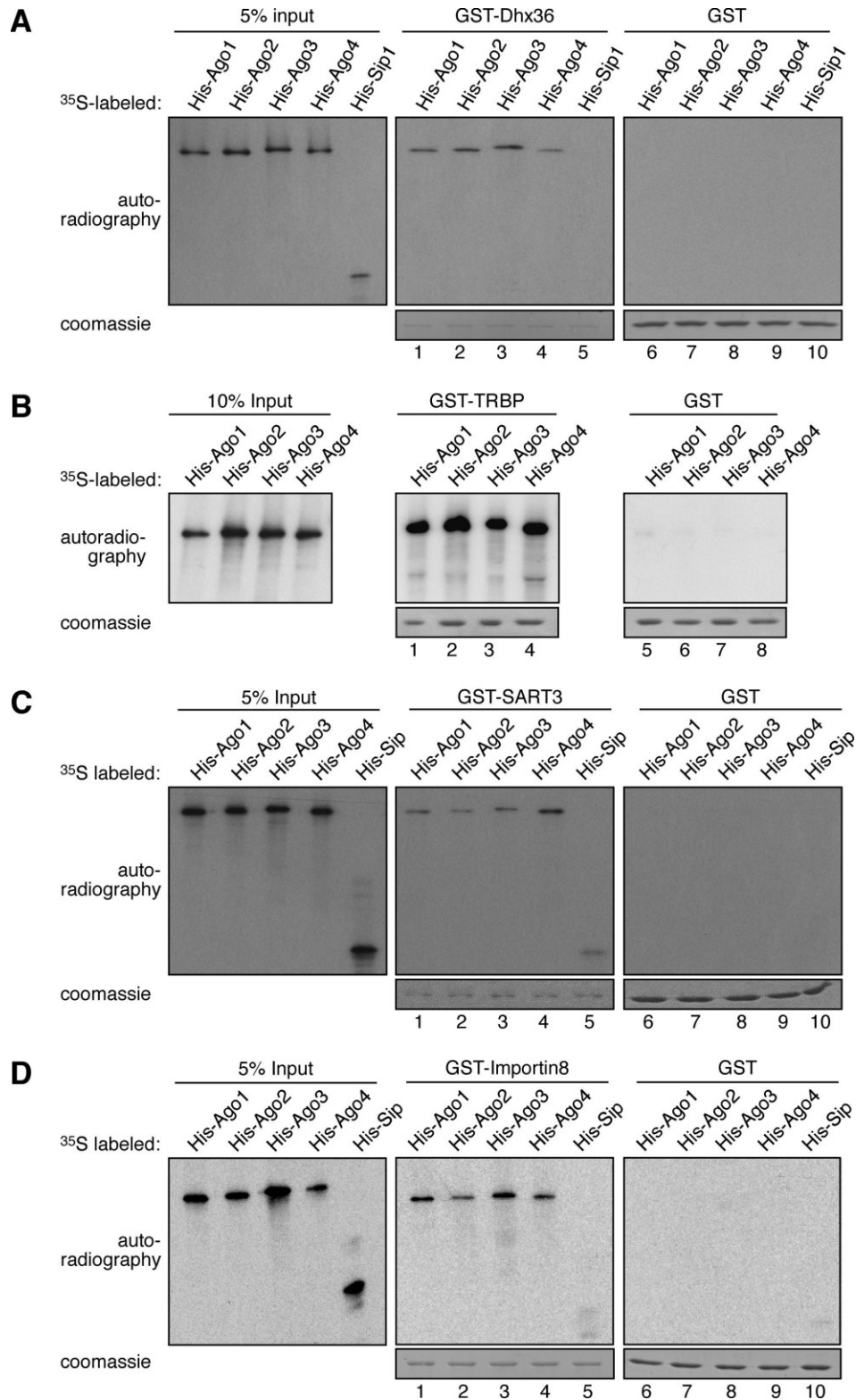
Figure 23: Verification of Ago-protein interaction by *in vitro* pull-down experiments
GST-DHX36 **(A)**, -TRBP **(B)**, -SART3 **(C)** and -Importin8 **(D)** fusion proteins (lanes 1-5) or GST alone (lanes 6-10) were immobilized on Glutathione sepharose beads and incubated with *in vitro* transcribed His-Ago1-4 or -Sip1. After separation by SDS-PAGE, bound proteins were detected by autoradiography. Coomassie staining of the immobilized proteins are shown below the respective panels. Left panels show 5 % **(A, C, D)** or 10 % **(B)** of the ^{35}S-labeled proteins used in lanes 1-10.

46

While in the mass spectrometry analysis, SART3 could only be detected in Ago1 complexes, co-immunoprecipitation experiments also showed a RNA-independent interaction with Ago2. This was confirmed by the *in vitro* binding assay. Moreover, a consistent binding of GST-SART3 to all four Ago proteins was observed (Figure 23C).

In vitro interaction studies with Ago1-4 were also performed for Importin 8 (Ipo8), an import receptor that had been identified as interaction partner of Ago2, Ago3 and Ago4 by mass spectrometry (Supplementary Table 4; Weinmann et al., 2009). All four Ago proteins interacted with GST-Ipo8, whereas no signal was observed in control reactions where GST alone was supplied as binding partner (Figure 23D).

2.2.6. Characterization of the Ago interaction factor PTCD3

Mass spectrometry analysis identified the pentatricopeptide repeat domain protein PTCD3 as a component of Ago1/2 complex II. While functional details about PTCD3 were missing, its characteristic PPR domains have been implicated in RNA binding (Schmitz-Linneweber and Small, 2008). Therefore, the presence of PTCD3 in Ago complexes prompted us to investigate the possible role of this previously uncharacterized protein in Ago function.

The PPR (pentatricopeptide repeat)-containing proteins constitute a large family of proteins involved in post-transcriptional processes. PPR proteins have been found in large numbers in plants and are predicted to be located primarily in organelles (Delannoy et al., 2007). In the human system, however, only seven PPR proteins were identified (Holzmann et al., 2008; Lightowlers and Chrzanowska-Lightowlers, 2008) and PTCD3 was found to associate with the small ribosomal subunit of mitochondrial ribosomes in the meantime (Davies et al., 2009).

To validate the interaction between Ago1/2 and PTCD3, FLAG/HA-tagged PTCD3 was co-transfected into HEK 293 cells together with myc-tagged Ago1, -Ago2 or -GFP. Immunoprecipitations were performed using anti-myc antibodies and samples were incubated in the presence or absence of RNase A as described before (Figure 24A). Western blotting for the HA-tag yielded a constant signal in both Ago1- and Ago2 samples, indicating a direct protein-protein interaction.

However, these results could not be confirmed by *in vitro* pull-down experiments. Though recombinant expression of GST-PTCD3 yielded considerable protein amounts, binding to ^{35}S-labeled Ago1 through -4 could not be detected (Figure 24B). *In vitro* binding of RBM4 to His-Ago2, performed as a positive control, was clearly visible (lane 16, also compare Figure 32). Failure of GST-PTCD3 to bind Ago proteins might be due to incorrect folding in *E. coli*. However, as both Ago and PTCD3 proteins were overexpressed in the co-

immunoprecipitation experiment, it cannot be excluded that the observed signals are overexpression artefacts.
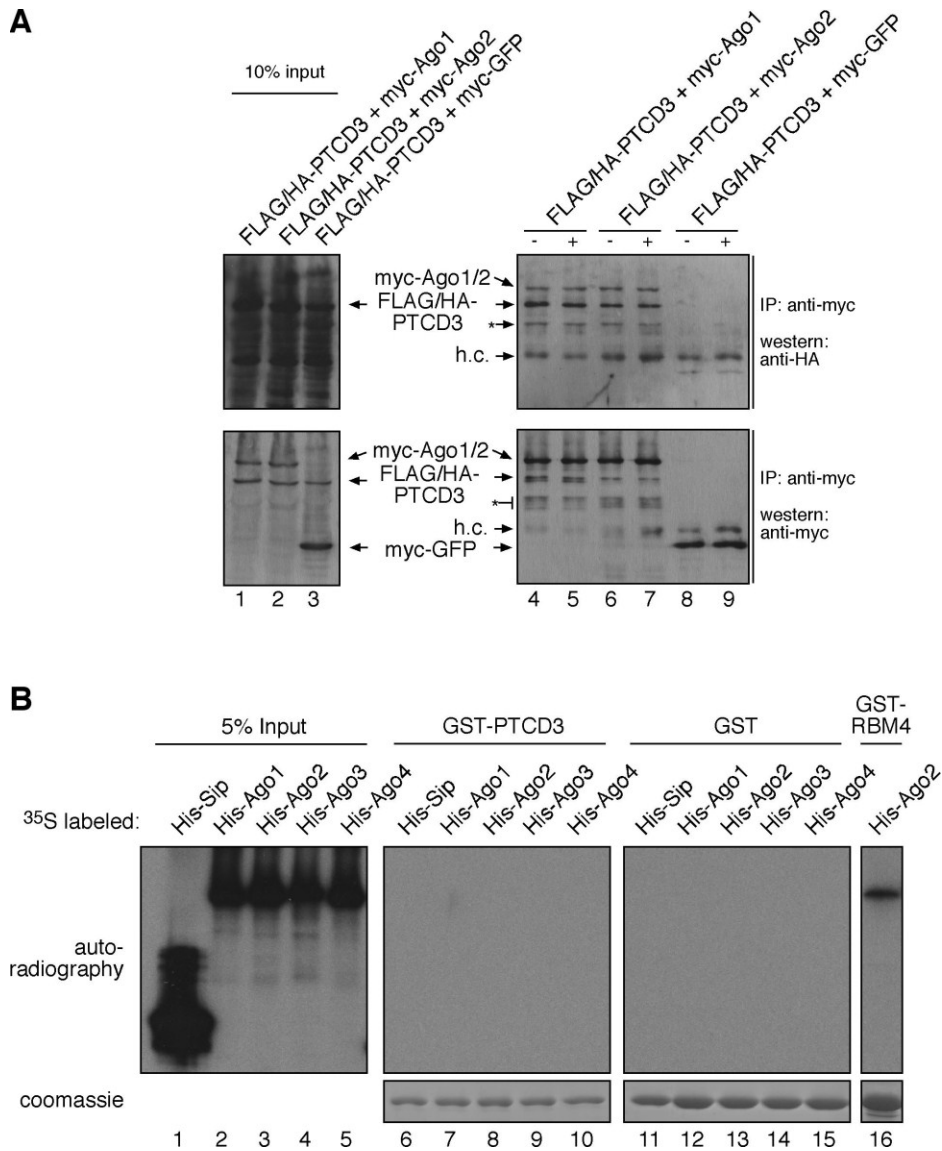
Figure 24: Analysis of Ago interaction with PTCD3
(A) FLAG/HA-tagged PTCD3 constructs were co-transfected into HEK 293 cells together with myc-tagged Ago1-, Ago2- and GFP-constructs. Lysates were subjected to immunoprecipitation using anti-myc antibodies and treated with RNase A as indicated (right panels). Samples were separated by SDS-PAGE and analyzed for co-precipitated FLAG/HA-PTCD3 using α-HA antibodies (upper right panel). Expression of the myc-constructs was analyzed by myc-western blot (lower right panel). To the left, 10 % of the input volumes for immunoprecipitation were loaded for western blotting. h.c.: heavy chain **(B)** GST-PTCD3 (lanes 6-10) or GST alone (lanes 11-15) as well as GST-RBM4 (lane 16) were immobilized on Glutathione sepharose and incubated with *in vitro* transcribed His-Ago1-4 or -Sip1 as indicated. After SDS-PAGE, bound proteins were visualized by autoradiography. Immobilized proteins were visualized by coomassie staining (lower panels). Lanes 1-5 show 5 % of the ^{35}S-labeled proteins used in lanes 6-16.

Nevertheless, sub-cellular localization of PTCD3 and Ago2 was analyzed by confocal laser microscopy. HEK 293 cells were co-transfected with myc-Ago2 and FLAG/HA-PTCD3 (Figure 25A). Cells were fixed and the tagged proteins were stained using α-HA or α-myc

antibodies. As expected, myc-Ago2 predominantly localized to cytoplasmic structures which are presumably P bodies. FLAG/HA-PTCD3 is diffusely localized to the cytoplasm, however, considerable amounts co-localized with myc-Ago2. P body localization could also be confirmed by co-localization of FLAG/HA-PTCD3 with the endogenous P body marker Lsm4 (Figure 25B).

Thus, PTCD3 can be regarded as a newly identified P body component. Its function related to Ago proteins, however, will have to be further elucidated.
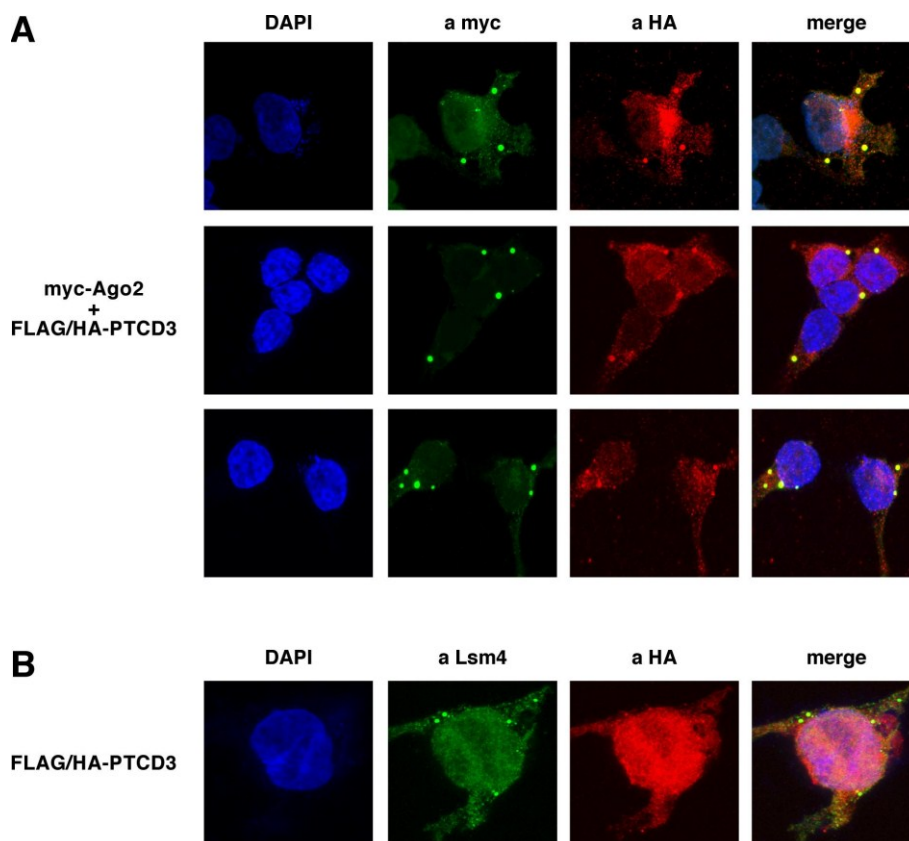
Figure 25: PTCD3 location within the cell
(A) Myc-Ago2 was co-expressed with FLAG/HA-PTCD3 in HEK 293 cells. Fixed cells were stained with DAPI as well as with α-HA and α-myc antibodies and the corresponding TexasRed- and FITC-conjugated secondary antibodies. Cells were analyzed using confocal laser microscopy and projections of 20 z-sections are shown. **(B)** HEK 293 cells expressing FLAG/HA-PTCD3 were probed for endogenous Lsm4 and overexpressed PTCD3 using α-Lsm4 and α-HA antibodies as described in **(A)**.

2.3. RBM4 AND ITS FUNCTION AS ARGONAUTE INTERACTION PARTNER

2.3.1. RBM4 is required for miRNA-guided gene silencing

To investigate the relevance of identified Ago mRNP components for miRNA function, a luciferase construct containing a perfectly complementary miR-21 target site in the 3'-UTR was generated. Binding of Ago complexes containing endogenous miR-21 to the reporter

mRNA results in target cleavage and -destruction and correspondingly in a decrease of luciferase levels. In combination with knock-down of Ago-associated proteins, the functional relevance of the respective interaction partner for Ago function can be tested. As a control, a mutant construct with imperfect miR-21 complementarity was cloned (Figure 26A).
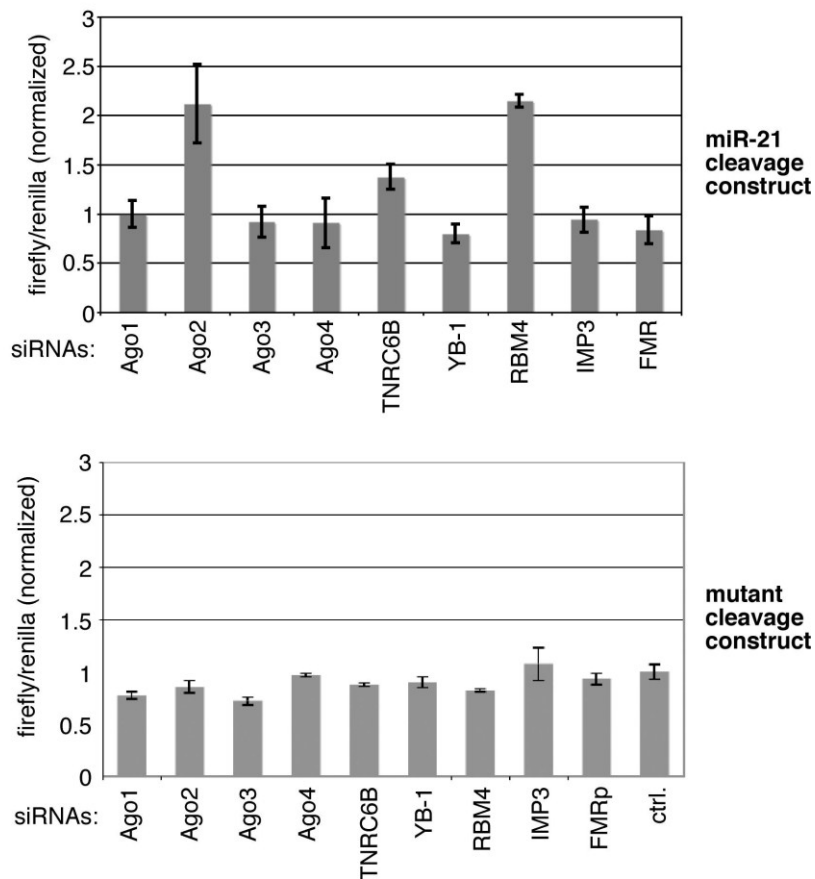
Figure 26: Effect of RBM4 knock-down on miRNA-guided gene silencing
(A) Schematic depiction of the miR-21 reporter construct and the corresponding control construct carrying a mutated miR-21 binding site. **(B)** SiRNAs against the indicated proteins were pre-transfected into HeLa cells. After 2 days, luciferase reporter constructs containing a complementary (upper panel) or a mutated (lower panel) binding site for miR-21 or a control vector lacking the miR-21 binding site were transfected and luminescence was measured after 96 h. Luciferase assays were done in triplicates. Results from the complementary or mutant reporters were normalized to those of the empty vector.

As expected, knock-down of Ago1, Ago3 and Ago4 had no effect, whereas siRNAs against Ago2 or TNRC6B led to a significant increase of luciferase expression (Figure 26B, upper panel). Strikingly, knock-down of RBM4 resulted in a strong increase of luciferase activity, indicating that RBM4 modulates miR-21-guided RNA cleavage. No effect was observed with the corresponding construct containing a mutated miR-21 binding site (lower panel).

To analyze whether RBM4 is also required for the regulation of natural miRNA targets, a luciferase construct containing the KRAS 3'-UTR was utilized. As KRAS is known to be a target of the miRNA let-7a, the effect of a let-7a inhibition was tested in a first experiment. Indeed, transfection of a 2'OMe-oligoribonucleotide antisense to let-7a resulted in a strong increase of luciferase signal, while translational repression was not affected by transfection of a control 2'OMe-oligonucleotide (Figure 27A, right panel).
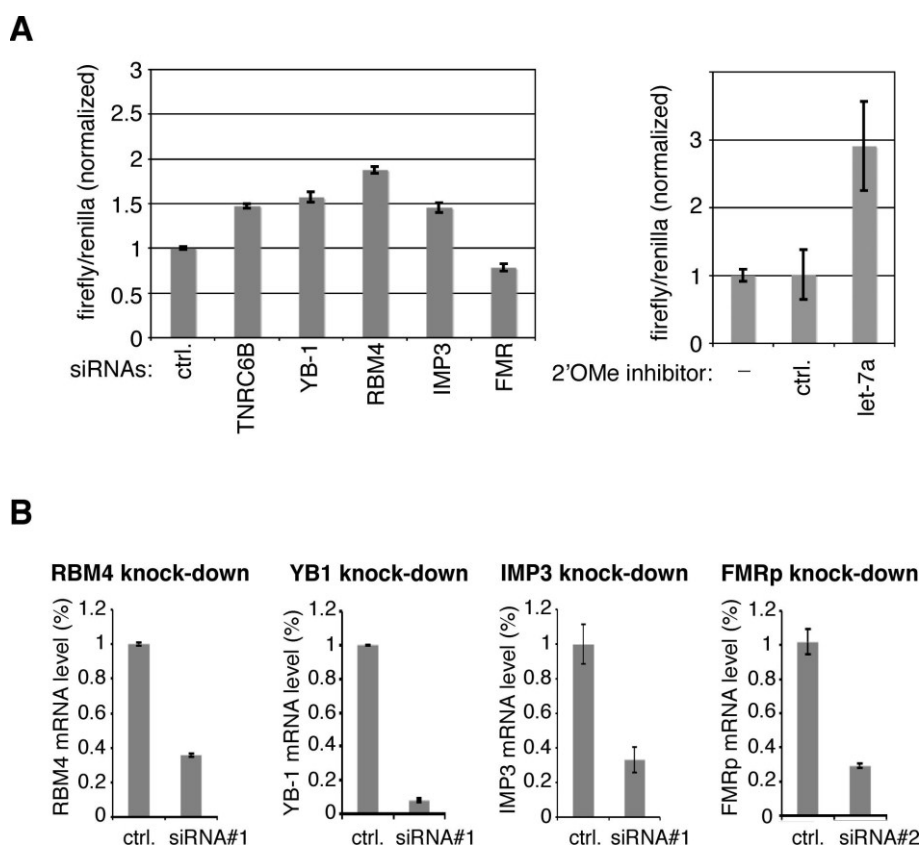
Figure 27: Regulation of the KRAS 3'-UTR mediated by Ago-interacting proteins
(A) The experiment was carried out as described in **(26B)**. A luciferase reporter construct containing the 3'-UTR of KRAS was used (left panel). 2'OMe inhibitors of the indicated miRNAs were co-transfected into HeLa cells together with the KRAS 3'-UTR reporter construct (right panel). Results were normalized to those of the empty vector. **(B)** HeLa cells were transfected with siRNAs against RBM4, YB-1, IMP3 and FMRp as well as a control siRNA (ctrl.) for 96 h. Total RNA was reverse transcribed and cDNA was amplified by qPCR with primers specific to the indicated proteins. mRNA levels relative to GAPDH mRNA were normalized to control transfections. The error bars are derived from three different experiments.

Next, the effects of the depletion of several proteins on the KRAS 3'-UTR reporter construct were analyzed. Knock-down of TNRC6B, a protein known to be involved in miRNA function, resulted in a signal increase as expected (Figure 27A, left panel). Further, cells depleted for YB-1, RBM4 or IMP3 showed stronger activity of the KRAS reporter construct, suggesting a function of these proteins in miRNA-mediated target regulation. Knock-down of FMRp, however, did not result in increased luciferase levels. Knock-down of the mentioned proteins was monitored by qRT-PCR as depicted in Figure 27B.

In an inverse experiment, luciferase levels were examined when RBM4 was overexpressed (Figure 28). Various amounts of FLAG/HA-RBM4 and -IMP3 were transfected into HeLa cells and luciferase activity was measured. Interestingly, IMP3 overexpression led to a slight increase in luciferase levels. RBM4 overexpression, however, resulted in a considerable decrease of luciferase activity, suggesting that RBM4 represses the KRAS 3'-UTR in a dose-dependent manner. Thus, results from RBM4 knock-down and overexpression experiments complement each other, confirming a function of RBM4 in the regulation of the KRAS 3'-UTR.
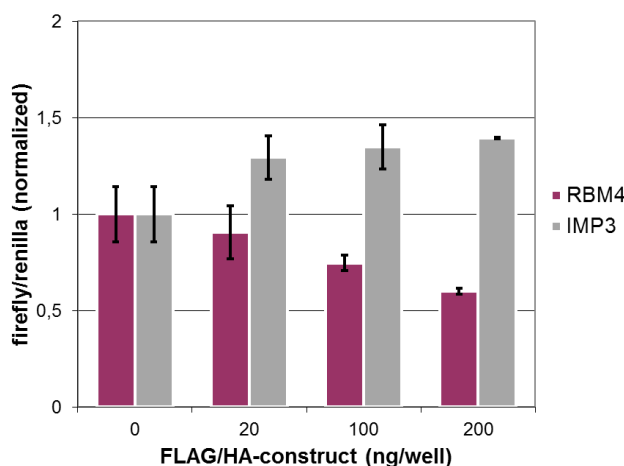
Figure 28: KRAS 3'-UTR regulation in RBM4 overexpression background
The indicated amounts of FLAG/HA-RBM4 and -IMP3 (control) encoding plasmids were co-transfected into HeLa cells together with the KRAS luciferase reporter plasmid. Luciferase assays were done in triplicates 48 h after transfection. KRAS data were normalized to those of the empty vector.

HMGA2, SERBP1, DNAJB11 and Raver2 have been identified and validated as miRNA targets before (Beitzinger et al., 2007; Mayr et al., 2007). Therefore, the luciferase reporter constructs containing the respective 3'-UTRs were transfected and luciferase activity was measured in an RBM4- or TNRC6B knock-down background (Figure 29). Indeed, luciferase activity was increased in the RBM4- and TNRC6B knock-down samples, indicating that RBM4 functions on various known miRNA targets.
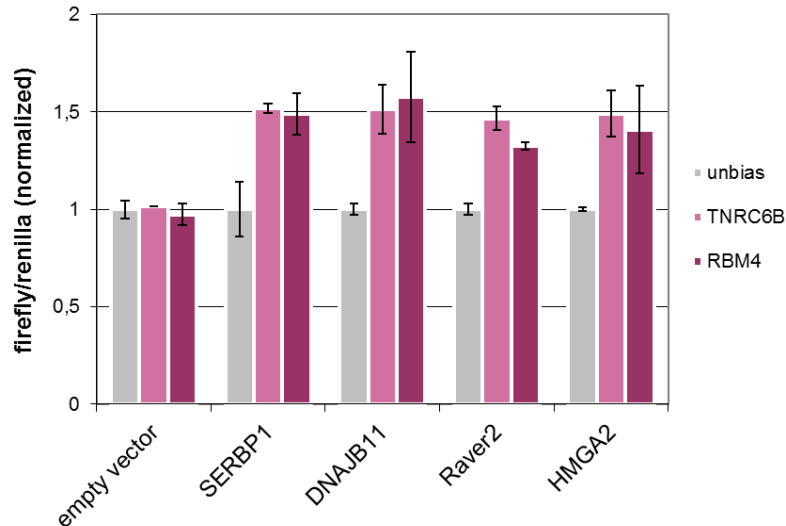
Figure 29: Effects of RBM4 knock-down on Ago target mRNAs
Experiments were carried out as in **(26B)**. Luciferase reporter constructs carrying the 3'-UTRs of the indicated Ago targets were transfected and results were normalized to control siRNA values and the empty vector.

2.3.2. RBM4 characterization and Ago interaction

RBM4 is an RNA binding protein with diverse functions within the cell. It was identified in association with Ago2 by mass spectrometry and the aforementioned luciferase reporter experiments point towards an additional role of RBM4 in regulation of a number of miRNA target mRNAs. Therefore, the RBM4 interaction with Ago proteins was addressed in more detail.

Revisiting the RBM4 migration behavior in sucrose gradients, HEK 293 lysates were fractionated and subjected to western blotting using antibodies specific to endogenous Ago1 and RBM4. RBM4 co-migrated with all three Ago complexes, a major share residing in complex III (Figure 30A) which is consistent with its identification in Ago2 complex III by mass spectrometry.

As RBM4 is known to be a nuclear-cytoplasmic shuttling protein, RBM4 distribution was analyzed in both compartments as well. Similar to Ago2, RBM4 was restricted to low molecular weight fractions in nuclear extracts (Figure 30B, upper panel). In the cytoplasmic extract, RBM4 can be detected in the fractions of all three Ago complexes (lower panel), confirming that RBM4 is part of the mRNP fraction in the cytoplasm.
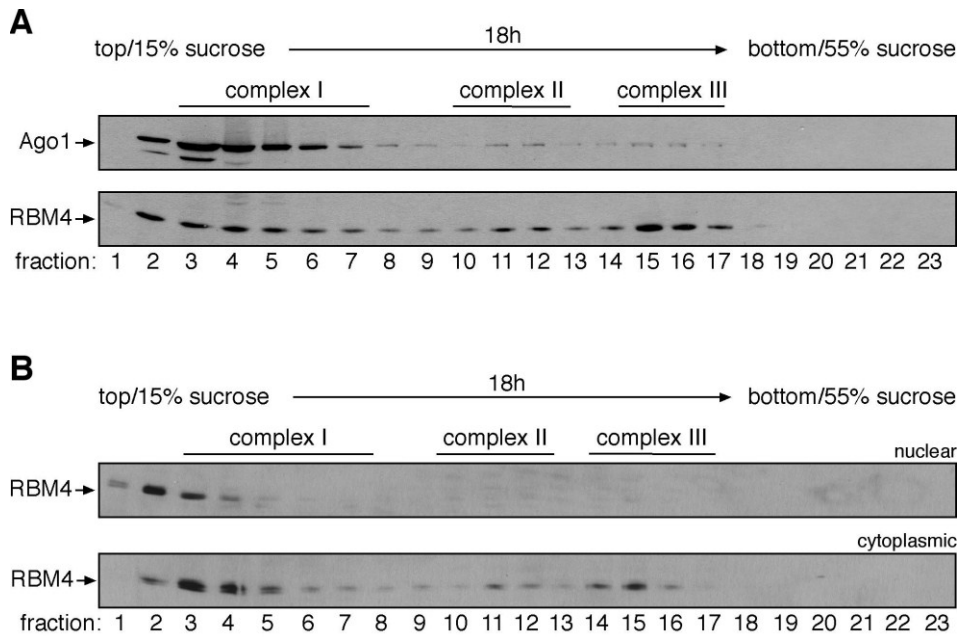
Figure 30: RBM4 gradient distribution
(A) HEK 293 lysates were separated by 15-55 % gradient centrifugation and individual fractions were analyzed for endogenous Ago1 (upper panel) and RBM4 (lower panel) using specific antibodies. **(B)** Nuclear (upper panel) and cytoplasmic (lower panel) lysates from HEK 293 cells were separated as in **(A)** and western blotting for endogenous RBM4 was performed.

Co-immunoprecipitation experiments reproducibly showed that FLAG/HA-RBM4 associates with endogenous Ago1 and Ago2 (Figure 22B, Figure 31, left panel). RNase treatment indicates that this interaction is at least partially RNA-dependent.

Northern blot analysis revealed that FLAG/HA-RBM4 co-immunoprecipitated endogenous miR-19b (Figure 31, right panel). However, the amount of co-purified miR-19b is very low compared to the levels bound to FLAG/HA-Ago2. It might therefore result rather from co-immunoprecipitated Ago proteins than from direct binding of RBM4 to miRNAs.
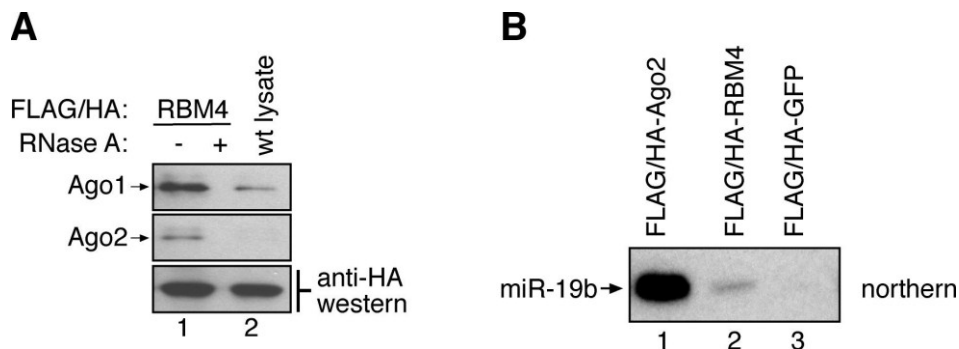
Figure 31: Association of RBM4 with Ago1, Ago2 and miRNAs
(A) FLAG/HA-RBM4 was immunoprecipitated as in **(22B)** and western blotting for endogenous Ago1 and Ago2 as well as the HA-tag of RBM4 (control) was performed. **(B)** Lysates from HEK 293 cells transfected with the indicated constructs were immunoprecipitated using α-FLAG antibodies and analyzed for miR-19b by northern blotting.

The RBM4 interaction with Ago proteins was further validated by *in vitro* pull-down experiments. Recombinant GST-RBM4 yielded a strong binding signal with His-Ago1 through -4, but not with the control protein His-Sip1. Interaction was not dependent on the miRNA binding abilities of Ago as an Ago2 mutant that is incapable of binding small RNAs (paz9; Liu et al., 2005) (Figure 32, lane 5) showed a signal equivalent to wild-type Ago2 (lane 2). Also, binding was specific for the RBM4 protein as control reactions supplying GST alone as binding partner did not yield any signal.
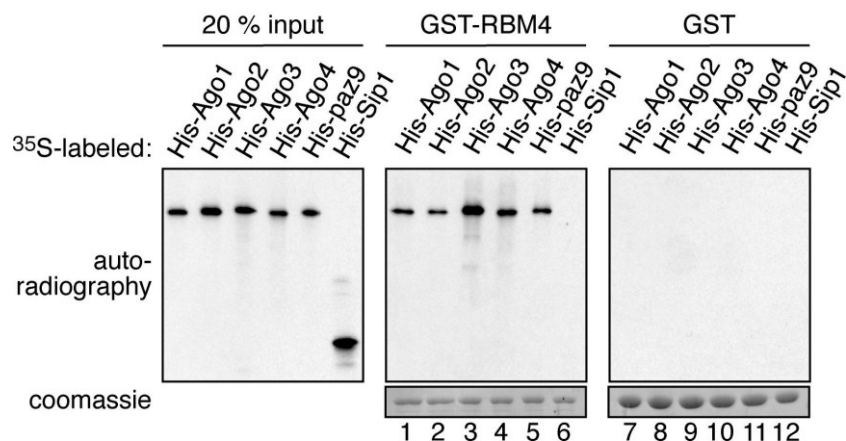
Figure 32: Analysis of RBM4-Ago binding by *in vitro* pull-down assay
GST-RBM4 (lanes 1-6) or GST (lanes 7-12) were immobilized on Glutathione sepharose and incubated with ^{35}S-labeled His-Ago1-4 (lanes 1-4 and 7-10), His-Ago2-paz9 mutant (lanes 5 and 11) or His-Sip1 (lanes 6 and 12). Bound proteins were separated by SDS-PAGE and visualized by coomassie staining (lower panels) or autoradiography (upper panels). The upper left panel shows 20 % of the ^{35}S-labeled proteins used in lanes 1-12.

RNase treatment during the incubation of the protein partners resulted in a clearly visible though slightly diminished binding signal (Figure 34C). This observation indicates that the Ago-RBM4 interaction may be stabilized by mRNA binding. Further, it confirms the data obtained by co-immunoprecipitation.

2.3.3. Identification of the RBM4 domains involved in Ago2 binding

To identify the domains necessary for establishment of the interaction between Ago2 and RBM4, *in vitro* binding experiments with various protein fragments and mutants were performed.

[35]S-labeled His-Ago2 as well as His-tagged fusion proteins containing the N-terminus, PAZ-, MID- or PIWI domains of Ago2 were incubated with GST-RBM4 and binding was assayed by autoradiography (Figure 33). As expected, RBM4 strongly interacted with full-length His-Ago2 (lane 1). Furthermore, binding was observed for His-PIWI and, though weaker, for the His-N-terminal domain (lanes 2 and 5). The PAZ- and MID domains seemed to be dispensable for GST-RBM4 binding (lanes 3 and 4). As a control for Ago protein levels, input

samples were analyzed (left panel). GST alone did not bind Ago or its fragments (lanes 7-12), also, the control protein His-Sip1 did not bind GST-RBM4 (lane 6).
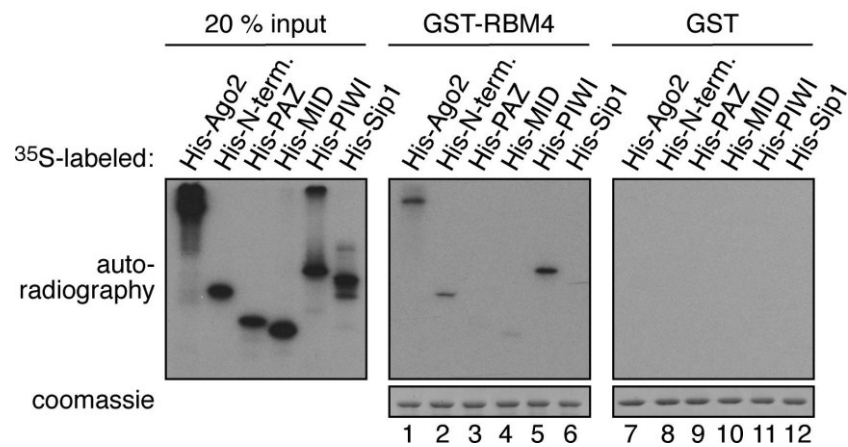
Figure 33: Identification of Ago domains involved in RBM4 binding
Experiments were carried out as in **(32)**, except that Ago2 constructs for the N-terminal (lanes 2 and 8), PAZ- (lanes 3 and 9), MID- (lanes 4 and 10) and PIWI- (lanes 5 and 11) domains of Ago2 were used for ^{35}S-labeling besides full-length His-Ago2 (lanes 1 and 7) and -Sip1 (lanes 6 and 12). Coomassie stained immobilized proteins are depicted in the lower panels. The upper left panel shows 20 % of the ^{35}S-labeled proteins used in lanes 1-12.

The determination of the RBM4 domains that are relevant for Ago2 binding was approached by cloning various fragments and deletion mutants as GST fusion proteins which are listed in Table 2 and depicted schematically in Figure 34A.
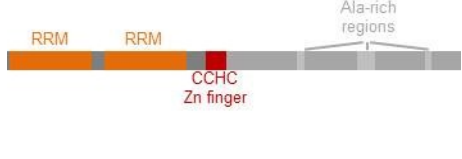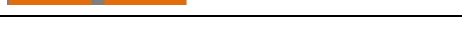
[35]S-labeled proteins were incubated with full-length His-Ago2 as described before and interaction was visualized by autoradiography. Deletion of the complete N-terminal part of RBM4 (ΔN) as well as deletion of both RNA recognition motifs (ΔRRM) abolished binding to His-Ago2 (Figure 34B, upper panel, lane 3 and 2, respectively). Deletion of the C-terminal part (ΔC, lane 4), however, did not interfere with Ago2 interaction, while an RBM4 fragment lacking both the Zn finger domain and the C-terminus (RRM+L2) showed slightly diminished Ago2 binding. Moreover, neither of the RRMs nor the Zn finger alone could facilitate interaction (Δ1, Δ2, Δ5, lanes 6, 7 and 10).

Removal of the Zn finger domain from the full-length protein led to a signal decrease, still, binding was not abolished completely (Δ6, lane 11), indicating a direct or indirect role for this domain in Ago2 interaction. This was also confirmed by mutant Δ14 carrying two mutations in the Zn finger domain that abolish its nucleic acid binding abilities (lane 19, Markus and Morris, 2006). Neither deletion of the RRM1 from the full-length protein nor from the N-terminal protein fragment resulted in diminished Ago2 interaction (Δ7 and Δ4, lanes 12 and 9). However, signal intensities decreased when the RRM2 was removed (Δ8 and Δ3, lanes 13 and 8). Besides the RRM2 and the Zn finger domains, the second linker region (L2) also seems to be involved in Ago2 binding, as both its deletion (Δ9, lane 14 compared to

RRM+L2, lane 5) and its replacement with an alanine-glycine-sequence of identical length (Δ10, lane 15) completely abolished *in vitro* binding to Ago2.

Table 2: Characteristics of the RBM4 mutants

Name	Schematic depiction	Amino acid residues	Internal deletions	Mutations
RBM4 RRM1 Linker L1 RRM2 Linker L2 Zn finger		1-364 3-68 69-78 79-144 145-159 160-176	-	-
ΔRRM		145-364	-	-
ΔN		177-364	-	-
ΔC		1-176	-	-
RRM+L2		1-159	-	-
Δ1		3-68	-	-
Δ2		79-144	-	-
Δ3		1-176	77-144	-
Δ4		69-176	-	-
Δ5		159-176	-	-
Δ6		1-364	160-179	-
Δ7		69-364	-	-
Δ8		1-364	78-144	-
Δ9		1-144	-	-
Δ10		1-364	-	L2 replaced by AAAAAAAGAAAAAAA sequence
Δ11		69-215	-	-
Δ12		1-215	-	-
Δ13		1-215	77-144	-
Δ14		1-364	-	Cys162 → Tyr Cys165 → Tyr
Δ15		1-364	-	Domain swap RRM1 ↔ RRM2
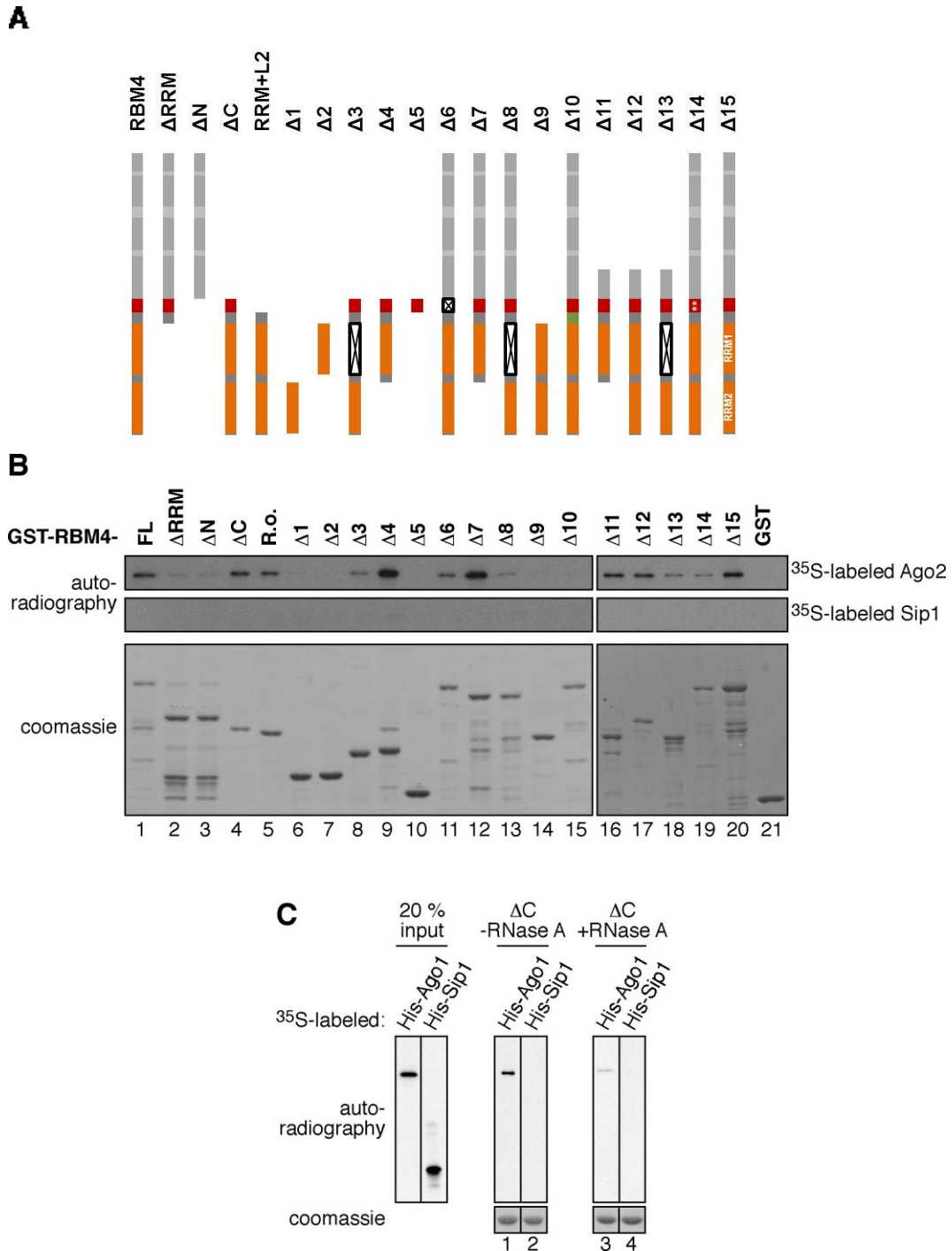
Figure 34: Identification of RBM4 motifs involved in Ago2 binding
(A) Schematic depiction of RBM4 and RBM4 fragments and mutants cloned. RNA recognition motifs are denoted in orange, the Zn-finger domain in red. The green stretch in mutant Δ10 symbolizes an alanine/glycine-stretch replacing the second linker domain. Two asterisks in mutant Δ14 depict Cys→Tyr mutations in positions 162 and 165 of the protein. **(B)** Experiments were carried out as in **(32)**, using ^{35}S-labeled His-Ago2 (upper panels) or His-Sip1 (middle panels) as well as the GST-tagged RBM4 mutants shown above and GST. Coomassie staining of the SDS PAGE gel is shown in the lowest panels. **(C)** Experiments were performed as in **(32)**. GST-RBM4 ΔC was incubated with His-Ago1 and -Sip in presence (right panel) or absence (middle panel) of RNase A.

As NMR measurements indicated that the deletion of the complete C-terminus might result in unfolding of the Zn finger domain (Birgitta Wöhrl, University of Bayreuth, personal communication), the mutants Δ4, ΔC and Δ3 were recloned carrying 11 additional amino acid

C-terminal of the Zn finger domain (Δ11, Δ12 and Δ13, respectively). However, this did not affect the binding behaviors in the *in vitro* pull-down experiments (compare lanes 16 and 9, lanes 17 and 4, lanes 18 and 8).

To further characterize the significance of the individual RRM domains for Ago2 binding, a domain swap was performed in mutant Δ15, rendering the RRM2 at the N-terminus of the protein and the RRM1 next to the L2 sequence. Interestingly, this did not have an influence on the binding signal (lane 20). As both RRM domains are still present in the Δ15 mutant, the shifted RRM2 could still function in Ago2 binding. Also, the RRM1 had been shown to partially compensate for a deletion of RRM2 (mutants Δ3, Δ8, Δ13). However, it cannot be excluded that the signal decrease in the latter mutants could be due to the fact that only RRM2 but not the first linker sequence L1 was deleted. In the resulting protein fragment, RRM1 and the Zn finger domain were separated not only by the required L2 sequence, but additionally by L1 which may have interfered with correct establishment of the binding surface.

To examine whether the *in vitro* binding properties of RBM4 could also be recapitulated with endogenous Ago from cell lysate, the immobilized RBM4 fragments were incubated with HEK 293 lysate and binding of Ago1 was analyzed by western blotting (Figure 35). Consistent with the *in vitro* data, Ago1 was co-purified with the ΔC- and RRM+L2 mutants as well as with the Δ4 and Δ7 mutants lacking RRM1. Weaker Ago1 signals, as might have been expected in analogy to the *in vitro* pull-down experiments, may not be visible due to background signals.
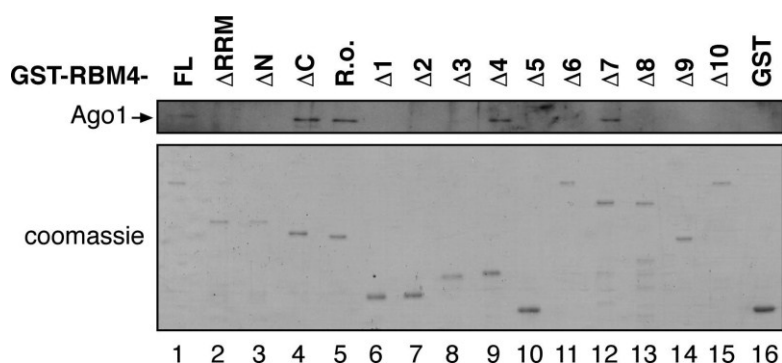
Figure 35: Interaction of GST-RBM4 mutants with endogenous Ago1
GST-RBM4, RBM4 mutants shown in **(34A)** and GST were immobilized on Glutathione sepharose and incubated with lysates from HEK 293 cells. Samples were analyzed for co-precipitated endogenous Ago1 by western blotting using specific antibodies.

Together, the results from the *in vitro* binding experiments indicate that the interaction of RBM4 and Ago2 is facilitated by the N-terminal and PIWI domains of Ago2 while the minimal Ago2-binding RBM4 fragment comprises the Zn finger-domain and one RRM domain (presumably RRM2) as well as the second linker domain L2.

2.3.4. Effects of RBM4 on RISC activity, Dicer activity and binding

As depicted in Figure 33, RBM4 interacts with the PIWI domain of Ago2. Interestingly, it has been shown that Dicer binding to Ago takes place at the PIWI domain as well (Tahbaz et al., 2004). Therefore, we tested whether RBM4 binding might interfere with the Ago-Dicer interaction by competing for the binding to the Ago PIWI domain. To address this, RISC and Dicer activities as well as the level of co-immunoprecipitated Dicer were analyzed in presence of recombinant RBM4.
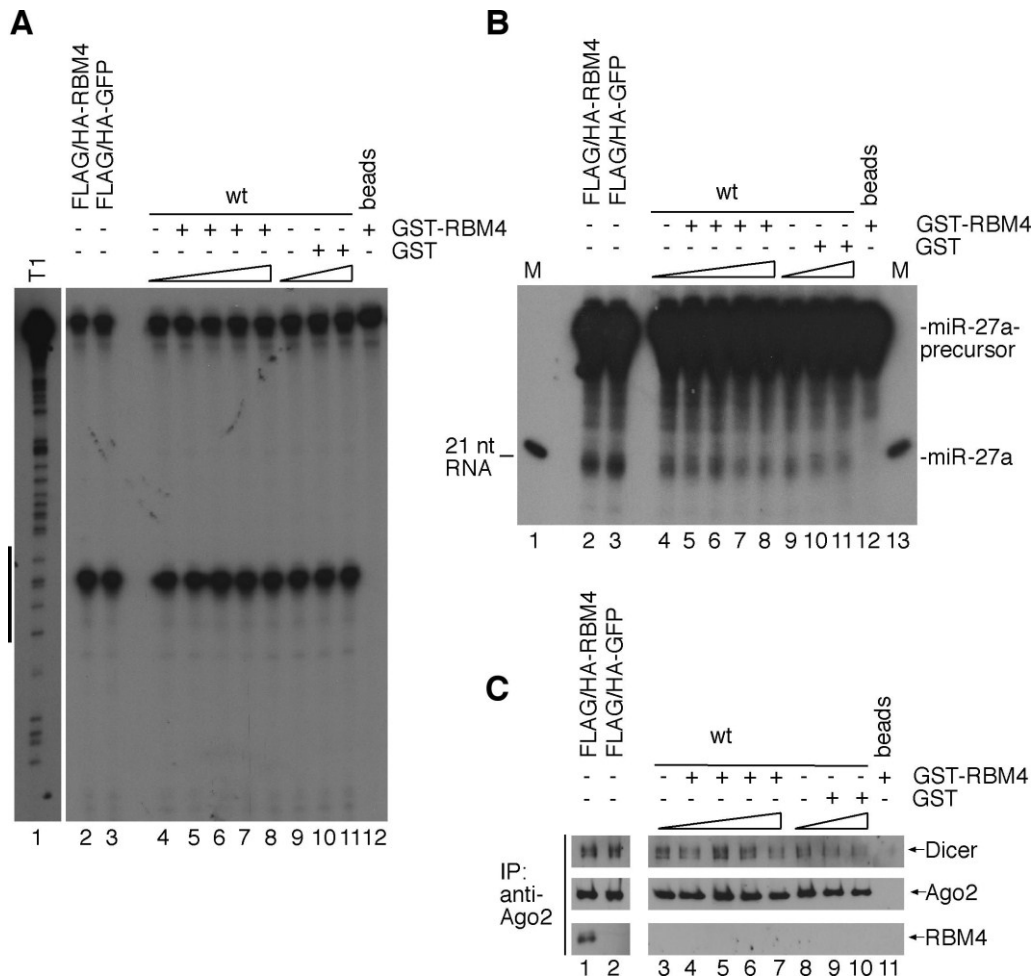
Figure 36: Effect of RBM4 on RISC activity, Dicer activity and levels of Ago-associated Dicer
(A) HEK 293 cell lysates were incubated with varying amounts of GST-RBM4 (lanes 4-8) or GST (lanes 9-11) prior to immunoprecipitation of endogenous Ago2. Ago2 from FLAG/HA-RBM4 or -GFP containing HEK 293 cell lysates (lanes 2 and 3) was immunoprecipitated directly. A RISC assay using a ^{32}P-cap-labeled substrate of miR-19b was carried out as in **(15)**. T1 indicates RNase T1 digestion of the RNA substrate (lane 1). The RNA sequence complementary to miR-19b is indicated by a black bar to the left. **(B)** Immunoprecipitations were performed as in **(A)**. Samples were incubated with an internally ^{32}P-labeled pri-miR-27a substrate and analyzed by RNA PAGE as in **(16A)**. A 21-nucleotide marker is shown to both sides (M). **(C)** Immunoprecipitation was performed as in **(A)**. Samples were analyzed for endogenous Dicer (upper panel), Ago2 (middle panel) and RBM4 (lower panel) by western blotting using specific antibodies.

HEK 293 lysate was incubated with varying amounts of GST-RBM4 prior to immunoprecipitation with antibodies specific to Ago2. Endonucleolytic activity was assayed

by incubation with a ^{32}P-cap-labeled RNA substrate of miR-19b. Samples showed constant RISC activity independent of the level of GST-RBM4 introduced (Figure 36A, lanes 4-8), as did samples that had been pre-incubated with GST alone (lanes 9-11). Also, transient transfection of FLAG/HA-RBM4 (lane 2) did not interfere with endonucleolytic activity compared to the GFP control (lane 3).

The same set of samples was used for assaying Dicer activity. Levels of mature miR-27a remained constant in presence of FLAG/HA- or GST-RBM4 (Figure 36B).

Also, the levels of endogenous Dicer that co-immunoprecipitated with Ago2 did not change upon RBM4 addition as demonstrated by western blotting using specific antibodies (Figure 36C). Notably, GST-RBM4 was hardly detectable by western blotting while overexpressed FLAG/HA-RBM4 clearly co-precipitated with Ago2.

Together, binding of RBM4 to Ago2 did not displace Ago-Dicer interaction. Despite binding of both proteins to the same Ago domain, neither Dicer levels nor its activity was affected by the presence of RBM4. The same is also true for Ago2 RISC activity, indicating that RBM4 function in relation to Ago proteins is restricted to transcriptional and/or translational regulation.

2.3.5. RNA recognition motifs as a potential binding platform for Ago proteins

Besides RBM4, a number of other RRM domain containing proteins were identified by mass spectrometry analysis of Ago1/2 complexes. This implied that RRM-containing proteins might act as a general binding platform for Ago proteins to their target mRNAs, possibly by promoting Ago complex binding or stabilizing an Ago-target mRNA interaction.

To further examine the role of RRM domains in Ago binding, three proteins, which had been validated as Ago interactors by co-immunoprecipitation experiments (see Figure 22), were recombinantly expressed as GST fusion proteins (schematic depiction in Figure 37A). Moreover, the corresponding deletion mutants lacking the RRM domain were created.

In vitro pull-down experiments using GST-IMP3, -SART3 and -Matrin3 together with ^{35}S-labeled His-Ago2 could not confirm the hypothesis that protein binding to Ago is generally mediated by the RRM-domain. Recombinant expression of GST-Matrin3 and its deletion mutant was not efficient, as observed by coomassie staining (Figure 37B, lanes 5 and 6, lower panel); still, an interaction with Ago2 could not be detected at all (lanes 5 and 6, upper panel), not even by long-term film exposure (not shown). GST-IMP3 as well as GST-SART3 interacted strongly with His-Ago2, though (lanes 3 and 7). However, deletion of the RRM domain from these proteins did not prevent their interaction with Ago2 (lanes 4 and 8), indicating that in these cases the RRM domain is not essential for Ago binding.
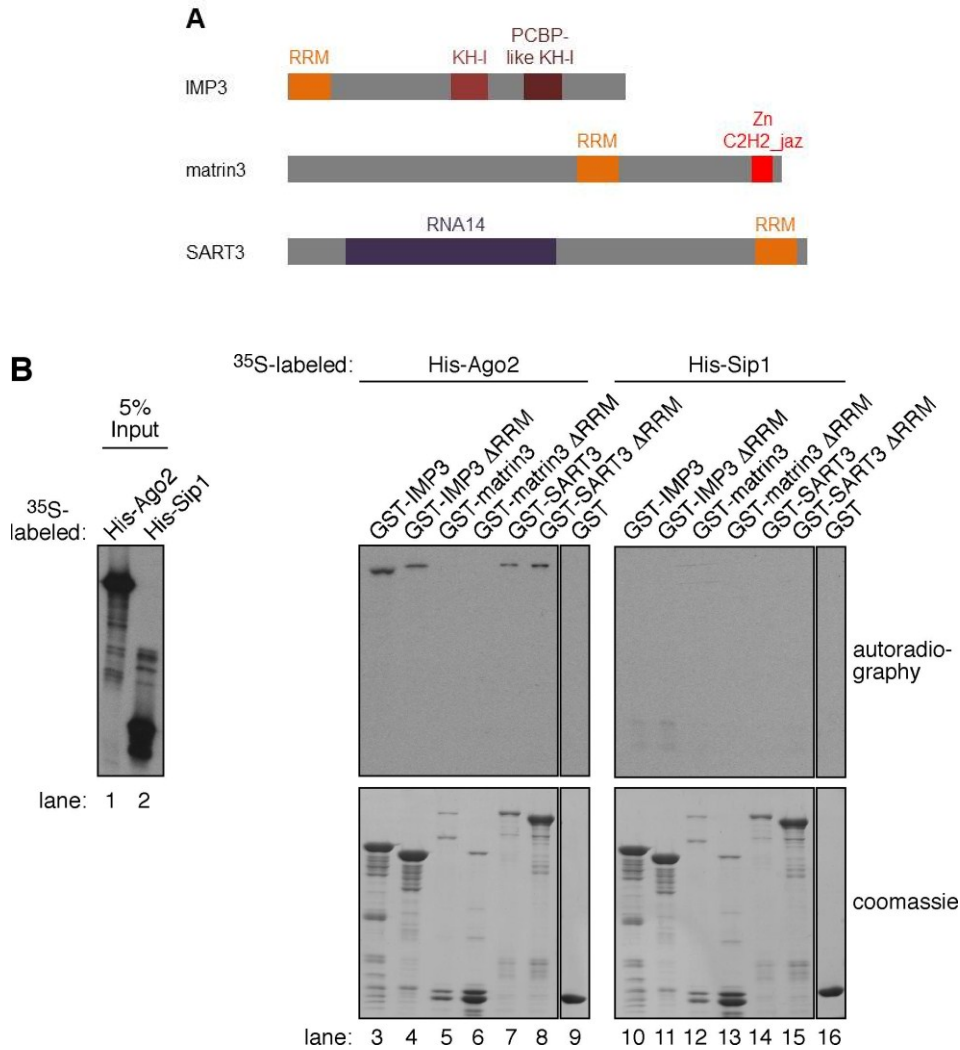
Figure 37: General influence of RRM domains on Ago binding
(A) Schematic depiction of Ago-interacting proteins. **(B)** GST-IMP3, -Matrin3, -SART3 and the respective RRM-deleted mutants as well as GST alone were immobilized on Glutathione sepharose and incubated with *in vitro* transcribed His-Ago2 or -Sip1. Protein separation and detection was performed as described in **(23)**.

2.3.6. Sequence and structure analysis of the RBM4 RNA recognition motifs

While RRM domains apparently do not generally act in Ago binding, the aforementioned results still indicate that Ago binding to RBM4 requires the RRM domain 2 of RBM4, while the RRM domain 1 is dispensable. This could point towards distinct functions of the individual RRM domains, with RRM1 binding the target mRNA and RRM2 acting in protein-protein-interaction with Ago.

Generally, three different forms of RNA recognition motifs are distinguished: canonical and non-canonical RNA binding RRM domains as well as protein-binding RRM domains (Table 3, Maris et al., 2005; Eulalio et al., 2009b). As these forms differ in structure and sequence, the analysis of both RRM domains of RBM4 might provide closer insight on their function. The

structure of the complete RBM4 protein has not yet been published. However, the structure of both RRM domain 1 and 2 is available from the Protein Data Bank (PDB IDs: 2DGT and 2DNQ, respectively).
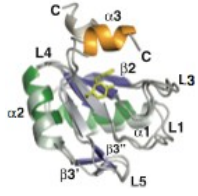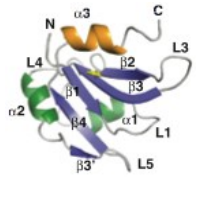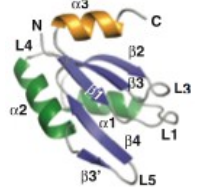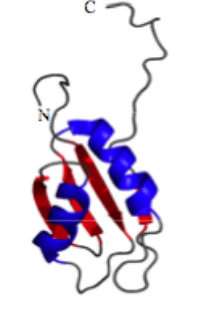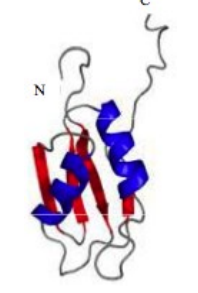
As characteristic for RNA recognition motifs, both RRM domains of RBM4 fold into a $\beta_1\alpha_1\beta_2\beta_3\alpha_2\beta_4$ topology in solution, with a four-stranded antiparallel β-sheet flanked on one side by two α-helices (Table 3; Maris et al., 2005). An additional third α-helix α_3, as described for a number of RRM domains, is not visible from the structure models.

Canonical RNA-binding RRM domains are characterized by two conserved sequence areas, RNP1 (ribonucleoprotein domain 1) ([RK]-[G]-**[FY]**-[GA]-**[FY]**-[ILV]-[X]-[FY]) on β-strand β_3 and RNP2 ([ILV]-**[FY]**-[ILV]-[X]-[N]-[L]) on β-strand β_1, providing aromatic side chains to the surface of the β-sheet (positions depicted in bold; Maris et al., 2005) and thereby allowing for interaction with nucleic acids. In protein-binding RRMs as well as in non-canonical RNA-binding RRMs, these aromatic residues are often replaced by aliphatic amino acids (Eulalio et al., 2009b).

Comparison of the RRM domains of RBM4 with these conserved sequences revealed that RRM1 adheres to the sequence motifs very well, with all three aromatic residues in place. The RNP1 motif of RRM2 matched the classical motif as well, while the aromatic residue in position 2 of the RNP2 was missing.

This rather points towards an RNA- or RNA/protein binding function of the RRM2 of RBM4, however, structural analysis of the RRM2 in complex with interacting proteins as Ago2 could clarify the exact binding properties of this domain.

Table 3: RRM domains - different interaction modes

RRM binding properites	Protein name	PDB-ID	ribonucleoprotein domain 1 (RNP1)	RNP2	RRM structure	Reference
RRM binding motif			[RK]-[G]-[**FY**]-[GA]-[**FY**]-[ILV]-[X]-[FY]	[ILV]-[**FY**]-[ILV]-X-N-L		Reviewed in Maris et al., 2005
Canonical RNA binding	U1A	1FHT/ 1URN	R-G-**Q**-A-**F**-V-I-F	I-**Y**-I-N-N-L		Nagai et al., 1990; Oubridge et al., 1994; Avis et al., 1996
Non-canonical RNA binding	hnRNP F (qRRM1)	2HGL	S-G-**E**-A-**F**-V-E-L	V-K-L-R-G-L		Dominguez and Allain, 2006
Protein binding	*Dm* GW182	2WBR	Q-G-**I**-A-**L**-C-K-Y	L-**L**-L-K-N-L		Eulalio et al., 2009
	RBM4 RRM1	2DNQ	K-N-**Y**-G-**F**-V-H-I	L-**F**-I-G-N-L		PDB
	RBM4 RRM2	2DGT	K-D-**Y**-A-**F**-V-H-M	L-**H**-V-G-N-I		PDB

64

2.3.7. Validation of translational effects of RBM4 on reported targets

To identify further common mRNA targets of RBM4 and Ago proteins and to analyze RBM4-Ago interactions on target mRNAs in detail, the 3'-UTRs of human Period1 (Per1), Flotillin1 (FLOT1) and Ras homolog C (RhoC) were cloned into a luciferase reporter construct. It was shown by others before that Per1 expression is translationally regulated by RBM4 (Kojima et al., 2007). FLOT1 and RhoC have been identified as targets of RBM4 as well (Lin and Tarn, 2005).

MiRNA target prediction by TargetScan and PicTar implied that all three 3'-UTRs should be targeted by a number of miRNAs as listed in Table 4. Thus, Ago proteins should associate with these 3'-UTRs.

Table 4: Predicted miRNA-binding sites within the 3'-UTR of RBM4 targets

mRNA	RBM4 binding site	Reference	Predicted miRNA binding sites
Per1 3'-UTR	5'-UAUUUUUUUUUUUAA-UACAAAAUGACAAAAU-3'	Kojima et al., 2006	miR-15b, miR-24, miR-29a/b/c, miR-133b, miR-136, miR-146a/b, miR-185
FLOT1 3'-UTR	5'-GCUCCCCUUG-3'	Lin and Tarn, 2005	miR-31, miR-124, miR-506
RhoC 3'-UTR	5'-GCCUUUCCUA-3'	Lin and Tarn, 2005	miR-17-5P, miR-20a/b, miR-93, miR-106a/b, miR-138, miR-142-5P, miR-302a/b/c/d, miR-372

To validate the 3'-UTRs as Ago targets, several of the listed miRNAs were inhibited by transfection of 2'OMe-antisense oligonucleotides. Values were normalized to those of HeLa cells not subjected to 2'OMe-treatment (untransf.). Moreover, 2'OMe-oligonucleotides against GFP and the Epstein Barr virus miRNAs BART5 and EBV-3P were used as controls. Surprisingly, miRNA inhibition did not have an effect on the expression levels of either reporter construct (Figure 38A, upper panels and lower left panel), even though - according to information from *Ambion* - some of the tested miRNAs are supposed to be moderately to strongly expressed in HeLa cells (http://www.ambion.com/techlib/resources/miRNA/expression.html). HMGA2, which served as a positive control, was strongly up-regulated upon let-7a inhibition (Figure 38A, lower right panel), indicating that transfection was efficient.
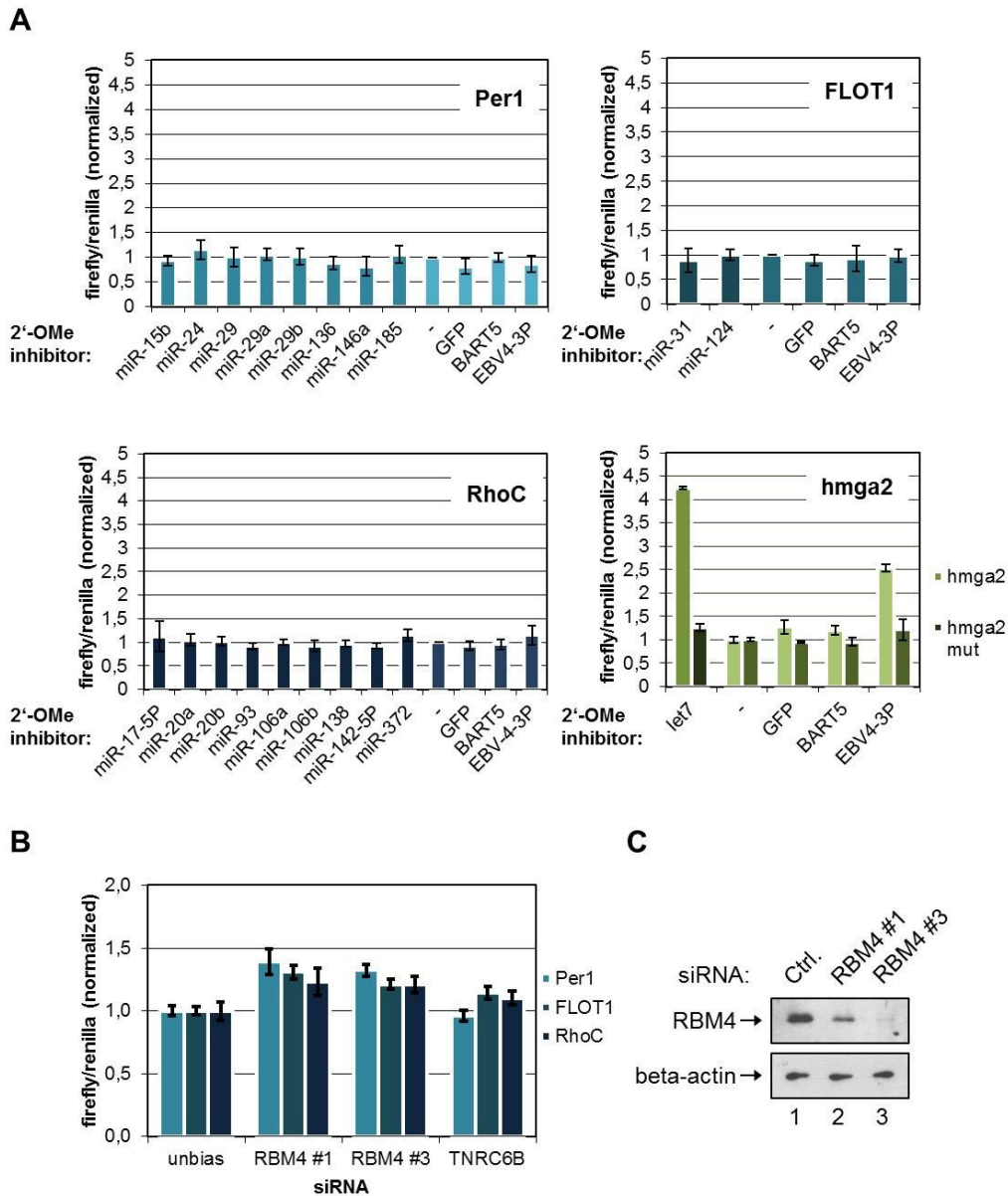
Figure 38: RBM4-mediated regulation of reported mRNA targets
(A) 2'OMe inhibitors to the indicated miRNAs were co-transfected into HeLa cells together with pMIR-RNL-Tk luciferase constructs carrying the 3'-UTRs of Per1 (upper left panel), FLOT1 (upper right panel), RhoC (lower left panel), HMGA2 (lower right panel) and a mutated HMGA2 3'-UTR sequence lacking let-7a binding sites (mut, lower right panel) as in **(27A)**. **(B)** SiRNAs against the indicated proteins were pre-transfected into HeLa cells. After 2 days, pMIR-RNL-Tk reporter constructs carrying the Per1-, FLOT1- and RhoC 3'-UTRs were transfected and luminescence was measured 96 h after the first transfection. Luciferase assays were done in triplicates. Results were normalized to those of the empty vector. **(C)** HeLa cells were transfected with the indicated siRNAs and lysed after 96h. Lysates were subjected to western blotting using antibodies against RBM4 (upper panel) and beta-actin (control, lower panel).

Nevertheless, regulation of Per1-, FLOT1- and RhoC 3'-UTR reporter constructs was also analyzed in an RBM4 knock-down background (Figure 38B). While depletion of RBM4 was efficient (Figure 38C, upper panel, lanes 2 and 3), the luciferase signal was not significantly increased (Figure 38B). Hence, RBM4 knock-down could not be shown to interfere with translation regulation of these mRNAs in the utilized system. Notably, also TNRC6B

depletion did not influence luciferase levels, arguing again against miRNA-mediated regulation of Per1-, FLOT1- and RhoC 3'-UTRs. Together, this suggests that miRNA target site prediction on these mRNAs was not accurate and the analyzed 3'-UTRs were not regulated by the examined miRNAs. Still, in these cases RBM4 might exert its function via one of its additional regulatory pathways.

2.3.8. Putative RBM4 binding motifs and their effect on translation

A number of studies have been published concerning the RNA binding preferences of RBM4; however, their results are controversial. The Tarn lab reported a CU-rich RBM4 binding motif (Lin and Tarn, 2005), while analysis of RNA targets of the *Drosophila* homolog LARK pointed towards an A-rich binding element containing one or more ACAAA motifs (Huang et al., 2007). A systematic analysis of RNA binding specificities of several RNA binding proteins, however, showed a binding preference of RBM4 towards GC-rich sequences within an unstructured sequence context (Ray et al., 2009; Kazan et al., 2010).

Table 5 summarizes K_D values obtained by anisotropy measurements of the RBM4 Δ4 (RRM2-L2-Zn finger) fragment together with 6-FAM labeled CU-rich RNA fragments (Ströh, 2009). However, binding of GC-rich RNAs to RBM4 Δ4 was not analyzed in this experiment.

Table 5: Anisotropy measurements with RBM4 Δ4 fragment

RNA	sequence	K_D value (µM)
RNA A	5'-GGUCUCUCUG-3'	25.4 ± 1.3
RNA B	5'-UAGGGAACC-3'	-
RNA C	5'-UGCUCUUUA-3'	49.1 ± 4.1
RNA D	5'-CACAUUCCA-3'	-
RNA E	5'-AAAAUUAA-3'	-

In order to analyze the effect of different RNA motifs on translational regulation of RNA, luciferase reporter constructs were created, carrying a miR-21 binding site and a putative RBM4 binding motif within a 190 nt random DNA sequence in 3'-position of the luciferase ORF. As controls, constructs carrying a control RNA (crtl. I) and additionally a mutated miR-21 binding site (ctrl. II) were used. Sequences of the tested putative RBM4 binding motifs and reporter constructs are schematically depicted in Figure 39A.
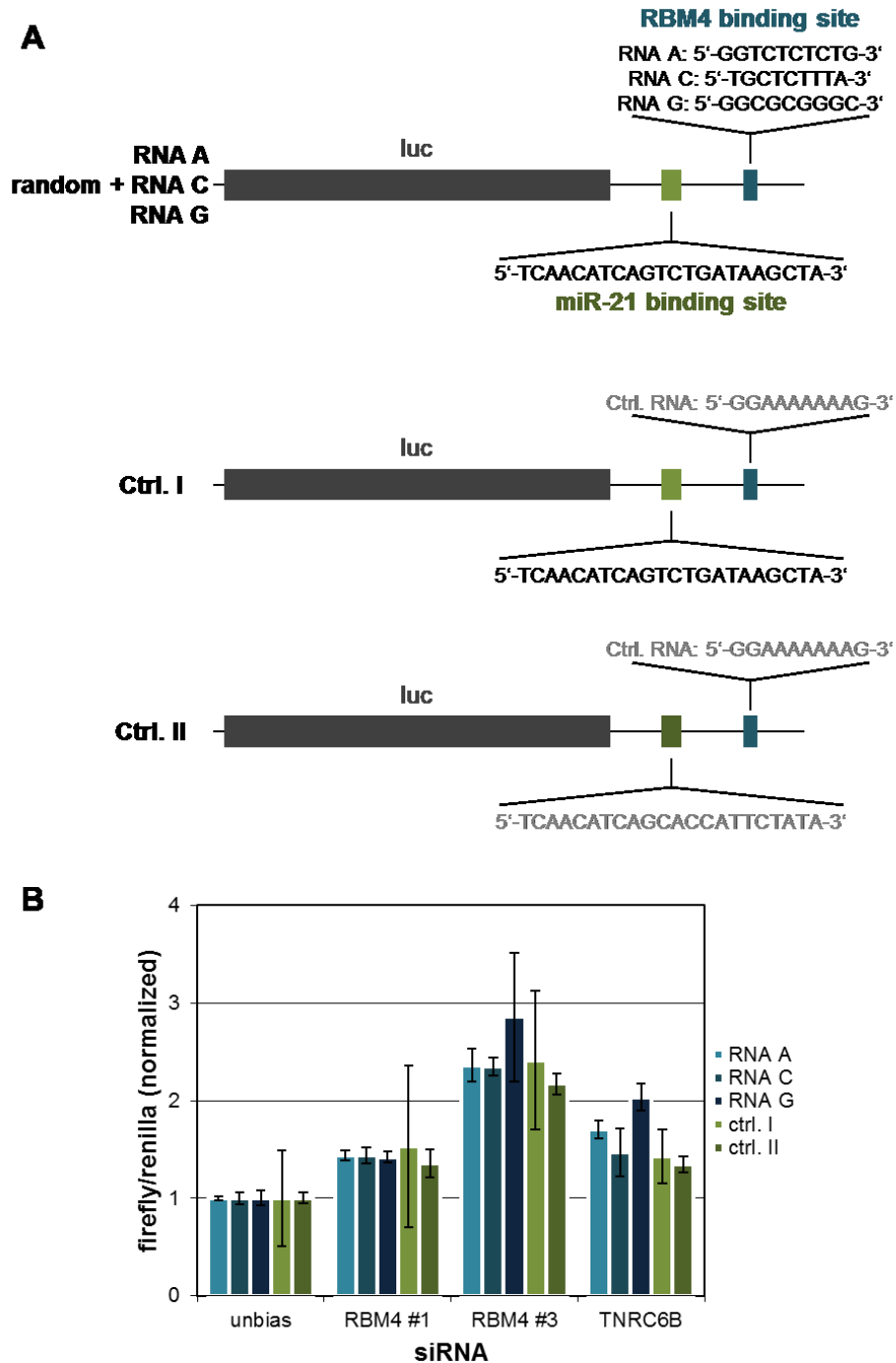
Figure 39: Regulation of an artificial RNA target by both RBM4 and Ago
(A) Schematic depiction of luciferase constructs carrying a miR-21 binding site as well as a potential RBM4 binding motif (as indicated) within a 190 nt random DNA sequence in 3' position to the luciferase ORF (upper panel). Control constructs either lack the RBM4 binding site (ctrl. I, middle panel) or additionally carry a mutated miR-21 binding site (ctrl. II, lower panel). **(B)** pMIR-RNL luciferase constructs indicated in **(A)** were transfected into HeLa cells depleted for the indicated proteins. Luminescence was measured 96 h after siRNA transfection. Luciferase assays were done in triplicates. Results were normalized to those of the empty vector.

Transfection of the constructs into RBM4- or TNRC6B-depleted HeLa cells caused a moderate to strong increase of the luciferase signal. However, this was also true for the control constructs, indicating that this effect was not specific for Ago and RBM4 binding (Figure 39B).
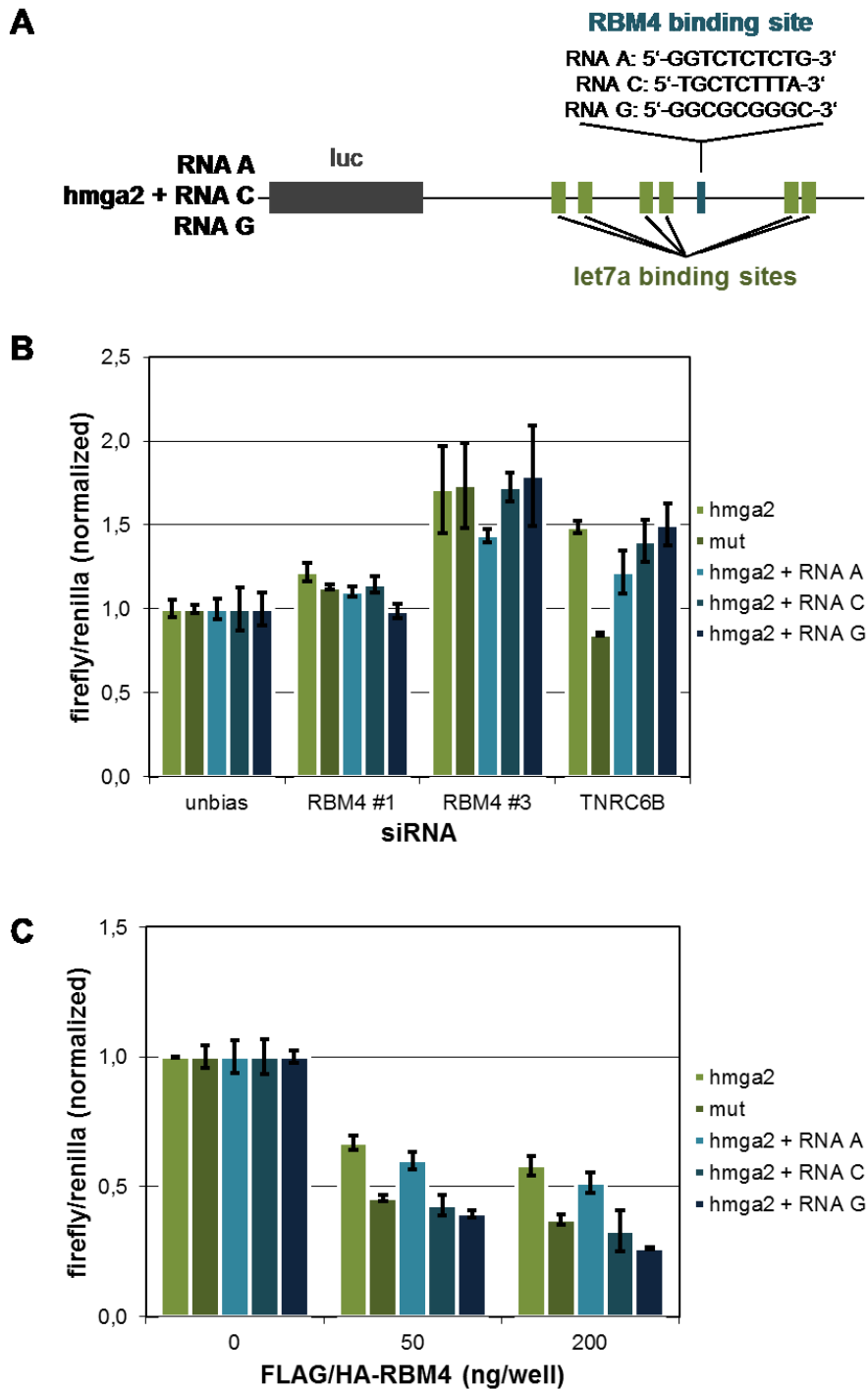
Figure 40: Effects of the introduction of a putative RBM4 binding site into the HMGA2 3'-UTR
(A) Schematic drawing of luciferase reporter constructs carrying a modified HMGA2 3'-UTR with an artificially inserted potential RBM4 binding motif. Residual let-7a binding sites are indicated in green, the position of the respective RBM4 binding motif is indicated in blue. **(B)** Experiments were performed as in **(39B)**. HMGA2 3'-UTR, a mutated HMGA2 3'-UTR lacking let-7a binding sites (mut) as well as the constructs indicated in **(A)** were transfected. **(C)** The indicated amounts of a FLAG/HA-RBM4-encoding plasmid were co-transfected into HeLa cells together with the indicated luciferase reporter plasmids. Luciferase assays were done in triplicates 48 h after transfection. Results were normalized to those of the empty vector.

To place the putative RBM4 binding sites into a more natural context, the respective RNA motifs were cloned into the HMGA2 3'-UTR (Figure 40A). Transfection of the constructs into

RBM4-depleted HeLa cells produced an up-regulation with siRNA #3. However, this effect was indiscriminate of the introduced RBM4 binding motifs and even the mutated let-7a binding sites, indicating that in the current position, the RBM4 binding site is not interfering with translational repression and that HMGA2 repression is also maintained in absence of let-7a binding sites under these conditions (Figure 40B), maybe by other miRNAs.

A similar pattern was also detected when RBM4 was overexpressed. As described before for the KRAS reporter construct (Figure 28), overexpression of FLAG/HA-RBM4 resulted in a firefly signal decrease (Figure 40C). This was even more explicit with the constructs carrying the RBM4 binding motifs. However, the signal decrease was also visible when the mutated HMGA2 3'-UTR was transfected.

To analyze whether RBM4 binding to the mRNAs of the HMGA2 reporter constructs containing RBM4 binding motifs was detectable, HEK 293 cells were transfected and lysates were subjected to immunoprecipitation using antibodies specific to RBM4. Co-precipitated RNA was reverse-transcribed and mRNA levels were quantified by qPCR (Figure 41). Indeed, enrichment of HMGA2 mRNA containing RNA A or RNA G was detected while HMGA2 +RNA C mRNA levels equaled those of HMGA2 alone. The mutated HMGA2 mut mRNA was only slightly enriched.
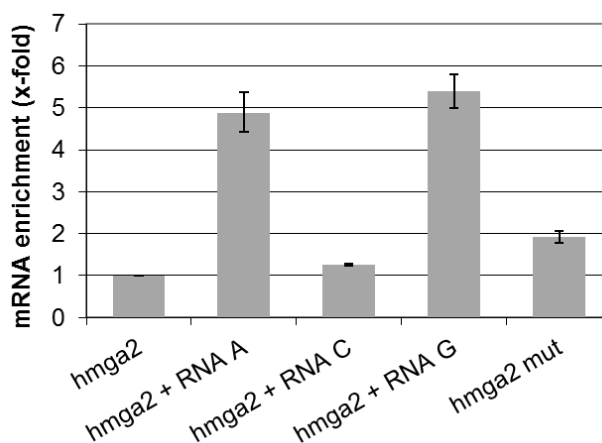
Figure 41: Binding of RBM4 to modified HMGA2 reporter mRNA
HeLa cells were transfected with the pMIR-RNL luciferase constructs from **(40)**. After 48h, cells were lyzed and lysates were subjected to immunoprecipitation using α-RBM4 antibodies. RNA was isolated from the beads and reverse transcribed. cDNA was amplified by qPCR with primers specific to the firefly luciferase ORF. mRNA levels were normalized to those of renilla luciferase mRNA.

This is to a certain degree consistent with the aforementioned anisotropy results, as RNA C binding to RBM4 Δ4 was weaker than that of RNA A. RNA G binding had not been tested with this method.

Together, these results indicate that RBM4 shows an affinity to the GC-rich RNA G sequence. It also binds the RNA A motif which is CU-rich, but flanked by G residues. RBM4 binding might therefore also be influenced by the presence of these G residues, as significant binding to RNA C, which predominantly consists of U residues, was not detected. However, an effect on miRNA-mediated translational regulation could not be shown, indicating that the sequence context might be important for RBM4 function as well.

Thus, it would be interesting to identify common targets of RBM4 and Ago proteins in an *in vivo* context allowing for a detailed analysis or their interaction on a target mRNA. First attempts on this behalf have been made using the PAR-CLiP method (Hafner et al., 2010) in collaboration with Mihaela Zavolan (University of Basel). However, experimental conditions of this method will have to be further modified in order to gain information on potential target mRNAs.

In summary, RBM4 was found to influence Ago function in luciferase systems using artificial as well as natural 3'-UTR constructs. It strongly interacted with all four human Ago proteins, specifically via the Ago PIWI and – to a smaller extent – also the N-terminal domain. RBM4 binding to the Ago PIWI domain did not interfere with Dicer binding to the same domain. RBM4 binding to Ago was mediated by the second RNA recognition motif (RRM2), the Zinc finger domain and the intermediate linker region, while the N-terminal RRM1 was dispensable for Ago interaction. However, distinct functions of the two RRM domains with respect to RNA or protein binding properties could not be deduced from sequence or structure of the isolated domains. Also, despite the considerable number of RRM containing proteins identified in Ago complexes, a general function of the RRM domain in Ago interaction could not be demonstrated. MiRNA effects on some known RBM4 targets could not be verified by a luciferase reporter approach, even though miRNA target prediction programs produced a number of potential miRNA binding sites in the 3'-UTRs of the respective transcripts. Different RBM4 RNA binding motifs were tested in combination with miRNA binding sites in completely and partially artificial luciferase constructs. However, the requirements of efficient RBM4-Ago cooperation seem to be more complex and could not be efficiently mimicked. The sequence of the preferred RNA binding motif of RBM4 is still controversial. Therefore, additional experiments such as the PAR-CLiP approach will be necessary for a closer analysis of RBM4 binding preferences on target mRNAs also common to Ago proteins. Further, the identification of common RBM4 and Ago targets may allow for detailed investigation of the molecular interaction mechanism of RBM4 and Ago proteins.

3. DISCUSSION

While small RNAs have become a widespread tool in the molecular analysis of proteins, many details about their endogenous functions in mammals are still elusive.

Ago proteins directly interact with small RNAs and constitute the core of small RNA guided effector complexes. The regulation of their various functions presumably involves a large number of regulatory proteins. In order to analyze factors interacting with Ago proteins to facilitate regulation of gene expression, this work aimed at the identification and characterization of human Ago protein complexes using biochemical and proteomic approaches.

3.1. CHARACTERIZATION OF HUMAN AGO COMPLEXES

In a first approach, the incorporation of Ago proteins into protein complexes with distinct molecular weight was examined. Sucrose gradient results indicate that both Ago1 and Ago2 reside in three distinct protein complexes ranging from about 11S to more than 30S. While all three complexes contain miRNAs, they differ in Dicer- and RISC activities. Moreover, both Ago1 and -2 were also detected in the low molecular weight fractions of gradients from nuclear extracts, underlining a role for Ago proteins in nuclear processes. This finding is consistent with observations by Ohrt and colleagues, who demonstrated the existence of a small nuclear Ago-containing complex of about 158 kDa in addition to a large cytoplasmic complex (about 3 MDa) using fluorescence correlation and cross-correlation spectroscopy (Ohrt et al., 2008).

The smallest cytoplasmic Ago complex, termed complex I, contains the largest Ago portion and has a molecular weight of about 250-350 kDa. It is characterized by RISC- as well as Dicer activity and is insensitive to RNase treatment. Complex III, sedimenting at a molecular weight of more than 900 kDa, is associated with Dicer activity only. Further, it co-migrates with a miRNA target mRNA implying that Ago complex III consists of miRNA-regulated mRNPs. Consistently, both complex III and the smaller complex II (~600-700 kDa) are RNase sensitive. Complex II, however, is lacking Dicer and subsequently miRNA processing abilities as well as RISC activity. Hence, it may contain a Dicer-free miRNP population, for which also the size difference could account. However, further experiments will be necessary to investigate its functional relevance.

3.2. IDENTIFICATION OF AGO INTERACTION PARTNERS BY A PROTEOMIC APPROACH

As a first approach, the incorporation of Ago proteins into protein complexes with distinct molecular weights was analyzed. Mass spectrometric analysis of pooled Ago complex fractions identified a large number of proteins associated with Ago1 and Ago2. Besides proteins that were known to participate in gene silencing, a major number of identified proteins could be assigned to the DEAD/DExH-box or heterogenous nuclear ribonucleoprotein (hnRNP) families. These two RNA binding protein families show high functional diversity and act on all aspects of eukaryotic RNA metabolism, including pre-mRNA splicing, ribosome biogenesis, mRNA export, regulation of translation and mRNA degradation (Linder, 2006; Han et al., 2010). Furthermore, the majority of the remaining proteins can be assigned to mRNA binding and RNA metabolism as well.

Interestingly, size addition of the proteins identified in Ago complex I would suggest a much bigger complex than 250-350 kDa, as was observed in the sucrose gradients. Indeed, complex I can be further subdivided into three complexes referred to as complex Ia-c with distinct RISC- and Dicer activities. Complex Ia probably contains a Dicer-free minimal RISC of about 200 kDa (Martinez et al., 2002; Haley and Zamore, 2004), hence it is able to cleave an RNA substrate but lacks Dicer activity. Complex Ib associates with Dicer as well as RISC activity and presumably corresponds to a trimeric Ago-Dicer-TRBP complex (Gregory et al., 2005). In complex Ic, Ago might interact with other proteins identified by mass spectrometry.

In *Drosophila*, an 80S Ago containing protein complex has been described which is endonucleolytically active and hence was termed "holo-RISC" (Pham et al., 2004). This holo-RISC complex contains Dicer2, its function within the complex, however, remains unclear. In this work, a human Ago complex, termed complex III, was identified sedimenting with a S value of approximately 30-40. Strikingly, Ago complex III also associates with Dicer and is capable of generating mature miRNAs from pre-miRNAs. Yet, in contrast to *Drosophila* holo-RISC, Ago2 complex III exhibits no RISC activity. This observation might be explained by association of the miRNA-containing Ago complexes with target mRNAs resulting in the formation of silenced mRNPs. While being loaded with a target mRNA, miRNA binding to an exogenous target RNA and its subsequent cleavage may not be possible. Consistent with this model, the known let-7a target KRAS (Johnson et al., 2005) was found to co-migrate with Ago complex III in sucrose gradients. In combination with the large number of co-purified RNA binding proteins, this observation indicates that Ago complex III consists of a variety of large mRNPs that contain presumably translationally repressed miRNA target mRNAs. Consistently, a number of proteins sedimenting in Ago complex III have been reported to be associated with mRNPs and also with small RNA function in different organisms.
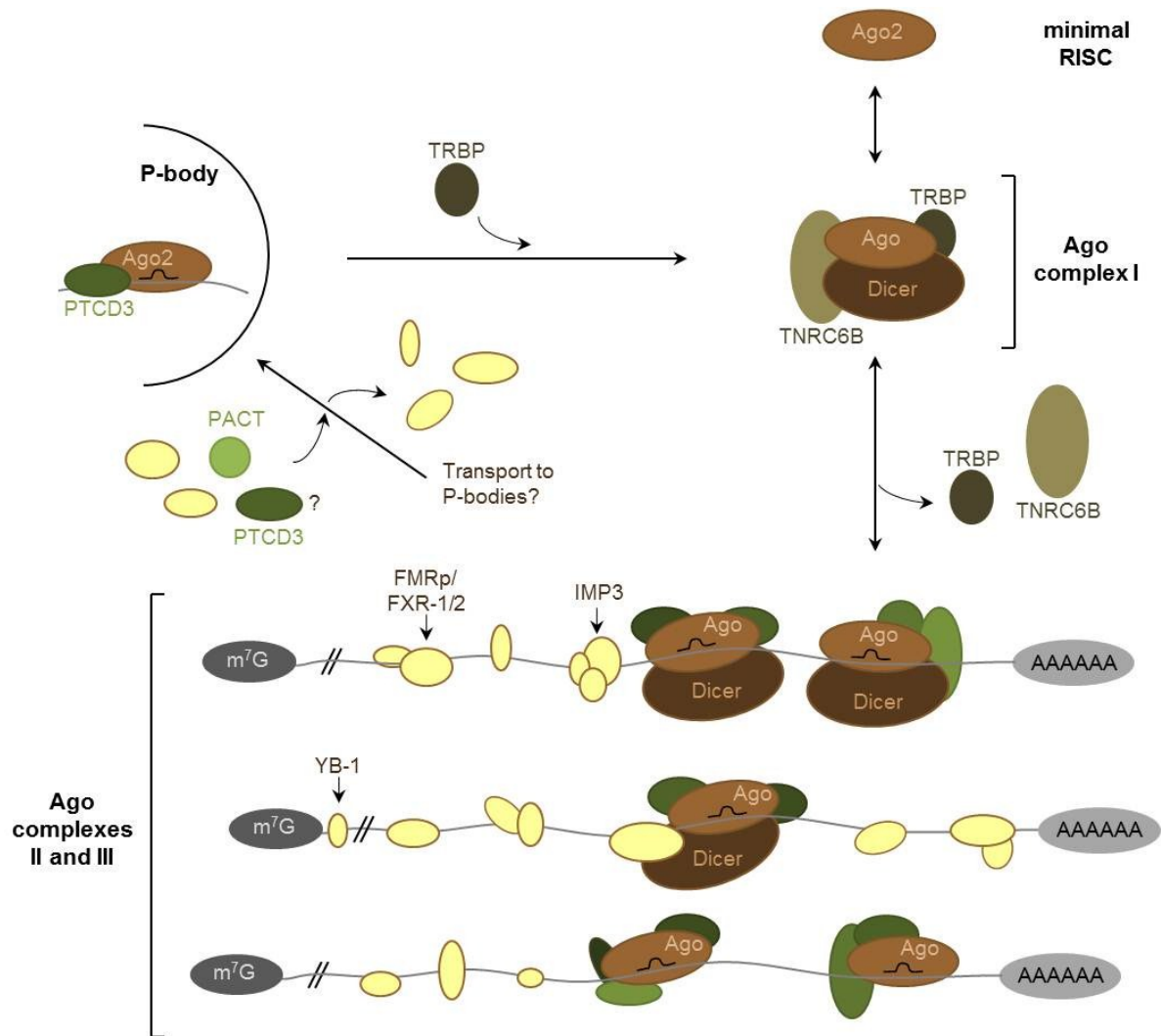
Figure 42: Model of Ago protein complex organization in the cytoplasm of mammalian cells

Among the DEAD/DExH-box containing proteins that co-purified with Ago was DDX5, an orthologue of *Drosophila* p68, which has been identified as a component of the Drosha-containing microprocessor complex together with hnRNP U, hnRNP U-like, and the heterodimer NF-90/NF-45 (Gregory et al., 2004). Interestingly, NF-90 possesses a dsRNA binding domain and has been reported to play a role in the nuclear export of viral stem-loop structured RNAs. Further, it associates with Exportin 5, the nuclear export factor that facilitates pre-miRNA transport to the cytoplasm (Gwizdek et al., 2004). Moreover, NF-90 has also been implicated in translation regulation of specific mRNAs (Shi et al., 2005). It is therefore conceivable that NF-90 might be involved in nuclear miRNA maturation and subsequent export as well as in miRNA function in the cytoplasm.

Previous data had already shown that Gemin3 and -4 co-sediment with a 15 S complex together with miRNAs and Ago proteins (Mourelatos et al., 2002). Also, DDX18 had been implicated in Drosha function before, presumably with a helicase function (Gregory et al., 2004). Consistently, these proteins were also detectable in the present study. Furthermore,

RNA helicase A (RHA/DHX9) has been demonstrated to be required for RISC formation and effective silencing of cognate mRNAs (Robb and Rana, 2007). Strikingly, DDX6, another DEAD-box helicase that was reported to be required for miRNA function (Chu and Rana, 2006), was not among the identified Ago interaction factors.

Besides its function in nonsense-mediated decay, UPF1 has been shown to target correct mRNAs to P bodies (Sheth and Parker, 2006) and to interact with the mRNA decapping enzymes DCP1 and DCP2. Notably, the present co-immunoprecipitation experiments point towards an RNA-independent interaction between UPF1 and Ago1/2, hence it would be tempting to speculate that the function of UPF1 in P bodies is closely connected to the miRNA pathway.

Mass spectrometry analysis also detected DHX36 (RHAU), a DExH-box protein involved in deadenylation of AU-rich mRNAs (Tran et al., 2004). It has been reported that miRNAs are involved in deadenylation of specific mRNAs in Zebrafish as well as in mammals (Giraldez et al., 2006; Wu et al., 2006). DHX36 could therefore be an Ago associated factor that recruits the deadenylation machinery to specific miRNA targets. Interestingly, among the Ago interactors tested for co-immunoprecipitation with Ago1 and -2, DHX36 was the only protein that showed a distinct binding behavior: while interaction with Ago2 was insensitive to RNase treatment, the interaction with Ago1 seemed to be dependent on RNA. Unfortunately, this result could not be confirmed in *in vitro* pull-down experiments, where DHX36 associated indiscriminately with all four Ago proteins. Still, this *in vitro* observation could be due to the absence of further interaction partners and may not reflect the actual protein interplay within the cell.

Besides DEAD/DExH box-containing proteins, poly(A)-binding proteins and a large number of mRNA binding proteins involved in translation, such as YB-1, IMP1 and -3, HuR and FMRp as well as its homologues FXR1 and FXR2, were present in the analysis.

An RNA-binding protein that showed RNA-dependent interactions with Ago1 and -2 in this study was HuR (ELAV1). HuR has been reported to influence the stability of A-rich mRNAs (Eberhardt et al., 2007). Moreover, it was shown to release the miR-122 repressed CAT-1 mRNA from cytoplasmic P bodies upon cellular stress and to activate its translation by facilitating its entry into polysomes (Bhattacharyya et al., 2006a). The Y-Box binding protein 1 (YB-1) competes with the eIF4E-translation initiation complex for the binding to the 5'-cap-structures of mRNAs, thereby repressing translation. Further it also seems to stabilize repressed mRNAs in a cap-dependent manner (Evdokimova et al., 2006). Like HuR, YB-1 co-purified with Ago1 and -2 in an RNA-dependent manner. As YB-1 depletion results in an up-regulation of a KRAS 3'-UTR reporter construct, its cooperation with Ago proteins in translational repression seems possible. IMP1 and -3 modulate localization, translation and mRNA stability of their targets (Yisraeli, 2005). Upon environmental stress, IMP1 retains

specific mRNAs in stress granules and prevents their premature decay in P bodies (Stohr et al., 2006).

The human fragile X mental retardation protein (FMRp) as well as its *Drosophila* homologue dFMR associates with Dicer, Ago2, miRNAs and other miRNA pathway components (Caudy et al., 2002; Ishizuka et al., 2002; Jin et al., 2004a; Jin et al., 2004b; Xu et al., 2008). Recently, it was further shown to be involved in the regulation of miRNA maturation as phosphorylation of FMRp precludes its binding to Dicer and results in an accumulation of 80 nt RNA species, presumably pre-miRNAs (Cheever and Ceman, 2009). Consistently, FMRp and also FXR2 were found in Ago complex III which shows Dicer activity. However, this would rather suggest that FMRp and FXR2 associate with large translationally silenced mRNPs. FXR1, on the other hand, has been shown to enhance translation of AU-rich mRNAs together with Ago2 under specific cellular conditions (Vasudevan and Steitz, 2007). Interestingly, FXR1 is also present in our mass spectrometry data supporting the concept that Ago proteins interact with a variety of mRNPs and within such an interaction network specific proteins influence Ago activity.

Notably, a number of proteins were identified with only one of the two Ago proteins. Especially mentionable is SART3, a protein implicated in pre-mRNA splicing and transcriptional regulation (Bell et al., 2002). SART3 was found with a comparatively high number of matched peptides in all three Ago1 complexes, but not at all with Ago2. Co-immunoprecipitation approaches suggested a RNA-independent interaction. An exclusive binding to Ago1, however, could neither be verified by co-immunoprecipitation nor by *in vitro* pull-down experiments. The same is true for other proteins that seemingly co-purified with only one Ago protein. Further, it cannot be excluded that overexpression of tagged proteins in some cases interferes with endogenous interaction behavior.

Generally, the present mass spectrometry data in combination with verifying experiments suggest that Ago1 and Ago2 bind a highly similar set of proteins. This is also affirmed by mass spectrometry data from another study on Ago3 and Ago4, though in this case analysis was restricted to visible protein bands in the SDS PAGE gel and therefore confines to a restricted view on associated protein factors (Weinmann et al., 2009).

Meanwhile, proteins associated with Ago1-4, Dicer and TNRC6A-C as well as bound mRNAs were analyzed in another study (Landthaler et al., 2008). To a certain degree, its results resembled those of the present study. Besides a large number of hnRNPs, Landthaler and colleagues identified 6 DEAD/DExH-box containing proteins including DDX5 and RHA, but not DDX6, and a number of additional RNA binding proteins, e.g. IMP1 and -3, HuR and YB-1, and protein components of the small and large ribosomal subunits. Co-immunoprecipitation results for YB-1, IMP3 and HuR were consistent with those of the present work. In general, the number of proteins listed in the above study is lower compared

to the present work. This could partly be attributed to differences in sample preparation, e.g. a double purification strategy that may reduce experimental noise but also might interfere with binding conditions thereby eliminating existing Ago-protein interactions. As also observed in the present work, Landthaler et al. report that the set of immunoprecipitated proteins is highly similar for Ago1 through -4. Further, also the set of mRNAs co-purifying with the four Ago proteins is strikingly similar, suggesting that Ago1-4 bind to similar mRNPs. This could also explain the high analogy detected on the proteomic level. Generally, the above study confirms the results obtained by the present work.

Taken together, the present data suggest that miRNA-containing Ago complexes are recruited to miRNA target mRNAs that already carry a variety of different mRNA binding or regulatory proteins (Figure 42). Depending on the composition of such cytoplasmic RNPs, these regulatory units are either directed to P bodies or other cellular sites. Ago-containing miRNPs therefore contribute to a global mRNA regulatory network which is unique to each individual mRNA. MiRNP complexes are probably highly dynamic structures that are constantly rearranged in order to determine the fate of a given mRNA in response to environmental or cellular signals. *Trans*-acting factors establish a regulatory network that is able to fine-tune the translational regulation of specific mRNAs. Ideally, an investigation of miRNA function will therefore have to include the analysis of the whole protein network associated with a given mRNA.

3.3.   PTCD3 AS A NOVEL P BODY COMPONENT

PTCD3, a member of the pentatricopeptide (PPR) domain protein family, was identified in complex II of Ago1 and Ago2. PPR domain proteins constitute a large protein family in plants, located mainly in mitochondria and chloroplasts. They are characterized by a degenerate 35-amino acid motif, repeated in tandem up to 30 times, that are supposed to bind RNA and act as platform for RNA processing complexes (reviewed in Schmitz-Linneweber and Small 2008). In mammals, however, only seven PPR proteins were identified to date, all of which were predicted to be mitochondrial (Holzmann et al. 2008; Lightowlers and Chrzanowska-Lightowlers 2008). Still, a minor portion of the cellular pool of the PPR protein LRPPRC has been found to share RNA targets with hnRNP A1 in the nucleus, indicating a function outside mitochondria (Mili and Pinol-Roma 2003).

The human PTCD3 protein has previously been reported to associate with the small subunit of the mitochondrial ribosome and to be involved in mitochondrial translation (Davies, Rackham et al. 2009). Surprisingly, in our hands, overexpressed PTCD3 co-localized with

co-expressed Ago2 as well as with endogenous Lsm4, indicating its localization in cytoplasmic P bodies. Also, co-immunoprecipitation experiments with overexpressed proteins indicated a RNA-independent interaction of PTCD3 with Ago1 and Ago2. However, PTCD3 depletion did not significantly interfere with luciferase levels of miRNA-regulated reporter constructs (not shown). While immunofluorescence results point towards PTCD3 as a new P body component, this finding will have to be further validated and an endogenous Ago-PTCD3 interaction will have to be characterized functionally to eliminate the possibility that the described observations might be attributed to overexpression.

3.4.   ANALYSIS OF AGO2-RBM4 INTERACTIONS

Prior to this work, RBM4 had been reported to be a primarily nuclear RNA-binding protein with implications in alternative splicing and exon selection (Lai et al., 2003; Lin and Tarn, 2005). Meanwhile, additional roles for RBM4 in translational regulation have been described (Kojima et al., 2007; Lin et al., 2007; Lin and Tarn, 2009).

Co-immunoprecipitation experiments verified the interaction between Ago1/2 and RBM4 identified by mass spectrometry. While RNase treatment decreased signal levels in these experiments, *in vitro* pull-down assays indicated a strong binding of GST-RBM4 to Ago1-4. However, when RNase was included in the pull-down sample, a signal decrease was detectable as well. Since the chosen conditions for the RNase treatment also destroyed Ago-bound miRNAs, this might be attributed to a conformational change in the Ago protein upon target RNA binding which in turn may promote RBM4 binding.

Also, *in vitro* binding to an Ago2 mutant deficient in miRNA binding (paz9; Liu et al., 2005) seemingly contradicts northern blotting results that demonstrate co-precipitation of endogenous miR-19b with FLAG/HA-RBM4 (compare Figure 31B and Figure 32). However, given the low miRNA levels in the RBM4-northern blot sample, co-purified miR-19b probably rather originated from associated endogenous Ago proteins than from direct binding of the miRNA to RBM4.

Sucrose gradient centrifugation revealed that a large portion of endogenous RBM4 co-migrated with Ago complex III and associated mRNPs, which is consistent with a role of RBM4 in translational regulation. Still, RBM4 was also found to co-sediment with Ago complexes I and II. Corresponding with aforementioned reports (Lai et al., 2003; Markus and Morris, 2006), RBM4 was also detected in low-molecular weight fractions of nuclear extracts.

To identify the protein domains involved in binding of Ago2 to RBM4, *in vitro* pull-down experiments were performed with a number of protein fragments and mutants. These studies revealed that on the Ago2 side, interaction is mainly mediated by the PIWI domain, with a

minor additional signal from the N-terminal domain. Within the RBM4 protein, the minimal Ago binding domains include the second RNA recognition motif (RRM2), the CCHC-type Zn finger domain and the intermediate second linker sequence (L2, Figure 43). Pull-down experiments from wild-type HEK 293 lysates using immobilized recombinant GST-RBM4 mutants confirmed the *in vitro* data.
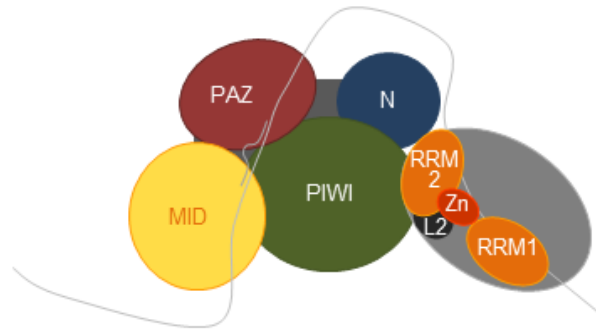
Figure 43: Ago2-RBM4 interaction model on a common target mRNA

Besides RBM4, the Ago2 PIWI domain is also bound by the miRNA-processing enzyme Dicer (Tahbaz et al., 2004). This raised the question whether RBM4 might compete with Dicer for Ago binding due to sterical hindrances. To address this, Ago2 was precipitated from HEK 293 lysates supplemented with various amounts of GST-RBM4 and levels of co-precipitated endogenous Dicer were analyzed. However, no changes could be detected in Dicer levels. Also, neither Dicer- nor RISC activity was altered upon GST-RBM4 addition, indicating that RBM4 binding does not prevent Dicer binding to Ago2 and functions aside small RNA maturation and siRNA-mediated RNA cleavage (Figure 44). Still, Dicer was not very efficient in these assays.

The finding that RBM4 binds to Ago2 via the RRM2-L2-Zn finger domains is in contrast to previous reports, claiming that protein-protein interaction is mediated by the alanine-rich C-terminal domain of RBM4 (Lai et al., 2003). However, previous studies in *Drosophila* stated that the RRM2 as well as the Zn-finger domain of the *Drosophila* homologue LARK are involved in translational repression (McNeil et al., 2001). This would be consistent with a proposed role of this RBM4 part in Ago binding and consequently in miRNA-mediated translational repression.

RNA recognition motifs have been shown to have different RNA and/or protein binding properties depending on their exact sequence and structure (Maris et al., 2005; Eulalio et al., 2009b). Given that a considerable number of proteins identified in the mass spectrometry approach carry RRM domains, it would be tempting to speculate that these domains function as a general binding platform that guides Ago proteins to their target mRNAs. To investigate

the importance of these domains in some of the further identified Ago interactors, *in vitro* pull-down assays were performed with RRM-deletion mutants of SART3, Matrin3 and IMP3. However, no effect on Ago binding could be detected in either of the mutants, indicating that Ago binding is conveyed by structures other than the RRM domain in these proteins.
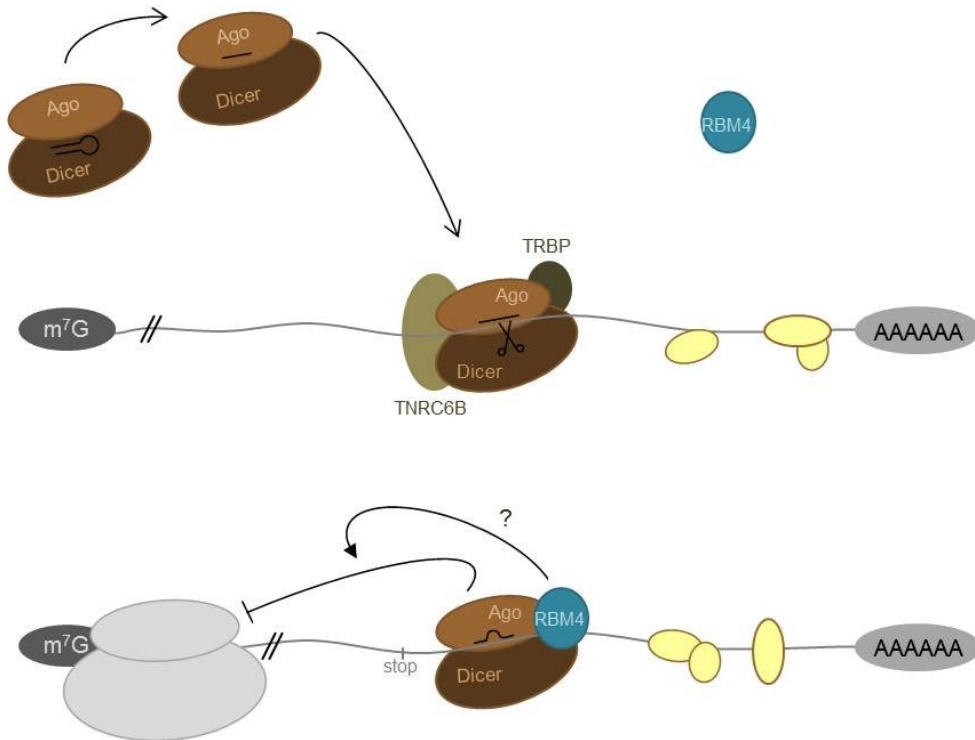
Figure 44: Model of putative RBM4 functions in concert with Ago proteins
RBM4 binds Ago proteins as well as RNA and presumably stabilizes Ago binding to a target mRNA and enhances translational repression. Involvement of RBM4 in small RNA processing or mRNA cleavage was not observed.

To elucidate the exact mode of Ago binding to RBM4 and the function of the individual domains in the RBM4 binding properties, it would now be interesting to perform a structural analysis of Ago or its PIWI domain together with the minimal binding RBM4 fragment (RRM2-L2-Zn finger) on a common target mRNA.

3.5. APPROACHES TO IDENTIFY *m*RNA TARGETS COMMON TO A*GO*2 AND RBM4 PROTEINS

Besides its usefulness for structural investigations, the identification of mRNA targets common to RBM4 and Ago proteins would also be interesting in terms of a closer biochemical characterization of the *in vivo* binding and interaction properties of the proteins.

To demonstrate the functional relevance of RBM4 in miRNA-guided translational regulation, luciferase reporter constructs carrying the 3'-UTR of several Ago targets were used. RBM4 as well as TNRC6B knock-down in these experiments resulted in an increase of the luciferase signal, indicating that RBM4 is indeed involved in translational repression. However, to identify a common RBM4 and Ago target that shows stronger regulation, several additional constructs were tested.

It was shown that the RBM4 homologue LARK regulates expression of the circadian clock protein Period1 (Per1) in mouse by binding to the 3'-UTR of the Per1 mRNA (Kojima et al., 2007). Moreover, the Flotillin1 (FLOT1) and RhoC 3'-UTRs were identified as RBM4 targets (Lin and Tarn, 2005). A miRNA database check revealed several predicted miRNA binding sites in all of these 3'-UTR sequences, suggesting miRNA-guided regulation in addition to RBM4 binding. However, knock-down of RBM4 did not significantly increase luciferase levels. As, furthermore, neither transfection of inhibitory 2'OMe antisense oligonucleotides nor knock-down of TNRC6B – which served as a positive control – showed effects on the luciferase signals, Per1, FLOT1 and RhoC could not be proven to be regulated by the miRNA pathway and therefore seemed unsuitable for further investigations on RBM4-Ago interactions.

Reports about RNA binding preferences of RBM4 are controversial. While Huang et al. claimed that the *Drosophila* homologue LARK precipitated A-rich elements with one or more "ACAAA" motifs, Lin and Tarn identified RBM4 binding to CU-rich RNA elements (Lin and Tarn, 2005; Huang et al., 2007). Based on a newly developed method called "RNAcompete" and subsequent bioinformatical data analysis, the labs of Morris and Hughes identified a binding preference of RBM4 to GC-rich sequences within an unstructured RNA context (Ray et al., 2009; Kazan et al., 2010). Data from anisotropy measurements obtained in collaboration with Birgitta Wöhrl (University of Bayreuth) using the RBM4 Δ4 mutant and short CU-rich RNA oligonucleotides yielded K_D values in the lower micromolar range, indicating a rather weak binding of RBM4 to these RNA sequences (Ströh, 2009). Unfortunately, GC-rich sequences were not included in the measurements. Based on these data, artificial reporter constructs were created carrying a miR-21 binding site and the putative RBM4 binding motifs (either CU- or GC-rich) within a 190 nt arbitrary DNA sequence lacking further miRNA binding sites. However, specific regulation of the luciferase levels

could not be observed with any of these reporter constructs. To test for the effect of RBM4 binding in a more natural setting, the putative RBM4 binding motifs were introduced into the HMGA2 3'-UTR reporter construct. Though knock-down of RBM4 increased HMGA2-coupled luciferase levels as expected, the introduction of RBM4 binding motifs could not further enhance this effect. Notably, also a reporter construct carrying the mutated HMGA2 3'-UTR lacking let-7a binding sites was up-regulated in RBM4-depleted cells, but not in TNRC6B knock-down cells, pointing towards a general effect of RBM4 in translation regulation rather than specific miRNA-mediated repression in this setting. Still, RBM4 could immunoprecipitate both RNA A- (CU-rich motif) and RNA G-(GC-rich motif) containing HMGA2 reporter mRNA from HEK 293 lysates, unfortunately not providing further convincing evidence for either binding motif. However, as the RNA A-motif is flanked by G residues, it cannot be excluded that the presence of these residues may have influenced RBM4 binding. Together, requirements for RBM4 binding and interaction with Ago proteins are obviously more complex and cannot easily be simulated based on the current knowledge. Apart from the controversial reports concerning RBM4 binding preferences, it is yet unknown in which distance RBM4 binding to the RNA takes place with respect to miRNA sites or whether the presence of several miRNA or RBM4 binding sites might influence protein interaction and subsequent target mRNA regulation. Against this background, it would be even more interesting to identify common natural targets of RBM4 and Ago proteins.

In a first attempt to achieve this, the PAR-CLiP method (Hafner et al., 2010) has been applied to mRNAs that co-purified with endogenous RBM4. In this method, photoactivatable 4-thiouridine was incorporated into cellular mRNA transcripts, followed by UV-induced cross-linking of these transcripts to associated proteins. After partial RNase T1 digestion, RNA fragments bound to RBM4 were radioactively labeled at the 5' end and subjected to SDS-PAGE. After removal of protein components, RNA was reverse transcribed, amplified and used for Solexa sequencing to identify RNA identity and, simultaneously, the RNA motif bound by RBM4. Surprisingly, only little RNA fragments could be annotated to mRNA sequences, while the rRNA fraction was disproportionally high (Mihaela Zavolan, University of Basel, personal communication). This could be explained on the one hand by a severe depletion of uridine residues in the RBM4 binding motif – assuming a preference of RBM4 for GC-rich RNA sequences – resulting in low cross-linking efficiencies using 4-thiouridine. On the other hand, treatment of immunoprecipitated RBM4 targets with RNase T1, which cuts RNA after G residues, might lead to an over-digestion of the RNA fragments providing fragments that are too short for sequencing or mapping. While these preliminary results point towards a preference of RBM4 to GC-rich RNA sequences, the experiment will have to be modified in order to confirm this theory and to identify shared RBM4-Ago mRNA targets, allowing for a more detailed analysis of the action and interaction mode of these proteins.

Notably, a recent publication from the Tarn lab has underlined the relevance of RBM4 for Ago-mediated translational repression (Lin and Tarn, 2009). The authors demonstrated that RBM4 is phosphorylated upon cell differentiation of murine myoblasts and transiently translocates to cytoplasmic granules where it co-localizes with P body components as GW182, DCP1 or Ago2. RBM4 was further shown to associate with certain muscle-specific miRNAs upon differentiation and overexpression of RBM4 resulted in repression of a target reporter construct in a dose-dependent manner (Lin and Tarn, 2009), similar to the effects observed with the KRAS 3'-UTR construct (Figure 28). Further immunoprecipitation and reporter assay approaches implied that RBM4 might enhance association of Ago-miRNA complexes with their target mRNA, presumably by promoting or stabilizing the interaction. However, overexpression of RBM4 probably also had general effects on translation as transient expression of RBM4 in HEK 293 cells which lack endogenous miR-1 resulted in down-regulation of a miR-1 reporter construct. This was also detectable with a natural target construct carrying a miR-1 binding site. Still, co-expression of miR-1 and RBM4 further enhanced the inhibitory effect conveyed by miR-1 or RBM4 expression alone. Notably, all of these experiments were performed in an overexpression background with an ectopically expressed miRNA. Therefore, further studies on this topic using a more natural setting are still elusive, which again underlines the importance of identifying natural mRNA targets that are simultaneously regulated by RBM4 and the miRNA machinery.

Interestingly, while the above study suggests that RBM4 promotes Ago binding to a target mRNA and to enforce miRNA-mediated translational regulation, the *Drosophila* RBM4 homologue LARK has been shown to physically interact with and stabilize dFMR, collectively regulating eye development as well as circadian behavior in flies (Sofola et al., 2008). FMRp is also a known component of the miRNA machinery in *Drosophila* and humans (Meister and Tuschl, 2004, Table 1), hence it would be tempting to speculate that RBM4 and FMRp work together with Ago proteins in miRNA-guided regulatory processes. As, depending on its phosphorylation status, FMRp also seems to have an effect on miRNA maturation (Cheever and Ceman, 2009), it might provide a link between miRNA function and processing in a more complex chain of regulatory events within the cell, presumably involving a number of additional protein factors whose role is yet unknown.

4. MATERIALS AND METHODS

4.1. MATERIALS

4.1.1. Chemicals and enzymes

Unless stated otherwise, chemicals were purchased from *Amersham Biosciences* (Buckinghamshire, UK), *Applichem* (Darmstadt, Germany), *Biorad* (Hercules, USA), *Merck* (Darmstadt, Germany), *Qiagen* (Hilden, Germany), *Roth* (Karlsruhe, Germany) and *Sigma-Aldrich* (Munich, Germany).

Radiochemicals were purchased from *Perkin Elmer* (Waltham, USA), enzymes from *New England Biolabs* (Ipswich, USA) and *Fermentas* (Burlington, Canada).

DNA oligonucleotides were ordered from *Metabion* (Martinsried, Germany), siRNAs and 2'OMe-oligonucleotides were produced by in-house service facilities.

4.1.2. Plasmids

pCS2-myc$_6$-FA	encodes for an N-terminal myc$_6$-tag and a *Fse*I-*Asc*I cloning cassette (donation from O. Stemmann, University of Bayreuth)
pET28a	encodes for N- and C-terminal His-tag (*Novagen,* Bloemfontein, South Africa)
pGEX6P-1	encodes for an N-terminal GST-tag (*Amersham-Pharmacia*)
pIRES-VP5	encodes for an N-terminal Flag/HA tag (Meister et al., 2004)
pMIR-RNL	is modified from the commercially available pMIR-REPORT vector (*Ambion*; Beitzinger et al., 2007). It encodes for the *Phototinus pylaris* luciferase (termed firefly in this work) under the control of a CMV promotor. A *Renilla reniformis* luciferase (termed renilla) under the control of a SV40 promotor was PCR-amplified from the pRL-SV40 plasmid (*Promega*, Madison, USA) and inserted into the *Ssp*I site of pMIR-REPORT. The firefly coding sequence is flanked by a multiple cloning site (MCS) at its 3' end, allowing for the introduction of regulatory sequences into the 3'-UTR.
pMIR-RNL-Tk	is based on the pMIR-RNL vector. The CMV promotor of the firefly luciferase was replaced by a HSV-Tk promotor which was PCR-cloned from the pRL-Tk plasmid (*Promega*, Madison, USA).

4.1.3. Antibodies

Antigen	Source	Dilution	Application	Reference / Manufacturer
α-Ago1 [1C9]	rat hybridoma supernatant, monoclonal	1:10	WB	(Beitzinger et al., 2007)
α-Ago2 [11A9]	rat hybridoma supernatant, monoclonal	1:50	WB	(Rudel et al., 2008)
α-alpha-tubulin	mouse, monoclonal	1:5000	WB	*Sigma-Aldrich*
α-Ddb1	goat, polyclonal	1:500	WB	*Serotec*
α-DDX5	goat, polyclonal	1:2000	WB	*Abcam*
α-Dicer [13D6]	mouse, monoclonal	1:1000	WB	*Abcam*
α-HA [16B12]	mouse, monoclonal HA.11	1:1000 1:200	WB IF	*Covance*
α-hnRNP C1/C2 [4F4]	mouse, monoclonal	1:1000	WB	*Abcam*
α-hnRNP U [3G6]	mouse, monoclonal	1:1000	WB	*Abcam*
α-IMP1	rabbit, monoclonal	1:1000	WB	kindly provided by S. Hüttelmayer, University of Halle (Huttelmaier et al., 2005)
α-IMP3	rabbit, monoclonal	1:1000	WB	kindly provided by S. Hüttelmayer, University of Halle
α-Lsm4	chicken, monoclonal	1:200	IF	*Geneway*
α-myc	rabbit, polyclonal	1:3000 1:200	WB IF	*Sigma*
α-NF-45	rabbit, polyclonal	1:1000	WB	(Isken et al., 2007)
α-NF-90	rabbit, polyclonal	1:1000	WB	(Isken et al., 2007)
α-RBM4 [6E10]	rat hybridoma supernatant, monoclonal	1:10	WB	(Pfuhl et al., 2008)
α-RCC1	rabbit, polyclonal	1:2000	WB	(Hetzer et al., 2000)
α-RmC [16D2]	rat, monoclonal	undiluted	IP	E. Kremmer, Helmholtz-Zentrum, Munich
α-rpS6	rabbit, monoclonal	1:1000	WB	*Cell signaling tech.*
α-SART3	rabbit, polyclonal	1:125	WB	this work
α-SMNRP [7B10]	mouse, monoclonal	1:1000	WB	(Meister et al., 2000)
α-TRBP	rabbit, polyclonal	1:125	WB	(Loef, 2006)
α-YB-1	rabbit, polyclonal	1:1000	WB	*Abcam*
α-chicken IgG, FITC-conjugated	rabbit, polyclonal	1:500	IF	*Sigma*
α-goat IgG, peroxidase conjugated	rabbit, polyclonal	1:5000	WB	*Abcam*
α-mouse IgG, TexasRed-conjugated	horse, polyclonal	1:500	IF	*Vector laboratories*

85

Antigen	Source	Dilution	Application	Reference / Manufacturer
α-mouse IgG, peroxidase conjugated	goat, polyclonal	1:5000	WB	*Sigma*
α-rabbit IgG, FITC-conjugated	goat, polyclonal	1:500	IF	*Sigma*
α-rabbit IgG, peroxidase conjugated	goat, polyclonal	1:7500	WB	*Sigma*
α-rat IgG, peroxidase conjugated	goat, polyclonal	1:5000	WB	*Jackson laboratories*

4.1.4. Bacterial strains and cell lines

cell lines:	HEK 293 HeLa
bacterial strains:	*E. coli* XL1 blue *E. coli* BL21

4.1.5. Cell culture media

For cultivation of cell lines, the following medium was used:

DMEM complete	500 ml	DMEM (*PAA*, Pasching, Austria)
	10%	fetal bovine serum (*Biochrom*, Berlin, Germany)
	1%	Penicillin/Streptomycin (*PAA*, Pasching, Austria)
OptiMEM (*Invitrogen*)		

4.1.6. Buffers and solutions

DNA loading dye (5x)	15 g	Saccharose
	50 ml	H_2O
	0.025 %	Xylene cyanol
RNA loading dye (1x)	90 %	Formamide
	0.025 %	Xylene cyanol
	0.025 %	Bromophenol blue
		in 1x TBE
Protein sample buffer (4x)	400 mM	Tris pH 6.8
	5 mM	EDTA
	50 %	Glycerol
	1 %	SDS
	0.01 %	Bromophenol blue
Coomassie staining solution	45 % (v/v)	methanol
	10 % (v/v)	acetic acid
	0.35 % (w/v)	Coomassie brilliant blue G250
Coomassie destaining solution	30 % (v/v)	methanol
	10 % (v/v)	acetic acid
LB (lysogenic broth) medium	1 % (w/v)	Trpyton
	1 % (w/v)	NaCl
	0.5 % (w/v)	Yeast extract
Phosphate buffered saline (PBS)	130 mM	NaCl
	774 mM	Na_2HPO_4
	226 mM	NaH_2PO_4
TBE buffer (1x)	89 mM	Tris pH 8.3
	89 mM	boric acid
	2.5 mM	EDTA
5 % stacking gel (SDS-PAGE)	5 %	Acrylamide-Bis solution (37.5:1, 30 % w/v) (*Serva*)
	75 mM	Tris-HCl pH 6.8
	0.1 %	SDS
	0.1 %	APS
	0.05 %	TEMED
10 % separation gel (SDS-PAGE)	10 %	Acrylamide-Bis solution (37.5:1, 30 % w/v) (*Serva*)
	400 mM	1.5 M Tris-HCl pH 8.8
	0.1 %	SDS
	0.1 %	APS
	0.05 %	TEMED
SDS running buffer (1x)	200 mM	Glycine
	25 mM	Tris pH 7.5
	25 mM	SDS

Towbin buffer (1x, for semi-dry western blotting)	38,6 mM 48 mM 0.0037 % (w/v) 20 %	Glycine Tris SDS Methanol	
Wash buffer (for western blotting)	300 mM 150 mM 0.25 %	Tris pH 7.5 NaCl Tween-20	
Chemiluminescence detection	100 mM 1.2 mM 0.68 %	Tris pH 8.5 Luminol p-cumaric acid H_2O_2 (30 %) components were mixed directly before use	in 10 ml in 150 μl 11 μl
2x HEPES (for calcium phosphate transfection)	274 mM 54.6 mM 1.5 mM	NaCl HEPES Na_2HPO_4	
Cell lysis buffer	150 mM 25 mM 2 mM 1 mM 0.5 mM 0.5 %	KCl Tris pH 7.5 EDTA NaF DTT NP-40	
Roeder A buffer	10 mM 10 mM 1.5 mM 0.5 mM 0.5 mM	Hepes-KOH pH 7.9 KCl $MgCl_2$ DTT PMSF	
Roeder C low buffer	5 % (v/v) 420 mM 1.5 mM 0.5 mM 0.2 mM 20 mM 0.5 mM	Glycerol KCl $MgCl_2$ DTT EDTA Hepes-KOH pH 7.9 PMSF	
Dicer lysis buffer	150 mM 20 mM 0.25 % 1.5 mM 0.5 mM	NaCl Tris pH 7.5 NP-40 $MgCl_2$ AEBSF	
Lysis buffer (for polysome gradients)	1/10 V 0.5 % 0.5 % 60 U/ml 3 mM	10x hypotonic buffer Triton X-100 Na-deoxycholate Ribolock DTT	

Hypotonic buffer (10x, for polysome gradients)	50 mM	Tris pH 7.5
	15 mM	KCl
	25 mM	MgCl$_2$
Polysome gradient buffer	20 mM	Tris pH 7.5
	80 mM	NaCl
	5 mM	MgCl$_2$
Gradient buffer (10x)	1.5 M	KCl
	0.25 M	Tris pH 7.5
	20 mM	EDTA
IP wash buffer	300 mM	NaCl
	50 mM	Tris pH 7.5
	5 mM	MgCl$_2$
	0.05 %	NP-40
8% denaturing RNA gel (RNA-PAGE)	32 %	SequaGel Concentrate (*national diagnostics*, Atlanta, USA)
	58 %	SequaGel Diluent
	10 %	SequaGel Buffer
	0.1 %	APS
	0.05 %	TEMED
TM buffer for 5'-cap labeling	1 mM	ATP
	0.2 mM	GTP
	10 U/ml	Ribolock
	100 mM	KCl
	1.5 mM	MgCl$_2$
	0.5 mM	DTT
Urea buffer for T1 digestion	10 M	Urea
	1.5 mM	EDTA
	0.05 %	Bromophenol blue
	0.05 %	Xylene cyanol
Elution buffer	300 mM	NaCl
	2 mM	EDTA
Proteinase K buffer	300 mM	NaCl
	200 mM	Tris pH 7.5
	25 mM	EDTA
	2 %	SDS
Proteinase K storage buffer	20 mg/ml	Proteinase K
	50 mM	Tris, pH 8.0
	1 mM	CaCl$_2$
	50 % (v/v)	Glycerol
Hybridization solution	7.5 ml	20x SSC
	0.6 ml	1M Na$_2$HPO$_4$, pH 7.2
	21 ml	10% SDS
	0.6 ml	50x Denhardt´s solution
	0.3 ml	Sonicated salmon sperm DNA (10mg/ml)

20x SSC	3 M 0.3 M	NaCl Sodium citrate adjust pH to 7.1
Denhardt´s solution (50x)	1 % 1 % 1 %	Albumin fraction V Polyvinylpyrrolidon K30 Ficoll 400
Lysis buffer pH 7.5 (for recombinant protein expression)	500 mM 50 mM 5 mM	NaCl Tris pH 7.5 $MgCl_2$
Wash buffer pH 8.0 (for recombinant protein expression)	500 mM 50 mM 5 mM	NaCl Tris pH 8.0 $MgCl_2$
Renilla buffer	2.2 mM 220 mM 0.44 mg/ml 1.1 M 1.3 mM 1.43 μM	EDTA K_2PO_4 pH 5.1 BSA NaCl NaN_3 Coelenterazine (*P.J.K.* GmbH, Kleinblitterdorf, Germany)
Firefly buffer	470 μM 530 μM 270 μM 20 mM 5.34 mM 0.1 mM 33.3 mM	D-Luciferine (*P.J.K.* GmbH, Kleinblitterdorf, Germany) ATP (*P.J.K. GmbH*) Coenzyme A (*P.J.K.* GmbH) Tricine Magnesiumsulfate heptahydrate EDTA DTT

4.2. METHODS

4.2.1. Molecular biological methods

4.2.1.1. General methods

Molecular biological methods (DNA/RNA gel electrophoresis, -extraction, -precipitation and concentration determination of nucleic acid, PCR, etc.) that are not described in detail here, were performed as described in Sambrook et al. (Sambrook, 1989) or according to the manufacturer´s instructions. There, also the composition of buffers and solutions not listed above can be found.

Plasmid DNA from *E. coli* was isolated using the "Plasmid MiniKit I" (*Omega BioTek*, Darmstadt, Germany) or the "NucleoBond Xtra Midi"-Kit (*Macherey Nagel*, Düren, Germany). For elution of DNA fragments from agarose gels, the "NucleoSpin"-Kit (*Macherey Nagel*, Darmstadt, Germany) was used. RNA isolation from cells was carried out using the "Prep Ease RNA Spin Kit" (*USB*, High Wycombe, UK).

Transformation of Plasmid-DNA into *E. coli* strains XL1 Blue and BL21(DE) was performed according to the calcium phosphate method (Sambrook, 1989).

4.2.1.2. Cloning of protein-coding DNA fragments from human cDNA libraries

To amplify cDNAs for the protein expression constructs used in this work, the "Human Brain (whole) Marathon-Ready cDNA" library (*Clontech*, Mountain View, USA) was used as template in a polymerase chain reaction (PCR). Specific primers were designed to carry restriction sites for the restriction enyzmes used in the cloning reaction at their 5'- or 3'-ends, respectively. PCR amplifications were performed using the Phusion Polymerase (*Finnzymes*, Espoo, Finland). PCR products were cloned into vectors that allow for protein expression in cell culture (pIRES-VP5, pCS2-myc$_6$-FA, pDEST puro) or bacterial cultures (pGEX6P-1, pET28a) as well as *in vitro* coupled T7-transcription/translation (pET28a). Based on the cDNA constructs, mutants were cloned in an analogous manner.

The following table lists the protein coding constructs used in this thesis.

Table 6: protein coding plasmid constructs

protein	amino acids	construct	plasmid	5'-/3'- restriction site	changes in amino acid sequence
Ago1	1-857	FH-Ago1	pIRES-VP5	*NotI/EcoRI*	-
		myc-Ago1	pCS2-myc₆-FA	*FseI/AscI*	-
		His-Ago1	pET28a	*EcoRI/NotI*	-
Ago2	1-859	FH-Ago2	pIRES-VP5	*NotI/EcoRI*	-
		myc-Ago2	pCS2-myc₆-FA	*FseI/AscI*	-
		His-Ago2	pET28a	*EcoRI/NotI*	-
	1-226	His-A2 N	pET28a	*EcoRI/NotI*	-
	227-371	His-A2 MID	pET28a	*EcoRI/NotI*	-
	372-516	His-A2 PAZ	pET28a	*EcoRI/NotI*	-
	372-516	His-A2 paz9	pET28a	*EcoRI/NotI*	(Liu et al., 2005)
	517-817	His-A2 PIWI	pET28a	*EcoRI/NotI*	-
Ago3	1-860	FH-Ago3	pIRES-VP5	*NotI/EcoRI*	-
		His-Ago3	pET28a	*EcoRI/NotI*	-
Ago4	1-861	FH-Ago4	pIRES-VP5	*NotI/EcoRI*	-
		His-Ago4	pET28a	*EcoRI/NotI*	-
DDX5	1-614	FH-DDX5	pIRES-VP5	*NotI/BamHI*	-
DDX30	1-1252	FH-DDX30	pIRES-VP5	*NotI/EcoRI*	-
DDX47	1-455	FH-DDX47	pIRES-VP5	*NotI/EcoRI*	-
DHX36	1-979	FH-DHX36	pIRES-VP5	*NotI/BamHI*	-
		GST-DHX36	pGEX6P-1	*BamHI/XhoI*	-
Dicer	1-1922	FH-Dicer	pDEST puro		-
GFP	1-239	FH-GFP	pIRES-VP5	*NotI/EcoRI*	-
		myc-GFP	pCS2-myc₆-FA	*FseI/AscI*	-
hnRNP C		FH-hnRNP C	pIRES-VP5	*NotI/EcoRI*	-
hnRNP U	1-824	FH-hnRNP U	pIRES-VP5	*NotI/EcoRI*	-
HuR	1-326	FH-HuR	pIRES-VP5	*NotI/EcoRI*	-
IMP1	1-577	FH-IMP1	pIRES-VP5	*NotI/EcoRI*	-
IMP3	1-579	FH-IMP3	pIRES-VP5	*NotI/EcoRI*	-
		GST-IMP3	pGEX6P-1	*EcoRI/XhoI*	-
	72-579	GST-IMP3 ΔRRM	pGEX6P-1	*EcoRI/XhoI*	Δ 1-71
Importin8	1-1037	FH-Importin8	pIRES-VP5	*NotI/BamHI*	-
		GST-Importin8	pGEX6P-1	*BamHI/NotI*	-
Matrin3	1-847	FH-Matrin3	pIRES-VP5	*NotI/BamHI*	-
		GST-Matrin3	pGEX6P-1	*BamHI/NotI*	-
		GST-Matrin3 ΔRRM	pGEX6P-1	*BamHI/NotI*	Δ 497-567
PABP-C1	1-636	FH-PABP-C1	pIRES-VP5	*NotI/BamHI*	-
PACT	1-313	GST-PACT	pGEX6P-1	*BamHI/XhoI*	-
PTCD3	1-689	FH-PTCD3	pIRES-VP5	*NotI/EcoRI*	-

protein	amino acids	construct	plasmid	5'-/3'-restriction site	changes in amino acid sequence
PTCD3		GST-PTCD3	pGEX6P-1	*BamHI/XhoI*	-
RBM4	1-364	FH-RBM4	pIRES-VP5	*NotI/BamHI*	-
		GST-RBM4	pGEX6P-1	*BamHI/XhoI*	-
	145-364	GST-RBM4 ΔRRM	pGEX6P-1	*BamHI/XhoI*	Δ 1-144
	177-364	GST-RBM4 ΔN	pGEX6P-1	*BamHI/XhoI*	Δ 1-176
	1-176	GST-RBM4 ΔC	pGEX6P-1	*BamHI/XhoI*	Δ 177-364
	1-159	GST-RBM4 RRM+L2	pGEX6P-1	*BamHI/XhoI*	Δ 160-364
	3-68	GST-RBM4 Δ1	pGEX6P-1	*BamHI/XhoI*	Δ 1-2, 69-364
	79-144	GST-RBM4 Δ2	pGEX6P-1	*BamHI/XhoI*	Δ 1-78, 145-364
	1-176	GST-RBM4 Δ3	pGEX6P-1	*BamHI/XhoI*	Δ 77-144
	69-176	GST-RBM4 Δ4	pGEX6P-1	*BamHI/XhoI*	Δ 1-68, 177-364
	160-176	GST-RBM4 Δ5	pGEX6P-1	*BamHI/XhoI*	Δ 1-159, 177-364
	1-364	GST-RBM4 Δ6	pGEX6P-1	*BamHI/XhoI*	Δ 160-179
	69-364	GST-RBM4 Δ7	pGEX6P-1	*BamHI/XhoI*	Δ 1-68
	1-364	GST-RBM4 Δ8	pGEX6P-1	*BamHI/XhoI*	Δ 77-144
	1-144	GST-RBM4 Δ9	pGEX6P-1	*BamHI/XhoI*	Δ 145-364
	1-364	GST-RBM4 Δ10	pGEX6P-1	*BamHI/XhoI*	aa 145-159 replaced by AAAAAAAGAAAAAAA
	69-215	GST-RBM4 Δ11	pGEX6P-1	*BamHI/XhoI*	Δ 1-68, 216-364
	1-215	GST-RBM4 Δ12	pGEX6P-1	*BamHI/XhoI*	Δ 216-364
	1-215	GST-RBM4 Δ13	pGEX6P-1	*BamHI/XhoI*	Δ 77-144
	1-364	GST-RBM4 Δ14	pGEX6P-1	*BamHI/XhoI*	Cys_{162} and Cys_{165} mutated to Tyr
	1-364	GST-RBM4 Δ15	pGEX6P-1	*BamHI/XhoI*	domain swap RRM1↔RRM2
RHA/DHX9	1-1270	FH-RHA	pIRES-VP5	*NotI/BamHI*	-
SART3	1-963	FH-SART3	pIRES-VP5	*NotI/EcoRI*	-
		GST-SART3	pGEX6P-1	*EcoRI/XhoI*	-
		GST-SART3 ΔRRM	pGEX6P-1	*EcoRI/XhoI*	Δ 802-873
Sip1	1-280	His-Sip1	pET28a	*BamHI/NotI*	-
TRBP	1-345	GST-TRBP	pGEX6P-1	*BamHI/NotI*	-
UPF1/RENT1	1-1118	FH-UPF1	pIRES-VP5	*NotI/EcoRI*	-

4.2.1.3.   Cloning of luciferase reporter constructs

The constructs used for luciferase reporter assays are based on the pMIR-REPORT miRNA reporter plasmid (*Ambion*). Modifications to this vector have been described in section 4.1.2. To yield the miR-21 cleavage reporter construct, the following DNA oligonucleotides were annealed, digested with *SacI* and *NaeI* and inserted into the *SacI* and *NaeI* restriction sites of the pMIR-RNL-Tk vector: 5'-CGCTGAGCTCATCGCCACCTTGTTTAAGCCTCAACATC AGTCTGATAAGCTAATTAGACCTACGCACTCCAGGCCGGCTCGC-3' and 5'-GCGAGCCG GCCTGGAGTGCGTAGGTCTAATTAGCTTATCAGACTGATGTTGAGGCTTAAACAAGGTG GCGATGAGCTCAGCG-3'. Analogously, a construct carrying a mutated miR-21 binding site was cloned using the following DNA oligonucleotides: 5'-CGCTGAGCTCATCGCCACCTTGTTTAAGCCTCAACATCAGCACCATTCTATAATTAGA CCTACGCACTCCAGGCCGGCTCGC-3' and 5'-GCGAGCCGGCCTGGAGTGCGTAGGT CTAATTATAGAATGGTGCTGATGTTGAGGCTTAAACAAGGTGGCGATGAGCTCAGCG-3'. A 3'-UTR fragment from the KRAS mRNA was PCR-amplified from a published construct (Johnson et al., 2005) and inserted into the *SacI* and *NaeI* restriction sites of the pMIR-RNL-Tk vector. The SERBP1, DNAJB11 and Raver2 reporter constructs have been reported before (Beitzinger et al., 2007). Additionally, the HMGA2 3'-UTR sequence was PCR amplified from HEK 293 cDNA using oligonucleotides 5'-CTCTGAGCTCTACTAATA GTTTGTTGATCTG-3' and 5'-CGCTGCCGGCGACCAAACTTTATTACTCATT-3' and cloned into the pMIR-RNL-Tk construct via the *SacI* and *NaeI* restriction sites. An HMGA2 3'-UTR reporter construct with mutated let-7a binding sites (Weinmann et al., 2009) was used as control.

FLOT1-, RhoC- and Per1 3'-UTRs were cloned into the pMIR-RNL-Tk vector via the *SacI* and *NaeI* restriction sites accordingly.

To produce an artificial 3'-UTR containing a miR-21 binding site as well as a putative RBM4 binding site, a random 190 nt-sequence was created using the website http://www.bioinformatics.org/sms2/random_dna.html. A miR-21 binding site (5'-TCAACATCAGTCTGATAAGCTA-3') was placed in position 51-72 and the potential RBM4 binding motifs RNA A (5'-GGTCTCTCTG-3'), RNA C (5'-TGCTCTTTA-3') or RNA G (5'-GGCGCGGGC-3') in position 131-140 of the 3'-UTR. According to miRBase, this sequence did not harbor any miRNA sites except the miR-21 binding site. Additionally, a construct carrying a control RNA (5'-GGAAAAAAAG-3', ctrl. I) was created. In another control plasmid, the miR-21 binding site was replaced by a mutated sequence (5'-TCAACATCAGCACCATTCTATA-3', ctrl. II) besides the control RNA sequence. DNA fragments were cloned into the pMIR-RNL vector using the *SacI* and *NaeI* restriction sites. The putative RBM4 binding motifs were introduced into the HMGA2 3'-UTR by PCR-based

mutagenesis in position 1471-1480 of the 3'-UTR sequence. This sequence alteration did neither interfere with known let-7 binding sites nor with additional miRNA sites as identified by PicTar or TargetScan. The PCR product was inserted into the *SacI* and *NaeI* restriction sites of the pMIR-RNL plasmid.

4.2.1.4.   Preparation of cell extracts

Standard cell extracts were prepared by scraping cells in 500 µl/15 cm dish cell lysis buffer. Cell debris was sedimented in a 10-minute centrifugation at 17000 *g* and 4 °C and supernatants were transferred to new reaction tubes.

For Dicer assays, cell lysates were prepared in the same way, except that EDTA-free Dicer lysis buffer was used.

Polyribosome fractionation from HEK 293 cells was carried out according to Pillai et al. (Pillai et al., 2005). For lysate preparation, cells were treated for 5 minutes with 100 µg/ml cyclohexamide to block translation and washed once with PBS and 1x hypotonic lysis buffer, each containing 100 µg/ml cyclohexamide. Cells were lysed by scraping in 500 µl/15 cm dish hypotonic lysis buffer containing cyclohexamide and cell debris was removed by centrifugation at 3500 *g* for 8 minutes at 4 °C.

The preparation of nuclear and cytoplasmic extracts was based on the method described by Dignam et al. (Dignam et al., 1983). 1 x 10^9 HEK 293 cells were collected by centrifugation at 350 *g* for 10 minutes and washed once in PBS. The volume of the cell pellet was estimated and cells were resuspended in 5 volumes Roeder A buffer and incubated for 10 minutes on ice. After another centrifugation step, cells were resuspended in 2 volumes Roeder A buffer, transferred to a glass douncer and lysed with 10 pestle strokes. Cell nuclei were sedimented by a 10-minute centrifugation at 1200 *g* and 4 °C and cytoplasmic extracts were transferred to new reaction tubes. The pelleted nuclei were resuspended in 3 ml buffer Roeder C-low and homogenized with 15 pestle strokes in a glass douncer. Samples were centrifuged at 17000 *g* for 30 minutes at 4 °C and supernatants were transferred to new reaction tubes.

4.2.1.5.   Immunoprecipitation and pull-down of proteins

For immunoprecipitation of FLAG/HA-tagged proteins, 20 µl FLAG agarose beads (*Sigma,* St. Louis, USA) were added to the lysates and incubated for 2-3 h at 4 °C. After washing three times with IP wash buffer and once with PBS, samples were transferred to fresh reaction tubes and used for further experiments. For subsequent western blotting analysis, samples were mixed with 20 µl protein sample buffer and heated to 95 °C for 5 minutes

before separation by SDS-PAGE. Myc-tagged proteins were immunoprecipitated in the same manner using 20 µl anti-myc-agarose (*Sigma*) per sample.

For immunoprecipitation of endogenous Ago1, Ago2 or RBM4, the corresponding antibodies were coupled to 20 µl Protein G Sepharose (*GE Healthcare*) for 3-12 h at 4 °C, followed by a 2-3 h incubation with cell lysates. Hybridoma supernatants were used undiluted for antibody coupling. Further steps were performed analogous to the FLAG-immunoprecipitation.

After the washing steps, samples destined for RNase A treatment were incubated with 100 mg/ml RNase A (*Qiagen*) for 1 h at 4 °C, washed twice with PBS and transferred to fresh reaction tubes.

Pull-down experiments in cell lysates were performed with various recombinantly expressed RBM4 mutants and fragments. GST fusion proteins were incubated with Glutathion Sepharose (*GE Healthcare*) for 2 h at 4 °C. Beads were washed twice with PBS and HEK 293 lysates were added. After incubation at 4 °C for 2 h, beads were washed three times with IP wash buffer and once with PBS, transferred to fresh reaction tubes and analyzed for endogenous Ago2 by western blotting.

4.2.1.6. Preparation of sucrose density gradients

For standard sucrose gradient centrifugation, a gradient ranging from 15 % to 55 % sucrose in 1x gradient buffer was used. Gradients were set up in 14x89 mm polyallomer centrifuge tubes (*Beckman*, Palo Alto, USA) using the Gradient Master 107ip system (*Biocomp*, New Brunswick, Canada) according to manufacturer´s instructions and cooled to 4 °C. Cells were lysed in 500 µl/15cm plate cell lysis buffer and cell debris was removed by centrifugation at 17000 *g* for 10 minutes at 4 °C. A maximum volume of 750 µl was loaded per gradient. Lysates were separated by centrifugation at 30000 rpm in a SW41 rotor for 18 h at 4 °C in an Optima L-90K ultracentrifuge (*Beckman* Coulter GmbH). Acceleration was set to "low" and the brake was turned off. 500 µl fractions were taken manually and 20 µl/fraction were used directly for western blotting in order to check for protein distribution. 5-25 % gradients were prepared accordingly. To determine indicated S values, Catalase (11S), apoferritin (17S) and thyroglobin (19S) (all *Sigma*) were separated on a 15-55 % sucrose gradient and protein distribution was visualized by SDS-PAGE and subsequent coomassie staining.

For polyribosome fractionation, gradients ranging from 0.5-1.5 M sucrose in 20 mM Tris pH 7.5, 80 mM NaCl and 5 mM $MgCl_2$ were prepared. Lysates were separated by centrifugation at 36000 rpm in a SW41 rotor for 2 h at 4 °C and fractionated. For western blotting, 20 µl/fraction were mixed with 4x protein sample buffer.

4.2.1.7. RNA extraction from cultured cells

Extraction of total RNA was performed using peqGold TriFast (*Peqlab*, Erlangen, Germany) according to the manufacturer´s protocol. After precipitation, the RNA pellet was washed with 80 % ethanol, air-dried and dissolved in ddH$_2$O.

RNA from immunopurified samples was directly isolated from antibody coupled beads by adding 200 µl Proteinase K buffer containing 40 µg Proteinase K. The samples were incubated at 65 °C for 20 minutes, followed by RNA extraction using 200 µl phenol/chloroform/isoamylalcohol (25:24:1). For subsequent RNA precipitation, the aqueous phase was mixed with 2.5 volumes of absolute ethanol, incubated at -20 °C O/N and RNA was pelleted by centrifugation at 17 000 *g* for 30 minutes at 4 °C. Pellets were washed with 70 % (mRNA preparation) or 80 % (miRNA isolation) ethanol, air-dried and dissolved in an appropriate volume of ddH$_2$O. Input samples were prepared accordingly.

4.2.1.8. Reverse transcription (RT) - cDNA synthesis

Prior to cDNA synthesis, RNA was subjected to DNase I treatment in order to remove potential DNA contaminations. 11.5 µl RNA were incubated with 1 µl DNase I, 1.5 µl of the corresponding 10x buffer and 1 µl RiboLock (all *Fermentas*) at 37 °C for 30 minutes followed by enzyme inactivation at 70 °C for 10 minutes. The subsequent cDNA synthesis reaction with a final reaction volume of 30 µl was performed using First Strand cDNA Synthesis Kit (*Fermentas*) according to manufacturer´s instructions. The cDNA samples were diluted 1:10 with supplied DEPC-H$_2$O and used for quantitative PCR.

4.2.1.9. Quantitative PCR (qPCR)

Quantitative PCR analysis was carried out in 15 µl reactions containing 7.5 µl Mesa Green qPCR MasterMix Plus (*Eurogentec*, Cologne, Germany), 0.2 µl each of forward and reverse primers (10 µM) and 5 µl cDNA in a MyiQ *BioRad* (Hercules, USA) *real-time* detection system.

The primers utilized for *real-time* PCR analysis are listed in the following table.

Table 7: Primers used for quantitative PCR

Name	Target mRNA	Primer sequence (5'→3')
RBM4	RBM4 (ORF)	CTTGAGGTGGGATGTGTGTG GCAGGAGAGGAAAGGAAAGG
YB-1	YB-1 (ORF)	AAGTGATGGAGGGTGCTGAC TGCGTCGGTAATTGAAGTTG
IMP3	IMP3 (ORF)	AGTTGTTGTCCCTCGTGACC AGCCTTCTGTTGTTGGTGCT
FMRp	FMRp (ORF)	CACCTCAAAGCGAGCACATA CAATAGCAGTGACCCCAGGT
GAPDH	GAPDH (ORF)	TGGTATCGTGGAAGGACTCATGAC ATGCCAGTGAGCTTCCCGTTCAGC
luc	firefly luciferase (ORF)	GTGTTCGTCTTCGTCCCAGT GCTGGGCGTTAATCAGAGAG
renilla	renilla luciferase (ORF)	ATGGGATGAATGGCCTGATA CAACATGGTTTCCACGAAGA
KRAS	KRAS (3'-UTR)	TTTTAGGACTCTTCTTCCATATTA TGGGGCATGTGGAAGGTAGGGAGG

4.2.1.10. Semi-quantitative RT-PCR for miRNAs

For detection of miRNA association with Ago complexes, HEK 293 cells were transiently transfected with FLAG/HA-Ago1 or -Ago2, cell lysates were subjected to gradient centrifugation and Ago complexes were immunoprecipitated from individual fractions using FLAG agarose. RNA was isolated and reverse transcription and semi-quantitative PCR was performed using mirVana qRT-PCR miRNA Detection Kit, miRVana qRT-PCR Primer Sets for miRNAs let-7a and miR-16 (all *Ambion*) and *Taq* polymerase (*Fermentas*). Aliquots from the PCR product were taken after different cycle numbers and separated on a 3 % agarose gel.

4.2.1.11. RNA polyacrylamide gel electrophoresis (RNA-PAGE)

RNA samples were separated by denaturing RNA polyacrylamide gel electrophoresis using the SequaGel System Kit (*national diagnostics*, Atlanta, USA) with an acrylamide concentration of 8% (RISC assay), 12 % (Dicer assay) or 15 % (northern blotting). The gel was pre-run for 10-15 minutes at 300 V. As running buffer, 1x TBE was used. Before loading, the pockets were rinsed thoroughly with running buffer and the gel was run at 300-500 V (northern blotting, Dicer assay) or 65 W (RISC assay).

4.2.1.12. Dicer assay

To assay for Dicer activity, an *in vitro* transcribed pri-miR-27a substrate was used (Landthaler et al., 2004; Meister et al., 2005). The template for pri-miR-27a transcription was generated by PCR amplification from human genomic DNA using the primers 5-GGCTGGAACGGAGGGCACAGCTAG-3' and 5'-GGTAACTGGCTGCTAGGAAGGTGCGG-3'. In a second round of PCR, a T7 promotor sequence was introduced using the following, partially overlapping, primers: 5'-AGGCAGACAGGCGGCAGCAG-3' and 5'-TAATACGACTCACTATACGAGGATGCTGCCCGG-3'. For *in vitro* transcription, 3 µl PCR product were incubated with 8 µl 5x NTP Mix (A/C/G/U = 5/5/8/0.1 mM), 8 µl 5x T7 buffer, 0.2 µl DTT (1M), 1 µl T7 polymerase and 5 µl [α-^{32}P]-UTP (3000 Ci/mmol) in a 40 µl reaction at 37 °C for 2 h. RNA sample buffer was added and RNA was purified by 10 % denaturing RNA-PAGE. After detection by autoradiography, the RNA was gel eluted in 300 µl elution buffer (300 mM NaCl, 2 mM EDTA) O/N at 4 °C under vigorous shaking and recovered by ethanol precipitation.

To provide a size marker, 10 pmol of an arbitrary single-stranded siRNA oligonucleotide was incubated with 0.1 µl [γ-^{32}P]-ATP and 0.1 µl T4 polynucleotide kinase in a 10 µl reaction for 5 minutes at 37 °C. Purification was performed in parallel to the Dicer substrate and the size marker was highly diluted before use.

Cell lysis and immunoprecipitations were performed as described earlier (section 4.2.1.5). For Dicer activity assays, 10 µl of Ago- or Dicer containing beads were incubated in 20 µl PBS containing 5 mM ATP, 7.5 mM MgCl$_2$, 10 U/ml RNasin (*Promega*, Madison, USA) and *in vitro* transcribed RNA (2 Bq/cm^2) at 37 °C. After 1 h, the reaction was stopped by proteinase K digestion and RNA precipitation was performed as described before. Samples were analyzed by 12 % denaturing RNA-PAGE and signals were detected by autoradiography.

4.2.1.13. RISC assay

The RISC cleavage assay as well as the RNA substrate used in this work have been described previously (Meister et al., 2004; and as a detailed protocol in Stöhr, 2011).

In short, the RNA cleavage substrate was obtained by *in vitro* transcription of a PCR product containing a perfect complementary sequence to miR-19b. 20 µl 5x NTP mix (A/C/G/U = 5/5/8/2 mM), 20 µl T7 transcription buffer, 0.5 µl DTT (1M), 1 µl T7 RNA polymerase and 5 µl PCR product in a total reaction volume of 100 µl were incubated for 2 h at 37 °C before adding RNA sample buffer. RNA was separated by 8 % denaturing RNA-PAGE, detected by UV shadowing, gel eluted in 300 µl elution buffer O/N at 4 °C and recovered by ethanol precipitation.

Subsequently, the RNA substrate was ^{32}P-cap labeled: 40 pmol *in vitro* transcribed RNA was incubated with 2 µl Guanylyltransferase (*Gibco/BRL*, Bethesda, MD), 2 µl 10x buffer (0.4 M Tris pH 8.0, 60 mM MgCl$_2$, 100 mM DTT, 20 mM spermidine), 0.25 µl RNasin (*Promega*, Madison, USA), 1 µl S-adenosyl-methionine (500 µM, *Sigma*), 1 µl DTT (100 mM) and 2 µl [α-^{32}P]-GTP (3000 Ci/mmol) in a 20 µl reaction at 37 °C for 3 h. Purification of the labeled RNA substrate by RNA-PAGE was performed as described above (section 4.2.1.12).

10 µl of Ago- or Dicer containing beads were incubated in a 25 µl reaction containing 5 nM target RNA, 1 mM ATP, 0.2 mM GTP, 10 U/ml RNasin (*Promega*, Madison, USA), 100 mM KCl, 1.5 mM MgCl$_2$ and 0.5 mM DTT for 1.5 h at 30 °C. RNA was Proteinase K digested, extracted as described before and analyzed by 8 % denaturing RNA-PAGE using a sequencing gel apparatus Model S2 (*Gibco/BRL*, Bethesda, MD). For a marker, substrate RNA subjected to digestion by RNase T1 was used (Stöhr, 2011).

Signals were detected by autoradiography using BioMax MS films and an intensifying HE Transcreen screen (both *Kodak*).

4.2.1.14. Northern blotting

Northern blotting was performed as described before (Lagos-Quintana et al., 2001) using the following probe against miR-19b: 5'-TCAGTTTTGCATGGATTTGCACA-3'. Samples were mixed with an equal volume of denaturing RNA sample buffer and heated to 95 °C for 5 minutes. RNA was separated by RNA-PAGE on a 12 % denaturing polyacrylamide gel and transferred to Hybond-N membrane (*Amersham Bioscience*, Buckinghamshire, UK) by semidry blotting using 0.5x TBE with constant amperage (3 mA/cm^2) for 1 h. To cross-link the RNA, the membrane was subjected to UV radiation (1200 J for 30s) and subsequently incubated at 80 °C for 1 h.

Pre-hybridization was performed in 5x SSC, 20 mM Na$_2$HPO$_4$ pH 7.2, 7 % SDS, 1x Denhardt´s solution and 10 µg sonicated salmon sperm DNA for 1 h at 50 °C. A 5'-^{32}P-labeled probe (see below) was added for hybridization O/N at 50 °C. Subsequently, the membrane was washed twice with 5x SSC and 1 % SDS and once with 1x SSC and 1x SDS for 10 minutes each. Exposure to Kodak BioMax MS films was performed with an intensifying HE Transcreen screen (*Kodak*, Stuttgart, Germany) at -80 °C.

For northern probe preparation, 10 pmol of the DNA oligonucleotide were radiolabeled in a 30 µl T4-Polynucleotide kinase reaction with 30 µCi of [γ-^{32}P]-ATP at 37 °C for 30 minutes. The reaction was stopped by addition of 30 µl EDTA (30 mM) and incubation at 95 °C for 5 minutes. Subsequently, the probe was purified using MicroSpin G-25 columns (*Amersham Bioscience*, Buckinghamshire, UK).

4.2.1.15. Mass spectrometry analysis

Lysates from transiently FLAG/HA-Ago1 or -Ago2 transfected HEK 293 cells were separated by sucrose density centrifugation. Fractions corresponding to complexes I to III, respectively, were pooled, subjected to immunoprecipitation using FLAG beads and separated by SDS-PAGE. After coomassie staining, gel lanes were cut into pieces of similar size (23 slices) and subjected to in-gel trypsinization (Shevchenko et al., 1996). Extracted peptides were analyzed by liquid chromatography-coupled tandem MS [LC-MS/MS] on a Q-ToF Ultima mass spectrometer (*Waters*). MSMS spectra of doubly and triply charged precursors were acquired for max. 3.3 s (0.1 s interscan time). Raw data were processed and transformed into a peaklist using MassLynx software 4.0 (*Waters*) with the following settings: i) Smoothing: smooth window (channels) 3.0, number of smooths 3 using Savitzky Golay algorithm; ii) Centroiding: min. peak width at half high: 4, centroid top, 80 %.

The peak list of fragment spectra was searched against the NCBI non-redundant database (NCBInr) with a mass accuracy of 0.2 Da for the parent ion (MS) and 0.2 Da for the fragment ions (MS/MS) using Mascot. The peptides were constrained to be tryptic with a maximum of one missed cleavage. Carbamidomethylation of cysteines was considered as a fixed modification whereas oxidation of methionine residues was considered as a variable modification. The highest scoring peptide from each protein as well as single hit peptides entry was manually inspected to eliminate false positives in the data set.

4.2.1.16. Recombinant protein expression

For recombinant expression of proteins or protein fragments, the corresponding plasmids were introduced into *E. coli* BL21(DE3) by heat shock transformation. LB medium was inoculated with transformed bacteria and cultured at 37 °C to an OD_{600} of about 0.8. After induction with 1 mM IPTG, cultures were transferred to 18 °C and incubated O/N. Bacteria were harvested by centrifugation (6000 g, 10 min, 4 °C), resuspended in 35 ml lysis buffer for recombinant protein expression and disrupted by sonication (4 x 30 s, amplitude 35 %) on ice using a Sonopuls H2070 sonicator with a TT13 sonotrode (both *Bandelin electronic*, Berlin, Germany). After centrifugation at 20000 *g* for 30 minutes at 4 °C, supernatants were either shock-frozen and stored at -80 °C or directly used for affinity purification.

4.2.1.17. Affinity purification of recombinant GST- and His-fusion proteins

For affinity purification of GST fusion proteins, *E. coli* extracts were incubated with Glutathion sepharose (*GE Healthcare*) for 2 h at 4 °C, followed by three washes with lysis buffer pH 7.5. Beads were transferred to PolyPrep columns (*Biorad*) and washed with wash buffer pH 8.0.

Purified GST fusion proteins were eluted using wash buffer pH 8.0 containing 3 mg/ml L-Glutathione (*Sigma*) and dialyzed O/N at 4 °C against PBS containing 100 µM AEBSF.

4.2.1.18. Western Blotting

For Western blot analysis, proteins were separated by 10 % SDS-PAGE (unless percentage stated otherwise) and transferred to Hybond ECL nitrocellulose membrane (*GE Healthcare*) by semi-dry western blotting at 7 V and room temperature for 3 h using 1x Towbin blotting buffer.

The membrane was blocked by incubation in wash buffer containing 10 % milk powder for 30-60 minutes followed by 3 five-minute washes with wash buffer. Primary antibodies were added to the blot in the indicated dilutions and incubated for a minimum time of 1 h, followed by three ten-minute washes with wash buffer. After one-hour incubation with the peroxidase-conjugated secondary antibody, membranes were again subjected to 3 ten-minute washes in wash buffer followed by a two-minute incubation in chemiluminescence detection solution. Signals were detected using Hyperfilm ECL films (*GE Healthcare*).

4.2.1.19. Immunofluorescence (IF)

HEK 293 cells were seeded onto coverslips in 6 well plates to give a cell density of 25 %. 5 h after seeding, cells were transfected with 0.1 µg DNA per well and plasmid as described in section 4.2.2.2. 2 days after transfection, cells were fixed for 15 minutes in ice-cold PBS containing 3.7 % formaldehyde. The reaction was stopped by adding PBS/100 mM glycine for 5 minutes and cells were permeabilized in PBS/0.2 % Triton X-100/3 % BSA for 10 min. Cover slips were washed once with IF buffer (PBS/0.1 % TWEEN-20/0.2 % BSA) and primary antibodies were added for 1 h. After 3 washes with IF buffer, cells were incubated with secondary antibodies for 1 h in the dark. Cells were washed once with IF buffer containing a final concentration of 1 µg/ml DAPI and then three times with IF buffer and mounted to slides using Vectashield mounting medium (*Vectorlabs*). Images were recorded using a TCS SP2 confocal laser microscope (*Leica Microsystems*, Germany). 20 z-sections of the cells were recorded and processed to maximum projections using the Leica confocal software. Adobe Photoshop was used to superimpose the images.

4.2.1.20. Coupled *in vitro* transcription/translation

For coupled *in vitro* transcription and translation from pET28a constructs, the TnT T7 Quick Coupled Transcription/Translation System (*Promega*, Madison, USA) was used.

2 µg plasmid DNA, 0.5 µl RiboLock, 2 µl Easy Tag L-[^{35}S]-Methionine (1000 Ci/mmol) and 40 µl reticulocyte lysate were incubated for 3 h at 30 °C. To check for successful translation, 1 µl per sample was separated by SDS-PAGE, the gel was incubated for 30 minutes in 30 % acetic acid and for 45 minutes in Amplify Reagent (*GE Healthcare*). The gel was dried and autoradiography was detected using BioMax MS films and a Transcreen LE intensifying screen (both *Kodak*).

4.2.1.21. *In vitro* pull-down analysis

To assay for direct binding of two proteins, one component was expressed as a GST-fusion protein, while the other component was radioactively labeled during *in vitro* translation (see above). Test samples from GST-protein lysates were separated by SDS-PAGE and protein amounts were leveled by estimating the intensity of protein bands in the gel after coomassie staining. Levels of radioactively labeled proteins were adjusted by checking autoradiography signals from the test gel described above.

For the actual binding assay, GST-fusion proteins were incubated with 20 µl Glutathion Sepharose (*GE Healthcare*) in a rotating wheel for 2 h at 4 °C. Samples were washed twice with PBS and transferred to new reaction tubes. Radioactively labeled proteins were added to the beads and samples were incubated on ice for 1.5 h. Beads were stirred every 10 minutes. Subsequently, samples were washed three times with IP wash buffer and once with PBS and transferred to new reaction tubes. The supernatant was removed completely and proteins were denatured by adding 20 µl protein sample buffer and heating to 95 °C for 5 minutes. Samples were separated by SDS-PAGE, followed by coomassie staining and a 45-minute incubation in Amplify Reagent (*GE Healthcare*). The gel was dried and autoradiography was detected using BioMax MS films and a Transcreen LE intensifying screen (both *Kodak*).

4.2.2. Cell biological methods

4.2.2.1. Culturing of mammalian cells

HEK 293 and HeLa cells were cultured in Dulbecco´s Modified Eagle´s Medium (DMEM, *PAA*, Pasching, Austria) supplied with 10 % (v/v) fetal bovine serum (FBS, *Gibco*) and 1 % (v/v) penicillin/streptomycin (*PAA*, Pasching, Austria) at 37 °C and 5 % CO_2. Cells were passaged every 2-3 days after incubation with trypsin-EDTA (*PAA*, Pasching, Austria) and seeded to new culture plates. HeLa cells were washed once with PBS prior to trypsin-EDTA treatment.

4.2.2.2. Calcium phosphate transfections

The calcium phosphate transfection method was used for transient transfection of HEK 293 cells. Cells were plated 3-5 h prior to transfection at about 30 % confluency. Per 15 cm dish, 10 µg plasmid DNA was mixed with 153 µl $CaCl_2$ (2M) in a volume of 1250 µl. 1250 µl 2x HEPES buffer was added drop-wise under gentle agitation. The transfection mixture was sprinkled onto the cells and incubated for 2 d before harvest.

4.2.2.3. SiRNA transfections

For knock-down experiments, HeLa cells were reverse transfected in 6-well format with 100 pmol siRNA per well using 5 µl Lipofectamine RNAiMAX reagent (*Invitrogen,* Carlsbad, USA) according to manufacturer´s instructions. For knock-down experiments, cells were cultured in medium without penicillin/streptomycin.

Cells were harvested 4 days post-transfection, total RNA was extracted and mRNA levels were analyzed by qPCR.

The following siRNAs were used in this work:

Table 8: siRNA sequences

name	5'→3' sequence (sense strand)	5'→3' sequence (antisense strand)
Ago1	GAGAAGAGGUGCUCAAGAAUU	UUCUUGAGCACCUCUUCUCUU
Ago2	GCACGGAAGUCCAUCUGAAUU	UUCAGAUGGACUUCCGUGCUU
Ago3	GAAAUUAGCAGAUUGGUAAUU	UUACCAAUCUGCUAAUUUCUU
Ago4	GGCCGGAGCUAAUAGCAAUUU	AUUGCUAUUAGCUCCGGCCUU
ctrl.	UUGUCUUGCAUUCGACUAAUU	UUAGUCGAAUGCAAGACAAUU
FMRp #1	GGCAGCUUGCCUCGAGAUUUU	AAUCUCGAGGCAAGCUGCCUU
FMRp #2	CCUCCUGUAGGUUAUAAUAUU	UAUUAUAACCUACAGGAGGUU

name	5'→3' sequence (sense strand)	5'→3' sequence (antisense strand)
FMRp #3	GAACGUCUAAGAUCUGUUAUT	UAACAGAUCUUAGACGUUCUT
FMRp #4	ACAGGUACUUUGUCUAAGAUT	UCUUAGACAAAGUACCUGUUT
RBM4 #1	UUACGGCUUUGUGCACAUAUT	UAUGUGCACAAAGCCGUAAUT
RBM4 #2	GGAGCUUCGAGCCAAGUUUUT	AAACUUGGCUCGAAGCUCCUT
RBM4 #3	GAGUGUCCGAUAGAUCGUUUT	AACGAUCUAUCGGACACUCUT
TNRC6B	GGCCUUGUAUUGCCAGCAAUT	UUGCUGGCAAUACAAGGCCUT
YB-1 #1	AACCUUCGUUGCGAUGACCUT	GGUCAUCGCAACGAAGGUUUT
YB-1 #2	GCAGACCGUAACCAUUAUAUT	UAUAAUGGUUACGGUCUGCUT
YB-1 #3	AGAAGGUCAUCGCAACGAAUT	UUCGUUGCGAUGACCUUCUUT
ZBP3 #1	UCCAGAACGCACUAUUACAUT	UGUAAUAGUGCGUUCUGGAUT

4.2.2.4. Luciferase assays

HeLa cells were seeded in culture medium to 96 well plates 5 h prior to transfection to give 50 % confluency. SiRNAs were transfected at 10 nM final concentration using HiPerfect (*Qiagen*) according to the manufacturer´s instructions. After 2 d, cells were passaged in an 1:3 ratio and seeded into a new 48 well plate. On the following day, medium was changed to OptiMEM (*Invitrogen*). Cells were subsequently transfected with reporter plasmids using 0.5 µl/well Lipofectamine (*Invitrogen,* Carlsbad, USA) and 0.125 µg/well reporter plasmid according to manufacturer´s instructions. Medium was changed to culture medium after 24 h and cells were lyzed after another 24 h in 50 µl/well passive lysis buffer (*Promega*, Madison, USA).

In later experiments, knock-down was performed using RNAiMAX as described above. Cells were seeded to 96 well plates after 2.5 d in culture medium without penicillin/streptomycin and transfected 6 h later using 0.25 µl Lipofectamine 2000 (*Invitrogen,* Carlsbad, USA) and 50 ng/well reporter plasmid. After 36 h, cells were lyzed in 50 µl/well passive lysis buffer (*Promega*, Madison, USA).

Luminescence was measured in a Mithras LB 940 luminometer (*Berthold Technologies*, Bad Wildbad, Germany) using firefly luciferase buffer and renilla luciferase buffer (sterile filtered). Samples were assayed in 3-4 replicates. For each siRNA, the firefly/renilla luminescence ratios of the reporter plasmids were normalized to the corresponding empty vector.

For miRNA inhibition experiments, 20 pmol of the 2'-O-methyl (2'-OMe) oligoribonucleotides were co-transfected with reporter plasmid (50 ng/well) in 96-well format with Lipofectamine 2000 (*Invitrogen*) according to manufacturer´s instructions. Cells were lyzed 24 h later in 50 µl/well passive lysis buffer (*Promega*) and luminescence was measured and normalized as described above.

For over-expression experiments, reporter plasmids (50 ng/well) were co-transfected with FLAG/HA-tagged constructs as indicated using 0.25 µl/well Lipofectamine 2000 (*Invitrogen*) according to manufacturer´s instructions. After 36 h, cells were lyzed in 50 µl/well passive lysis buffer (*Promega*) and luminescence was measured as described above. Again, results were normalized to those of the empty vector.

Table 9: luciferase reporter constructs

reporter construct name	vector backbone	insert	reference
miR-21 cleavage	pMIR-RNL-Tk	miR-21 cleavage site (perfect complementary)	cloned in this work
miR-21 cleavage mutant	pMIR-RNL-Tk	mutated miR-21 cleavage site (mismatches in pos. 3-6 and 9-12 of miR-21)	cloned in this work
KRAS	pMIR-RNL-Tk	kras 3'-UTR	(Johnson et al., 2005)
HMGA2	pMIR-RNL-Tk	HMGA2 3'-UTR (NM_003483.4)	(Mayr et al., 2007)
HMGA2 mut	pMIR-RNL-Tk	HMGA2 3'-UTR with mutated let-7 binding sites	cloned in this work
SERBP1	pMIR-RNL	serbp1 3'-UTR	(Beitzinger et al., 2007)
DNAJB11	pMIR-RNL	dnajb11 3'-UTR	(Beitzinger et al., 2007)
Raver2	pMIR-RNL	raver 2 3'-UTR	(Beitzinger et al., 2007)
Per1	pMIR-RNL-Tk	Per1 3'-UTR (NM_002616.2)	(Kojima et al., 2007)
FLOT1	pMIR-RNL-Tk	FLOT1 3'-UTR (NM_005803.2)	(Lin and Tarn, 2005)
RhoC	pMIR-RNL-Tk	RhoC 3'-UTR (NM_175744.4)	(Lin and Tarn, 2005)
random + RNA A	pMIR-RNL	random DNA (190 nt)* + miR-21 binding site + putative RBM4 binding motif A	cloned in this work
random + RNA C	pMIR-RNL	random DNA (189 nt) * + miR-21 binding site + putative RBM4 binding motif C	cloned in this work
random + RNA G	pMIR-RNL	random DNA (190 nt) * + miR-21 binding site + putative RBM4 binding motif G	cloned in this work
random ctrl. I	pMIR-RNL	random DNA (190 nt) * + miR-21 binding site + ctrl. RNA binding motif	cloned in this work
random ctrl. II	pMIR-RNL	random DNA (190 nt) * + mutated miR-21 binding site + ctrl. RNA motif	cloned in this work
HMGA2 + RNA A	pMIR-RNL	HMGA2 3'-UTR + putative RBM4 binding motif A	cloned in this work
HMGA2 + RNA C	pMIR-RNL	HMGA2 3'-UTR + putative RBM4 binding motif C	cloned in this work
HMGA2 + RNA G	pMIR-RNL	HMGA2 3'-UTR + putative RBM4 binding motif G	cloned in this work

ABBREVIATIONS

3'-UTR	3'-untranslated region	**h**	hour
5'-UTR	5'-untranslated region	**HA**	haemagglutinin
AEBSF	4-(2-Aminoethyl) benzenesulfonyl fluoride	**HEK**	human embryonic kidney
Ago	Argonaute	**HEPES**	4-(2-Hydroxyethyl)piperazine-1-ethanesulfonic acid
APS	ammonium persulfate	**HSC**	heat shock cognate
ATP	adenosine triphosphate	**HSP**	heat shock protein
AUB	Aubergine	**IgG**	immunoglobulin class G
BSA	bovine serum albumin	**IPTG**	Isopropyl β-D-1-thiogalactopyranoside
bp	base pair	**IRES**	internal ribosome entry site
casiRNA	*cis*-acting siRNA	**k**	kilo
C. elegans	*Caenorhabditis elegans*	**KRAS**	Kirsten rat sarcoma viral oncogene homologue
Ci	Curie	**l**	liter
DNA	deoxyribonucleic acid	**M**	molar
cDNA	complementary DNA	**tRNA**	transfer RNA
d	deoxy	**mRNA**	messenger RNA
Da	Dalton	**miRNA**	microRNA
ddH$_2$O	double-distilled water	**miRNP**	micro-ribonucleoprotein
DGCR8	DiGeorge syndrome critical region 8	**natsiRNA**	natural antisense transcript-derived siRNA
Dm	Drosophila melanogaster	**nt**	nucleotides
DUF	domain of unknown function		
dNTP	2'-deoxyribonucleoside triphosphate	**O/N**	over-night
ds	double-stranded	**ORF**	open reading frame
dsRBD	double-stranded RNA binding domain	**P**	phosphate
DTT	1,4-dithiothreitol	**PAA**	polyacrylamide
E. coli	*Escherichia coli*	**PABP**	poly(A)-binding protein
EDTA	ethylenediaminetetraacetic acid	**PAGE**	polyacrylamide gel electrophoresis
FCS	fetal calf serum	**PAZ**	piwi-argonaute-zwille
FH	Flag-HA	**PBS**	phospate buffered saline
g	gravitational constant	**P bodies**	processing bodies
GFP	green fluorescent protein	**PCR**	polymerase chain reaction
GTP	guanosine triphosphate	**Per1**	Period1

107

piRNA	Piwi-interacting RNA		**S**	Svedberg unit (sedimentation coefficient)
PMSF	phenylmethylsulfonyl fluoride		**SD**	standard deviation
Pol	polymerase		**SDS**	sodium dodecyl sulfate
pre-miRNA	precursor miRNA		**siRNA**	small interfering RNA
pri-miRNA	primary miRNA		**snoRNA**	small nucleolar RNA
qPCR	quantitative *real time* polymerase chain reaction		**ss**	single-stranded
RdRP	RNA dependent RNA polymerase		**tasiRNA**	*trans*-acting siRNA
rpm	revolutions per minute		**TEMED**	N,N,N',N'-Tetramethylethylenediamine
RT	room temperature		**TNRC6**	trinucleotide repeat containing 6
RISC	RNA induced silencing complex		**Tris**	tris(hydroxymethyl)aminomethane
RNA	ribonucleic acid		**UBA**	ubiquitin-associated domain
RNAi	RNA interference		**UTP**	uridine triphosphate
RNP	ribonucleoprotein		**v/v**	volume in volume
rRNA	ribosomal RNA		**wt**	wild-type
RRM	RNA recognition motif		**w/v**	weight per volume

FIGURE INDEX

TABLE INDEX

APPENDIX

Supplementary Table 1: Mass spectrometry data on Ago 1 complex I

protein	Acc.No.	Mass	Queries matched	Protein score	Seq cov (%)	Peptide score	Pep delta	Pep sequence
eukaryotic translation initiation factor 2C, 1 (Ago1) [Homo sapiens]	gi|6912352	97152	26	2058	58	87	-0,0038	K.NASYNLDPYIQEFGIK.V
Dicer	gi|21665773	217490	7	383	5	112	0,1540	K.SNAETATDLVVLDR.Y
squamous cell carcinoma antigen recognized by T cells 3 (SART3) [Homo sapiens]	gi|7661952	109865	6	158	6	40	0,0663	R.YSQYLDR.Q
Na+/K+ -ATPase alpha 1 subunit isoform a proprotein [Homo sapiens]	gi|21361181	112824	2	72	1	39	0,0775	R.LNIPVSQVNPR.D
unnamed protein product [Homo sapiens]	gi|34535987	148788	1	24	-	24	0,0190	K.EPLLHFR.R
DNA damage binding protein 1 (Damage-specific DNA binding protein 1) (DDB p127 subunit) (DDBa) (UV-damaged DNA-binding protein 1)	gi|418316	126901	4	92	3	50	0,0530	K.LLASINSTVR.L
sirtuin 1 [Homo sapiens]	gi|7657575	81630	1	68	1	68	0,0590	R.GDIFNQVVPR.C
HSPC273 [Homo sapiens]	gi|6841196	25891	1	66	4	66	0,0725	R.ELGENLDQILR.A
E1B-55kDa-associated protein (hnRNP U-like) [Homo sapiens]	gi|3319956	95750	1	48	0	48	0,0579	K.INEEISVK.H
programmed cell death 1 precursor [Homo sapiens]	gi|4826890	31687	1	20	2	20	0,0633	R.RTGQPLK.E
heat shock 90kDa protein [Homo sapiens]	gi|56204416	83212	12	686	24	61	0,0464	K.SIYYITGESK.E
Skb1Hs (PRMT5) [Homo sapiens]	gi|48145599	72638	12	749	25	75	0,0108	K.AAILPTSIFLTNK.K
aralar2 [Homo sapiens]	gi|6523256	74093	3	115	6	86	0,0492	K.TVELLSGVVDQTK.D
chaperonin (HSP60)	gi|306890	60986	7	374	21	55	0,0037	R.VTDALNATR.A
translation initiation factor eIF-2b delta subunit [Homo sapiens]	gi|6563202	57563	1	60	2	60	0,0320	R.VGTAQLALVAR.A
elongation factor Tu [Homo sapiens]	gi|31092	50095	5	194	10	54	0,0206	K.IGGIGTVPVGR.V
RuvB-like 2 [Homo sapiens]	gi|5730023	51125	2	89	4	47	0,0332	K.GTEVQVDDIKR.V
Dnj3/Cpr3 [Homo sapiens]	gi|2352904	46277	1	145	10	32	0,0337	R.ELYDRYGEQGLR.E
trans-activation-responsive RNA-binding protein - human (TRBP) (fragment)	gi|107904	38814	1	36	2	36	0,0358	R.FIEIGSGTSK.K
KIAA0115 [Homo sapiens]	gi|473947	50680	1	31	1	31	0,0317	K.SSLNPILFR.G
MEP50 protein (MEP50) [Homo sapiens]	gi|13559060	36701	5	390	22	93	0,0469	K.VWDLAQQVVLSSYR.A
signal sequence receptor, alpha [Homo sapiens]	gi|4507237	32163	1	44	3	44	0,0306	K.GEDFPANNIVK.F
solute carrier family 25 member 3 isoform a precursor [Homo sapiens]	gi|6031192	40069	1	54	3	54	0,0282	R.IQTQPGYANTLR.D
S3 ribosomal protein [Homo sapiens]	gi|7765076	26699	2	206	25	68	0,0322	R.ELAEDGYSGVEVR.V
solute carrier family 25, member 5 [Homo sapiens]	gi|4502099	32874	7	190	22	49	0,0239	K.LLLQVQHASK.Q
Solute carrier family 25, member A6 [Homo sapiens]	gi|15928608	32905	7	204	22	49/48	0,0239/ 0,0088	K.LLLQVQHASK.Q / R.GNLANVIR.Y
solute carrier family 25 member 4 variant [Homo sapiens]	gi|62089114	29328	3	131	11	47	0,0142	R.GNLANVIR.Y
transmembrane protein 33 [Homo sapiens]	gi|8922491	27933	1	56	4	56	0,0113	R.ALLANALTSALR.L
ribosomal protein L23 [Homo sapiens]	gi|4506605	14856	1	28	5	28	0,0137	K.NLYIISVK.G
Ribosomal protein S27-like protein [Homo sapiens]	gi|13277528	9472	1	58	9	58	0,0133	R.LTEGCSFR.R + Carb.
ribosomal protein L38 [Homo sapiens]	gi|3088356	4291	1	38	27	38	0,0253	K.QSLPPGLAVK.E
ribosomal protein S6	gi|225901	28633	1	28	3	28	0,0224	K.LIEVDDER.K

Supplementary Table 2: Mass spectrometry data on Ago1 complex II

protein	Acc.No.	Mass	Queries matched	Protein score	Seq cov %	Peptide score	Pep delta	Pep sequence
eukaryotic translation initiation factor 2C, 1 (Ago1) [Homo sapiens]	gi|6912352 gi|38649144	97152 97151	30 5	2142 332	62 12	76/76 63	0,0133/ 0,0398 0,0179	K.LLANYFEVDIPK.I / K.NASYNLDPYIQEFGIK.V R.VLPAPILQYGGR.N
splicing factor 3b, subunit 1 isoform 1 [Homo sapiens]	gi|54112117	145738	6	460	8	69	0,0353	R.GGDSIGETPTPGASK.R

111

protein	Acc.No.	Mass	Queries matched	Protein score	Seq cov %	Peptide score	Pep delta	Pep sequence
Splicing factor 3B subunit 2 (Spliceosome associated protein 145) (SAP 145) (SF3b150) (Pre-mRNA splicing factor SF3b 145 kDa subunit)	gi|2498883	97596	5	158	6	57	0,0227	R.AAVLLEQER.Q
RNA helicase A [Homo sapiens]	gi|1806048	140788	9	382	10	58	0,0264	R.GISHVIVDEIHER.D
KIAA0017 protein [Homo sapiens]	gi|40788938	139414	9	302	7	62	0,0263	R.SVAGGFVYTYK.L
DEAH (Asp-Glu-Ala-His) box polypeptide 30 isoform 1 (Ddx30) [Homo sapiens]	gi|20336294	133854	4	189	6	44	0,0273	K.AIFQQPPVGVR.K
hnRNP U protein [Homo sapiens]	gi|32358	88890	4	286	5	110	0,0361	R.NFILDQTNVSAAAQR.R
squamous cell carcinoma antigen recognized by T cells 3 (SART3) [Homo sapiens]	gi|7661952	109865	4	151	5	58	0,0224	R.ALEYLKQEVEER.F
spliceosomal protein SAP 155 [Homo sapiens]	gi|4033735	145723	1	51	0	51	0,0237	R.QQAADLISR.T
gemin4 [Homo sapiens]	gi|7657122	119913	1	45	-	45	0,0193	R.GLTQIQSR.I
F-box and leucine-rich repeat protein 13 [Homo sapiens]	gi|24432072	83887	1	35	2	17	0,0223	K.THFCTWRDIAR.T + Carb
KIAA1488 protein (Dhx36) [Homo sapiens]	gi|7959237	97766	1	27	1	27	0,0334	R.LGGIAYFLSR.L
RNA helicase Gu - human (fragment)	gi|2135315	89196	4	117	-	40	0,043	K.STYEQVDLIGK.K
transcription factor NF-AT 90K chain – human	gi|1082856	73293	3	114	-	52	0,0559	R.EDITQSAQHALR.L
ATP-dependent RNA helicase #46 [Homo sapiens]	gi|2696613	92770	1	112	3	44	0,06	R.YGVIILDEAHER.T
motor protein [Homo sapiens]	gi|516764	79659	2	88	3	46	0,0521	R.GVYSEETLR.A
hypothetical protein LOC55037 [Homo sapiens]	gi|38683855	78500	4	232	7	53	0,0595	K.DISEAALKER.I
ZNF326 protein [Homo sapiens]	gi|31807861	33426	2	109	7	61	0,0775	R.SGYGFNEPEQSR.F
NSAP1 protein [Homo sapiens]	gi|5031512	62617	2	102	4	60	0,0886	R.TGYTLDVTTGQR.K
Skb1Hs (PRMT5) [Homo sapiens]	gi|2323410	72740	3	90	5	32	0,0664	R.GPLVNASLR.A
mRNA-binding protein CRDBP [Homo sapiens]	gi|7141072	63417	3	145	6	50	0,1205	R.DQTPDENDQVIVK.I
poly(A) binding protein, cytoplasmic 1 [Homo sapiens]	gi|46367787	70626	4	128	-	66	0,0246	R.IVATKPLYVALAQR.K
E2IG3 [Homo sapiens]	gi|6457340	63528	1	35	1	35	0,084	K.GGIPNVEGAAK.L
ribosomal protein L4 [Homo sapiens]	gi|16579885	47667	1	153	6	56	0,0646	K.AAAAAAALQAK.S
heterogeneous nuclear ribonucleoprotein H2 (H') [Homo sapiens]	gi|6065880	49232	1	61	3	61	0,0995	K.HTGPNSPDTANDGFVR.L
DNA-binding protein B (Homo sapiens)	gi|181486	39954	9	538	28	115	0,1146	K.GAEAANVTGPGGVPVQGS K.Y
elongation factor Tu [Homo sapiens]	gi|31092	50095	4	130	9	37	0,0854	R.YEEIVKEVSTYIK.K
HNRPF protein [Homo sapiens]	gi|16876910	45671	1	66	3	66	0,0805	K.HSGPNSADSANDGFVR.L
Rev interacting protein Rip-1	gi|1326184	33263	2	60	6	37	0,0634	R.SVSFEQAVR.I
translation initiation factor (Ddx48) [Homo sapiens]	gi|496902	46803	1	13	3	13	0,1046	R.GIYAYGFEKPSAIQQR.A
NF45 protein	gi|532313	44669	2	117	5	65	0,0579	K.VLQSALAAIR.H
LYAR [Homo sapiens]	gi|49065522	43626	1	92	3	92	0,0949	R.ELLEQISAFDNVPR.K
KIAA0264 [Homo sapiens]	gi|1665795	47767	1	89	4	58	0,0533	R.LIDNISSR.E
MEP50 protein (MEP50) [Homo sapiens]	gi|13559060	36701	1	31	4	31	0,0842	R.YRSDGALLLGASSLSGR.C
mitochondrial ribosomal protein S5 [Homo sapiens]	gi|13994259	47976	2	105	5	73	0,0862	R.AIITICR.L + Carb
ionizing radiation resistance conferring protein – human	gi|7430427	43584	3	104	-	45	0,0508	R.NATDAVGIVLK.E
Mitochondrial ribosomal protein S22 [Homo sapiens]	gi|14424546	41254	2	169	12	30	0,0572	K.DQAAEGINLIK.V
60S acidic ribosomal protein P0 (L10E)	gi|3041728	33236	2	229	14	57	0,1075	R.GTIEILSDVQLIK.T
ribosomal protein L6 [Homo sapiens]	gi|36138	32841	3	99	10	46	0,0912	R.SVFALTNGIYPHK.L
Hypothetical protein PRO1855 [Homo sapiens]	gi|16877878	34909	2	42	7	28	0,152	K.LVTLPVSFAQLK.N
ribosomal protein S3a [Homo sapiens]	gi|4506723	29926	7	279	35	57	0,1812	R.EVQTNDLKEVVNK.L
prohibitin 2 [Homo sapiens]	gi|6005854	33276	2	143	12	74	0,1698	K.LLLGAGAVAYGVR.E
ribosomal protein S2 [Homo sapiens]	gi|15055539	31305	8	442	40	63	0,1102	R.GTGIVSAPVPK.K
mitochondrial ribosomal protein S2 [Homo sapiens]	gi|55958121	30460	1	32	2	32	0,1113	K.GIILFISR.N
ribosomal protein S6	gi|337514	28614	3	173	31	59	0,1626	L.LFNLSKEDDVR.E
S3 ribosomal protein [Homo sapiens]	gi|7765076	26699	6	350	33	72	0,1654	R.ELAEDGYSGVEVR.V
ATP synthase, H+ transporting, mitochondrial F1 complex, gamma subunit isoform H (heart) precursor [Homo sapiens] ?alpha subunit found	gi|4885079	32860	1	106	8	67	0,1784	R.IYGLGSLALYEK.A
solute carrier family 25 member 3 isoform a precursor [Homo sapiens]	gi|6031192	40069	1	50	3	50	0,187	R.IQTQPGYANTLR.D
ribosomal protein S4	gi|227229	29664	4	208	18	64	0,1729	K.VNDTIQIDLETGK.I
ribosomal protein L7 [Homo sapiens]	gi|35903	29164	3	178	12	81	0,1303	R.IALTDNALIAR.S
ribosomal protein L14 [Homo sapiens]	gi|1620022	23788	1	49	5	49	0,1671	K.LVAIVDVIDQNR.A
unnamed protein product [Homo sapiens]	gi|34392	24191	1	33	3	33	0,11	K.ATFDAISK.T
prohibitin [Homo sapiens]	gi|4505773	29786	4	203	16	83	0,1505	R.FDAGELITQR.E
ADP.ATP translocase	gi|339721	28042	4	182	15	63	0,1574	R.AAYFGIYDTAK.G

protein	Acc.No.	Mass	Queries matched	Protein score	Seq cov %	Peptide score	Pep delta	Pep sequence
ribosomal protein L13 [Homo sapiens]	gi|15431297	24247	1 / 2	101 / 79	11 / 8	67 / 46	0,2710 / 0,1869	K.STESLQANVQR.L / R.VATWFNQPAR.K
ribosomal protein L10 [Homo sapiens]	gi|5174431	24561	5	290	38	52	0,2486	R.GAFGKPQGTVAR.V
ribosomal protein L13a [Homo sapiens]	gi|6912634	23562	4	244	29	68	0,2626	K.YQAVTATLEEK.R
ribosomal protein S9	gi|550023	22558	4	123	16	48	0,2173	R.LFEGNALLR.R
mitochondrial ribosomal protein S23 [Homo sapiens]	gi|16554604	21757	2	55	11	37	0,3242	K.APIQDIWYHEDR.I
ribosomal protein L19 [Homo sapiens]	gi|4506609		1	56	4	56	0,1872	K.LLADQAEAR.R
mitochondrial ribosomal protein S15 [Homo sapiens]	gi|16554611	29823	1	46	3	46	0,2045	K.IVANPEDTR.S
ribosomal protein L29 [Homo sapiens]	gi|793843	17656	1	93	10	51	0,2829	K.AQAAAPASVPAQAPK.R
Ribosomal protein S5 [Homo sapiens]	gi|550021	22763	1	45	4	45	0,2053	R.QAVDVSPLR.R
Ribosomal protein L17 [Homo sapiens]	gi|42542645	21402	6	391	51	46	0,2477	R.YSLDPENPTK.S
ribosomal protein L24 [Homo sapiens]	gi|4506619	17768	3	327	30	62	0,2436	R.TDGKVFQFLNAK.C
ribosomal protein S7 [Homo sapiens]	gi|4506741	22113	2	36	8	18 / 18	0,1832 / 0,2003	R.ELNITAAK.E / K.HVVFIAQR.R
RPL21 protein [Homo sapiens]	gi|38649057	18553	1	36	9	36	0,3273	R.VYNVTQHAVGIVVNK.Q
FUS interacting protein (serine-arginine rich) 1 [Homo sapiens]	gi|55961039	22122	1	31	6	31	0,2568	R.YLRPPNTSLFVR.N
ribosomal protein L26	gi|292435	17278	4	169	28	43	0,1556	K.YVIYIER.V
ribosomal protein L11 [Homo sapiens]	gi|14719845	20112	3	152	19	77	0,2808	K.VLEQLTGQTPVFSK.A
ribosomal protein L23a [Homo sapiens]	gi|1574942	17629	2	117	13	68	0,2592	R.LAPDYDALDVANK.I
ribosomal protein L18a [Homo sapiens]	gi|11415026	20749	1	24	3	24	0,1656	K.NFGIWLR.Y
ribosomal protein L27a [Homo sapiens]	gi|4506625	16551	4	142	14	76	0,1704	K.TGAAPIIDVVR.S
ribosomal protein L28	gi|550019	15752	3	132	17	62	0,2314	K.QTYSTEPNNLK.A
ribosomal protein L35 [Homo sapiens]	gi|6005860	14543	2	122	21	49	0,2655	R.VLTVINQTQKENLR.K
Ribosomal protein S18 [Homo sapiens]	gi|75517276	17708	3	233	30	89	0,1868	R.AGELTEDEVER.V
ribosomal protein S26 [Homo sapiens]	gi|296452	12922	2	221	31	124	0,2636	R.DISEASVFDAYVLPK.L
ribosomal protein L23 [Homo sapiens]	gi|4506605	14856	2	148	30	34	0,1091	K.NLYIISVK.G
ribosomal protein homologous to yeast S24 [Homo sapiens]	gi|36142	14707	2	135	25	59	0,2588	K.HGYIGEFEIIDDHR.A
ribosomal protein S23 [Homo sapiens]	gi|3088342	6465	2	110	38	69	0,1774	K.VANVSLLALYK.G
PREDICTED: similar to ribosomal protein S27 [Homo sapiens]	gi|51463957	18745	1	86	-	41	0,2139	K.DLLHPSPEEEKR.K
ribosomal protein L38 [Homo sapiens]	gi|3088356	4291	2	79	59	51	0,2235	R.YLYTLVITDKEK.A
splicing factor 3B, 14 kDa subunit [Homo sapiens]	gi|7706326	14576	2	71	16	42	0,2498	R.GTAYVVYEDIFDAK.N
ribosomal protein L31 [Homo sapiens]	gi|1655596	14084	2	67	28	32	0,2614	K.LYTLVTYVPVTTFK.N
mitochondrial ribosomal protein S16 [Homo sapiens]	gi|7705626	15335	2	41	18	38	0,1442	K.LVALNLDR.I
ribosomal protein L35a [Homo sapiens]	gi|16117791	12530	1	36	13	28	0,1292	K.IEGVYAR.D
PHD-finger 5A [Homo sapiens]	gi|14249398	12397	1	33	6	33	0,1486	K.TDLFYER.K

Supplementary Table 3: Mass spectrometry data on Ago1 complex III

protein	Acc.No.	Mass	Queries matched	Protein score	Seq cov %	Peptide score	Pep delta	Pep sequence
eukaryotic translation initiation factor 2C, 1 (Ago1) [Homo sapiens]	gi|6912352	97152	24	1797	60	89	0,2587	K.LLANYFEVDIPK.I
Transcription factor (TFIIIC) alpha chain, partial [Homo sapiens]	gi|2342740	209464	2	105	1	43	0,1593	R.GYYSPGIVSTR.N
RNA helicase A – human	gi|1082769	141984	20	1135	26	64	0,1842	K.LAQFEPSQR.Q
hnRNP U protein [Homo sapiens]	gi|32358	88890	12	401	16	95	0,2567	K.SSGPTSLFAVTVAPPGAR.Q
MYB binding protein 1a [Homo sapiens]	gi|7657351	148758	12	628	13	69	0,1538	K.ALVDILSEVSK.A
ubiquitin	gi|229532	8446	1	26	12	26	0,1429	R.TLSDYNIQK.E
Dicer [Homo sapiens]	gi|5019620	218673	2	62	0	62	0,1331	R.AQTASDAGVGVR.S
U5 snRNP-specific 200kD protein [Homo sapiens]	gi|3255965	194356	2	46	0	27	0,1184	R.TYTQLVR.L
polymerase (RNA) I polypeptide A, 194kDa [Homo sapiens]	gi|7661686	194068	1	32	-	32	0,1293	R.GYLTPTSAR.E
proliferation-inducing protein 32 [Homo sapiens]	gi|45643460	162923	11	421	9	84	0,2010	K.SLYDEVAAQGEVVR.K
PELP1 [Homo sapiens]	gi|21426922	136556	7	320	7	65	0,1701	R.LPSLGAGFSQGLK.H
coatomer protein [Homo sapiens]	gi|1002369	138244	6	247	6	53	0,1850	K.LVGQSIIAYLQK.K
DEAH (Asp-Glu-Ala-His) box polypeptide 30 isoform 1 (Ddx30) [Homo sapiens]	gi|20336294	133854	14	662	16	76	0,2654	R.ENYLEENLLYAPSLR.F

113

protein	Acc.No.	Mass	Queries matched	Protein score	Seq cov %	Peptide score	Pep delta	Pep sequence
regulator of nonsense transcript stability (RENT1) [Homo sapiens]	gi|1575536	123039	8	293	9	51 / 51	0,1395 / 0,1640	R.YGVIIVGNPK.A / R.EAIIPGSVYDR.S
squamous cell carcinoma antigen recognized by T cells 3 (SART3) [Homo sapiens]	gi|7661952	109865						
Splicing factor 3B subunit 3 (Spliceosome associated protein 130) (SAP 130) (SF3b130) (Pre-mRNA splicing factor SF3b 130 kDa subunit) (STAF130)	gi|19863446	135507	2	82	-	46	0,1859	R.FLAVGLVDNTVR.I
spliceosomal protein SAP 155 [Homo sapiens]	gi|4033735	145723	1	32	1	14	0,1482	K.TEILPPFFK.H
unnamed protein product [Homo sapiens]	gi|7023011	113841	3	84	2	52	0,1564	R.QSILNSLSR.G
novel S-100/ICaBP type calcium binding domain and EF hand domain containing protein [Homo sapiens]	gi|12314268	24325	1	54	-	54	0,2037	R.SVVTVIDVFYK.Y
KIAA1488 protein (Dhx36) [Homo sapiens]	gi|7959237	97766	1	38	1	38	0,1752	R.LGGIAYFLSR.L
matrin 3 [Homo sapiens]	gi|6563246	95138	1	36	1	36	0,1478	K.SFQQSSLSR.D
Chain A, Human Dna Topoisomerase I (70 Kda) In Non-Covalent Complex With A 22 Base Pair Dna Duplex	gi|3659924	69975	5	210	11	65	0,2323	R.TYNASITLQQQLK.E
gemin4 [Homo sapiens]	gi|7657122	119913	3	123	-	52	0,2582	R.LLETVIDVSTADR.A
Nucleolin (Protein C23)	gi|128841	76298	3	94	-	42	0,3323	R.SISLYYTGEKGQNQDYR.G
serine protein kinase SRPK1 – human	gi|630737	74273	1	45	-	45	0,2781	K.SAEAYTETALDEIR.L
RNA helicase Gu - human (fragment)	gi|2135315	89196	5	142	-	41	0,2663	K.STYEQVDLIGKK.T
NF-90 [Homo sapiens]	gi|5006602	82749	9	470	18	47	0,2972	K.AVSDWIDEQEK.G / R.IFVNDDR.H
nbla10363 [Homo sapiens]	gi|19911062	105622	3	132	4	41	0,1882	K.SLQATALR.I
fragile X mental retardation syndrome related protein 2 [Homo sapiens]	gi|4758410	74083	4	122	6	62	0,3632	K.AGYSTDESSSSSLHATR.T
novel protein [Homo sapiens]	gi|5578958	81192	1	50	3	31	0,3445	R.GLHSQNFTQALLER.M
DEAD (Asp-Glu-Ala-Asp) box polypeptide 50 [Homo sapiens]	gi|55664207	82514	2	48	4	27	0,2840	R.GVTYLFPIQVK.T
motor protein [Homo sapiens]	gi|516764	79659	1	41	1	41	0,3122	K.VVSQYHELVVQAR.D
90kDa heat shock protein	gi|306891	83242	1	37	1	37	0,2755	K.ADLINNLGTIAK.S
general transcription factor IIIC, polypeptide 4, 90kDa [Homo sapiens]	gi|6912400	91943	1	31	1	31	0,2307	K.QVDLIDLVR.W
RNA helicase (Ddx18) [Homo sapiens]	gi|1498229	68416	3	201	7	77	0,3234	K.LGNGINIIVATPGR.L
motor protein [Homo sapiens]	gi|516768	83626	3	117	5	52	0,2728	R.YSTSGSSGLTTGK.I
ZNF326 protein [Homo sapiens]	gi|47125447	57787	2	112	4	72	0,3989	R.ESVLTATSILNNPIVK.A
FMR1	gi|182673	74981	1	22	1	22	0,2391	R.LQIDEQLR.Q
polyadenylate binding protein II [Homo sapiens]	gi|693937	58481	16	808	39	66	0,2400	R.IVATKPLYVALAQR.K
putative G-binding protein [Homo sapiens]	gi|3153873	65375	2	78	4	52	0,2486	R.ADVDVQPYAFTTK.S
IGF-II mRNA-binding protein 1 (ZBP-1) [Homo sapiens]	gi|56237027	63441	10	499	21	92	0,3391	K.ITISSLQDLTLYNPER.T
IGF-II mRNA-binding protein 3 (ZBP-3) [Homo sapiens]	gi|30795212	63666	6	274	12	61	0,2814	R.DQTPDENDQVVVK.I
E2IG3 [Homo sapiens]	gi|6457340	63528	6	207	11	49	0,1862	K.GGIPNVEGAAK.L
PBK1 protein [Homo sapiens]	gi|3668141	58097	3	103	5	37	0,1655	R.LLPSLIGR.H
NSAP1 protein [Homo sapiens]	gi|5031512	62617	2	65	3	44	0,2641	R.NLANTVTEEILEK.A
hNop56 [Homo sapiens]	gi|2230878	66807	2	62	3	39	0,1809	R.VVSLSEYR.Q
G22P1 [Homo sapiens]	gi|49457432	69829	1	53	1	53	0,2187	R.DSLIFLVDASK.A
KIAA1273 protein [Homo sapiens]	gi|6382028	68066	2	47	3	35	0,1802	R.QTVLESIR.T
Similar to ribophorin I [Homo sapiens]	gi|14124942	64542	1	31	1	31	0,1624	K.IILPEGAK.N
heterogeneous nuclear ribonucleoprotein L [Homo sapiens]	gi|11527777	64046	1	55	1	55	0,2128	R.SSSGLLEWESK.S
t-complex polypeptide 1 [Homo sapiens]	gi|36796	60356	1	37	1	37	0,1868	R.YPVNSVNILK.A
testis-specific poly(A)-binding protein [Homo sapiens]	gi|11610605	70072	1	33	2	33	0,2196	R.IVATKPLYVALAQR.K
ribophorin II precursor – human	gi|88567	69273	1	29	-	29	0,1694	R.YIANTVELR.V
Ost-I [Homo sapiens]	gi|41386665	102111	1	13	1	13	0,1875	R.HLCDQFSAEIAR.R + Carb.
ribosomal protein L4 [Homo sapiens]	gi|16579885	47667	5	279	19	43	0,1513	R.NIPGITLLNVSK.L
DEAD (Asp-Glu-Ala-Asp) box polypeptide 47 isoform 1 [Homo sapiens]	gi|20149629	50615	2	85	5	43	0,1470	R.DIIGLAETGSGK.T
nuclear RNA helicase (Ddx39) [Homo sapiens]	gi|1905998	49046	1	45	2	45	0,1370	R.ILVATNLFGR.G
translation initiation factor (KIAA0111) [Homo sapiens]	gi|496902	46803	6	207	15	51	0,1949	R.ETQALILAPTR.E
Ribosomal protein P0 [Homo sapiens]	gi|12654583	34253	7	519	43	76	0,0606	K.TSFFQALGITTK.I
Mov10	gi|14424568	43599	6	52	6	52	0,06	R.ITGNPVVTNP.I
NF45 protein	gi|532313	44669	8	469	25	64 / 64	0,0115 / 0,0249	K.VLQSALAAIR.H / K.ILPTLEAVAALGNK.V
PAK/PLC-interacting protein 1 [Homo sapiens]	gi|14211689	44076	1	44	2	44	0,1426	K.LALSVGTDK.T
unnamed protein product [Homo sapiens]	gi|31092	50095	1	37	2	37	0,1690	K.IGGIGTVPVGR.V
KIAA1756 protein [Homo sapiens]	gi|12698057	116668	1	30	0	30	0,0590	R.AELEKVLR.A

protein	Acc.No.	Mass	Queries matched	Protein score	Seq cov %	Peptide score	Pep delta	Pep sequence
R32184_1 [Homo sapiens]	gi|3025445	47276	1	26	2	26	0,1660	K.SVLGGQDQLR.V
WS beta-transducin repeats protein [Homo sapiens]	gi|4704417	47537	1	24	2	24	0,1765	K.YLATCADDR.T + Carb.
HNRPC protein [Homo sapiens]	gi|13937888	33578	4	349	20	71	0,0539	R.VFIGNLNTLVVK.K
RNA polymerase I subunit isoform 2 [Homo sapiens]	gi|4759046	38623	2	93	5	49	0,0182	R.VVLGEFGVR.N
ribosomal protein L6 [Homo sapiens]	gi|36138	32841	7	265	22	50	0,0414	K.FVIATSTK.I
EBNA1 binding protein 2 [Homo sapiens]	gi|5803111	34798	1	55	3	55	0,0383	R.ESYDDVSSFR.A
B23 nucleophosmin (280 AA) [Homo sapiens]	gi|825671	30919	2	109	7	57	0,0379	K.GPSSVEDIK.A
hnRNP-E2 [Homo sapiens]	gi|460773	38556	1	56	3	56	0,0448	K.IANPVEGSTDR.Q
HuR RNA binding protein	gi|1022961	36039	1	73	3	73	0,0541	R.VLVDQTTGLSR.G
putative dimethyladenosine transferase [Homo sapiens]	gi|3646270	17915	1	46	6	46	0,0453	K.SSAVQQLLEK.N
prohibitin 2 [Homo sapiens]	gi|6005854	33276	10	513	35	90	0,0478	K.FNASQLITQR.A
ribosomal protein S3a [Homo sapiens]	gi|4506723	29926	4	278	38	56	0,0516	R.EVQTNDLKEVVNK.L
ribosomal protein S6	gi|337514	28614	2	289	16	73	0,0372	K.LIEVDDER.K
SMN-interacting protein 1 isoform alpha [Homo sapiens]	gi|4506961		1	32	2	32	0,0362	R.TPQEYLR.R
PREDICTED: hypothetical protein XP_499151 [Homo sapiens]	gi|51467206	12243	1	22	-	22	0,1148	K.VCSWPVDLDSK.G
distal-less homeobox 4 isoform a [Homo sapiens]	gi|20143962	26246	1	22	6	22	0,0799	-.MTSLPCPLPGRDASK.A + Oxid.
ribosomal protein L7a [Homo sapiens]	gi|4506661	29977	11	535	50	92	0,0422	R.AGVNTVTTLVENK.K
Ribosomal protein L8 [Homo sapiens]	gi|15341853	27993	7	311	27	76	0,0493	R.ASGNYATVISHNPETK.K
ribosomal protein S2 [Homo sapiens]	gi|15055539	31305	6	277	25	48	0,0565	K.TYSYLTPDLWK.E
S3 ribosomal protein [Homo sapiens]	gi|7765076	26699	3	165	18	67	0,0604	R.ELAEDGYSGVEVR.V
solute carrier family 25 member 3 isoform a precursor [Homo sapiens]	gi|6031192	40069	1	50	3	50	0,0594	R.IQTQPGYANTLR.D
scar protein	gi|337930	27386	10	423	42	90	0,0455	K.VNDTIQIDLETGK.I
ribosomal protein L7 [Homo sapiens]	gi|35903	29164	6	304	36	83	0,0317	R.IALTDNALIAR.S
prohibitin [Homo sapiens]	gi|4505773	29786	6	308	23	89	0,0292	K.AAIISAEGDSK.A
ADP.ATP translocase	gi|339721	28042	2	79	9	42	0,0444	R.AAYFGIYDTAK.G
Unknown (protein for MGC:117326) [Homo sapiens]	gi|76779245	36999	10	440	27	98	0,0343	R.IALTDNALIAR.S
ribosomal protein S4	gi|227229	29664	2	82	9	57	0,0297	R.LSNIFVIGK.G
ribosomal protein S8 [Homo sapiens]	gi|55961080	2186	2	79	13	64	0,0221	K.ISSLLEEQFQQGK.L
60S ribosomal protein L13	gi|6831614	24378	1	72	5	72	0,0266	K.STESLQANVQR.L
ribosomal protein L13 [Homo sapiens]	gi|15431297	24247	2	139	16	72	-0,0036	K.STESLQANVQR.L
ribosomal protein L14 [Homo sapiens]	gi|1620022	23788	1	86	5	86	0,0163	K.LVAIVDVIDQNR.A
ribosomal protein L19 [Homo sapiens]	gi|4506609		1	72	4	72	-0,0192	K.LLADQAEAR.R
ribosomal protein L18 [Homo sapiens]	gi|4506607	21621	7	453	41	103	-0,0268	K.ILTFDQLALDSPK.G
ribosomal protein L13a [Homo sapiens]	gi|6912634	23562	4	237	28	68	-0,0100	K.YQAVTATLEEK.R
ribosomal protein L15 [Homo sapiens]	gi|15431293	24131	4	140	18	65	-0,0128	R.SLQSVAEER.A
ribosomal protein S9	gi|550023	22558	9	373	39	49	0,0154	R.LGVLDEGK.M
ribosomal protein L10 [Homo sapiens]	gi|5174431	24561	2	83	17	35	-0,0132	R.GAFGKPQGTVAR.V
Ribosomal protein S5 [Homo sapiens]	gi|15929961	22862	1	51	4	51	-0,0091	R.QAVDVSPLR.R
ribosomal protein L29 [Homo sapiens]	gi|793843	17656	2	130	15	56	-0,0696	K.AQAAAPASVPAQAPKR.T
ribosomal protein S7 [Homo sapiens]	gi|4506741	22113	5	196	18	46	-0,0254	K.VETFSGVYK.K
Ribosomal protein L17 [Homo sapiens]	gi|42542645	21402	3	198	23	51	-0,0285	R.YSLDPENPTK.S
L21 ribosomal protein	gi|619788	17646	2	80	17	43	-0,0441	R.VYNVTQHAVGIVVNK.Q
ribosomal protein L24 [Homo sapiens]	gi|4506619	17768	3	191	21	45	-0,0534	R.TDGKVFQFLNAK.C
ribosomal protein L18a [Homo sapiens]	gi|11415026	20749	2	43	30	43	-0,0278	R.IFAPNHVVAK.S
ribosomal protein L11 [Homo sapiens]	gi|14719845	20112	7	363	31	97	-0,0372	K.VLEQLTGQTPVFSK.A
ribosomal protein L26 [Homo sapiens	gi|4506621	17248	3	243	26	33	-0,0321	K.DDEVQVVR.G
ribosomal protein L12 [Homo sapiens]	gi|55665101	17808	3	165	24	65	-0,0607	K.HSGNITFDEIVNIAR.Q
ribosomal protein L23a [Homo sapiens]	gi|1574942	17629	2	108	13	59	-0,0328	R.LAPDYDALDVANK.I
ribosomal protein L27a [Homo sapiens]	gi|4432754	3706	1	57	32	57	-0,0284	K.TGAAPIIDVVR.S
ribosomal protein L28	gi|550019	15752	5	338	43	52 / 52	-0,0343 / -0,0738	K.GVVVVIKR.R / K.QTYSTEPNNLKAR.N
ribosomal protein L11 [Homo sapiens]	gi|495126	20103	3	215	16	55	-0,0786	K.VLEQLTGQTPVFSKAR.Y
ribosomal protein S13 [Homo sapiens]	gi|553640	13313	4	101	24	50	-0,0420	K.GLTPSQIGVILR.D
PREDICTED: similar to 60S ribosomal protein L32 [Homo sapiens]	gi|51467067	52271	1	64	-	39	-0,0630	R.AAQLAIRVTNPNAR.Q
ribosomal protein L35 [Homo sapiens]	gi|6005860	14543	2	142	21	47	-0,0744	R.VLTVINQTQKENLR.K
ribosomal protein S26 [Homo sapiens]	gi|296452	12922	2	168	31	73	-0,0614	R.DISEASVFDAYVLPK.L
ribosomal protein L23 [Homo sapiens]	gi|4506605	14856	2	247	51	39	-0,0393	K.GSAITGPVAK.E
Ribosomal protein S15a [Homo sapiens]	gi|12804561	14770	3	209	60	74	-0,0769	K.HGYIGEFEIIDDHR.A
ribosomal protein L37a [Homo sapiens]	gi|4506643	10268	1	132	39	102	-0,0533	K.TVAGGAWTYNTTSAVTVK.S

protein	Acc.No.	Mass	Queries matched	Protein score	Seq cov %	Peptide score	Pep delta	Pep sequence
PREDICTED: similar to ribosomal protein S27 [Homo sapiens]	gi|51463957	18745	1	94	-	41	-0,0609	K.DLLHPSPEEEKR.K

Supplementary Table 4: Mass spectrometry data on Ago2 complex I

protein	Acc.No.	Mass	Queries matched	Protein score	Seq cov %	Peptide score	Pep delta	Pep sequence
eukaryotic initiation factor 2C2 (Ago2) [Homo sapiens]	gi|29171734	97146	12	1104	40	91	0,0204	R.SVSIPAPAYYAHLVAFR.A
solute carrier family 25 member 3 isoform a precursor [Homo sapiens]	gi|6031192	40069	5	217	14	62	0,0382	R.IQTQPGYANTLR.D
Dicer [Homo sapiens]	gi|5019620	218673	6	353	5	112	0,0632	K.SNAETATDLVVLDR.Y
KIAA1093 protein [Homo sapiens]	gi|14133235	183156	3	169	3	74	0,0779	K.TGSVGSWGAAR.G
HsGCN1 [Homo sapiens]	gi|2282576	211377	1	41	0	41	0,0405	K.ASLLDPVPEVR.T
Na+,K+ ATPase [Homo sapiens]	gi|1359715	111901	1	122	3	47	0,0305	R.LNIPVSQVNPR.D
RNA-binding protein 10 (RNA-binding motif protein 10) (DXS8237E)	gi|12644371	103396	1	40	1	40	0,0326	R.DGLGSDNIGSR.M
HSPC273 [Homo sapiens]	gi|6841196	25891	1	95	10	74	0,1177	R.ELGENLDQILR.A
importin 4 [Homo sapiens]	gi|18700635	118642	1	70	1	41	0,0912	R.ELLLPDTER.I
DNA damage binding protein 1 (Damage-specific DNA binding protein 1) (DDB p127 subunit) (DDBa) (UV-damaged DNA-binding protein 1) (UV-DDB 1)	gi|418316	126901	1	31	2	24	0,1030	K.VTLGTQPTVLR.T
importin 8 [Homo sapiens	gi|53759103	119861	1	30	0	30	0,1061	K.IINFAPSLLR.I
eukaryotic translation initiation factor 2C, 3 (Ago3) [Homo sapiens]	gi|56204478	71165	12	1104	16	91	0,0204	R.SVSIPAPAYYAHLVAFR.A
Heat shock protein 90 [Homo sapiens]	gi|56204416	83212	8	520	13	81	0,0209	R.GVVDSEDLPLNISR.E
PREDICTED: similar to liver phosphofructokinase isoform b; 6-phosphofructokinase, liver type; liver-type 1-phosphofructokinase; phosphofructokinase 1	gi|55657570	85437	1	53	-	48	0,0934	R.FDEATQLR.G
initation factor 4B [Homo sapiens]	gi|288100	69183	1	32	2	32	0,1246	R.AASIFGGAKPVDTAAR.E
MTHSP75	gi|292059	73734	2	25	6	33	0,0469	R.QAVTNPNNTFYATKR.L
Skb1Hs [Homo sapiens]	gi|82581643	72520	10	710	25	66	0,1128	K.YSQYQQAIYK.C
aralar2 [Homo sapiens]	gi|6523256	74093	2	100	2	61	0,1153	R.LQVAGEITTGPR.V
proteasome subunit p58 [Homo sapiens]	gi|2656092	60968	1	44	2	44	0,0964	R.VYEFLDKLDVVR.S
glycoprotein-associated amino acid transporter hb0,+AT1 [Homo sapiens]	gi|5823978	53436	1	32	1	32	0,0358	K.VLSYISVRR.L
Chaperonin [Homo sapiens]	gi|49522865	61016	5	348	10	79	0,0927	K.NAGVEGSLIVEK.I
mitogen-activated protein kinase kinase kinase 7 interacting protein 1 isoform alpha [Homo sapiens]	gi|5174703	54610	1	64	2	64	0,1068	K.YGYTDIDLLSAAK.S
TATA binding protein interacting protein 49 kDa [Homo sapiens]	gi|4506753	50196	1	61	2	61	0,0746	K.QAASGLVGQENAR.E
elongation factor Tu	gi|556301	50132	4	196	10	65	0,0505	K.THINIVVIGHVDSGK.S
RuvB-like 2 [Homo sapiens]	gi|5730023	51125	2	140	4	82	0,0451	R.GLGLDDALEPR.R
trans-activation-responsive RNA-binding protein - human (TRBP) (fragment)	gi|107904	38814	1	46	2	46	0,0250	R.FIEIGSGTSK.K
unnamed protein product [Homo sapiens]	gi|31092	50095	3	88	6	39	0,0260	K.IGGIGTVPVGR.V
HNRPF protein [Homo sapiens]	gi|16876910	45671	1	64	4	51	0,0328	R.YIEVFKSSQEEVR.S
26S proteasome regulatory chain 4 [validated] – human	gi|345717	49210	1	46	-	46	0,0247	K.GVILYGPPGTGK.T
MEP50 protein (MEP50) [Homo sapiens]	gi|13559060	36701	4	343	21	89	0,0813	K.VWDLAQQVVLSSYR.A
brain tumor associated protein LRRC4 [Homo sapiens]	gi|14495561	72671	1	47	1	47	0,0122	R.MAELKCR.T
otopetrin 2 [Homo sapiens]	gi|30039714	62195	1	43	1	43	0,0044	R.EAVAIVSTPR.S
Cl channel	gi|228672	25872	1	92	5	92	0,0186	K.GLGTGTLYIAESR.L
7-dehydrocholesterol reductase [Homo sapiens]	gi|3171089	53073	1	38	1	38	0,0129	R.YTAAVPYR.L
oxidase (cytochrome c) assembly 1-like [Homo sapiens]	gi|4826880	55262	1	37	1	37	0,0062	R.NQLELAAR.G
[Human pre-mRNA splicing factor SF2p32, complete sequence.], gene product	gi|338043	30888	4	469	33	81	0,0706	R.EVSFQSTGESEWK.D
emerin [Homo sapiens]	gi|4557553	28976	1	40	3	40	0,0357	R.APGAGLGQDR.Q
Solute carrier family 25, member A6 [Homo sapiens]	gi|15928608	32905	12	420	33	66	0,0461	K.LLLQVQHASK.Q
solute carrier family 25, member 5 [Homo sapiens]	gi|4502099	32874	11	362	32	71	0,0513	K.DFLAGGVAAAISK.T
transmembrane protein 33 [Homo sapiens]	gi|8922491	27933	2	90	8	60	0,0839	R.ALLANALTSALR.L
ADP.ATP translocase	gi|339721	28042	1	25	4	25	0,0780	R.AAYFGIYDTAK.G
signal sequence receptor, delta [Homo sapiens]	gi|5454090	18987	1	87	13	44	0,0744	R.FFDEESYSLLR.K

protein	Acc.No.	Mass	Queries matched	Protein score	Seq cov %	Peptide score	Pep delta	Pep sequence
ribosomal protein S20 [Homo sapiens]	gi|3088340	6853	1	38	20	38	0,0502	R.LIDLHSPSEIVK.Q
ribosomal protein L23 [Homo sapiens]	gi|4506605	14856	2	86	20	35	0,0407	K.GSAITGPVAK.E
NADH dehydrogenase (ubiquinone) 1 alpha subcomplex, 4, 9kDa [Homo sapiens]	gi|75517917	9364	2	52	22	37	0,0487	K.FYSVNVDYSK.L
ribosomal protein S27 [Homo sapiens]	gi|4432748	7686	1	49	17	49	0,0437	-.DLLAPSPEEEKR.K
ribosomal protein L38 [Homo sapiens]	gi|3088356	4291	1	29	27	29	0,0371	K.QSLPPGLAVK.E
c-myc binding protein [Homo sapiens]	gi|1785851	11945	1	24	10	24	0,0610	K.LAQYEPPQEEK.R

Supplementary Table 5: Mass spectrometry data on Ago2 complex II

protein	Acc.No.	Mass	Queries matched	Protein score	Seq cov %	Peptide score	Pep delta	Pep sequence
eukaryotic translation initiation factor 2C, 2 (Ago2) [Homo sapiens]	gi|29171734	97146	20	1819	53	86	0,0231	R.SVSIPAPAYYAHLVAFR.A
ubiquitin	gi|229532	8446	1	30	12	30	-0,0019	R.TLSDYNIQK.E
proliferation-inducing protein 32 [Homo sapiens]	gi|45643460	162923	3	224	4	65	-0,008	K.LTVAENEAETK.L
hornerin [Homo sapiens]	gi|28557150	48569	1	48	3	48	-0,0294	R.GPYESGSGHSSGLGHR.E
RNA helicase A [Homo sapiens]	gi|1806048	140788	7	444	11	87	-0,0199	R.ELDALDANDELTPLGR.I
splicing factor 3b, subunit 1 isoform 1 [Homo sapiens]	gi|54112117	145738	2	133	3	47	-0,0142	R.ATVNTFGYIAK.A
Splicing factor 3B subunit 3 (Spliceosome associated protein 130) (SAP 130) (SF3b130) (Pre-mRNA splicing factor SF3b 130 kDa subunit) (STAF130)	gi|19863446	135507	6	222	-	53	-0,0221	R.FLAVGLVDNTVR.I
coatomer protein [Homo sapiens]	gi|1002369	138244	2	85	2	39	-0,0162	R.TLDLPIYVTR.V
Splicing factor 3B subunit 2 (Spliceosome associated protein 145) (SAP 145) (SF3b150) (Pre-mRNA splicing factor SF3b 145 kDa subunit)	gi|2498883	97596	1	62	1	62	-0,0147	R.AAVLLEQER.Q
hnRNP U protein [Homo sapiens]	gi|32358	88890	9	390	13	96	-0,0305	R.NFILDQTNVSAAAQR.R
DEAH (Asp-Glu-Ala-His) box polypeptide 30 isoform 1 (Ddx30) [Homo sapiens	gi|20336294	133854	5	257	7	46	-0,0193	K.AIVLAAIFR.C
RNA-binding protein 10 (RNA-binding motif protein 10) (DXS8237E)	gi|12644371	103396	1	63	1	63	-0,0462	R.ESATADAGYAILEKK.G
gemin4 [Homo sapiens]	gi|7657122	119913	2	81	-	57	-0,0126	R.LLETVIDVSTADR.A
DHX36 protein (KIAA1488) [Homo sapiens]	gi|23243423	111426	1	70	2	61	-0,0344	R.LGGIAYFLSR.L
RNA helicase Gu - human (fragment)	gi|2135315	89196	3	142	-	59	0,0074	R.AAVIGDVIR.V
NF-90	gi|1082856	73293	2	118	-	47	0,0057	R.IFVNDDR.H
ATP-dependent RNA helicase #46 [Homo sapiens]	gi|2696613	92770	1	81	2	38	0,0033	R.YGVIILDEAHER.T
hypothetical protein LOC55037 [Homo sapiens]	gi|38683855	78500	3	129	3	45	0,0180	R.SPALQVLR.E
Gemin3	gi|14209614	92163	1	30	0	30	1,2	K.EGLEKPVEIIR.H
polyadenylate binding protein II [Homo sapiens]	gi|693937	58481	7	262	20	66	0,0315	R.IVATKPLYVALAQR.K
Skb1Hs (PRMT 5) [Homo sapiens]	gi|2323410	72740	3	166	4	65	0,0228	R.GPLVNASLR.A
thyroid autoantigen 70kDa (Ku antigen) [Homo sapiens]	gi|57165052	69799	1	36	2	36	0,0367	K.NIYVLQELDNPGAK.R
E2IG3 [Homo sapiens]	gi|6457340	63528	1	36	1	36	0,005	K.GGIPNVEGAAK.L
sodium bicarbonate cotransporter-like protein [Homo sapiens]	gi|10567590	118582	1	20	1	20	0,0657	K.FEEKVEEGGER.W
DNA-binding protein B (YB-1)	gi|181486	39954	4	222	11	87	-0,1458	K.GAEAANVTGPGGVPVQGSK.Y
RuvB-like 2 [Homo sapiens]	gi|12653319	51125	2	69	4	44	-0,0949	R.GLGLDDALEPR.Q
Ribosomal protein L4 [Homo sapiens]	gi|12655035	47667	1	68	4	32	-0,1009	R.NIPGITLLNVSK.L
unnamed protein product [Homo sapiens]	gi|31092	50095	1	55	2	55	-0,0852	K.IGGIGTVPVGR.V
KIAA0115 [Homo sapiens]	gi|473947	50680	1	45	1	45	-0,0815	K.SSLNPILFR.G
nuclear RNA helicase (Ddx39) [Homo sapiens]	gi|1905998	49046	1	18	2	18	-0,1250	R.ILVATNLFGR.G
NF45 protein	gi|532313	44669	4	258	12	70	-0,0847	K.VLQSALAAIR.H
ribosomal protein L3	gi|337580	45440	2	89	7	38	-0,08	R.HGSLGFLPR.K
KIAA1756 protein [Homo sapiens]	gi|12698057	116668	1	38	0	38	-0,1676	R.AELEKVLR.A
MRPS27 protein [Homo sapiens]	gi|38014602	25008	2	105	10	55	-0,0913	R.EALDVLGAVLK.A
HNRPC protein [Homo sapiens]	gi|13937888	33578	3	184	12	71	-0,1095	R.VFIGNLNTLVVK.K
7-dehydrocholesterol reductase [Homo sapiens]	gi|3171089	53073	1	38	1	38	-0,0803	R.YTAAVPYR.L
protein translation initiation factor 2C2; EIF2C2 [Homo sapiens]	gi|6468775	42502	1	29	0	29	-0,0889	R.ELLIQFYK.S
Mitochondrial ribosomal protein S22 [Homo sapiens]	gi|14424546	41254	2	98	6	60	-0,1498	K.ILTPIIFKEENLR.T
ribosomal protein L6 [Homo sapiens]	gi|36138	32841	2	79	5	45	-0,0726	K.FVIATSTK.I
fibrillarin	gi|182592	33797	1	51	3	51	-0,1100	R.TNIIPVIEDAR.H
ribosomal protein S2 [Homo sapiens]	gi|15055539	31305	6	475	35	54	-0,1249	K.TYSYLTPDLWK.E

117

protein	Acc.No.	Mass	Queries matched	Protein score	Seq cov %	Peptide score	Pep delta	Pep sequence
hypothetical protein LOC84319 [Homo sapiens]	gi|14150167	31792	1	31	3	31	-0,0925	K.QGGLNLSPLK.F
prohibitin 2 [Homo sapiens]	gi|6005854	33276	6	389	29	78	-0,1100	K.FNASQLITQR.A
ribosomal protein S3a [Homo sapiens]	gi|4506723	29926	6	245	28	52	-0,0928	K.LITEDVQGK.N
ribosomal protein S6	gi|337514	28633	4	182	25	58	-0,09	K.LIEVDDR.K
S3 ribosomal protein [Homo sapiens]	gi|7765076	26699	12	725	65	75	-0,1272	R.ELAEDGYSGVEVR.V
ATP synthase, H+ transporting, mitochondrial F1 complex, gamma subunit isoform H (heart) precursor [Homo sapiens]	gi|4885079	32860	2	160	12	59	-0,0931	K.SEVATLTAAGK.E
Ribosomal protein L8 [Homo sapiens]	gi|15341853	27993	1	49	4	49	-0,0799	R.AVVGVVAGGGR.I
solute carrier family 25 member 3 isoform a precursor [Homo sapiens]	gi|6031192	40069	1	27	1	27	-0,0692	R.TVEALYK.F
scar protein	gi|337930	27386	7	330	32	64	-0,1010	K.DANGNSFATR.L
prohibitin [Homo sapiens]	gi|4505773	29786	5	159	19	62	-0,0952	K.AAIISAEGDSK.A
PREDICTED: similar to SLC25A5 protein [Homo sapiens]	gi|51460683	40069	3	127	-	50	-0,1368	R.VKLLLQVQHASK.Q
Solute carrier family 25, member A6 [Homo sapiens]	gi|15928608	32905	3	126	10	47	-0,1097	R.AAYFGVYDTAK.G
Similar to ribosomal protein S8 [Homo sapiens]	gi|13542987	9277	3	161	41	99	-0,1323	K.ISSLLEEQFQQGK.L
ribosomal protein S9	gi|550023	22558	9	351	36	52	-0,0945	R.LFEGNALLR.R
ribosomal protein S5	gi|550021	22763	1	147	14	58	-0,0871	R.QAVDVSPLR.R
ribosomal protein L24 [Homo sapiens]	gi|4506619	17768	2	197	26	50	-0,1190	R.QINWTVLYR.R
ribosomal protein L29 [Homo sapiens]	gi|793843	17656	1	38	9	38	-0,1299	K.AQAAAPASVPAQAPK.R
ribosomal protein L13a [Homo sapiens]	gi|6912634	23562	1	31	3	31	-0,0735	R.KFAYLGR.L
Ribosomal protein L17 [Homo sapiens]	gi|42542645	21402	4	231	34	59	-0,1090	R.YSLDPENPTK.S
homology to rat ribosomal protein L23	gi|306549	16730	2	99	14	68	-0,1240	R.LAPDYDALDVANK.I
ribosomal protein L27a [Homo sapiens]	gi|4432754	3706	1	76	32	76	-0,0830	K.TGAAPIIDVVR.S
ribosomal protein L26	gi|292435	17278	3	186	26	47	-0,1496	K.ANGTTVHVGIHPSK.V
ribosomal protein L27a [Homo sapiens]	gi|4506625	16551	4	170	29	76	-0,1032	K.TGAAPIIDVVR.S
ribosomal protein L11 [Homo sapiens]	gi|495126	20103	1	111	7	111	-0,1332	K.VLEQLTGQTPVFSK.A
Ribosomal protein S18 [Homo sapiens]	gi|75517910	17708	1	90	11	70	-0,0951	R.VLNTNIDGR.R
ribosomal protein L31	gi|1655596	14084	2	46 / 32	11 / 7	46 / 32	-0,1070 / -0,1004	K.LYTLVTYVPVTTFK.N / R.SAINEVVTR.E
ribosomal protein S26 [Homo sapiens]	gi|296452	12922	2	147	20	100	-0,1180	R.DISEASVFDAYVLPK.L
Ribosomal protein S15a [Homo sapiens]	gi|12804561	14770	1	92	20	45	-0,0610	K.IVVNLTGR.L
ribosomal protein L35 [Homo sapiens]	gi|6005860	14543	2	78	18	45	-0,0876	R.VLTVINQTQK.E
histone H2A.5 - human	gi|70686	14047	1	68	12	56	-0,0626	R.AGLQFPVGR.V
pro-ubiquitin	gi|340062	17434	2	43	21	26	-0,136	K.CCLTYCFNKPEDK.- + Carb.
Ring finger protein 149 [Homo sapiens]	gi|32425835	43151	1	15	2	15	-0,1652	K.GREILELVQK.G

Supplementary Table 6: Mass spectrometry data on Ago2 complex III

protein	Acc.No.	Mass	Queries matched	Protein score	Seq cov %	Peptide score	Pep delta	Pep sequence
eukaryotic translation initiation factor 2C, 2 (Ago2) [Homo sapiens]	gi|29171734	97146	17	1170	40	62	-0,0935 (-0,147)	K.AVQVHQDTLR.T (R.SVSIPAPAYYAHLVAFR.A)
ubiquitin	gi|229532	8446	2	56	21	56 / 21	-0,1095 / -0,0765	K.TITLEVEPSDTIENVK.A / R.TLSDYNIQK.E
Dicer [Homo sapiens]	gi|5019620	218673	1	46	0	36	-0,0649	R.YTAVVLNR.L
MYB binding protein 1a [Homo sapiens]	gi|7657351	148758	1	36	2	40	-0,0738	R.SPSLLQSGAK.K
proline and glutamic acid rich nuclear protein isoform [Homo sapiens]	gi|3168604	109069	1	51	1	51	-0,1009	R.TGSAVAPVHPPNR.S
RNA helicase A	gi|1082769	141984	4	146	3	39	-0,0787	K.VFDPVPVGVTK.V
DEAH (Asp-Glu-Ala-His) box polypeptide 30 isoform 1 (Ddx30)[Homo sapiens]	gi|20336294	133854	2	33	1	18	-0,0661	K.NLLNSVIGR.A
Splicing factor 3B subunit 3 (Spliceosome associated protein 130) (SAP 130) (SF3b130) (Pre-mRNA splicing factor SF3b 130 kDa subunit) (STAF130)	gi|19863446	135507	1	27	-	27	-0,0797	R.FLAVGLVDNTVR.I
hnRNP U protein [Homo sapiens]	gi|32358	88890	4	213	6	52	-0,1008	K.LLEQYKEESK.K
matrin 3 [Homo sapiens]	gi|6563246	95138	1	39	1	39	-0,0686	K.SFQQSSLSR.D
gemin4 [Homo sapiens]	gi|7657122	119913	3	150	-	75	-0,1312	K.VLQPHPVTPSDTETR.W
hect domain and RLD 5 [Homo sapiens]	gi|7705931	116773	1	54	-	54	-0,0795	K.FLVFLTGTDR.L
polyadenylate binding protein II [Homo sapiens]	gi|693937	58481	9	414	24	66	-0,1173	R.IVATKPLYVALAQR.K
Skb1Hs [Homo sapiens]	gi|2323410	72740	1	41	1	41	-0,0620	R.EFIQEPAK.N
mRNA-binding protein CRDBP [Homo sapiens]	gi|7141072	63417	2	118	5	52	-0,1047	R.DQTPDENDQVIVK.I
FXR1	gi|1730139	69649	10	40	15	41	0,04	R.LQIDEQLR.Q

protein	Acc.No.	Mass	Queries matched	Protein score	Seq cov %	Peptide score	Pep delta	Pep sequence
Ribosomal protein L4 [Homo sapiens]	gi|12655035	47667	4	287	21	50	-0,2030	R.QPYAVSELAGHQTSAESWGTGR.A
Y box-binding protein [Mus musculus]	gi|55451	35822	3	158	11	85	-0,1388	R.SVGDGETVEFDVVEGEK.G
unnamed protein product [Homo sapiens]	gi|31092	50095	1	47	2	47	-0,0860	K.IGGGIGTVPVGR.V
ribosomal protein L3	gi|337580	45440	4	218	14	57	-0,1166	K.NNASTDYDLSDK.S
KIAA1756 protein [Homo sapiens]	gi|12698057	116668	1	33	0	33	-0,1734	R.AELEKVLR.A
NF45 protein	gi|532313	44669	2	134	9	53	-0,0943	K.VLQSALAAIR.H
HNRPC protein [Homo sapiens]	gi|14250048	33578	2	106	8	45	-0,0822	R.VPPPPPIAR.A
ribosomal protein L6 [Homo sapiens]	gi|36138	32841	4	169	11	60	-0,0788	K.FVIATSTK.I
Stomatin (EPB72)-like 2 [Homo sapiens]	gi|14603403	38494	1	43	2	43	-0,1070	R.ATVLESEGTR.E
Mov10	gi|144244568	43599	7	23	5	23	0,8	R.ITGNPVVTNP.I
EBNA1 binding protein 2 [Homo sapiens]	gi|5803111	34798	1	36	3	36	-0,0823	R.QAQAAVLAVLPR.L
HNRPC protein [Homo sapiens]	gi|13937888	33578	3	152	12	58	-0,0926	K.SDVEAIFSK.Y
B23 nucleophosmin	gi|190238	9189	1	40	10	40	-0,0821	K.GPSSVEDIK.A
RNA binding motif protein 4 isoform 1 [Homo sapiens]	gi|4506445	40914	1	32	-	32	-0,0791	R.AEDAVEAIR.G
Ribosomal protein P0 [Homo sapiens]	gi|12654583	34253	5	310	21	61	-0,1265	R.GTIEILSDVQLIK.T
fibrillarin	gi|182592	33797	1	35	3	35	-0,1090	R.TNIIPVIEDAR.H
prohibitin 2 [Homo sapiens]	gi|6005854	33276	1	41	3	41	-0,0566	R.VLPSIVNEVLK.S
ribosomal protein S6	gi|225901	28633	2	64 / 38	4 / 3	64 / 38	-0,0725 / -0,0504	K.DIPGLTDTTVPR.R / K.LIEVDDER.K
ribosomal protein L7a [Homo sapiens]	gi|4506661	29977	6	236	21	73	-0,0820	R.AGVNTVTTLVENK.K
Ribosomal protein L8 [Homo sapiens]	gi|15341853	27993	5	187	21	80	-0,1253	R.ASGNYATVISHNPETK.K
S3 ribosomal protein [Homo sapiens]	gi|7765076	26699	3	177	14	57	-0,0749	R.TEIIILATR.T
unnamed protein product [Homo sapiens]	gi|34392	24191	1	39	4	39	-0,0797	K.TYSYLTPDLWK.E
ribosomal protein S4	gi|227229	29664	1	52	3	52	-0,0589	R.LSNIFVIGK.G
ADP.ATP translocase	gi|339721	28042	2	77	8	43	-0,1026	R.YFPTQALNFAFK.D
Ribosomal protein L7 [Homo sapiens]	gi|14250762	29207	5	228	20	61	-0,0853	R.IALTDNALIAR.S
ribosomal protein L10a [Homo sapiens]	gi|15431288	24816	2	84	13	37	-0,0633	R.DTLYEAVR.E
ribosomal protein S9	gi|550023	22558	4	139	18	47	-0,0619	R.LFEGNALLR.R
ribosomal protein L18	gi|4506607	21621	2	126	13	74	-0,0864	K.TAVVVGTITDDVR.V
ribosomal protein L13a [Homo sapiens]	gi|6912634	23562	1	70	9	54	-0,0788	K.YQAVTATLEEK.R
ribosomal protein L10	gi|414587	23903	1	42	4	42	-0,0652	R.SLQSVAEER.A
L21 ribosomal protein	gi|619788	17646	1	35	9	35	-0,1089	R.VYNVTQHAVGIVVNK.Q
ribosomal protein L24 [Homo sapiens]	gi|4506619	17768	1	109	14	52	-0,0820	R.QINWTVLYR.R
unnamed protein product [Homo sapiens]	gi|527578	16582	(1)	77	9	77	-0,1049	R.DLTTAGAVTQCYR.D + Carb:
ribosomal protein L11 [Homo sapiens]	gi|495126	20103	1	95	11	77	0,0258	K.VLEQLTGQTPVFSK.A
ribosomal protein L27a [Homo sapiens]	gi|4432754	3706	1	76	32	76	0,0092	K.TGAAPIIDVVR.S
amino acid starvation-induced protein	gi|202990	13865	1	30	11	30	-0,1136	K.EQIVPKPEEEVAQK.K
ribosomal protein L12 [Homo sapiens]	gi|55665101	17808	2	163	24	42	-0,0017	K.IGPLGLSPK.K
ribosomal protein L26 [Homo sapiens]	gi|4506621	17248	2	59	10	36	0,0115	K.DDEVQVVR.G
ribosomal protein S26 [Homo sapiens]	gi|456351	13035	1	78	13	78	-0,1098	R.DISEASVFDAYVLPK.L
ribosomal protein L28	gi|550019	15752	1	32	8	32	-0,1066	K.QTYSTEPNNLK.A
ribosomal protein S13	gi|553640	13313	3	129	34	54	-0,0858	K.GLTPSQIGVILR.D
ribosomal protein L35 [Homo sapiens]	gi|6005860	14543	2	123	21	48	-0,1371	R.VLTVINQTQKENLR.K
ribosomal protein L27 [Homo sapiens]	gi|4506623	15788	2	109	20	45	-0,0541	K.VVLVLAGR.Y
ribosomal protein S16 – mouse	gi|70920	16319	2	89	-	49	-0,0849	K.GPLQSVQVFGR.K
RPL23 protein [Homo sapiens]	gi|38571606	14875	1	83	18	37	-0,0601	K.NLYIISVK.G
60S ribosomal protein L34	gi|132910	13499	2	69	12	36	-0,0671	R.AFLIEEQK.I
acidic ribosomal phosphoprotein P1 [Homo sapiens]	gi|31979223	11392	1	53	14	53	-0,1187	K.AAGVNVEPFWPGLFAK.A
ribosomal protein L35a [Homo sapiens]	gi|16117791	12530	1	47	14	21	-0,0686	K.AIFAGYKR.G
ribosomal protein homologous to yeast S24 [Homo sapiens]	gi|36142	14707	1	47	6	47	-0,0634	K.IVVNLTGR.L
Ribosomal protein S27-like protein [Homo sapiens]	gi|13277528	9472	(1)	42	9	42	-0,0701	R.LTEGCSFR.R + Carb.
ribosomal protein S20 [Homo sapiens]	gi|3088340	6853	1	33	20	33	-0,1046	R.LIDLHSPSEIVK.Q
RPL37A protein [Homo sapiens]	gi|34783045	10137	(1)	28	8	28	-0,0723	K.YTCSFCGK.T + Carb.
unnamed protein product [Homo sapiens]	gi|32111	14164	1	27	27	27	-0,0586	R.AGLQFPVGR.V

REFERENCES

Ambros, V., Lee, R.C., Lavanway, A., Williams, P.T., and Jewell, D. (2003). MicroRNAs and other tiny endogenous RNAs in C. elegans. Curr Biol *13*, 807-818.

Aoki, K., Moriguchi, H., Yoshioka, T., Okawa, K., and Tabara, H. (2007). In vitro analyses of the production and activity of secondary small interfering RNAs in C. elegans. EMBO J *26*, 5007-5019.

Aravin, A., Gaidatzis, D., Pfeffer, S., Lagos-Quintana, M., Landgraf, P., Iovino, N., Morris, P., Brownstein, M.J., Kuramochi-Miyagawa, S., Nakano, T.*, et al.* (2006). A novel class of small RNAs bind to MILI protein in mouse testes. Nature *442*, 203-207.

Aravin, A.A., and Hannon, G.J. (2008). Small RNA silencing pathways in germ and stem cells. Cold Spring Harb Symp Quant Biol *73*, 283-290.

Aravin, A.A., Sachidanandam, R., Bourc'his, D., Schaefer, C., Pezic, D., Toth, K.F., Bestor, T., and Hannon, G.J. (2008). A piRNA pathway primed by individual transposons is linked to de novo DNA methylation in mice. Mol Cell *31*, 785-799.

Aravin, A.A., Sachidanandam, R., Girard, A., Fejes-Toth, K., and Hannon, G.J. (2007). Developmentally regulated piRNA clusters implicate MILI in transposon control. Science *316*, 744-747.

Babiarz, J.E., Ruby, J.G., Wang, Y., Bartel, D.P., and Blelloch, R. (2008). Mouse ES cells express endogenous shRNAs, siRNAs, and other Microprocessor-independent, Dicer-dependent small RNAs. Genes Dev *22*, 2773-2785.

Baillat, D., and Shiekhattar, R. (2009). Functional dissection of the human TNRC6 (GW182-related) family of proteins. Mol Cell Biol *29*, 4144-4155.

Bartel, D.P., and Chen, C.Z. (2004). Micromanagers of gene expression: the potentially widespread influence of metazoan microRNAs. Nat Rev Genet *5*, 396-400.

Behm-Ansmant, I., Rehwinkel, J., Doerks, T., Stark, A., Bork, P., and Izaurralde, E. (2006). mRNA degradation by miRNAs and GW182 requires both CCR4:NOT deadenylase and DCP1:DCP2 decapping complexes. Genes Dev *20*, 1885-1898.

Beitzinger, M., Peters, L., Zhu, J.Y., Kremmer, E., and Meister, G. (2007). Identification of human microRNA targets from isolated argonaute protein complexes. RNA Biol *4*, 76-84.

Bell, M., Schreiner, S., Damianov, A., Reddy, R., and Bindereif, A. (2002). p110, a novel human U6 snRNP protein and U4/U6 snRNP recycling factor. EMBO J *21*, 2724-2735.

Bernstein, E., Caudy, A.A., Hammond, S.M., and Hannon, G.J. (2001). Role for a bidentate ribonuclease in the initiation step of RNA interference. Nature *409*, 363-366.

Bhattacharyya, S.N., Habermacher, R., Martine, U., Closs, E.I., and Filipowicz, W. (2006a). Relief of microRNA-mediated translational repression in human cells subjected to stress. Cell *125*, 1111-1124.

Bhattacharyya, S.N., Habermacher, R., Martine, U., Closs, E.I., and Filipowicz, W. (2006b). Stress-induced reversal of microRNA repression and mRNA P-body localization in human cells. Cold Spring Harb Symp Quant Biol *71*, 513-521.

Birney, E., Stamatoyannopoulos, J.A., Dutta, A., Guigo, R., Gingeras, T.R., Margulies, E.H., Weng, Z., Snyder, M., Dermitzakis, E.T., Thurman, R.E.*, et al.* (2007). Identification and analysis of functional elements in 1% of the human genome by the ENCODE pilot project. Nature *447*, 799-816.

Bohnsack, M.T., Czaplinski, K., and Gorlich, D. (2004). Exportin 5 is a RanGTP-dependent dsRNA-binding protein that mediates nuclear export of pre-miRNAs. RNA *10*, 185-191.

Brennecke, J., Aravin, A.A., Stark, A., Dus, M., Kellis, M., Sachidanandam, R., and Hannon, G.J. (2007). Discrete small RNA-generating loci as master regulators of transposon activity in Drosophila. Cell *128*, 1089-1103.

Brennecke, J., Malone, C.D., Aravin, A.A., Sachidanandam, R., Stark, A., and Hannon, G.J. (2008). An epigenetic role for maternally inherited piRNAs in transposon silencing. Science *322*, 1387-1392.

Carthew, R.W., and Sontheimer, E.J. (2009). Origins and Mechanisms of miRNAs and siRNAs. Cell *136*, 642-655.

Caudy, A.A., Myers, M., Hannon, G.J., and Hammond, S.M. (2002). Fragile X-related protein and VIG associate with the RNA interference machinery. Genes Dev *16*, 2491-2496.

Cheever, A., and Ceman, S. (2009). Phosphorylation of FMRP inhibits association with Dicer. RNA *15*, 362-366.

Cheloufi, S., Dos Santos, C.O., Chong, M.M., and Hannon, G.J. (2010). A dicer-independent miRNA biogenesis pathway that requires Ago catalysis. Nature *465*, 584-589.

Chendrimada, T.P., Finn, K.J., Ji, X., Baillat, D., Gregory, R.I., Liebhaber, S.A., Pasquinelli, A.E., and Shiekhattar, R. (2007). MicroRNA silencing through RISC recruitment of eIF6. Nature *447*, 823-828.

Chendrimada, T.P., Gregory, R.I., Kumaraswamy, E., Norman, J., Cooch, N., Nishikura, K., and Shiekhattar, R. (2005). TRBP recruits the Dicer complex to Ago2 for microRNA processing and gene silencing. Nature *436*, 740-744.

Chu, C.Y., and Rana, T.M. (2006). Translation repression in human cells by microRNA-induced gene silencing requires RCK/p54. PLoS Biol *4*, e210.

Cifuentes, D., Xue, H., Taylor, D.W., Patnode, H., Mishima, Y., Cheloufi, S., Ma, E., Mane, S., Hannon, G.J., Lawson, N.D.*, et al.* (2010). A novel miRNA processing pathway independent of Dicer requires Argonaute2 catalytic activity. Science *328*, 1694-1698.

Czech, B., Zhou, R., Erlich, Y., Brennecke, J., Binari, R., Villalta, C., Gordon, A., Perrimon, N., and Hannon, G.J. (2009). Hierarchical rules for Argonaute loading in Drosophila. Mol Cell *36*, 445-456.

Davies, S.M., Rackham, O., Shearwood, A.M., Hamilton, K.L., Narsai, R., Whelan, J., and Filipovska, A. (2009). Pentatricopeptide repeat domain protein 3 associates with the mitochondrial small ribosomal subunit and regulates translation. FEBS Lett *583*, 1853-1858.

Davis, B.N., Hilyard, A.C., Lagna, G., and Hata, A. (2008). SMAD proteins control DROSHA-mediated microRNA maturation. Nature *454*, 56-61.

Davis, E., Caiment, F., Tordoir, X., Cavaille, J., Ferguson-Smith, A., Cockett, N., Georges, M., and Charlier, C. (2005). RNAi-mediated allelic trans-interaction at the imprinted Rtl1/Peg11 locus. Curr Biol *15*, 743-749.

Delannoy, E., Stanley, W.A., Bond, C.S., and Small, I.D. (2007). Pentatricopeptide repeat (PPR) proteins as sequence-specificity factors in post-transcriptional processes in organelles. Biochem Soc Trans *35*, 1643-1647.

Denli, A.M., Tops, B.B., Plasterk, R.H., Ketting, R.F., and Hannon, G.J. (2004). Processing of primary microRNAs by the Microprocessor complex. Nature *432*, 231-235.

Dignam, J.D., Lebovitz, R.M., and Roeder, R.G. (1983). Accurate transcription initiation by RNA polymerase II in a soluble extract from isolated mammalian nuclei. Nucleic Acids Res *11*, 1475-1489.

Doench, J.G., Petersen, C.P., and Sharp, P.A. (2003). siRNAs can function as miRNAs. Genes Dev *17*, 438-442.

Doench, J.G., and Sharp, P.A. (2004). Specificity of microRNA target selection in translational repression. Genes Dev *18*, 504-511.

Easow, G., Teleman, A.A., and Cohen, S.M. (2007). Isolation of microRNA targets by miRNP immunopurification. RNA *13*, 1198-1204.

Eberhardt, W., Doller, A., Akool el, S., and Pfeilschifter, J. (2007). Modulation of mRNA stability as a novel therapeutic approach. Pharmacol Ther *114*, 56-73.

Elbashir, S.M., Harborth, J., Lendeckel, W., Yalcin, A., Weber, K., and Tuschl, T. (2001a). Duplexes of 21-nucleotide RNAs mediate RNA interference in cultured mammalian cells. Nature *411*, 494-498.

Elbashir, S.M., Lendeckel, W., and Tuschl, T. (2001b). RNA interference is mediated by 21- and 22-nucleotide RNAs. Genes Dev *15*, 188-200.

Elbashir, S.M., Martinez, J., Patkaniowska, A., Lendeckel, W., and Tuschl, T. (2001c). Functional anatomy of siRNAs for mediating efficient RNAi in Drosophila melanogaster embryo lysate. EMBO J *20*, 6877-6888.

Ender, C., Krek, A., Friedlander, M.R., Beitzinger, M., Weinmann, L., Chen, W., Pfeffer, S., Rajewsky, N., and Meister, G. (2008). A human snoRNA with microRNA-like functions. Mol Cell *32*, 519-528.

Ender, C., and Meister, G. (2010). Argonaute proteins at a glance. J Cell Sci *123*, 1819-1823.

Eulalio, A., Behm-Ansmant, I., and Izaurralde, E. (2007a). P bodies: at the crossroads of post-transcriptional pathways. Nat Rev Mol Cell Biol *8*, 9-22.

Eulalio, A., Behm-Ansmant, I., Schweizer, D., and Izaurralde, E. (2007b). P-body formation is a consequence, not the cause, of RNA-mediated gene silencing. Mol Cell Biol *27*, 3970-3981.

Eulalio, A., Helms, S., Fritzsch, C., Fauser, M., and Izaurralde, E. (2009a). A C-terminal silencing domain in GW182 is essential for miRNA function. RNA *15*, 1067-1077.

Eulalio, A., Huntzinger, E., and Izaurralde, E. (2008). GW182 interaction with Argonaute is essential for miRNA-mediated translational repression and mRNA decay. Nat Struct Mol Biol *15*, 346-353.

Eulalio, A., Tritschler, F., Buttner, R., Weichenrieder, O., Izaurralde, E., and Truffault, V. (2009b). The RRM domain in GW182 proteins contributes to miRNA-mediated gene silencing. Nucleic Acids Res *37*, 2974-2983.

Eulalio, A., Tritschler, F., and Izaurralde, E. (2009c). The GW182 protein family in animal cells: new insights into domains required for miRNA-mediated gene silencing. RNA *15*, 1433-1442.

Evdokimova, V., Ovchinnikov, L.P., and Sorensen, P.H. (2006). Y-box binding protein 1: providing a new angle on translational regulation. Cell Cycle *5*, 1143-1147.

Fabian, M.R., Mathonnet, G., Sundermeier, T., Mathys, H., Zipprich, J.T., Svitkin, Y.V., Rivas, F., Jinek, M., Wohlschlegel, J., Doudna, J.A.*, et al.* (2009). Mammalian miRNA RISC recruits CAF1 and PABP to affect PABP-dependent deadenylation. Mol Cell *35*, 868-880.

Fabian, M.R., Sonenberg, N., and Filipowicz, W. (2010). Regulation of mRNA translation and stability by microRNAs. Annu Rev Biochem *79*, 351-379.

Fire, A., Xu, S., Montgomery, M.K., Kostas, S.A., Driver, S.E., and Mello, C.C. (1998). Potent and specific genetic interference by double-stranded RNA in Caenorhabditis elegans. Nature *391*, 806-811.

Forstemann, K., Horwich, M.D., Wee, L., Tomari, Y., and Zamore, P.D. (2007). Drosophila microRNAs are sorted into functionally distinct argonaute complexes after production by dicer-1. Cell *130*, 287-297.

Forstemann, K., Tomari, Y., Du, T., Vagin, V.V., Denli, A.M., Bratu, D.P., Klattenhoff, C., Theurkauf, W.E., and Zamore, P.D. (2005). Normal microRNA maturation and germ-line stem cell maintenance requires Loquacious, a double-stranded RNA-binding domain protein. PLoS Biol *3*, e236.

Friedman, R.C., Farh, K.K., Burge, C.B., and Bartel, D.P. (2009). Most mammalian mRNAs are conserved targets of microRNAs. Genome Res *19*, 92-105.

Ghildiyal, M., Seitz, H., Horwich, M.D., Li, C., Du, T., Lee, S., Xu, J., Kittler, E.L., Zapp, M.L., Weng, Z.*, et al.* (2008). Endogenous siRNAs derived from transposons and mRNAs in Drosophila somatic cells. Science *320*, 1077-1081.

Ghildiyal, M., and Zamore, P.D. (2009). Small silencing RNAs: an expanding universe. Nat Rev Genet *10*, 94-108.

Giot, L., Bader, J.S., Brouwer, C., Chaudhuri, A., Kuang, B., Li, Y., Hao, Y.L., Ooi, C.E., Godwin, B., Vitols, E.*, et al.* (2003). A protein interaction map of Drosophila melanogaster. Science *302*, 1727-1736.

Giraldez, A.J., Mishima, Y., Rihel, J., Grocock, R.J., Van Dongen, S., Inoue, K., Enright, A.J., and Schier, A.F. (2006). Zebrafish MiR-430 promotes deadenylation and clearance of maternal mRNAs. Science *312*, 75-79.

Girard, A., Sachidanandam, R., Hannon, G.J., and Carmell, M.A. (2006). A germline-specific class of small RNAs binds mammalian Piwi proteins. Nature *442*, 199-202.

Gregory, R.I., Chendrimada, T.P., Cooch, N., and Shiekhattar, R. (2005). Human RISC couples microRNA biogenesis and posttranscriptional gene silencing. Cell *123*, 631-640.

Gregory, R.I., Yan, K.P., Amuthan, G., Chendrimada, T., Doratotaj, B., Cooch, N., and Shiekhattar, R. (2004). The Microprocessor complex mediates the genesis of microRNAs. Nature *432*, 235-240.

Grimson, A., Farh, K.K., Johnston, W.K., Garrett-Engele, P., Lim, L.P., and Bartel, D.P. (2007). MicroRNA targeting specificity in mammals: determinants beyond seed pairing. Mol Cell *27*, 91-105.

Gu, S., Jin, L., Zhang, F., Sarnow, P., and Kay, M.A. (2009). Biological basis for restriction of microRNA targets to the 3' untranslated region in mammalian mRNAs. Nat Struct Mol Biol *16*, 144-150.

Guil, S., and Caceres, J.F. (2007). The multifunctional RNA-binding protein hnRNP A1 is required for processing of miR-18a. Nat Struct Mol Biol *14*, 591-596.

Gunawardane, L.S., Saito, K., Nishida, K.M., Miyoshi, K., Kawamura, Y., Nagami, T., Siomi, H., and Siomi, M.C. (2007). A slicer-mediated mechanism for repeat-associated siRNA 5' end formation in Drosophila. Science *315*, 1587-1590.

Gwizdek, C., Ossareh-Nazari, B., Brownawell, A.M., Evers, S., Macara, I.G., and Dargemont, C. (2004). Minihelix-containing RNAs mediate exportin-5-dependent nuclear export of the double-stranded RNA-binding protein ILF3. J Biol Chem *279*, 884-891.

Haase, A.D., Jaskiewicz, L., Zhang, H., Laine, S., Sack, R., Gatignol, A., and Filipowicz, W. (2005). TRBP, a regulator of cellular PKR and HIV-1 virus expression, interacts with Dicer and functions in RNA silencing. EMBO Rep *6*, 961-967.

Hafner, M., Landthaler, M., Burger, L., Khorshid, M., Hausser, J., Berninger, P., Rothballer, A., Ascano, M., Jungkamp, A.C., Munschauer, M.*, et al.* (2010). PAR-CliP--a method to identify transcriptome-wide the binding sites of RNA binding proteins. J Vis Exp.

Haley, B., and Zamore, P.D. (2004). Kinetic analysis of the RNAi enzyme complex. Nat Struct Mol Biol *11*, 599-606.

Hamilton, A., Voinnet, O., Chappell, L., and Baulcombe, D. (2002). Two classes of short interfering RNA in RNA silencing. EMBO J *21*, 4671-4679.

Hamilton, A.J., and Baulcombe, D.C. (1999). A species of small antisense RNA in posttranscriptional gene silencing in plants. Science *286*, 950-952.

Hammell, C.M., Lubin, I., Boag, P.R., Blackwell, T.K., and Ambros, V. (2009). nhl-2 Modulates microRNA activity in Caenorhabditis elegans. Cell *136*, 926-938.

Hammond, S.M., Bernstein, E., Beach, D., and Hannon, G.J. (2000). An RNA-directed nuclease mediates post-transcriptional gene silencing in Drosophila cells. Nature *404*, 293-296.

Han, J., Lee, Y., Yeom, K.H., Kim, Y.K., Jin, H., and Kim, V.N. (2004). The Drosha-DGCR8 complex in primary microRNA processing. Genes Dev *18*, 3016-3027.

Han, J., Lee, Y., Yeom, K.H., Nam, J.W., Heo, I., Rhee, J.K., Sohn, S.Y., Cho, Y., Zhang, B.T., and Kim, V.N. (2006). Molecular basis for the recognition of primary microRNAs by the Drosha-DGCR8 complex. Cell *125*, 887-901.

Han, S.P., Tang, Y.H., and Smith, R. (2010). Functional diversity of the hnRNPs: past, present and perspectives. Biochem J *430*, 379-392.

Hartig, J.V., Esslinger, S., Bottcher, R., Saito, K., and Forstemann, K. (2009). Endo-siRNAs depend on a new isoform of loquacious and target artificially introduced, high-copy sequences. EMBO J *28*, 2932-2944.

Hartig, J.V., and Forstemann, K. (2011). Loqs-PD and R2D2 define independent pathways for RISC generation in Drosophila. Nucleic Acids Res.

Henke, J.I., Goergen, D., Zheng, J., Song, Y., Schuttler, C.G., Fehr, C., Junemann, C., and Niepmann, M. (2008). microRNA-122 stimulates translation of hepatitis C virus RNA. EMBO J *27*, 3300-3310.

Heo, I., Joo, C., Cho, J., Ha, M., Han, J., and Kim, V.N. (2008). Lin28 mediates the terminal uridylation of let-7 precursor MicroRNA. Mol Cell *32*, 276-284.

Hetzer, M., Bilbao-Cortes, D., Walther, T.C., Gruss, O.J., and Mattaj, I.W. (2000). GTP hydrolysis by Ran is required for nuclear envelope assembly. Mol Cell *5*, 1013-1024.

Hock, J., and Meister, G. (2008). The Argonaute protein family. Genome Biol *9*, 210.

Holzmann, J., Frank, P., Loffler, E., Bennett, K.L., Gerner, C., and Rossmanith, W. (2008). RNase P without RNA: identification and functional reconstitution of the human mitochondrial tRNA processing enzyme. Cell *135*, 462-474.

Horwich, M.D., Li, C., Matranga, C., Vagin, V., Farley, G., Wang, P., and Zamore, P.D. (2007). The Drosophila RNA methyltransferase, DmHen1, modifies germline piRNAs and single-stranded siRNAs in RISC. Curr Biol *17*, 1265-1272.

Hu, W., Sweet, T.J., Chamnongpol, S., Baker, K.E., and Coller, J. (2009). Co-translational mRNA decay in Saccharomyces cerevisiae. Nature *461*, 225-229.

Huang, Y., Genova, G., Roberts, M., and Jackson, F.R. (2007). The LARK RNA-binding protein selectively regulates the circadian eclosion rhythm by controlling E74 protein expression. PLoS One *2*, e1107.

Humphreys, D.T., Westman, B.J., Martin, D.I., and Preiss, T. (2005). MicroRNAs control translation initiation by inhibiting eukaryotic initiation factor 4E/cap and poly(A) tail function. Proc Natl Acad Sci U S A *102*, 16961-16966.

Huttelmaier, S., Zenklusen, D., Lederer, M., Dictenberg, J., Lorenz, M., Meng, X., Bassell, G.J., Condeelis, J., and Singer, R.H. (2005). Spatial regulation of beta-actin translation by Src-dependent phosphorylation of ZBP1. Nature *438*, 512-515.

Hutvagner, G., McLachlan, J., Pasquinelli, A.E., Balint, E., Tuschl, T., and Zamore, P.D. (2001). A cellular function for the RNA-interference enzyme Dicer in the maturation of the let-7 small temporal RNA. Science *293*, 834-838.

Hutvagner, G., and Simard, M.J. (2008). Argonaute proteins: key players in RNA silencing. Nat Rev Mol Cell Biol *9*, 22-32.

Iki, T., Yoshikawa, M., Nishikiori, M., Jaudal, M.C., Matsumoto-Yokoyama, E., Mitsuhara, I., Meshi, T., and Ishikawa, M. (2010). In vitro assembly of plant RNA-induced silencing complexes facilitated by molecular chaperone HSP90. Mol Cell *39*, 282-291.

Ishizuka, A., Siomi, M.C., and Siomi, H. (2002). A Drosophila fragile X protein interacts with components of RNAi and ribosomal proteins. Genes Dev *16*, 2497-2508.

Isken, O., Baroth, M., Grassmann, C.W., Weinlich, S., Ostareck, D.H., Ostareck-Lederer, A., and Behrens, S.E. (2007). Nuclear factors are involved in hepatitis C virus RNA replication. RNA *13*, 1675-1692.

Iwasaki, S., Kawamata, T., and Tomari, Y. (2009). Drosophila argonaute1 and argonaute2 employ distinct mechanisms for translational repression. Mol Cell *34*, 58-67.

Iwasaki, S., Kobayashi, M., Yoda, M., Sakaguchi, Y., Katsuma, S., Suzuki, T., and Tomari, Y. (2010). Hsc70/Hsp90 chaperone machinery mediates ATP-dependent RISC loading of small RNA duplexes. Mol Cell *39*, 292-299.

Jackson, A.L., and Linsley, P.S. (2004). Noise amidst the silence: off-target effects of siRNAs? Trends Genet *20*, 521-524.

Jannot, G., Boisvert, M.E., Banville, I.H., and Simard, M.J. (2008). Two molecular features contribute to the Argonaute specificity for the microRNA and RNAi pathways in C. elegans. RNA *14*, 829-835.

Janowski, B.A., Huffman, K.E., Schwartz, J.C., Ram, R., Nordsell, R., Shames, D.S., Minna, J.D., and Corey, D.R. (2006). Involvement of AGO1 and AGO2 in mammalian transcriptional silencing. Nat Struct Mol Biol *13*, 787-792.

Jin, P., Alisch, R.S., and Warren, S.T. (2004a). RNA and microRNAs in fragile X mental retardation. Nat Cell Biol *6*, 1048-1053.

Jin, P., Zarnescu, D.C., Ceman, S., Nakamoto, M., Mowrey, J., Jongens, T.A., Nelson, D.L., Moses, K., and Warren, S.T. (2004b). Biochemical and genetic interaction between the fragile X mental retardation protein and the microRNA pathway. Nat Neurosci *7*, 113-117.

Jinek, M., and Doudna, J.A. (2009). A three-dimensional view of the molecular machinery of RNA interference. Nature *457*, 405-412.

Johnson, S.M., Grosshans, H., Shingara, J., Byrom, M., Jarvis, R., Cheng, A., Labourier, E., Reinert, K.L., Brown, D., and Slack, F.J. (2005). RAS is regulated by the let-7 microRNA family. Cell *120*, 635-647.

Johnston, M., Geoffroy, M.C., Sobala, A., Hay, R., and Hutvagner, G. (2010). HSP90 protein stabilizes unloaded argonaute complexes and microscopic P-bodies in human cells. Mol Biol Cell *21*, 1462-1469.

Kahvejian, A., Svitkin, Y.V., Sukarieh, R., M'Boutchou, M.N., and Sonenberg, N. (2005). Mammalian poly(A)-binding protein is a eukaryotic translation initiation factor, which acts via multiple mechanisms. Genes Dev *19*, 104-113.

Kar, A., Havlioglu, N., Tarn, W.Y., and Wu, J.Y. (2006). RBM4 interacts with an intronic element and stimulates tau exon 10 inclusion. J Biol Chem *281*, 24479-24488.

Kawamata, T., Seitz, H., and Tomari, Y. (2009). Structural determinants of miRNAs for RISC loading and slicer-independent unwinding. Nat Struct Mol Biol *16*, 953-960.

Kazan, H., Ray, D., Chan, E.T., Hughes, T.R., and Morris, Q. (2010). RNAcontext: a new method for learning the sequence and structure binding preferences of RNA-binding proteins. PLoS Comput Biol *6*, e1000832.

Ketting, R.F., Fischer, S.E., Bernstein, E., Sijen, T., Hannon, G.J., and Plasterk, R.H. (2001). Dicer functions in RNA interference and in synthesis of small RNA involved in developmental timing in C. elegans. Genes Dev *15*, 2654-2659.

Khvorova, A., Reynolds, A., and Jayasena, S.D. (2003). Functional siRNAs and miRNAs exhibit strand bias. Cell *115*, 209-216.

Kim, J., Krichevsky, A., Grad, Y., Hayes, G.D., Kosik, K.S., Church, G.M., and Ruvkun, G. (2004). Identification of many microRNAs that copurify with polyribosomes in mammalian neurons. Proc Natl Acad Sci U S A *101*, 360-365.

Kim, V.N., Han, J., and Siomi, M.C. (2009). Biogenesis of small RNAs in animals. Nat Rev Mol Cell Biol *10*, 126-139.

Kinch, L.N., and Grishin, N.V. (2009). The human Ago2 MC region does not contain an eIF4E-like mRNA cap binding motif. Biol Direct *4*, 2.

Kiriakidou, M., Tan, G.S., Lamprinaki, S., De Planell-Saguer, M., Nelson, P.T., and Mourelatos, Z. (2007). An mRNA m7G cap binding-like motif within human Ago2 represses translation. Cell *129*, 1141-1151.

Kirino, Y., Kim, N., de Planell-Saguer, M., Khandros, E., Chiorean, S., Klein, P.S., Rigoutsos, I., Jongens, T.A., and Mourelatos, Z. (2009). Arginine methylation of Piwi proteins catalysed by dPRMT5 is required for Ago3 and Aub stability. Nat Cell Biol *11*, 652-658.

Klattenhoff, C., Bratu, D.P., McGinnis-Schultz, N., Koppetsch, B.S., Cook, H.A., and Theurkauf, W.E. (2007). Drosophila rasiRNA pathway mutations disrupt embryonic axis specification through activation of an ATR/Chk2 DNA damage response. Dev Cell *12*, 45-55.

Kloosterman, W.P., Wienholds, E., Ketting, R.F., and Plasterk, R.H. (2004). Substrate requirements for let-7 function in the developing zebrafish embryo. Nucleic Acids Res *32*, 6284-6291.

Knight, S.W., and Bass, B.L. (2001). A role for the RNase III enzyme DCR-1 in RNA interference and germ line development in Caenorhabditis elegans. Science *293*, 2269-2271.

Kojima, S., Matsumoto, K., Hirose, M., Shimada, M., Nagano, M., Shigeyoshi, Y., Hoshino, S., Ui-Tei, K., Saigo, K., Green, C.B.*, et al.* (2007). LARK activates posttranscriptional expression of an essential mammalian clock protein, PERIOD1. Proc Natl Acad Sci U S A *104*, 1859-1864.

Kong, Y.W., Cannell, I.G., de Moor, C.H., Hill, K., Garside, P.G., Hamilton, T.L., Meijer, H.A., Dobbyn, H.C., Stoneley, M., Spriggs, K.A.*, et al.* (2008). The mechanism of micro-RNA-mediated translation repression is determined by the promoter of the target gene. Proc Natl Acad Sci U S A *105*, 8866-8871.

Kuramochi-Miyagawa, S., Watanabe, T., Gotoh, K., Totoki, Y., Toyoda, A., Ikawa, M., Asada, N., Kojima, K., Yamaguchi, Y., Ijiri, T.W.*, et al.* (2008). DNA methylation of retrotransposon genes is regulated by Piwi family members MILI and MIWI2 in murine fetal testes. Genes Dev *22*, 908-917.

Lagos-Quintana, M., Rauhut, R., Lendeckel, W., and Tuschl, T. (2001). Identification of novel genes coding for small expressed RNAs. Science *294*, 853-858.

Lai, M.C., Kuo, H.W., Chang, W.C., and Tarn, W.Y. (2003). A novel splicing regulator shares a nuclear import pathway with SR proteins. EMBO J *22*, 1359-1369.

Landgraf, P., Rusu, M., Sheridan, R., Sewer, A., Iovino, N., Aravin, A., Pfeffer, S., Rice, A., Kamphorst, A.O., Landthaler, M.*, et al.* (2007). A mammalian microRNA expression atlas based on small RNA library sequencing. Cell *129*, 1401-1414.

Landthaler, M., Gaidatzis, D., Rothballer, A., Chen, P.Y., Soll, S.J., Dinic, L., Ojo, T., Hafner, M., Zavolan, M., and Tuschl, T. (2008). Molecular characterization of human Argonaute-containing ribonucleoprotein complexes and their bound target mRNAs. RNA *14*, 2580-2596.

Landthaler, M., Yalcin, A., and Tuschl, T. (2004). The human DiGeorge syndrome critical region gene 8 and Its D. melanogaster homolog are required for miRNA biogenesis. Curr Biol *14*, 2162-2167.

Lau, N.C., Seto, A.G., Kim, J., Kuramochi-Miyagawa, S., Nakano, T., Bartel, D.P., and Kingston, R.E. (2006). Characterization of the piRNA complex from rat testes. Science *313*, 363-367.

Lee, Y., Ahn, C., Han, J., Choi, H., Kim, J., Yim, J., Lee, J., Provost, P., Radmark, O., Kim, S.*, et al.* (2003). The nuclear RNase III Drosha initiates microRNA processing. Nature *425*, 415-419.

Lee, Y., Hur, I., Park, S.Y., Kim, Y.K., Suh, M.R., and Kim, V.N. (2006). The role of PACT in the RNA silencing pathway. EMBO J *25*, 522-532.

Lee, Y., Jeon, K., Lee, J.T., Kim, S., and Kim, V.N. (2002). MicroRNA maturation: stepwise processing and subcellular localization. EMBO J *21*, 4663-4670.

Lee, Y., Kim, M., Han, J., Yeom, K.H., Lee, S., Baek, S.H., and Kim, V.N. (2004a). MicroRNA genes are transcribed by RNA polymerase II. EMBO J *23*, 4051-4060.

Lee, Y.S., Nakahara, K., Pham, J.W., Kim, K., He, Z., Sontheimer, E.J., and Carthew, R.W. (2004b). Distinct roles for Drosophila Dicer-1 and Dicer-2 in the siRNA/miRNA silencing pathways. Cell *117*, 69-81.

Lewis, B.P., Burge, C.B., and Bartel, D.P. (2005). Conserved seed pairing, often flanked by adenosines, indicates that thousands of human genes are microRNA targets. Cell *120*, 15-20.

Li, J., Yang, Z., Yu, B., Liu, J., and Chen, X. (2005). Methylation protects miRNAs and siRNAs from a 3'-end uridylation activity in Arabidopsis. Curr Biol *15*, 1501-1507.

Lian, S., Jakymiw, A., Eystathioy, T., Hamel, J.C., Fritzler, M.J., and Chan, E.K. (2006). GW bodies, microRNAs and the cell cycle. Cell Cycle *5*, 242-245.

Lightowlers, R.N., and Chrzanowska-Lightowlers, Z.M. (2008). PPR (pentatricopeptide repeat) proteins in mammals: important aids to mitochondrial gene expression. Biochem J *416*, e5-6.

Lin, J.C., Hsu, M., and Tarn, W.Y. (2007). Cell stress modulates the function of splicing regulatory protein RBM4 in translation control. Proc Natl Acad Sci U S A *104*, 2235-2240.

Lin, J.C., and Tarn, W.Y. (2005). Exon selection in alpha-tropomyosin mRNA is regulated by the antagonistic action of RBM4 and PTB. Mol Cell Biol *25*, 10111-10121.

Lin, J.C., and Tarn, W.Y. (2009). RNA-binding motif protein 4 translocates to cytoplasmic granules and suppresses translation via argonaute2 during muscle cell differentiation. J Biol Chem *284*, 34658-34665.

Linder, P. (2006). Dead-box proteins: a family affair--active and passive players in RNP-remodeling. Nucleic Acids Res *34*, 4168-4180.

Lingel, A., Simon, B., Izaurralde, E., and Sattler, M. (2003). Structure and nucleic-acid binding of the Drosophila Argonaute 2 PAZ domain. Nature *426*, 465-469.

Lingel, A., Simon, B., Izaurralde, E., and Sattler, M. (2004). Nucleic acid 3'-end recognition by the Argonaute2 PAZ domain. Nat Struct Mol Biol *11*, 576-577.

Liu, J., Carmell, M.A., Rivas, F.V., Marsden, C.G., Thomson, J.M., Song, J.J., Hammond, S.M., Joshua-Tor, L., and Hannon, G.J. (2004). Argonaute2 is the catalytic engine of mammalian RNAi. Science *305*, 1437-1441.

Liu, J., Valencia-Sanchez, M.A., Hannon, G.J., and Parker, R. (2005). MicroRNA-dependent localization of targeted mRNAs to mammalian P-bodies. Nat Cell Biol *7*, 719-723.

Liu, Q., Rand, T.A., Kalidas, S., Du, F., Kim, H.E., Smith, D.P., and Wang, X. (2003). R2D2, a bridge between the initiation and effector steps of the Drosophila RNAi pathway. Science *301*, 1921-1925.

Liu, Y., Ye, X., Jiang, F., Liang, C., Chen, D., Peng, J., Kinch, L.N., Grishin, N.V., and Liu, Q. (2009). C3PO, an endoribonuclease that promotes RNAi by facilitating RISC activation. Science *325*, 750-753.

Loef, M. (2006). Identifizierung von essentiellen Komponenten der miRNA-vermittelten Genregulation (Diploma thesis). In Institut für Biochemie (Würzburg, University of Würzburg).

Lund, E., Guttinger, S., Calado, A., Dahlberg, J.E., and Kutay, U. (2004). Nuclear export of microRNA precursors. Science *303*, 95-98.

Lytle, J.R., Yario, T.A., and Steitz, J.A. (2007). Target mRNAs are repressed as efficiently by microRNA-binding sites in the 5' UTR as in the 3' UTR. Proc Natl Acad Sci U S A *104*, 9667-9672.

Ma, E., MacRae, I.J., Kirsch, J.F., and Doudna, J.A. (2008). Autoinhibition of human dicer by its internal helicase domain. J Mol Biol *380*, 237-243.

Ma, J.B., Ye, K., and Patel, D.J. (2004). Structural basis for overhang-specific small interfering RNA recognition by the PAZ domain. Nature *429*, 318-322.

MacRae, I.J., and Doudna, J.A. (2007). Ribonuclease revisited: structural insights into ribonuclease III family enzymes. Curr Opin Struct Biol *17*, 138-145.

MacRae, I.J., Zhou, K., and Doudna, J.A. (2007). Structural determinants of RNA recognition and cleavage by Dicer. Nat Struct Mol Biol *14*, 934-940.

Macrae, I.J., Zhou, K., Li, F., Repic, A., Brooks, A.N., Cande, W.Z., Adams, P.D., and Doudna, J.A. (2006). Structural basis for double-stranded RNA processing by Dicer. Science *311*, 195-198.

Maniataki, E., and Mourelatos, Z. (2005). A human, ATP-independent, RISC assembly machine fueled by pre-miRNA. Genes Dev *19*, 2979-2990.

Maris, C., Dominguez, C., and Allain, F.H. (2005). The RNA recognition motif, a plastic RNA-binding platform to regulate post-transcriptional gene expression. FEBS J *272*, 2118-2131.

Markus, M.A., Heinrich, B., Raitskin, O., Adams, D.J., Mangs, H., Goy, C., Ladomery, M., Sperling, R., Stamm, S., and Morris, B.J. (2006). WT1 interacts with the splicing protein RBM4 and regulates its ability to modulate alternative splicing in vivo. Exp Cell Res *312*, 3379-3388.

Markus, M.A., and Morris, B.J. (2006). Lark is the splicing factor RBM4 and exhibits unique subnuclear localization properties. DNA Cell Biol *25*, 457-464.

Markus, M.A., and Morris, B.J. (2009). RBM4: a multifunctional RNA-binding protein. Int J Biochem Cell Biol *41*, 740-743.

Maroney, P.A., Yu, Y., Fisher, J., and Nilsen, T.W. (2006). Evidence that microRNAs are associated with translating messenger RNAs in human cells. Nat Struct Mol Biol *13*, 1102-1107.

Martinez, J., Patkaniowska, A., Urlaub, H., Luhrmann, R., and Tuschl, T. (2002). Single-stranded antisense siRNAs guide target RNA cleavage in RNAi. Cell *110*, 563-574.

Martinez, J., and Tuschl, T. (2004). RISC is a 5' phosphomonoester-producing RNA endonuclease. Genes Dev *18*, 975-980.

Mathonnet, G., Fabian, M.R., Svitkin, Y.V., Parsyan, A., Huck, L., Murata, T., Biffo, S., Merrick, W.C., Darzynkiewicz, E., Pillai, R.S.*, et al.* (2007). MicroRNA inhibition of translation initiation in vitro by targeting the cap-binding complex eIF4F. Science *317*, 1764-1767.

Matranga, C., Tomari, Y., Shin, C., Bartel, D.P., and Zamore, P.D. (2005). Passenger-strand cleavage facilitates assembly of siRNA into Ago2-containing RNAi enzyme complexes. Cell *123*, 607-620.

Mayr, C., Hemann, M.T., and Bartel, D.P. (2007). Disrupting the pairing between let-7 and Hmga2 enhances oncogenic transformation. Science *315*, 1576-1579.

McNeil, G.P., Schroeder, A.J., Roberts, M.A., and Jackson, F.R. (2001). Genetic analysis of functional domains within the Drosophila LARK RNA-binding protein. Genetics *159*, 229-240.

REFERENCES

McNeil, G.P., Zhang, X., Genova, G., and Jackson, F.R. (1998). A molecular rhythm mediating circadian clock output in Drosophila. Neuron *20*, 297-303.

McNeil, G.P., Zhang, X., Roberts, M., and Jackson, F.R. (1999). Maternal function of a retroviral-type zinc-finger protein is essential for Drosophila development. Dev Genet *25*, 387-396.

Meister, G., Buhler, D., Laggerbauer, B., Zobawa, M., Lottspeich, F., and Fischer, U. (2000). Characterization of a nuclear 20S complex containing the survival of motor neurons (SMN) protein and a specific subset of spliceosomal Sm proteins. Hum Mol Genet *9*, 1977-1986.

Meister, G., Landthaler, M., Patkaniowska, A., Dorsett, Y., Teng, G., and Tuschl, T. (2004). Human Argonaute2 mediates RNA cleavage targeted by miRNAs and siRNAs. Mol Cell *15*, 185-197.

Meister, G., Landthaler, M., Peters, L., Chen, P.Y., Urlaub, H., Luhrmann, R., and Tuschl, T. (2005). Identification of novel argonaute-associated proteins. Curr Biol *15*, 2149-2155.

Meister, G., and Tuschl, T. (2004). Mechanisms of gene silencing by double-stranded RNA. Nature *431*, 343-349.

Miyoshi, K., Tsukumo, H., Nagami, T., Siomi, H., and Siomi, M.C. (2005). Slicer function of Drosophila Argonautes and its involvement in RISC formation. Genes Dev *19*, 2837-2848.

Miyoshi, T., Takeuchi, A., Siomi, H., and Siomi, M.C. (2010). A direct role for Hsp90 in pre-RISC formation in Drosophila. Nat Struct Mol Biol *17*, 1024-1026.

Moazed, D. (2009). Small RNAs in transcriptional gene silencing and genome defence. Nature *457*, 413-420.

Mourelatos, Z., Dostie, J., Paushkin, S., Sharma, A., Charroux, B., Abel, L., Rappsilber, J., Mann, M., and Dreyfuss, G. (2002). miRNPs: a novel class of ribonucleoproteins containing numerous microRNAs. Genes Dev *16*, 720-728.

Napoli, C., Lemieux, C., and Jorgensen, R. (1990). Introduction of a Chimeric Chalcone Synthase Gene into Petunia Results in Reversible Co-Suppression of Homologous Genes in trans. Plant Cell *2*, 279-289.

Nelson, P.T., Hatzigeorgiou, A.G., and Mourelatos, Z. (2004). miRNP:mRNA association in polyribosomes in a human neuronal cell line. RNA *10*, 387-394.

Newby, L.M., and Jackson, F.R. (1993). A new biological rhythm mutant of Drosophila melanogaster that identifies a gene with an essential embryonic function. Genetics *135*, 1077-1090.

Newby, L.M., and Jackson, F.R. (1996). Regulation of a specific circadian clock output pathway by lark, a putative RNA-binding protein with repressor activity. J Neurobiol *31*, 117-128.

Newman, M.A., Thomson, J.M., and Hammond, S.M. (2008). Lin-28 interaction with the Let-7 precursor loop mediates regulated microRNA processing. RNA *14*, 1539-1549.

Nielsen, C.B., Shomron, N., Sandberg, R., Hornstein, E., Kitzman, J., and Burge, C.B. (2007). Determinants of targeting by endogenous and exogenous microRNAs and siRNAs. RNA *13*, 1894-1910.

Nishida, K.M., Saito, K., Mori, T., Kawamura, Y., Nagami-Okada, T., Inagaki, S., Siomi, H., and Siomi, M.C. (2007). Gene silencing mechanisms mediated by Aubergine piRNA complexes in Drosophila male gonad. RNA *13*, 1911-1922.

Nottrott, S., Simard, M.J., and Richter, J.D. (2006). Human let-7a miRNA blocks protein production on actively translating polyribosomes. Nat Struct Mol Biol *13*, 1108-1114.

Nykanen, A., Haley, B., and Zamore, P.D. (2001). ATP requirements and small interfering RNA structure in the RNA interference pathway. Cell *107*, 309-321.

O'Carroll, D., Mecklenbrauker, I., Das, P.P., Santana, A., Koenig, U., Enright, A.J., Miska, E.A., and Tarakhovsky, A. (2007). A Slicer-independent role for Argonaute 2 in hematopoiesis and the microRNA pathway. Genes Dev *21*, 1999-2004.

Ohrt, T., Mutze, J., Staroske, W., Weinmann, L., Hock, J., Crell, K., Meister, G., and Schwille, P. (2008). Fluorescence correlation spectroscopy and fluorescence cross-correlation spectroscopy reveal the cytoplasmic origination of loaded nuclear RISC in vivo in human cells. Nucleic Acids Res *36*, 6439-6449.

Okamura, K., Hagen, J.W., Duan, H., Tyler, D.M., and Lai, E.C. (2007). The mirtron pathway generates microRNA-class regulatory RNAs in Drosophila. Cell *130*, 89-100.

Olsen, P.H., and Ambros, V. (1999). The lin-4 regulatory RNA controls developmental timing in Caenorhabditis elegans by blocking LIN-14 protein synthesis after the initiation of translation. Dev Biol *216*, 671-680.

Orban, T.I., and Izaurralde, E. (2005). Decay of mRNAs targeted by RISC requires XRN1, the Ski complex, and the exosome. RNA *11*, 459-469.

Orom, U.A., Nielsen, F.C., and Lund, A.H. (2008). MicroRNA-10a binds the 5'UTR of ribosomal protein mRNAs and enhances their translation. Mol Cell *30*, 460-471.

Packer, A.N., Xing, Y., Harper, S.Q., Jones, L., and Davidson, B.L. (2008). The bifunctional microRNA miR-9/miR-9* regulates REST and CoREST and is downregulated in Huntington's disease. J Neurosci *28*, 14341-14346.

Pak, J., and Fire, A. (2007). Distinct populations of primary and secondary effectors during RNAi in C. elegans. Science *315*, 241-244.

Parker, J.S., Roe, S.M., and Barford, D. (2005). Structural insights into mRNA recognition from a PIWI domain-siRNA guide complex. Nature *434*, 663-666.

Parker, R., and Sheth, U. (2007). P bodies and the control of mRNA translation and degradation. Mol Cell *25*, 635-646.

Paroo, Z., Ye, X., Chen, S., and Liu, Q. (2009). Phosphorylation of the human microRNA-generating complex mediates MAPK/Erk signaling. Cell *139*, 112-122.

Pauley, K.M., Eystathioy, T., Jakymiw, A., Hamel, J.C., Fritzler, M.J., and Chan, E.K. (2006). Formation of GW bodies is a consequence of microRNA genesis. EMBO Rep *7*, 904-910.

Pelisson, A., Sarot, E., Payen-Groschene, G., and Bucheton, A. (2007). A novel repeat-associated small interfering RNA-mediated silencing pathway downregulates complementary sense gypsy transcripts in somatic cells of the Drosophila ovary. J Virol *81*, 1951-1960.

Petersen, C.P., Bordeleau, M.E., Pelletier, J., and Sharp, P.A. (2006). Short RNAs repress translation after initiation in mammalian cells. Mol Cell *21*, 533-542.

Pfuhl, T., Mamiani, A., Durr, M., Welter, S., Stieber, J., Ankara, J., Liss, M., Dobner, T., Schmitt, A., Falkai, P.*, et al.* (2008). The LARK/RBM4a protein is highly expressed in cerebellum as compared to cerebrum. Neurosci Lett *444*, 11-15.

Pham, J.W., Pellino, J.L., Lee, Y.S., Carthew, R.W., and Sontheimer, E.J. (2004). A Dicer-2-dependent 80s complex cleaves targeted mRNAs during RNAi in Drosophila. Cell *117*, 83-94.

Pillai, R.S., Bhattacharyya, S.N., Artus, C.G., Zoller, T., Cougot, N., Basyuk, E., Bertrand, E., and Filipowicz, W. (2005). Inhibition of translational initiation by Let-7 MicroRNA in human cells. Science *309*, 1573-1576.

Qi, H.H., Ongusaha, P.P., Myllyharju, J., Cheng, D., Pakkanen, O., Shi, Y., Lee, S.W., and Peng, J. (2008). Prolyl 4-hydroxylation regulates Argonaute 2 stability. Nature *455*, 421-424.

Rajewsky, N. (2006). microRNA target predictions in animals. Nat Genet *38 Suppl*, S8-13.

Ramachandran, V., and Chen, X. (2008). Small RNA metabolism in Arabidopsis. Trends Plant Sci *13*, 368-374.

Rand, T.A., Petersen, S., Du, F., and Wang, X. (2005). Argonaute2 cleaves the anti-guide strand of siRNA during RISC activation. Cell *123*, 621-629.

Ray, D., Kazan, H., Chan, E.T., Pena Castillo, L., Chaudhry, S., Talukder, S., Blencowe, B.J., Morris, Q., and Hughes, T.R. (2009). Rapid and systematic analysis of the RNA recognition specificities of RNA-binding proteins. Nat Biotechnol *27*, 667-670.

Reuter, M., Chuma, S., Tanaka, T., Franz, T., Stark, A., and Pillai, R.S. (2009). Loss of the Mili-interacting Tudor domain-containing protein-1 activates transposons and alters the Mili-associated small RNA profile. Nat Struct Mol Biol *16*, 639-646.

Rigoutsos, I. (2009). New tricks for animal microRNAS: targeting of amino acid coding regions at conserved and nonconserved sites. Cancer Res *69*, 3245-3248.

Rivas, F.V., Tolia, N.H., Song, J.J., Aragon, J.P., Liu, J., Hannon, G.J., and Joshua-Tor, L. (2005). Purified Argonaute2 and an siRNA form recombinant human RISC. Nat Struct Mol Biol *12*, 340-349.

Robb, G.B., Brown, K.M., Khurana, J., and Rana, T.M. (2005). Specific and potent RNAi in the nucleus of human cells. Nat Struct Mol Biol *12*, 133-137.

Robb, G.B., and Rana, T.M. (2007). RNA helicase A interacts with RISC in human cells and functions in RISC loading. Mol Cell *26*, 523-537.

Rodriguez, A., Griffiths-Jones, S., Ashurst, J.L., and Bradley, A. (2004). Identification of mammalian microRNA host genes and transcription units. Genome Res *14*, 1902-1910.

Ruby, J.G., Jan, C.H., and Bartel, D.P. (2007). Intronic microRNA precursors that bypass Drosha processing. Nature *448*, 83-86.

Rudel, S., Flatley, A., Weinmann, L., Kremmer, E., and Meister, G. (2008). A multifunctional human Argonaute2-specific monoclonal antibody. RNA *14*, 1244-1253.

Rudel, S., Wang, Y., Lenobel, R., Korner, R., Hsiao, H.H., Urlaub, H., Patel, D., and Meister, G. (2010). Phosphorylation of human Argonaute proteins affects small RNA binding. Nucleic Acids Res.

Saito, K., Ishizuka, A., Siomi, H., and Siomi, M.C. (2005). Processing of pre-microRNAs by the Dicer-1-Loquacious complex in Drosophila cells. PLoS Biol *3*, e235.

Saito, K., Nishida, K.M., Mori, T., Kawamura, Y., Miyoshi, K., Nagami, T., Siomi, H., and Siomi, M.C. (2006). Specific association of Piwi with rasiRNAs derived from retrotransposon and heterochromatic regions in the Drosophila genome. Genes Dev *20*, 2214-2222.

Sambrook, J., Fritsch, E.F. and Maniatis, F. (1989). Molecular cloning: A Laboratory Manual (Cold Spring Harbour, N.Y., Cold Spring Laboratory Press).

Saraiya, A.A., and Wang, C.C. (2008). snoRNA, a novel precursor of microRNA in Giardia lamblia. PLoS Pathog *4*, e1000224.

Sasaki, T., Shiohama, A., Minoshima, S., and Shimizu, N. (2003). Identification of eight members of the Argonaute family in the human genome small star, filled. Genomics *82*, 323-330.

Schmitter, D., Filkowski, J., Sewer, A., Pillai, R.S., Oakeley, E.J., Zavolan, M., Svoboda, P., and Filipowicz, W. (2006). Effects of Dicer and Argonaute down-regulation on mRNA levels in human HEK293 cells. Nucleic Acids Res *34*, 4801-4815.

Schmitz-Linneweber, C., and Small, I. (2008). Pentatricopeptide repeat proteins: a socket set for organelle gene expression. Trends Plant Sci *13*, 663-670.

Schwamborn, J.C., Berezikov, E., and Knoblich, J.A. (2009). The TRIM-NHL protein TRIM32 activates microRNAs and prevents self-renewal in mouse neural progenitors. Cell *136*, 913-925.

Schwarz, D.S., Hutvagner, G., Du, T., Xu, Z., Aronin, N., and Zamore, P.D. (2003). Asymmetry in the assembly of the RNAi enzyme complex. Cell *115*, 199-208.

Schwarz, D.S., Hutvagner, G., Haley, B., and Zamore, P.D. (2002). Evidence that siRNAs function as guides, not primers, in the Drosophila and human RNAi pathways. Mol Cell *10*, 537-548.

Schwarz, D.S., Tomari, Y., and Zamore, P.D. (2004). The RNA-induced silencing complex is a Mg2+-dependent endonuclease. Curr Biol *14*, 787-791.

Seggerson, K., Tang, L., and Moss, E.G. (2002). Two genetic circuits repress the Caenorhabditis elegans heterochronic gene lin-28 after translation initiation. Dev Biol *243*, 215-225.

Selbach, M., Schwanhausser, B., Thierfelder, N., Fang, Z., Khanin, R., and Rajewsky, N. (2008). Widespread changes in protein synthesis induced by microRNAs. Nature *455*, 58-63.

Sheth, U., and Parker, R. (2006). Targeting of aberrant mRNAs to cytoplasmic processing bodies. Cell *125*, 1095-1109.

Shevchenko, A., Jensen, O.N., Podtelejnikov, A.V., Sagliocco, F., Wilm, M., Vorm, O., Mortensen, P., Boucherie, H., and Mann, M. (1996). Linking genome and proteome by mass spectrometry: large-

scale identification of yeast proteins from two dimensional gels. Proc Natl Acad Sci U S A *93*, 14440-14445.

Shi, L., Zhao, G., Qiu, D., Godfrey, W.R., Vogel, H., Rando, T.A., Hu, H., and Kao, P.N. (2005). NF90 regulates cell cycle exit and terminal myogenic differentiation by direct binding to the 3'-untranslated region of MyoD and p21WAF1/CIP1 mRNAs. J Biol Chem *280*, 18981-18989.

Sijen, T., Steiner, F.A., Thijssen, K.L., and Plasterk, R.H. (2007). Secondary siRNAs result from unprimed RNA synthesis and form a distinct class. Science *315*, 244-247.

Siomi, H., and Siomi, M.C. (2009). On the road to reading the RNA-interference code. Nature *457*, 396-404.

Smardon, A., Spoerke, J.M., Stacey, S.C., Klein, M.E., Mackin, N., and Maine, E.M. (2000). EGO-1 is related to RNA-directed RNA polymerase and functions in germ-line development and RNA interference in C. elegans. Curr Biol *10*, 169-178.

Sofola, O., Sundram, V., Ng, F., Kleyner, Y., Morales, J., Botas, J., Jackson, F.R., and Nelson, D.L. (2008). The Drosophila FMRP and LARK RNA-binding proteins function together to regulate eye development and circadian behavior. J Neurosci *28*, 10200-10205.

Song, J.J., Liu, J., Tolia, N.H., Schneiderman, J., Smith, S.K., Martienssen, R.A., Hannon, G.J., and Joshua-Tor, L. (2003). The crystal structure of the Argonaute2 PAZ domain reveals an RNA binding motif in RNAi effector complexes. Nat Struct Biol *10*, 1026-1032.

Song, J.J., Smith, S.K., Hannon, G.J., and Joshua-Tor, L. (2004). Crystal structure of Argonaute and its implications for RISC slicer activity. Science *305*, 1434-1437.

Stark, G.R., Kerr, I.M., Williams, B.R., Silverman, R.H., and Schreiber, R.D. (1998). How cells respond to interferons. Annu Rev Biochem *67*, 227-264.

Steiner, F.A., Hoogstrate, S.W., Okihara, K.L., Thijssen, K.L., Ketting, R.F., Plasterk, R.H., and Sijen, T. (2007). Structural features of small RNA precursors determine Argonaute loading in Caenorhabditis elegans. Nat Struct Mol Biol *14*, 927-933.

Stöhr, J.R., Meister, G. (2011). In vitro RISC cleavage assay (Berlin, Humana Press).

Stohr, N., Lederer, M., Reinke, C., Meyer, S., Hatzfeld, M., Singer, R.H., and Huttelmaier, S. (2006). ZBP1 regulates mRNA stability during cellular stress. J Cell Biol *175*, 527-534.

Ströh, L.J. (2009). Reinigung und strukturelle Untersuchung der potenziellen eukaryontischen Interaktionspartner RBM4 und Argonaut 2 (Diploma thesis). In Lehrstuhl für Struktur und Chemie der Biopolymere (Bayreuth, University of Bayreuth).

Taft, R.J., Glazov, E.A., Lassmann, T., Hayashizaki, Y., Carninci, P., and Mattick, J.S. (2009). Small RNAs derived from snoRNAs. RNA *15*, 1233-1240.

Tahbaz, N., Kolb, F.A., Zhang, H., Jaronczyk, K., Filipowicz, W., and Hobman, T.C. (2004). Characterization of the interactions between mammalian PAZ PIWI domain proteins and Dicer. EMBO Rep *5*, 189-194.

Tam, O.H., Aravin, A.A., Stein, P., Girard, A., Murchison, E.P., Cheloufi, S., Hodges, E., Anger, M., Sachidanandam, R., Schultz, R.M.*, et al.* (2008). Pseudogene-derived small interfering RNAs regulate gene expression in mouse oocytes. Nature *453*, 534-538.

Tarun, S.Z., Jr., and Sachs, A.B. (1996). Association of the yeast poly(A) tail binding protein with translation initiation factor eIF-4G. EMBO J *15*, 7168-7177.

Thermann, R., and Hentze, M.W. (2007). Drosophila miR2 induces pseudo-polysomes and inhibits translation initiation. Nature *447*, 875-878.

Till, S., Lejeune, E., Thermann, R., Bortfeld, M., Hothorn, M., Enderle, D., Heinrich, C., Hentze, M.W., and Ladurner, A.G. (2007). A conserved motif in Argonaute-interacting proteins mediates functional interactions through the Argonaute PIWI domain. Nat Struct Mol Biol *14*, 897-903.

Tolia, N.H., and Joshua-Tor, L. (2007). Slicer and the argonautes. Nat Chem Biol *3*, 36-43.

Tomari, Y., Du, T., Haley, B., Schwarz, D.S., Bennett, R., Cook, H.A., Koppetsch, B.S., Theurkauf, W.E., and Zamore, P.D. (2004a). RISC assembly defects in the Drosophila RNAi mutant armitage. Cell *116*, 831-841.

Tomari, Y., Du, T., and Zamore, P.D. (2007). Sorting of Drosophila small silencing RNAs. Cell *130*, 299-308.

Tomari, Y., Matranga, C., Haley, B., Martinez, N., and Zamore, P.D. (2004b). A protein sensor for siRNA asymmetry. Science *306*, 1377-1380.

Tran, H., Schilling, M., Wirbelauer, C., Hess, D., and Nagamine, Y. (2004). Facilitation of mRNA deadenylation and decay by the exosome-bound, DExH protein RHAU. Mol Cell *13*, 101-111.

Uchida, N., Hoshino, S., Imataka, H., Sonenberg, N., and Katada, T. (2002). A novel role of the mammalian GSPT/eRF3 associating with poly(A)-binding protein in Cap/Poly(A)-dependent translation. J Biol Chem *277*, 50286-50292.

Vagin, V.V., Sigova, A., Li, C., Seitz, H., Gvozdev, V., and Zamore, P.D. (2006). A distinct small RNA pathway silences selfish genetic elements in the germline. Science *313*, 320-324.

Vagin, V.V., Wohlschlegel, J., Qu, J., Jonsson, Z., Huang, X., Chuma, S., Girard, A., Sachidanandam, R., Hannon, G.J., and Aravin, A.A. (2009). Proteomic analysis of murine Piwi proteins reveals a role for arginine methylation in specifying interaction with Tudor family members. Genes Dev *23*, 1749-1762.

Vasudevan, S., and Steitz, J.A. (2007). AU-rich-element-mediated upregulation of translation by FXR1 and Argonaute 2. Cell *128*, 1105-1118.

Vasudevan, S., Tong, Y., and Steitz, J.A. (2007). Switching from repression to activation: microRNAs can up-regulate translation. Science *318*, 1931-1934.

Viswanathan, S.R., Daley, G.Q., and Gregory, R.I. (2008). Selective blockade of microRNA processing by Lin28. Science *320*, 97-100.

Voinnet, O. (2005). Non-cell autonomous RNA silencing. FEBS Lett *579*, 5858-5871.

Volpe, T., Schramke, V., Hamilton, G.L., White, S.A., Teng, G., Martienssen, R.A., and Allshire, R.C. (2003). RNA interference is required for normal centromere function in fission yeast. Chromosome Res *11*, 137-146.

Wakiyama, M., Takimoto, K., Ohara, O., and Yokoyama, S. (2007). Let-7 microRNA-mediated mRNA deadenylation and translational repression in a mammalian cell-free system. Genes Dev *21*, 1857-1862.

Wang, B., Love, T.M., Call, M.E., Doench, J.G., and Novina, C.D. (2006). Recapitulation of short RNA-directed translational gene silencing in vitro. Mol Cell *22*, 553-560.

Wang, B., Yanez, A., and Novina, C.D. (2008a). MicroRNA-repressed mRNAs contain 40S but not 60S components. Proc Natl Acad Sci U S A *105*, 5343-5348.

Wang, Y., Juranek, S., Li, H., Sheng, G., Tuschl, T., and Patel, D.J. (2008b). Structure of an argonaute silencing complex with a seed-containing guide DNA and target RNA duplex. Nature *456*, 921-926.

Wang, Y., Sheng, G., Juranek, S., Tuschl, T., and Patel, D.J. (2008c). Structure of the guide-strand-containing argonaute silencing complex. Nature *456*, 209-213.

Watanabe, T., Takeda, A., Tsukiyama, T., Mise, K., Okuno, T., Sasaki, H., Minami, N., and Imai, H. (2006). Identification and characterization of two novel classes of small RNAs in the mouse germline: retrotransposon-derived siRNAs in oocytes and germline small RNAs in testes. Genes Dev *20*, 1732-1743.

Watanabe, T., Totoki, Y., Toyoda, A., Kaneda, M., Kuramochi-Miyagawa, S., Obata, Y., Chiba, H., Kohara, Y., Kono, T., Nakano, T.*, et al.* (2008). Endogenous siRNAs from naturally formed dsRNAs regulate transcripts in mouse oocytes. Nature *453*, 539-543.

Weinmann, L., Hock, J., Ivacevic, T., Ohrt, T., Mutze, J., Schwille, P., Kremmer, E., Benes, V., Urlaub, H., and Meister, G. (2009). Importin 8 is a gene silencing factor that targets argonaute proteins to distinct mRNAs. Cell *136*, 496-507.

Wu, L., Fan, J., and Belasco, J.G. (2006). MicroRNAs direct rapid deadenylation of mRNA. Proc Natl Acad Sci U S A *103*, 4034-4039.

Xu, X.L., Li, Y., Wang, F., and Gao, F.B. (2008). The steady-state level of the nervous-system-specific microRNA-124a is regulated by dFMR1 in Drosophila. J Neurosci *28*, 11883-11889.

Yan, K.S., Yan, S., Farooq, A., Han, A., Zeng, L., and Zhou, M.M. (2003). Structure and conserved RNA binding of the PAZ domain. Nature *426*, 468-474.

Yang, J.S., Maurin, T., Robine, N., Rasmussen, K.D., Jeffrey, K.L., Chandwani, R., Papapetrou, E.P., Sadelain, M., O'Carroll, D., and Lai, E.C. (2010). Conserved vertebrate mir-451 provides a platform for Dicer-independent, Ago2-mediated microRNA biogenesis. Proc Natl Acad Sci U S A *107*, 15163-15168.

Yekta, S., Shih, I.H., and Bartel, D.P. (2004). MicroRNA-directed cleavage of HOXB8 mRNA. Science *304*, 594-596.

Yi, R., Qin, Y., Macara, I.G., and Cullen, B.R. (2003). Exportin-5 mediates the nuclear export of pre-microRNAs and short hairpin RNAs. Genes Dev *17*, 3011-3016.

Yisraeli, J.K. (2005). VICKZ proteins: a multi-talented family of regulatory RNA-binding proteins. Biol Cell *97*, 87-96.

Yoda, M., Kawamata, T., Paroo, Z., Ye, X., Iwasaki, S., Liu, Q., and Tomari, Y. (2010). ATP-dependent human RISC assembly pathways. Nat Struct Mol Biol *17*, 17-23.

Yu, B., Yang, Z., Li, J., Minakhina, S., Yang, M., Padgett, R.W., Steward, R., and Chen, X. (2005). Methylation as a crucial step in plant microRNA biogenesis. Science *307*, 932-935.

Yuan, Y.R., Pei, Y., Ma, J.B., Kuryavyi, V., Zhadina, M., Meister, G., Chen, H.Y., Dauter, Z., Tuschl, T., and Patel, D.J. (2005). Crystal structure of A. aeolicus argonaute, a site-specific DNA-guided endoribonuclease, provides insights into RISC-mediated mRNA cleavage. Mol Cell *19*, 405-419.

Zamore, P.D., Tuschl, T., Sharp, P.A., and Bartel, D.P. (2000). RNAi: double-stranded RNA directs the ATP-dependent cleavage of mRNA at 21 to 23 nucleotide intervals. Cell *101*, 25-33.

Zeng, Y., Sankala, H., Zhang, X., and Graves, P.R. (2008). Phosphorylation of Argonaute 2 at serine-387 facilitates its localization to processing bodies. Biochem J *413*, 429-436.

Zhang, H., Kolb, F.A., Jaskiewicz, L., Westhof, E., and Filipowicz, W. (2004). Single processing center models for human Dicer and bacterial RNase III. Cell *118*, 57-68.

Zhou, R., Hotta, I., Denli, A.M., Hong, P., Perrimon, N., and Hannon, G.J. (2008). Comparative analysis of argonaute-dependent small RNA pathways in Drosophila. Mol Cell *32*, 592-599.

Zipprich, J.T., Bhattacharyya, S., Mathys, H., and Filipowicz, W. (2009). Importance of the C-terminal domain of the human GW182 protein TNRC6C for translational repression. RNA *15*, 781-793.

ACKNOWLEDGEMENTS

CURRICULUM VITAE

PERSONAL DETAILS

Name	Julia Regina Stöhr
Birth name	Höck
Place of birth	Augsburg
Citizenship	German

EDUCATION

10/2005 - 02/2011	PhD student, Max Planck Institute of Biochemistry, Martinsried, Germany Laboratory of Dr. Gunter Meister
10/2003 - 09/2005	Master studies, Technical University Munich, Germany Degree: M. Sc. (Biochemistry)
10/2000 - 09/2003	Bachelor studies, Technical University Munich, Germany Degree: B. Sc. (Biochemistry)
06/2000	university entrance qualification Justus-von-Liebig-Gymnasium Neusäß, Germany

PUBLICATIONS

PRIMARY PUBLICATIONS

Coley AM, Parisi K, Masciantonio R, **Höck J**, Casey JL, Murphy VJ, Harris KS, Batchelor AH, Anders RF, Foley M.
The most polymorphic residue on Plasmodium falciparum apical membrane antigen 1 determines binding of an invasion-inhibitory antibody.
Infect Immun. 2006 May;74(5):2628-36.

Maier S, Staffler G, Hartmann A, **Höck J**, Henning K, Grabusic K, Mailhammer R, Hoffmann R, Wilmanns M, Lang R, Mages J, Kempkes B.
Cellular target genes of Epstein-Barr virus nuclear antigen 2.
J Virol. 2006 Oct;80(19):9761-71.

Höck J, Weinmann L, Ender C, Rüdel S, Kremmer E, Raabe M, Urlaub H, Meister G.
Proteomic and functional analysis of Argonaute-containing mRNA-protein complexes in human cells.
EMBO Rep. 2007 Nov;8(11):1052-60.

Barth S, Pfuhl T, Mamiani A, Ehses C, Roemer K, Kremmer E, Jäker C, **Höck J**, Meister G, Grässer FA.
Epstein-Barr virus-encoded microRNA miR-BART2 down-regulates the viral DNA polymerase BALF5.
Nucleic Acids Res. 2008 Feb;36(2):666-75.

Ohrt T, Mütze J, Staroske W, Weinmann L, **Höck J**, Crell K, Meister G, Schwille P.
Fluorescence correlation spectroscopy and fluorescence cross-correlation spectroscopy reveal the cytoplasmic origination of loaded nuclear RISC in vivo in human cells.
Nucleic Acids Res. 2008 Nov;36(20):6439-49.

Weinmann L, **Höck J**, Ivacevic T, Ohrt T, Mütze J, Schwille P, Kremmer E, Benes V, Urlaub H, Meister G.
Importin 8 is a gene silencing factor that targets argonaute proteins to distinct mRNAs.
Cell. 2009 Feb 6;136(3):496-507.

REVIEWS AND BOOK CHAPTERS

Höck J, Meister G.
The Argonaute protein family.
Genome Biol. 2008;9(2):210.

Stöhr J, Meister G.
In vitro RISC cleavage assay
in: Hobman TC, Duchaine TF (editors)
Argonaute Proteins: Methods and Protocols
Humana Press, Berlin; estimated Publication Date: April 2011